

**CLIMATE VARIABILITY AND CLIMATE CHANGE IN WATER RESOURCES
MANAGEMENT OF THE ZAMBEZI RIVER BASIN**

A thesis submitted in fulfilment of the
requirements for the degree of

DOCTOR OF PHILOSOPHY

Of

RHODES UNIVERSITY

Grahamstown

South Africa

By

SITHABILE TIRIVAROMBO

August 2012

DEDICATION

This thesis is dedicated to my sons Tatenda and Tapiwanashe

ACKNOWLEDGEMENTS

GLORY BE TO THE ALMIGHTY FOR IT IS IN HIM THAT WE DERIVE THE STRENGTH TO ACCOMPLISH OUR DREAMS

I express my sincere gratitude to my supervisor Professor Denis Hughes for all the kinds of support he provided throughout the entire course of my research right up to the completion of this thesis. Through his guidance, constructive criticisms and support, this thesis has been accomplished. I am particularly grateful for his patience during the time I was writing this thesis and for the numerous chapters he reviewed before the final thesis was approved. I will forever be grateful.

My gratitude is also extended to the Carnegie Corporation of New York through the Regional Initiative in Science and Education (RISE) Programme and the Sub-Saharan African Water Resources Network (SSAWRN) for providing a bursary for my PhD research. Special mention goes to the Schlumberger Foundation's Faculty for the Future Programme for the fellowship that enabled me to take care of my family even in the absence of employment. Your efforts to uplift the women faculty are greatly appreciated. Without the support of both organizations this thesis would not have been accomplished.

I am extremely grateful for the collaboration we had with my research colleagues Raphael and Jane, thank you for your support and encouragement. I am also thankful to Evison for assisting with the initial set up of the model and for providing guidance where it was needed and to Andrew Slaughter for the programming expertise. To Bolu, Paul and Nelson thank you so much for always reminding me of a smile even when the road was getting tougher.

Last but not least, I would like to thank my sons, Tatenda and Tapiwanashe for their patience as well as the emotional support they provided throughout the course of my study.

ABSTRACT

Water is recognised as a key driver for social and economic development in the Zambezi basin. The basin is riparian to eight southern African countries and the transboundary nature of the basin's water resources can be viewed as an agent of cooperation between the basin countries. It is possible, however, that the same water resource can lead to conflicts between water users. The southern African Water Vision for 'equitable and sustainable utilisation of water for social, environmental justice and economic benefits for the present and future generations' calls for an integrated and efficient management of water resources within the basin. Ensuring water and food security in the Zambezi basin is, however, faced with challenges due to high variability in climate and the available water resources. Water resources are under continuous threat from pollution, increased population growth, development and urbanisation as well as global climate change. These factors increase the demand for freshwater resources and have resulted in water being one of the major driving forces for development. The basin is also vulnerable due to lack of adequate financial resources and appropriate water resources infrastructure to enable viable, equitable and sustainable distribution of the water resources. This is in addition to the fact that the basin's economic mainstay and social well-being are largely dependent on rainfed agriculture. There is also competition among the different water users and this has the potential to generate conflicts, which further hinder the development of water resources in the basin.

This thesis has focused on the Zambezi River basin emphasising climate variability and climate change. It is now considered common knowledge that the global climate is changing and that many of the impacts will be felt through water resources. If these predictions are correct then the Zambezi basin is most likely to suffer under such impacts since its economic mainstay is largely determined by the availability of rainfall. It is the belief of this study that in order to ascertain the impacts of climate change, there should be a basis against which this change is evaluated. If we do not know the historical patterns of variability it may be difficult to predict changes in the future climate and in the hydrological resources and it will certainly be difficult to develop appropriate management strategies. Reliable quantitative estimates of water availability are a prerequisite for successful water resource plans. However, such initiatives have been hindered by paucity in data especially in a basin where gauging networks are inadequate and some of them have deteriorated. This is further compounded by shortages in resources, both human and

financial, to ensure adequate monitoring. To address the data problems, this study largely relied on global data sets and the CRU TS2.1 rainfall grids were used for a large part of this study. The study starts by assessing the historical variability of rainfall and streamflow in the Zambezi basin and the results are used to inform the prediction of change in the future. Various methods of assessing historical trends were employed and regional drought indices were generated and evaluated against the historical rainfall trends. The study clearly demonstrates that the basin has a high degree of temporal and spatial variability in rainfall and streamflow at inter-annual and multi-decadal scales.

The Standardised Precipitation Index, a rainfall based drought index, is used to assess historical drought events in the basin and it is shown that most of the droughts that have occurred were influenced by climatic and hydrological variability. It is concluded, through the evaluation of agricultural maize yields, that the basin's food security is mostly constrained by the availability of rainfall. Comparing the viability of using a rainfall based index to a soil moisture based index as an agricultural drought indicator, this study concluded that a soil moisture based index is a better indicator since all of the water balance components are considered in the generation of the index. This index presents the actual amount of water available for the plant unlike purely rainfall based indices, that do not account for other components of the water budget that cause water losses. A number of challenges were, however, faced in assessing the variability and historical drought conditions, mainly due to the fact that most parts of the Zambezi basin are ungauged and available data are sparse, short and not continuous (with missing gaps).

Hydrological modelling is frequently used to bridge the data gap and to facilitate the quantification of a basin's hydrology for both gauged and ungauged catchments. The trend has been to use various methods of regionalisation to transfer information from gauged basins, or from basins with adequate physical basin data, to ungauged basins. All this is done to ensure that water resources are accounted for and that the future can be well planned. A number of approaches leading to the evaluation of the basin's hydrological response to future climate change scenarios are taken.

The Pitman rainfall-runoff model has enjoyed wide use as a water resources estimation tool in southern Africa. The model has been calibrated for the Zambezi basin but it should be acknowledged that any hydrological modelling process is characterised by many uncertainties

arising from limitations in input data and inherent model structural uncertainty. The calibration process is thus carried out in a manner that embraces some of the uncertainties. Initial ranges of parameter values (maximum and minimum) that incorporate the possible parameter uncertainties are assigned in relation to physical basin properties. These parameter sets are used as input to the uncertainty version of the model to generate behavioural parameter space which is then further modified through manual calibration. The use of parameter ranges initially guided by the basin physical properties generates streamflows that adequately represent the historically observed amounts. This study concludes that the uncertainty framework and the Pitman model perform quite well in the Zambezi basin.

Based on assumptions of an intensifying hydrological cycle, climate changes are frequently expected to result in negative impacts on water resources. However, it is important that basin scale assessments are undertaken so that appropriate future management strategies can be developed. To assess the likely changes in the Zambezi basin, the calibrated Pitman model was forced with downscaled and bias corrected GCM data. Three GCMs were used for this study, namely; ECHAM, GFDL and IPSL. The general observation made in this study is that the near future (2046-2065) conditions of the Zambezi basin are expected to remain within the ranges of historically observed variability. The differences between the predictions for the three GCMs are an indication of the uncertainties in the future and it has not been possible to make any firm conclusions about directions of change. It is therefore recommended that future water resources management strategies account for historical patterns of variability, but also for increased uncertainty. Any management strategies that are able to satisfactorily deal with the large variability that is evident from the historical data should be robust enough to account for the near future patterns of water availability predicted by this study. However, the uncertainties in these predictions suggest that improved monitoring systems are required to provide additional data against which future model outputs can be assessed.

TABLE OF CONTENTS

| | |
|--|------|
| DEDICATION | ii |
| ACKNOWLEDGEMENTS | iii |
| ABSTRACT | iv |
| TABLE OF CONTENTS | vii |
| LIST OF FIGURES | xiii |
| LIST OF TABLES | xiii |
| | |
| CHAPTER 1 INTRODUCTION AND OBJECTIVES OF THE STUDY | 1 |
| 1.1 Background of the study | 1 |
| 1.2 Problem statement and objectives of the study | 5 |
| | |
| CHAPTER 2 CLIMATE VARIABILITY AND CLIMATE CHANGE | 9 |
| 2.1 Introduction | 9 |
| 2.2 Climate variability and climate change | 9 |
| 2.2.1 Global climate variability | 10 |
| 2.2.2 Global atmospheric circulation | 10 |
| 2.2.3 Land-Ocean-Atmosphere interactions | 11 |
| 2.2.4 Variability in global water resources | 13 |
| 2.3 Climate variability in Africa | 14 |
| 2.4 Variability and water resources in southern Africa | 186 |
| 2.5 Extreme drought events | 18 |
| 2.6 Climate change and water resources | 22 |
| 2.6.1 General Circulation Models (GCMs) | 23 |
| 2.6.2 Downscaling | 25 |
| 2.6.3 Observed trends in global temperature and precipitation | 27 |
| 2.7 Impacts of climate variability and climate change in the Zambezi basin | 29 |
| 2.8 Application of models in water resources management | 30 |
| 2.8.1 Decision support systems in water resources management | 31 |
| 2.8.2 Types of water resource systems for decision making | 33 |
| 2.8.3 Software packages as decision support tools | 34 |
| 2.9 Hydrological modelling | 35 |
| 2.9.1 Uses of hydrological models | 36 |
| 2.9.2 Types of hydrological models | 37 |
| 2.9.3 Parameter estimation approaches | 38 |
| 2.9.4 Uncertainty in hydrological modelling | 42 |
| 2.9.5 Dealing with uncertainty in hydrological modelling | 44 |
| 2.9.6 Hydrological modelling in southern Africa | 45 |
| 2.10 Modelling the hydrological responses to climate change | 46 |
| 2.10.1 GCM uncertainty in predicting climate | 47 |
| 2.10.2 Uncertainty in assessing the hydrological impacts of climate change | 48 |
| 2.11 Summary of key aspects | 50 |
| | |
| CHAPTER 3 STUDY AREA AND AVAILABLE DATA | 52 |
| 3.1 The Zambezi River Basin | 52 |

| | | |
|---|---|------------|
| 3.1.1 | Geology and topography..... | 55 |
| 3.1.2 | Soils..... | 56 |
| 3.1.3 | Land cover | 58 |
| 3.1.4 | Climate..... | 59 |
| 3.1.5 | Runoff..... | 62 |
| 3.1.6 | Water resource use and management..... | 69 |
| 3.2 | Sources of data..... | 71 |
| CHAPTER 4 METHODOLOGICAL APPROACHES | | 79 |
| 4.1 | Introduction | 79 |
| 4.2 | SPATSIM - Spatial and Time Series Information Modelling..... | 79 |
| 4.2.1 | SPATSIM components | 80 |
| 4.2.2 | Generation of catchment averaged rainfall in SPATSIM..... | 83 |
| 4.2.3 | Drought analysis routines in SPATSIM | 85 |
| 4.2.4 | Applications - External linkages to SPATSIM..... | 88 |
| 4.3 | The Pitman model | 90 |
| 4.4 | Setting up the Pitman model in SPATSIM | 97 |
| 4.5 | Assessing the model performance..... | 99 |
| 4.6 | SPI, soil moisture and regional food security relationships..... | 101 |
| 4.6.1 | Drought and food security relationships..... | 101 |
| 4.6.2 | SPI and soil moisture relationships..... | 103 |
| 4.7 | Methods of detecting trends and changes in hydrological variables..... | 105 |
| 4.7.1 | Tests for trends..... | 106 |
| 4.7.2 | Change point analysis | 109 |
| 4.7.3 | Spectral analysis..... | 111 |
| 4.8 | Scenarios for climate change..... | 113 |
| 4.8.1 | Bias correction | 115 |
| 4.8.2 | Modelling the impact of climate change on the Zambezi River basin..... | 118 |
| CHAPTER 5 VARIABILITY IN RAINFALL AND STREAMFLOW | | 119 |
| 5.1 | Introduction | 119 |
| 5.2 | General characteristics of the rainfall time series | 121 |
| 5.2.1 | Spatial analysis of rainfall variability across the Zambezi basin..... | 123 |
| 5.2.2 | Inter-annual and decadal variability in rainfall in the Zambezi basin | 124 |
| 5.2.3 | Linear trend detection in mean annual precipitation..... | 128 |
| 5.2.4 | Change point analysis in rainfall..... | 130 |
| 5.2.5 | Detection of cyclic behaviour in rainfall time series | 132 |
| 5.2.6 | Seasonality in rainfall distribution..... | 135 |
| 5.3 | General characteristics of the streamflow time series..... | 136 |
| 5.3.1 | Inter-annual and decadal variability in streamflow in the Zambezi basin | 138 |
| 5.3.2 | Linear trend detection in mean annual streamflow..... | 141 |
| 5.3.3 | Change point analysis in streamflow | 142 |
| 5.3.4 | Detection of cyclic behaviour in streamflow | 145 |
| 5.3.5 | Seasonality in streamflow distribution..... | 146 |
| 5.4 | Discussion and conclusion | 147 |

| | |
|--|-----|
| CHAPTER 6 HYDROLOGICAL MODEL CALIBRATION FOR THE ZAMBEZI BASIN | 151 |
| 6.1 Introduction | 151 |
| 6.2 The calibration approach | 152 |
| 6.2.1 Assigning the initial parameter ranges | 153 |
| 6.2.2 Generating the parameter space using the uncertainty version of the Pitman model | 160 |
| 6.3 Calibration results | 163 |
| CHAPTER 7 VARIABILITY, REGIONAL DROUGHTS AND FOOD SECURITY IN THE ZAMBEZI BASIN | 179 |
| 7.1 Introduction | 179 |
| 7.2.1 Variability of agricultural droughts at six month time scales | 180 |
| 7.2.2 Dry and wet spells, 1901-2002 | 184 |
| 7.2.3 Historical droughts and variability at three month time scales | 187 |
| 7.3.1 Historical drought and agricultural production in the Zambezi basin | 189 |
| 7.3.2 SPI and maize yield relationships at sub-basin scales | 192 |
| 7.4 Discussion | 201 |
| 7.5 Simulated soil moisture and agricultural droughts | 203 |
| 7.5.1 Soil moisture SPI relationship | 203 |
| 7.5.2 Soil moisture yield relationship | 208 |
| 7.6 Discussion and conclusion | 214 |
| CHAPTER 8 IMPACTS OF CLIMATE CHANGE ON WATER RESOURCES IN THE ZAMBEZI BASIN | 218 |
| 8.1 Introduction | 218 |
| 8.2.1 Bias correction for rainfall | 221 |
| 8.2.2 Bias correction and change in potential evapotranspiration | 222 |
| 8.3 Future scenarios of change in rainfall | 225 |
| 8.4 Hydrological impacts of climate change (2046-2065) | 229 |
| 8.4.1 Changes in streamflow | 230 |
| 8.4.2 Uncertainty in future climate change projections | 234 |
| 8.5 Changes in soil moisture storage | 236 |
| 8.6 Extreme drought events | 238 |
| 8.7 Climate change and climate variability | 243 |
| 8.8 Discussion and conclusion | 245 |
| CHAPTER 9 CONCLUSION AND RECOMMENDATIONS | 249 |
| 9.1 Introduction | 249 |
| 9.2 Data issues and decision support tools | 249 |
| 9.3 Variability and its implications for droughts and food security | 251 |
| 9.4 Modelling the hydrological impacts of climate change | 253 |
| 9.5 Recommendations | 253 |
| 9.6 Conclusion | 256 |
| REFERENCES | 257 |

LIST OF FIGURES

| | | |
|-------------|---|-----|
| Figure 1 | Climate induced impacts on vulnerable and well adapted regions..... | 3 |
| Figure 2.1 | The earth's annual energy balance | 10 |
| Figure 2.2 | General global circulation patterns and a cross-section of tropospheric circulation | 11 |
| Figure 2.3 | Circulation patterns and convergence over Africa..... | 15 |
| Figure 2.4 | Average monthly rainfall totals | 16 |
| Figure 2.5 | Propagation of drought | 19 |
| Figure 2.6 | Schematic of climatic impacts and responses to anthropogenic drivers | 22 |
| Figure 2.7 | The four IPCC SRES scenarios | 24 |
| Figure 2.8 | Dynamical downscaling..... | 27 |
| Figure 2.9 | Global annual mean temperature..... | 28 |
| Figure 2.10 | Annual rainfall and lake levels for Lake Malawi for the period 1896-1994..... | 30 |
| Figure 2.11 | Common components of a decision support system | 33 |
| Figure 2.1 | Schematic of the steps involved in the formulation of hydrological models ... | 36 |
| Figure 2.13 | Cascading uncertainty in quantifying the hydrological impacts of climate change. | 49 |
| Figure 3.1 | Zambezi River basin..... | 53 |
| Figure 3.2 | Sub-basins of the Zambezi | 54 |
| Figure 3.3 | Catchments of the Zambezi basin | 55 |
| Figure 3.4 | Zambezi basin topography | 56 |
| Figure 3.5 | Dominant soil types in the Zambezi River basin | 57 |
| Figure 3.6 | Land use in the Zambezi River basin | 58 |
| Figure 3.7 | Mean annual rainfall (1961-1990) in the Zambezi River basin | 60 |
| Figure 3.8 | Lake Kariba water levels, 1961-2005 | 61 |
| Figure 3.9 | Zambezi basin mean annual runoff, 1970-1994..... | 64 |
| Figure 3.10 | Kariba Dam and Cahora Bassa Dam..... | 65 |
| Figure 3.11 | Wetlands in the Zambezi Delta | 66 |
| Figure 3.12 | CRU rainfall grids and local rainfall stations..... | 72 |
| Figure 3.14 | Runoff stations used in the study | 78 |
| Figure 4.1 | SPATSIM main screen..... | 81 |
| Figure 4.2 | Selecting data from the import item under the attribute menu..... | 82 |
| Figure 4.3 | Selecting data and specifying the variable type to be imported..... | 82 |
| Figure 4.4 | Example of (a) 1-dimensional and (b) 2-dimensional arrays in SPATSIM..... | 83 |
| Figure 4.5 | Selection of sub-catchments, search radius, interpolation period and time step. | 84 |
| Figure 4.6 | Procedure for generating and saving time series SPI..... | 87 |
| Figure 4.7 | Time series of SPI plotted in TSOFT..... | 88 |
| Figure 4.8 | Starting the render process and generating maps in SPATSIM | 88 |
| Figure 4.9 | Comparison of simulated and observed time series data in TSOFT | 89 |
| Figure 4.10 | TSOFT scatter plot display of simulated versus observed streamflow | 89 |
| Figure 4.11 | Schematic of the main components of the Pitman model | 91 |
| Figure 4.12 | Flow stations used to calibrate the Zambezi River basin..... | 99 |
| Figure 4.13 | An example showing the impacts of various factors on agricultural yield-red line. | 102 |
| Figure 4.14 | Graphical representation of the detrending process | 103 |

| | | |
|-------------|--|-----|
| Figure 4.15 | Example of Morlet Wavelet power spectrum showing El Niño activity | 104 |
| Figure 4.16 | Example of a cumulative sum plot of rainfall | 111 |
| Figure 4.17 | Illustration of a periodogram and spectral density | 113 |
| Figure 4.18 | Downscaled GCM grid points used in this study..... | 115 |
| Figure 4.19 | Bias in baseline precipitation with respect to historically observed precipitation | 116 |
| Figure 5.1 | Rainfall stations used for variability analysis | 120 |
| Figure 5.2 | Streamflow gauging stations used for variability analysis..... | 120 |
| Figure 5.3 | Spatial distribution of rainfall in the western part of the Zambezi basin. | 124 |
| Figure 5.4a | 5-year running trend in rainfall for example stations in the Zambezi River basin. | 125 |
| Figure 5.4b | 5-year running trend in rainfall for example stations in the Zambezi River basin. | 126 |
| Figure 5.5a | 10 and 20-year running trends in rainfall | 127 |
| Figure 5.5b | 10 and 20-year running trends in rainfall | 128 |
| Figure 5.6 | Sen's linear estimates of rainfall at example stations | 129 |
| Figure 5.7a | CUSUM and distribution plots of rainfall anomalies at example stations..... | 130 |
| Figure 5.7b | CUSUM and distribution plots of rainfall anomalies at example stations..... | 131 |
| Figure 5.8 | Significant step change at stations 8801322 and 24140..... | 132 |
| Figure 5.9a | Rainfall spectral densities for example cases in the Zambezi River basin..... | 134 |
| Figure 5.9b | Rainfall spectral densities for example cases in the Zambezi River basin..... | 135 |
| Figure 5.10 | Seasonal rainfall distribution during the periods 1931-1960 and 1961-1990 ... | 136 |
| Figure 5.11 | 5-year running trends in streamflow for example cases in the Zambezi..... | 139 |
| Figure 5.12 | 10 and 20-year running trends in streamflow for example cases in the Zambezi... | 140 |
| Figure 5.13 | Variability of rainfall and streamflow | 141 |
| Figure 5.14 | Sen's linear estimates of streamflow at example stations..... | 142 |
| Figure 5.15 | CUSUM and distribution plots of streamflow anomalies at example stations . | 143 |
| Figure 5.16 | Significant step changes at ZGP25 and 1291100..... | 144 |
| Figure 5.17 | Streamflow spectral densities for case examples in the Zambezi | 146 |
| Figure 5.18 | Mean monthly streamflow distribution | 147 |
| Figure 6.1 | Schematic of the hydrological modelling process for the Zambezi basin..... | 153 |
| Figure 6.2 | Variation of coefficients of efficiency against GW, ST and FT/POW + GW/GPOW | 161 |
| Figure 6.3 | Flow gauging stations used for calibrations..... | 163 |
| Figure 6.4 | Observed and simulated monthly streamflows for Luanginga and Zambezi 10166 | |
| Figure 6.5a | Observed and simulated monthly streamflows for Kafue 4 and Kafue 1 | 168 |
| Figure 6.5b | Observed and simulated monthly streamflows for Kafue 3 | 169 |
| Figure 6.6 | Observed and simulated monthly streamflows for catchments in Lake Kariba | 171 |
| Figure 6.7 | Observed and simulated monthly streamflows for Manyame and Mazowe | 172 |
| Figure 6.8a | Observed and simulated monthly streamflows for Luangwa..... | 173 |
| Figure 6.8b | Observed and simulated monthly streamflows for Namitete | 174 |
| Figure 6.9 | Observed and simulated monthly streamflows for validation tests..... | 175 |
| Figure 7.1a | 6 month SPIs from the upper sub-basins of the Zambezi | 181 |
| Figure 7.1b | 6 month SPIs for Lake Kariba, Kafue Luangwa and Lake Malawi sub-basins | 182 |
| Figure 7.1c | 6 month SPIs for Tete and Zambezi Delta | 183 |

| | | |
|--------------|--|-----|
| Figure 7.2 | 6 month SPIs (October to March) for 1921, 1940, 1948 and 1967..... | 184 |
| Figure 7.3 | Temporal evolution of cumulative SPI 6 during 1901-2002..... | 186 |
| Figure 7.4a | Historical JFM and OND SPIs for sub-basins in the Zambezi | 187 |
| Figure 7.4b | Historical JFM and OND SPIs for sub-basins in the Zambezi | 188 |
| Figure 7.5 | 3 month SPIs for 1969 OND, 1970 JFM, 1981 OND and 1982 JFM..... | 189 |
| Figure 7.6 | Total annual maize yield in the Zambezi basin..... | 190 |
| Figure 7.7 | Annual maize yields in some of the Zambezi basin countries (1961-2010)..... | 190 |
| Figure 7.8 | SPIs for 1969-70, 1982-83 and 1991-92 (OND and JFM)..... | 191 |
| Figure 7.9 | Observed and detrended maize yields for Zambia, Zimbabwe and Malawi ... | 194 |
| Figure 7.10 | Annual rainfall and maize yield in Zimbabwe during 1961-2002 | 195 |
| Figure 7.11 | Observed and detrended maize yields for Mozambique | 196 |
| Figure 7.12a | Correlation of SPI with detrended maize yield deviations (1961-2000)..... | 198 |
| Figure 7.12b | Correlation of SPI with detrended maize yield deviations (1961-2000)..... | 199 |
| Figure 7.12c | Correlation of SPI with detrended maize yield deviations (1961-2000)..... | 200 |
| Figure 7.13a | Correlations of soil moisture and SPI..... | 204 |
| Figure 7.13b | Correlations of soil moisture and SPI..... | 205 |
| Figure 7.14 | Wavelet power spectra of soil moisture and SPI for the Kabompo and Kafue. | 206 |
| Figure 7.15a | Correlations between soil moisture anomalies and detrended maize yields | 209 |
| Figure 7.15b | Correlations between soil moisture anomalies and detrended maize yields | 210 |
| Figure 7.15c | Correlations between soil moisture anomalies and detrended maize yields | 211 |
| Figure 7.16 | Wavelet power spectra of soil moisture and detrended maize yields..... | 212 |
| Figure 7.17 | Wavelet coherence between soil moisture and detrended maize yields..... | 213 |
| Figure 8.1 | Conversion of the GCM daily rainfall to monthly rainfall in SPATSIM..... | 220 |
| Figure 8.2 | Example of rainfall bias correction using the ECHAM, GFDL and IPSL..... | 222 |
| Figure 8.3 | Annual evapotranspiration increases predicted by ECHAM, GFDL, and IPSL | 223 |
| Figure 8.4a | Monthly rainfall distributions for the historical and near future periods | 225 |
| Figure 8.4b | Monthly rainfall distributions for the historical and near future periods | 226 |
| Figure 8.5 | Changes in mean monthly rainfall relative to the historical rainfall | 228 |
| Figure 8.6a | Changes in long term mean monthly rainfall | 228 |
| Figure 8.6b | Changes in long term mean monthly rainfall | 229 |
| Figure 8.7a | Flow duration curves for the historical and near future streamflows..... | 231 |
| Figure 8.7b | Flow duration curves for the historical and near future streamflows | 232 |
| Figure 8.8a | Future changes in streamflow relative to the historical flow..... | 233 |
| Figure 8.8b | Future changes in streamflow relative to the historical flow..... | 234 |
| Figure 8.9 | Comparison of the hydrological model parameter uncertainty and GCM uncertainty..... | 235 |
| Figure 8.10 | Changes in soil moisture relative to historical conditions..... | 237 |
| Figure 8.11a | Predicted JFM and OND SPIs for 2046-2065 | 238 |
| Figure 8.11b | Predicted JFM and OND SPIs for 2046-2065 | 239 |
| Figure 8.11c | Predicted JFM and OND SPIs for 2046-2065 | 240 |
| Figure 8.12a | Frequency and severity of droughts for the near future seasons | 241 |
| Figure 8.12b | Frequency and severity of droughts for the near future seasons | 242 |

LIST OF TABLES

| | | |
|-----------|--|-----|
| Table 3.1 | Basin countries, area and population details..... | 52 |
| Table 3.2 | Hydrological disasters in the Zambezi basin since 1980 | 62 |
| Table 3.3 | Water uses in the Zambezi basin | 63 |
| Table 3.4 | Water balance for the Zambezi River sub-basins 1969-1970 to 1993-1994 | 64 |
| Table 3.5 | Reservoirs and lakes in the Zambezi basin | 66 |
| Table 3.6 | Summary of sub-basin characteristics | 66 |
| Table 3.7 | ID and location of local stations | 73 |
| Table 3.8 | Comparison of CRU and local rainfall data..... | 76 |
| Table 3.9 | Identification and location of runoff stations..... | 77 |
| Table 4.1 | SPI categories and drought classes | 86 |
| Table 4.2 | Pitman model and reservoir model parameters..... | 92 |
| Table 4.3 | Required attributes for the Pitman model | 98 |
| Table 4.4 | Characteristics of the three GCMs availed for this study | 114 |
| Table 5.1 | Statistical parameters for mean annual precipitation using local rainfall data | 121 |
| Table 5.2 | Statistical parameters for catchment averaged rainfall using CRU data..... | 123 |
| Table 5.3 | Stations used for analysis of spatial variability in rainfall..... | 124 |
| Table 5.4 | Rainfall trend statistics for Mann-Kendall's and Sen's test..... | 128 |
| Table 5.5 | Fisher's Kappa and Bartlett's Kolmogorov-Smirnov statistical tests for rainfall..... | 133 |
| Table 5.6 | Statistical parameters for selected flow gauging stations in the Zambezi basin... | 138 |
| Table 5.7 | Mann-Kendall and Sen's tests for trends in streamflow | 141 |
| Table 5.8 | Step change statistics for stations ZGP25 and 1291100 | 145 |
| Table 5.9 | Fisher's Kappa and Bartlett's K-S statistical tests of streamflow..... | 145 |
| Table 6.1 | Initial parameter ranges for example sub-basins of the Zambezi | 158 |
| Table 6.2 | Initial parameter ranges for example sub-basins of the Zambezi | 159 |
| Table 6.3 | Summary statistics of streamflows based on untransformed and transformed data | 164 |
| Table 6.4 | Calibrated parameters for Upper Zambezi and Barotse..... | 164 |
| Table 6.5 | Calibrated parameters for the Kafue | 166 |
| Table 6.6 | Wetland and reservoir parameters for Kafue Flats, Lukanga, Itezhitezhi | 167 |
| Table 6.7 | Calibrated parameters for Lake Kariba, Tete, Luangwa and Namitete | 170 |
| Table 6.8 | Validation and calibration statistics for example sub-basins..... | 174 |
| Table 7.1 | Severe and extreme SPI 6 droughts between 1901 and 2002 | 183 |
| Table 7.2 | Mann Kendall test on SPI6 for the period 1901-2002 | 185 |
| Table 7.3 | Rank order correlation coefficients of SPI and detrended maize yield | 193 |
| Table 7.4 | Coincidence of SPI and yield deviation..... | 197 |
| Table 7.5 | Correlation of soil moisture anomaly with SPI..... | 204 |
| Table 7.6 | Coherency between SPI and soil moisture..... | 207 |
| Table 7.7 | Rank order correlation coefficients of soil moisture and detrended maize yield .. | 208 |
| Table 7.8 | Coherency between soil moisture and detrended maize yields | 213 |
| Table 8.1 | Mean monthly potential evapotranspiration changes | 224 |
| Table 8.2 | Changes in mean annual streamflow | 234 |
| Table 8.3 | Climate variability: Climate change - Signal to noise ratio for streamflow | 244 |

CHAPTER 1 INTRODUCTION AND OBJECTIVES OF THE STUDY

1.1 Background of the study

The global climate is inherently variable at different spatial and temporal scales. Palaeoclimatic records show that variability is not a recent development but it has occurred intermittently for millennia (Kabat and van Schaik, 2003). A series of complex feedback processes make up the earth's climate system whose major driver is solar radiation, and any fluctuations in the radiative forcing may cause variations in the climate thus resulting in increased variability. Freshwater resources are good indicators of climatic variability and have the potential to be greatly impacted by fluxes of moisture and energy that emanate from changes in atmospheric circulation. As such, most of the impacts of a changing and varying climate are likely to be felt through water resources (Chiew, 2007, IPCC, 2008). The potential threats of a variable and changing climate include alteration of hydrological variables such as precipitation, streamflow, soil moisture, groundwater recharge, evapotranspiration as well as changes to the timing and magnitude of the extreme events. Such changes will have varying impacts on societal well-being, ranging from water supply, health, food security, energy and the environment (Xu, 2000).

The different time scales at which climatic variability occurs have implications for the management of water resources. At daily time scales, local variation in weather may cause floods and storms while at seasonal time scales, increased variation in precipitation due to fluctuations in sea surface temperatures (SSTs) and changes in soil moisture storage may culminate into droughts (van den Hurk and Jacob, 2010). Decadal scale variability is important for implementing effective water management strategies such as the design of water resources infrastructure and the operating rules of water supply systems. The various impacts that occur at the different time scales of variability are a clear indication that water resources can no longer be managed under assumed stationary climatic conditions (Milly et al., 2008), but rather the dynamics of climate change must be considered in order to develop a well-informed water resources management strategy for the future.

Clearly, natural climate variability and climate change are not the only threats to water resources. Freshwater resources are under continued threats from a rapidly increasing population and

economic development, and as the standard of living improves, the demand for freshwater also increases. The United Nations Population Reference Bureau (UN, 2006a) projects a global population of about 8 billion by the year 2025, and the World Bank (2005) estimates that demands for water will exceed supply by 40% by 2030, while two-thirds of the global population could experience water stress by 2025. Human-induced activities such as urbanisation, changes in land cover, agriculture and industrialisation cause a variety of impacts on water resources and should also be considered alongside the impacts of climatic variability.

The IPCC (1997) has defined vulnerability as the extent to which climate may damage or harm a system. Kabat and van Schaik (2003) state that vulnerability is a function of location, coping capacity, exposure and sensitivity of the affected system to climate change. Sensitivity and coping capacity are mainly driven by the socioeconomic status of the system which includes factors such as income, nutritional status and access to basic services. Therefore an increasingly variable climate and a resource-driven adaptation strategy may put some of the world's poorest regions in a precarious position as they may not be able to afford some of the costly adaptation options. In Africa for example, high variability in climate has caused widespread human suffering and economic damage (Conway and Hulme, 1996). As the poorest continent, contributing 28% of the global poverty (World Bank, 2005) and with a high population growth rate which is expected to double by 2050 (Population Reference Bureau, 2009), Africa will become more vulnerable and even less able to adapt to climatic variability.

In the context of water resources management, vulnerability can be translated into an economy-driven water scarcity and a natural or physically-driven water scarcity. An economy-driven water scarcity is due to insufficient investment in water, as is the case in most of the poor regions of the world, whereas, a physically-driven water scarcity is caused by natural changes in the hydrological system, a situation common in economically developed regions (Koutsoyiannis, 2011). The IPCC (2001a) has prescribed the following as requirements for a well-adapted region: a stable and prosperous economy; adequate access to the necessary technologies; clear-cut rules, roles and responsibilities for implementing the adaptation strategies; well-coordinated systems for disseminating climate change information and equitable distribution of and access to resources. Unfortunately most of the economically developing regions fall short of these requirements. Figure 1 shows that economically developed regions have at their disposal,

resources to ensure that appropriate water management policies and infrastructure are in place and are thus well cushioned against the undesirable impacts of climate change on water resources.

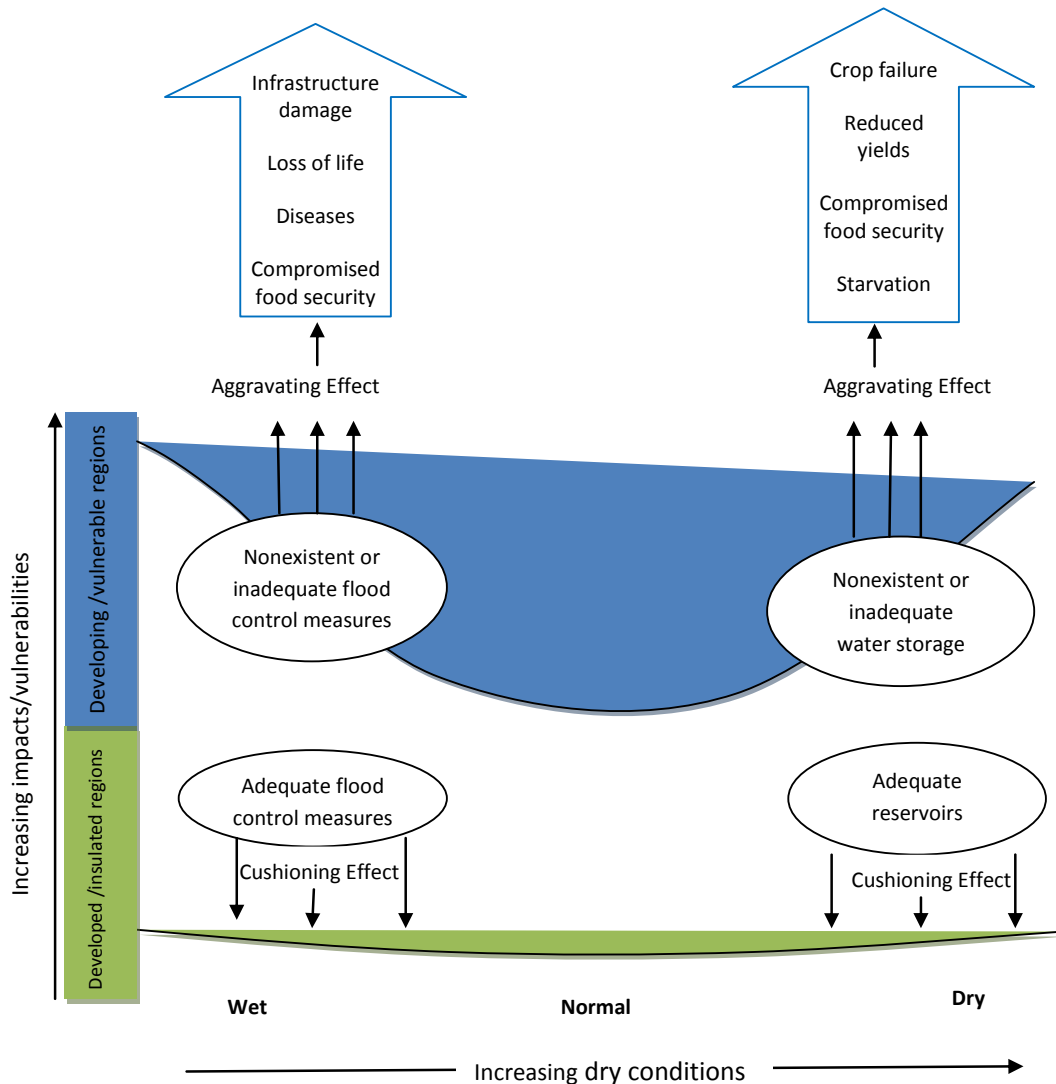


Figure 1 Climate induced impacts on vulnerable and well adapted regions. Shaded regions show extent and magnitude of impacts in vulnerable regions (top-blue) and in well adapted regions (bottom-green)

Vulnerability is higher within poor communities because most of them survive on subsistence agriculture and forestry whose viability is controlled by climatic conditions. High population growth rates, sharing of trans-boundary water resources, pest and disease infestation and unfavourable political environments are some of the compounding factors that add to the

vulnerability of poor regions. Climate variability and the looming threats of climate change, as well as uncertainties and knowledge gaps surrounding their manifestation, will exacerbate the hardships already being faced by the poor, thus making them more vulnerable. If vulnerability is not addressed, Africa may not be able to cope with the ramifications of climate change impacts in the future.

Climate change can generally be regarded as the long-term change in climatic variables such as precipitation and temperature caused by natural variability and/or by human-induced changes. Currently the term climate change is used in a broader sense to represent global warming as caused by anthropogenic increases in greenhouse gas concentrations. There is now compelling evidence that the global climate has become warmer and climate change is rapidly becoming a matter of global concern (IPCC, 2007). Long term records show that the mean global surface temperature increased by 0.6°C in the 20th century (IPCC, 2001b; Trenberth et al. 2007), while it is projected that by the year 2100, the mean temperature may increase by 1.0 to 3.5°C and the sea level will rise by 15 to 95cm. At the same time the concentration of atmospheric carbon dioxide, a major product of burning fossil fuels and a warming agent for atmospheric temperatures is expected to rise to more than double the pre-industrial levels by the end of the 21st century (IPCC, 1996a). Global warming is expected to cause changes in atmospheric circulation and to amplify the variability in climate. These changes may result in an intensified hydrological cycle and shifts in the occurrence and magnitude of flood and drought events thereby imposing huge impacts on the environment, agriculture and water management. Increased temperatures will also result in increased demand for water while increased evapotranspiration will reduce soil moisture and groundwater reserves with a consequent decrease in runoff.

In a world already faced by water scarcity and where almost 1.2 billion people (UN, 2006b) are without access to safe drinking water, increased water scarcity through climate change will worsen the vulnerability of the poor people who are already largely unable to cope with the impacts of climate variability and natural climatic hazards. As human beings face the additional risks of a changing climate, floods and droughts will result in food shortages and hunger. At the same time, the health and economy of the people, water supplies, energy and other water-

dependent services may be greatly compromised and, in shared river basins, more conflicts may be generated as people compete for a scarce water resource (Van Jaarsveldt et al., 2005, Elasha et al., 2006).

While managing water resources is complicated by natural climatic variability and extreme events, the situation will be worsened by anthropogenic changes in climate. There is high uncertainty as to how climate change will manifest itself and about how the climate system will respond to external forcings including influences such as land use changes, development and population expansion. This makes it difficult to predict exactly the timing and magnitude of climate change-induced events and the availability of water in the future. Uncertainty in climate predictions will continue to undermine the efforts being put towards promoting human social and economic development as well as safeguarding the environment (Todd et al., 2011). Despite the uncertainties, the imminent threats of climate change must still be acknowledged alongside the threats of climate variability and development impacts so that appropriate strategies may be developed to deal with the risks in the management of water resources.

1.2 Problem statement and objectives of the study

Due to high seasonal and inter-annual variations in rainfall (Hulme et al., 2001; Christensen et al., 2007), the African continent is highly vulnerable and severely impacted by the present variability in climate as well as predicted long-term climate change impacts. Vulnerability is further worsened by the presence of transboundary water basins, generally low income levels, inadequate resources, pest and disease infestation and poorly developed national and regional water institutions (Beyene et al., 2010). Future changes in the timing of hydrologically extreme events may have significant impacts on transboundary river basins where there is already competition for water and where most of the livelihoods depend on rain-fed agriculture. This study focuses on climate variability and climate change in the Zambezi River basin, a transboundary basin located in southern Africa and riparian to eight countries.

The Zambezi basin climate is semi arid and highly variable and climate change is expected to amplify natural climatic variability. Some of the major climate-induced events that have caused suffering amongst the basin population include cyclone-induced floods and droughts. For

example, in 2000, severe floods caused by Cyclone Eline resulted in over 700 deaths and over half a million were left homeless (Wamukonya et al, 2001). Inevitably, changes in streamflow as a result of climate variability and climate change will affect the availability and accessibility of water for various intended uses, with significant consequences on the rural poor as well as on hydroelectricity generation. It is therefore becoming increasingly necessary to consider the long term impacts of climate variability and climate change on the water resources of the Zambezi basin. Understanding the uncertainties and quantifying the impacts of climate variability and climate change will assist policy makers and water managers to adopt coherent and informed response strategies that reflect the state of scientific understanding of the likelihood of outcomes. Furthermore, incorporation of climate variability estimates into watershed management tools would make adaptation to future climate change easier.

A wealth of literature is available justifying the need to undertake investigations on the impacts of changing climates on water resources. Ziervogel et al. (2010) indicate that knowledge of vulnerabilities to climate variability as well as appropriate response strategies will enable the formulation of adaptation options that are based on the most appropriate design and implementation techniques. Kundzewicz (2008) advocates the incorporation of the current climate variability into water-related management as this would make adaptation to future climate change easier. Zhang et al. (2007) state that quantifying the hydrological impacts of climate change will assist in understanding the potential climate-related water problems and to make better planning decisions. Bardossy (2007) and Jacob and van den Hurk (2009) concur that understanding the potential impacts of a changing climate on streamflow is vital for design and management of water resources and that it can be explored through the use of complex numerical models, including the hydrological models (e.g. Knutti, 2011).

Given the situation in the Zambezi River basin, it is likely that the adverse water resources impacts caused by climate variability will be compounded by the threatening climate change. This thesis therefore aims at assessing historical and future variability and climate change impacts on water resources of the Zambezi River basin, with a view to generate catchment scale information that can assist in developing appropriate adaptation and mitigation strategies for the basin. The overall goal of this study is to quantify historical and future variability in water

resources availability and to assess the likely impacts on water resources management and decision making in the Zambezi River basin. Unlike other studies that place emphasis on the main river of the Zambezi, focussing on hydropower dams, this study focuses on the hydrological impacts of climate variability and climate change at the sub-basin scale in the Zambezi basin. The specific objectives identified to address the overall goal are:

1) **To identify major water resources and management issues in the basin.** To understand the water resource issues in the basin, various reviews of literature are undertaken in addition to physical observations.

2) **To assess the available climate, hydrology and water use data and to evaluate their appropriateness for addressing some of the objectives of this study.** Climate and hydrology data are collected from various sources and assessed for gaps, uncertainties and variability trends.

3) **To evaluate the appropriateness of existing data analysis and modelling tools in identifying patterns and trends and providing water resources management information.** In order to produce reliable information that can be of practical use, basin hydrological parameters that adequately characterise the basin should be obtained and for this purpose the Pitman monthly rainfall-runoff model will be calibrated for the Zambezi basin. To identify patterns and trends, appropriate statistical methods of analysis methods will be used.

4) **To perform a regional drought analysis and to assess the impacts of future climate change on the occurrence of droughts in the Zambezi basin.** Historical and future drought conditions will be assessed using the Standardised Precipitation Index (SPI) and simulated soil moisture data and the results validated by use of publicly available crop yield data. Simulated soil moisture storage will be compared against SPI to explore the viability of using it as an agricultural drought indicator. ***Floods and hydroelectricity generation are not addressed in this part of the study.***

5) **To evaluate available climate change scenario information in the context of predicting future water resources availability.** Identifying and evaluating the likely

impacts of climate change on water resources will help to develop appropriate adaptation strategies. Downscaled and bias-corrected climate change data obtained from available and accessible General Circulation Models are forced onto the Pitman hydrological model to generate future basin hydrology.

6) To improve understanding of risk and uncertainty within the Zambezi River basin. Water resources should be managed on the basis of the links between uncertainty and risk and it is thus necessary to incorporate uncertainty so that water managers can be able to tell the range of uncertainty within which they are working. An evaluation of uncertainties in data, the models and the prediction process will thus be undertaken.

7) To improve the understanding of vulnerability of the basin water resources to climate variability and climate change and to develop recommendations that can assist the future management of the basin water resources.

1.3 Outline of the thesis

This thesis is organized into nine chapters. Chapter 1 covers the introduction, significance of the study and research objectives. Chapter 2 reviews literatures which address the objectives of the study, the drivers of climate variability and climate change at global and local scales as well as the impacts of climate variability and change on water resources are presented. Hydrological modelling, methods of assessing the hydrological impacts of climate change, extreme events and their impacts with particular emphasis on droughts are reviewed. Chapter 3 describes the study area, data sources and the selection of gauging stations that are used in the study. Methodological approaches including the description of the Pitman model are presented in Chapter 4 and Chapter 5 assesses the historical variability of rainfall and streamflow in the Zambezi basin. The results of the Pitman model calibration for the Zambezi basin which incorporate the use of the uncertainty framework are presented in Chapter 6. Chapter 7 is devoted to the regional drought analysis and food security. The hydrological response of the Zambezi basin to the near future (2046-2065) climate change scenarios is examined in Chapter 8. Chapter 9 concludes the thesis by providing a discussion of the main findings and recommendations for further research and for improving the management of water resources in the Zambezi River basin.

CHAPTER 2 CLIMATE VARIABILITY AND CLIMATE CHANGE

2.1 Introduction

Climate is one of the most important limiting factors to societal well being with respect to food security, human health, ecosystems maintenance, energy and most importantly to the mapping and characterisation of the hydrological cycle. The earth's climate is driven by natural and anthropogenic factors such that changes to any of the forcing variables may cause fluctuations of the climate system resulting in a variable and changing system. The synergistic relationship between the climate and the hydrological cycle is such that if the climate becomes variable, the variability is also passed onto the water resources. Variability normally results in unreliable water supply which tends to have significant impacts on the most vulnerable communities. This situation can be worsened by the impacts of anthropogenic climate change on water resources.

This chapter presents a review of the nature of climate variability and its driving forces starting from a global scale to a regional scale which mainly focuses on southern Africa. The impacts of climate variability and climate change on water resources are explored after which the decision support systems to water resources management are discussed mainly based on modelling. The methods of quantifying the hydrological responses to climate change and which recognize the predictive uncertainties are also examined.

2.2 Climate variability and climate change

The IPCC (2001a) defines climate variability as the short term fluctuations about the mean of the climatic variables and these fluctuations are largely caused by natural climatic processes but they can be amplified by human activities. Climate change is defined as a statistically significant variation in either the mean state of the climate or its variability over an extended period of time. The minimum period required to make reasonable estimates of long-term changes in climate is 30 years (WMO, 1987). The hydrological cycle plays a crucial role in the global climate system as it is the major agent through which the various components of the climate system are coordinated. Any alterations to the climate, whether due to climatic variability or climate change

are therefore expected to have significant impacts on water resources (Chiew, 2007; Le Treut et al., 2007).

2.2.1 Global climate variability

The global climate is naturally variable; it has never been stable for any extended period of time (Kabat and van Schaik, 2003). Variability in climate is experienced through changes in space and time of variables such as precipitation, evapotranspiration, temperature and runoff. The state of the climate at any given time is influenced by the nature of energy and water cycles that interact between the land, oceans and the atmosphere, and these are driven by solar energy through absorption and emission of short wave solar radiation (Figure 2.1). The various drivers of global climate variability are outlined in the sections that follow.

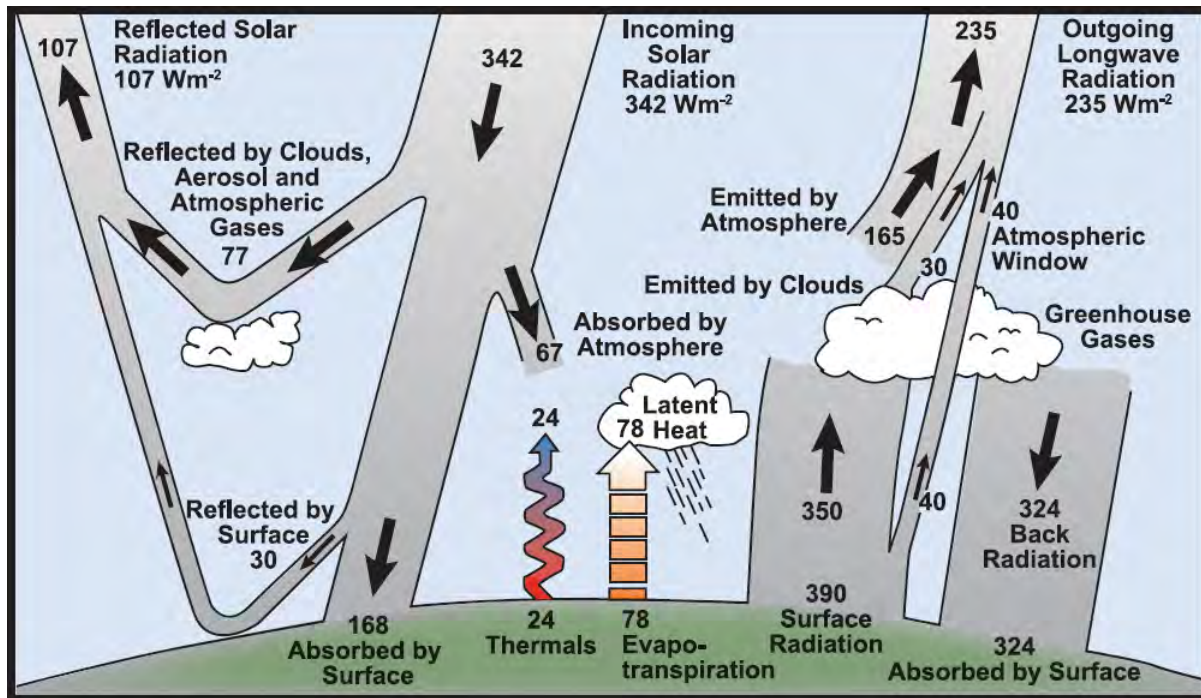


Figure 2.1 The earth's annual energy balance (after Kiehl and Trenberth, 1997)

2.2.2 Global atmospheric circulation

Variability in climate is largely caused by global circulations which occur as a result of the redistribution of global energy. Fluctuations in the climate system are generated when a forcing is applied such that an energy difference is created between the equator and the poles. This difference in energy invokes a flow of air masses so that the global energy balance can be

restored (Held et al., 1989; Pabon and Dorado, 2008). A simplified version of the general global circulation patterns is presented in Figure 2.2. A low pressure belt (the equatorial trough) is found at the equator and air masses flow towards this belt to make up for the pressure differences. As the earth rotates, air masses are deflected from their north-south direction either towards the right (Northern Hemisphere) or towards the left (Southern Hemisphere). The tropics in the latitudes 30° north and south are governed by the NE trade winds (northern hemisphere) and the SE trade winds (southern hemisphere). The air masses of these trade winds converge in the Inter-Tropical Convergence Zone (ITCZ). The ITCZ is a zone close to the equator where massive rain-bearing clouds form rain when the South East Trade Winds meet the North East Monsoon Winds. Under convection, the air rises to the upper atmosphere where it is met by a compensating poleward flow (Hadley cell). Sinking and diverging air-masses from the Hadley cell form a permanent Subtropical High Pressure Belt at about 20°-40° latitude. This belt is largely made up of anticyclones which are formed as a result of high pressure. Westerly winds (westerlies) prevail in the mid latitudes (between 60°-80° latitude). Polewards, above 60°, there is the Polar Front which is a mixture of cold polar air and warm tropical air. This mixture forms a meandering jetstream in the upper atmosphere. The ITCZ migrates north and south of the equator as a result of seasonal changes in global radiation (Tallaksen and Van Lanen, 2004) and as it shifts position, other circulation features (e.g. the jet stream and the sub-tropical high pressure belt) are also shifted.

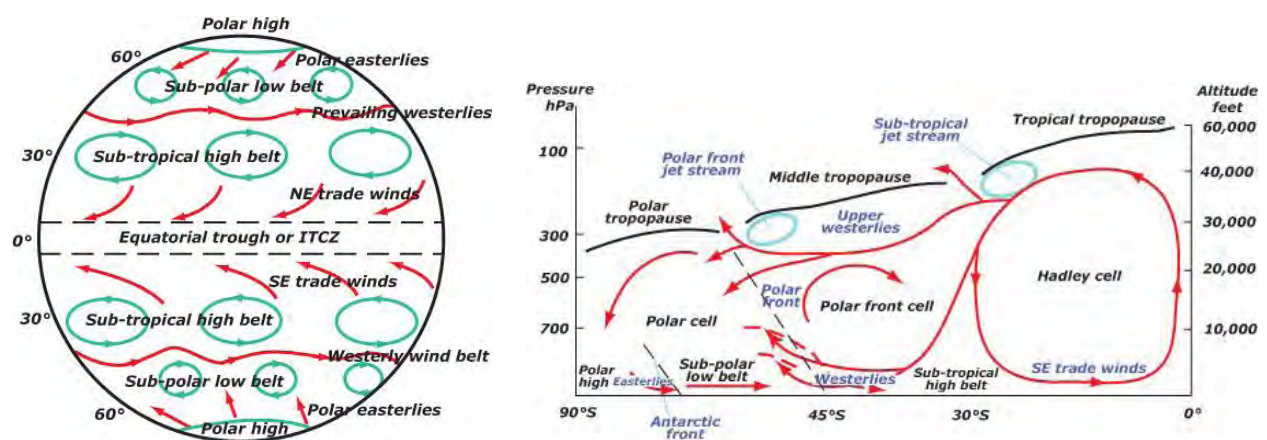


Figure 2.2 General global circulation patterns and a cross-section of tropospheric circulation (source Brandon, 2011)

2.2.3 Land-Ocean-Atmosphere interactions

In addition to the movement of the ITCZ, land, ocean and atmospheric interactions are responsible for modifying a region's climate. Gleick (2000) states that ocean-atmosphere feedback mechanisms and changes in sea surface temperatures (SSTs) play a large role in modifying a region's climate thereby contributing to climatic variability. Regional climate characteristics are influenced by surface features and processes such as topography and land-water distribution. Oceans store massive amounts of heat and through global teleconnections their currents can transport heat energy over large distances. Large amounts of evaporation are derived from the oceanic waters and as the oceanic air masses move onto the continents they condense and form precipitation (Pabon and Dorado, 2008). As the atmospheric conditions change, changes may also be imposed on the oceanic surfaces and these will in turn alter the weather conditions. Large scale processes that drive climatic variability include; the tropical Pacific events of El Niño and La Niña, the North Atlantic Oscillation (NAO); Pacific Decadal Oscillation (PDO) and the Indian Ocean Dipole (IDO) (Krishnamurti and Shukla, 2007; Lyons et al., 2011). These large scale ocean-atmosphere interactions and fluctuations are also responsible for the periodic cycles that are observed in the climatic patterns.

The El Niño Southern Oscillation (ENSO) is a well known feedback mechanism that occurs in the Pacific Ocean and is considered the largest driver of natural variability (Trenberth et al., 1998). ENSO is an unusual large-scale ocean-atmosphere system resulting in irregular and alternate cycles of warm and cool sea surface temperatures (SSTs) in the tropical Pacific Ocean. It occurs alongside the rise and fall in air pressure between the Asian and the eastern Pacific regions (Burroughs, 2007). When pressure is high in the Pacific Ocean, the pressure in the Indian Ocean from Africa to Australia is low and the pressure difference between the two is referred to as the Southern Oscillation (SO). A standard measure of the pressure difference is taken between Tahiti and Darwin (Australia) and this is referred to as the Southern Oscillation Index (SOI, Tallaksen and Van Lanen, 2004). El Niño is characterised by highly negative values of SOI signifying a reversal of the prevailing pressure conditions. When conditions are reversed the SSTs in the Pacific Ocean are also reversed and the cold water is replaced by warm water. When the opposite happens, it is termed La Niña and these two represent warm and cold events (Krishnamurti and Shukla, 2007). Changes in pressure due to the southern oscillation are also

linked to shifting of the position of the ITCZ and changes in rainfall distribution patterns particularly in the tropics. Teleconnections between the El Niño and La Niña events have been experienced in most parts of the world and they have also been linked to droughts (Chiew and McMahon, 2002). An irregular and alternate cycle of warm and cool sea surface temperatures (SSTs) that lasts 2 to 7 years has been observed in the entire global climate system (Hastenrath, 1996; Zhang et al., 1997).

2.2.4 Variability in global water resources

Precipitation is the main determining factor of variability in the water balance and in observed flows over space and time. Because of the inherent association between the hydrological cycle and the climate system, hydrological variability is inevitably driven by climatic variability while at the same time variability in climate can be observed through changes in temperature and precipitation (Peel et al., 2002, 2004). Consequently fluctuations in atmospheric circulation patterns which occur as fluxes of moisture and energy at the land surface have a large influence on the hydrological characteristics of a river system. Also, the shifting of the ITCZ and the fluctuation in sea surface temperatures are linked to spatial and temporal variations in global runoff (Schulze, 2005).

A study by McMahon et al. (1987) focusing on global runoff and precipitation clearly indicates how climate varies across the globe. The study shows that interannual variability differs between continents, while Australia and southern Africa are singled out to have the highest variability in precipitation and consequently in runoff. Although the observed differences could not be fully ascribed to precipitation alone, the study noted that for any given variation in precipitation, the variability in runoff of the two regions (Australia and southern Africa) was significantly higher than in the rest of the world. In another study using an expanded and improved annual runoff database, Peel et al. (2001) confirmed the observations made earlier by McMahon et al. (1987) that there are continental differences in annual runoff variability, they also concluded that the differences were primarily due to variations in annual precipitation at the continental scale. Continental differences in the annual runoff and precipitation were further confirmed in a re-analysis by Peel et al. (2004) whose results also revealed that annual runoff in the southern hemisphere was significantly higher than in the northern hemisphere. In a bid to further illustrate

runoff variability across the globe, McMahon et al. (2007a) undertook a study on 729 rivers worldwide in which it was concluded that southern Africa had the highest variability in mean annual runoff. The coefficients of variation of the mean annual runoff were ranked as: southern Africa 0.82, Australia 0.68, South America 0.37, northern Africa 0.29, Asia 0.29, North America 0.25, Europe 0.24 and South Pacific 0.22. In a related study aimed at assessing variability on a country basis, McMahon et al. (2007b) showed a wide range of mean annual runoff across the globe ranging from a country mean of 34 mm in southern Africa to 2 417 mm in Panama.

2.3 Climate variability in Africa

Africa is characterised by different types of climate ranging from humid equatorial, seasonally-arid tropics to sub-tropical Mediterranean (Hulme et al., 2001). African variability is attributable to fluctuations in global sea surface temperatures (SSTs) and to ENSO as well as to the shifting position of the ITCZ. The state of the climate is largely guided by effective moisture variability which in turn is a function of the change in position of the ITCZ (Hoerling et al. 2006; Lyons et al., 2011). In Africa, the seasons vary temporally and spatially such that most parts of southern Africa experience summer from September through late April while winter occurs mainly from late May and peaking during the months of June to July. The reverse is true for North Africa (Figure 2.3., Nicholson, 1996). These seasonal differences are due to the pressure belt over the Sahara and the location of the ITCZ (Nicholson, 2000). In July, the low pressure belt over the Sahara oscillates between the north east (NE) trade winds and the southwest (SW) monsoon while the two are separated by the ITCZ, located at 18-20⁰N. Southern Africa, East Africa and the Sahel are deemed to portray the highest levels of seasonal variation in Africa (Goulden et al., 2008).

The different climates that are observed in Africa are the major cause of the high rainfall variability in the continent (Hulme et al., 2001). SSTs are responsible for inter-decadal variability in rainfall, ENSO is normally responsible for the inter-annual variability and the ITCZ is responsible for seasonal variability. Since the ITCZ is a rain-bearing system, it influences the distribution of rainfall over Africa. In North Africa rainfall occurs during the July season, during this time, pressure is high over southern Africa. In January the situation is reversed such that rainfall occurs in southern Africa when the pressure is high in North Africa and while the ITCZ

is relocated to southern Africa. In general, frontal systems (westerlies) associated with the ITCZ and other circulation patterns determine the occurrence and amount of rainfall in a certain area. In areas where the circulations are prolonged, rainfall is high and this is particularly so for the pole-ward and equatorial zones where the average annual rainfall amounts to between 800 to 1 200 mm and 1 200 to 2 000 mm respectively. Desert areas lie in sub-tropical latitudes and are barely influenced by the westerlies thus they receive a very small amount (about 20 to 200 mm per year) of rainfall (Nicholson, 2000).

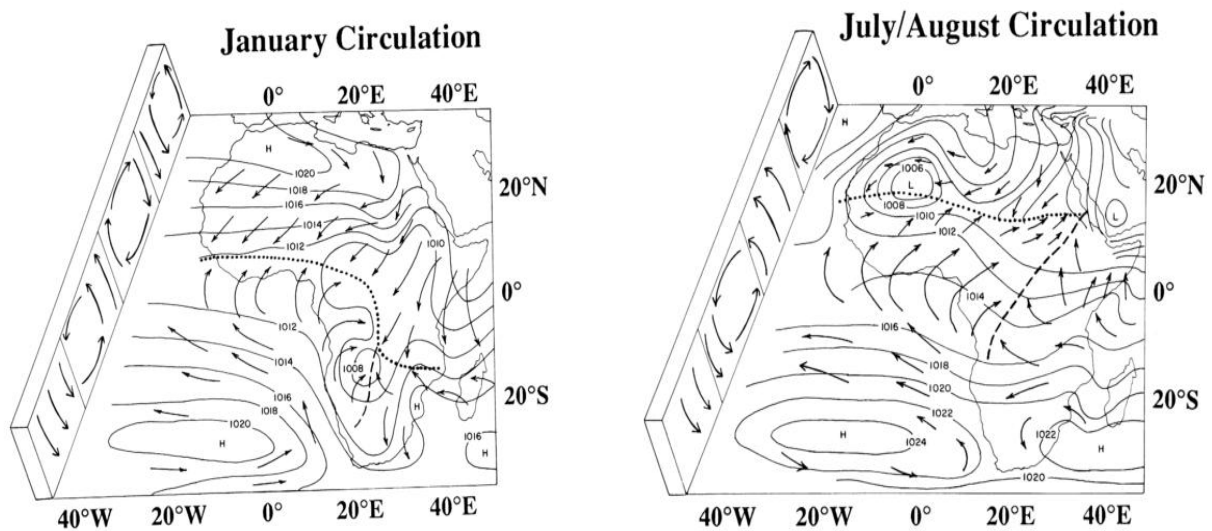


Figure 2.3 Circulation patterns and convergence over Africa, dotted lines show the ITCZ, dashed lines show other convergences (source: Nicholson, 1996).

The high coefficients of variation (>20%) in rainfall and runoff in most of the major rivers in Africa have been attributed to the high temporal and spatial variability in climate (Sutcliffe and Knott, 1987; Conway, 2002; Hamandawana, 2007). Hoerling et al. (2006) studied the 1950-1999 rainfall trends over Africa and concluded that fluctuations in SSTs and global atmospheric interactions were a major contributor to the dry conditions that had been experienced in the continent, in addition to the influence of the ITCZ. The dry conditions in the Sahel in the late twentieth century were reported to be associated with the warming of the South Atlantic Sea Surface Temperatures (Lamb, 1978; Folland et al., 1986) whereas the dry conditions in Southern Africa during 1950-1999 were attributed to the warming of the Indian Ocean.

2.4 Variability and water resources in southern Africa

Southern Africa lies between the South Atlantic and the Indian Ocean subtropical high-pressure cells. The region is subjected to the interaction of tropical easterly and westerly wind patterns that arise from outside the tropics. Most of the rainfall in the region originates from evaporation over the Indian Ocean, as well as wind systems originating from outside the region. Figure 2.4 shows the variation of rainfall in southern Africa. The influence of the ITCZ is largely centred between mid-Tanzania and southern Zimbabwe.

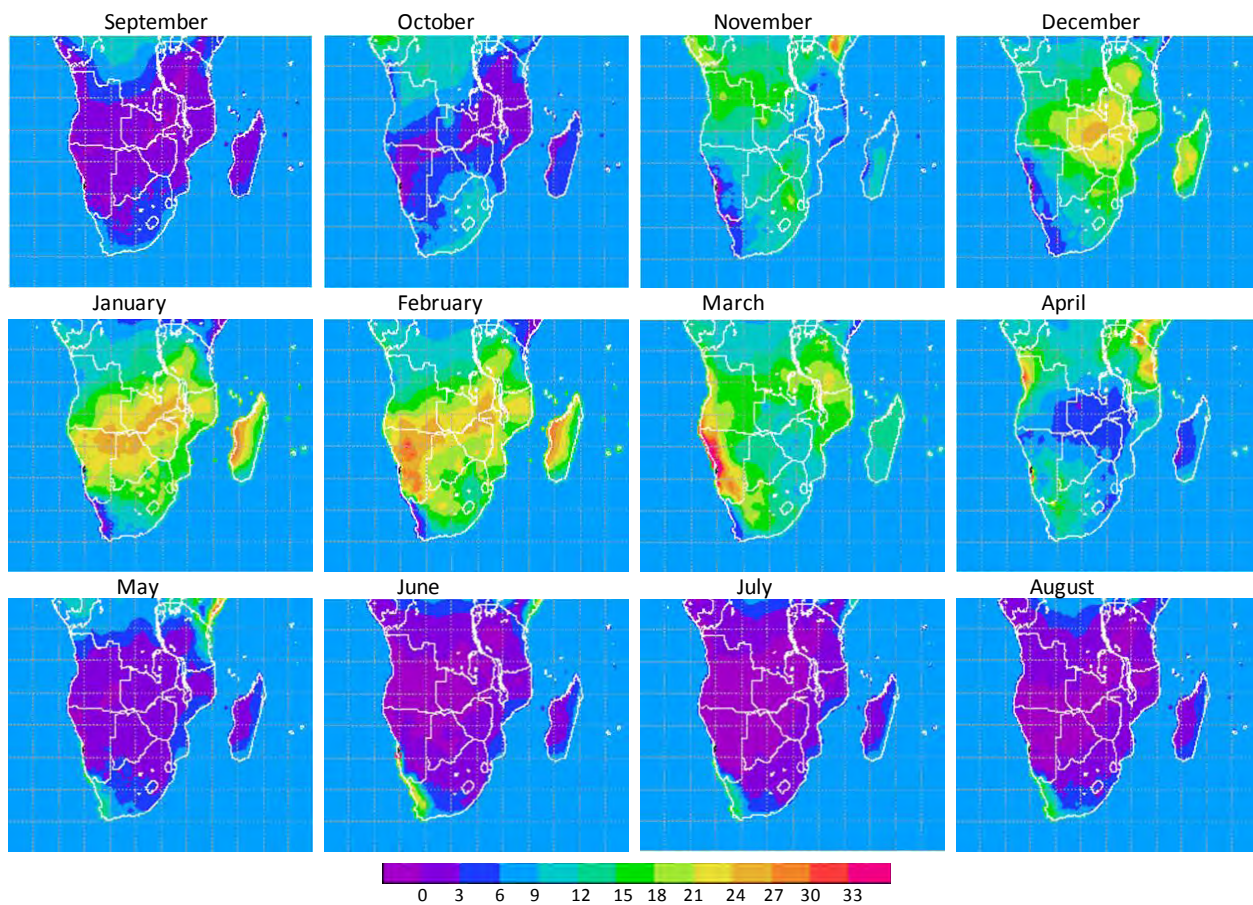


Figure 2.4 Average monthly rainfall totals expressed as percentages of the respective long-term means (modified from Engelbrecht, 2005)

Other rain bearing systems that influence rainfall variability in the region include; the tropical temperate troughs (TTTs, Todd and Washington, 1999) which are linked to the intense rainfall

that occurs from December to February, localised cyclonic flows found in the Mozambican channel between December and January and normally give rise to intense rainfall events and floods in Mozambique, the Angolan heat low which is also responsible for a cyclonic flow from the tropical Atlantic Ocean and brings convective rainfall to some parts of Angola, Namibia, Botswana, Tanzania, Zambia and Zimbabwe (Valimba, 2004). Another system, the Botswana Upper High, a middle level atmospheric condition of a high pressure cell that is usually centred over Botswana is known to push the ITCZ away in the northwards direction thereby causing periods of drought in the country (SARDC, 2008). Rainfall variability is also influenced by SSTs of the Indian, Pacific and Atlantic Oceans. The Indian Ocean is responsible for most of the moisture that prevails over the region and it is linked to the decadal variability that has been observed in the past (Reason and Mulenga, 1999). Tyson (1986) attributes the cyclic pattern of hydrological events that occurred in southern Africa in the past to short term feedback processes in the climate system and to the cyclic behaviour of the Southern Oscillation.

Through global teleconnections, ENSO events derived from the Pacific Ocean have a spatial and temporal influence on rainfall. However, different areas respond differently to ENSO, for example, when warm ENSO (Niño) events occur in the north east (e.g. Tanzania), the rest of the region is under the influence of cold ENSO (Niña) events and vice versa. Folland et al. (1986) demonstrated a strong correlation between SST anomalies and wet and dry conditions in Africa. Warm ENSO events are associated with low rainfall while the cold events bring in more rainfall (Richard et al, 2001). ENSO can be responsible for severe floods that are preceded by heavy rains as well as drought conditions in the region (Glanz et al., 1991; Thiaw et al., 1999). The severe droughts of 1967-73, 1981-83, 1986-87, 1991-92, 1993-95 and 1999-2000 are attributed to ENSO and floods that devastated Mozambique in 1999-2000 were a result of Cyclone Eline (Chenje and Johnson, 1996; WMO, 2000; National Drought Mitigation Center, 2000). From the Atlantic Ocean, the Benguela Niño produces some unusually warm waters within the Angola-Benguela Front. These warm conditions have been associated with increased rainfall along the adjacent coast line (Rouault et al., 2003). SSTs from the South Atlantic Ocean have generally been found to influence rainfall variations in the basin and significant correlations have been found between the SSTs and rainfall in various parts of the basin (e.g. Richard et al., 2001; Phillipon et al., 2002).

2.5 Extreme drought events

Drought is a natural climatic hazard which may cause a lot of human and environmental suffering. It is a temporary event which occurs largely as a result of insufficient precipitation during a given season and which may result in huge economic losses. Some regions, such as southern Africa, are already prone to droughts by virtue of inherent climatic variability and these drought events may be intensified by climate change thereby worsening the suffering of vulnerable communities. Compared to natural floods, droughts develop slowly, they creep in with time and can only be recognized once people and the environment start to feel their impact (Vicente-Serrano and Lopez-Moreno, 2005). Droughts are widespread in nature and thus can significantly impact the socio-economic status of an entire region (Sharma et al., 2009). Although it is difficult to avoid droughts, their impacts can be averted through an understanding of their nature and occurrence. It is therefore important that droughts are defined and quantified (Smakhtin and Hughes, 2004) in order to develop appropriate monitoring and mitigation strategies and policies.

Defining a drought is complicated by the fact that droughts are spatially and temporally variable, region-specific, context-dependent, and because they also occur with varying degrees of intensity, whilst their cumulative effect makes it difficult to identify their start and end (Quiring and Papakryiakou, 2003). Many conceptual definitions based on specific areas of interest and applications have been attached to droughts (Palmer, 1965; 1968). A simplified definition of drought is that, it is a recurrent and natural climatic event caused by a deficiency in precipitation compared to the long-term average rainfall (Kundzewicz, 1997; Pandey *et al.*, 2007). Because of their specific nature, and the time scale over which precipitation deficits prevail, droughts have been grouped into three main categories, namely; meteorological, agricultural and hydrological (streamflow), (Wilhite and Glantz, 1985; Heim, 2002). The difference is in the timescales of occurrence of the drought which are <3 months, 3 to 6 months and >12 months respectively. However, it should also be borne in mind that the different types of droughts can also be related to the impacts. A meteorological drought shows a prolonged departure of precipitation from the normal conditions, mainly in the form of moisture deficiency. If the dry conditions continue, the moisture deficit is propagated through the hydrological cycle giving rise to different types of drought. An agricultural drought is a result of the deficiency in soil moisture for a particular crop

at a particular time, and usually sets in when the available soil moisture has fallen to such a level that crop yield and agricultural production are reduced, this situation may be worsened by high rates of evaporation. Subsequent reductions in groundwater and streamflow may lead to hydrological droughts (Thomas, 1965; Panu and Sharma, 2002). Figure 2.5 illustrates the connection between the different types of droughts.

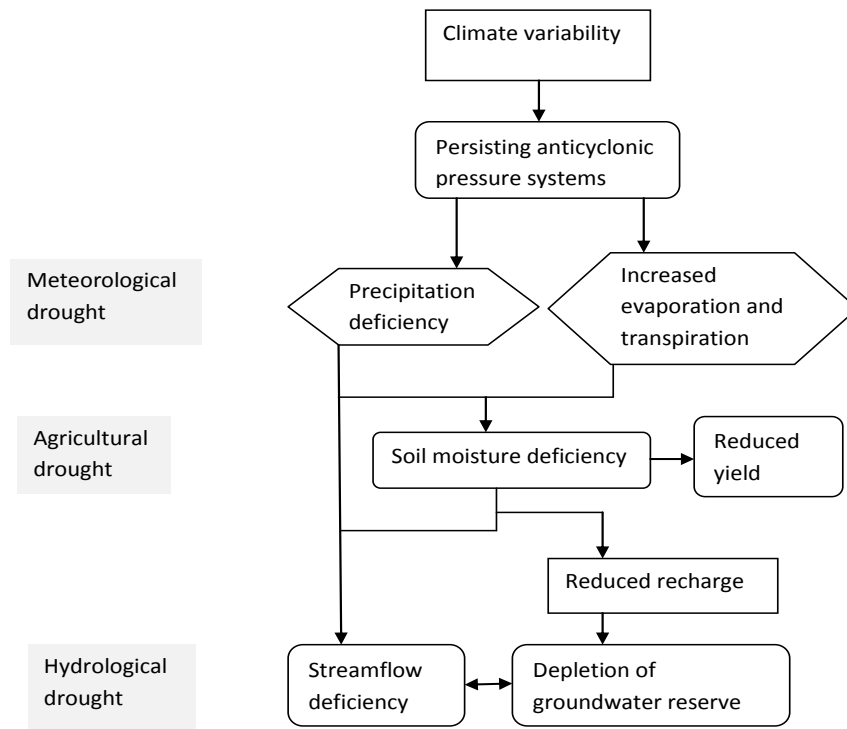


Figure 2.5 Propagation of drought (modified from Tallaksen and Van Lanen, 2004)

Soil moisture is a significant hydrological variable related to droughts and as indicated in Figure 2.5, it is the main link between meteorological drought and hydrological drought and it is the media by which rainfall is converted into runoff and groundwater storage (Tang and Piechota, 2009). Soil moisture deficit results in more infiltration and little runoff after precipitation whereas high soil moisture storage results in increased overland runoff and groundwater infiltration. High soil moisture also promotes plant growth while at the same it causes high evapotranspiration rates especially in summer. Keyantash and Dracup (2002) noted that soil moisture could be used as an indicator for agricultural potential and available water storage and it could also be used to reflect on the recent precipitation and antecedent conditions.

Monitoring Droughts

Droughts are regarded as non-events since it is impossible to determine with any precision their onset and their cessation. Nonetheless, it is possible to assess a drought with some degree of precision once it has started. Appropriate and timely interventions to the devastating impacts of droughts call for monitoring tools that are able to identify the intensity, duration and spatial extent of droughts. Drought indices are therefore used as the operational definitions for droughts. Droughts are treated as normally distributed continuous functions of hydro-meteorological variables such as rainfall, runoff, or temperature (Krasovskaia and Gottschalk, 1995). A number of drought indices are in place for monitoring droughts, each with its own advantages and limitations in terms of application. Among them are the Standardised Precipitation Index (SPI); Palmer Drought Severity Index (PDSI); the Crop Moisture Index (CMI); the Effective Drought Index (EDI); the Surface Water Supply Index (SWSI); Deciles, the Percent of Normal Index (PON) and a host of others. A detailed description of these indices is given in Smakhtin and Hughes (2004).

The Palmer Drought Severity Index (PDSI), (Palmer, 1965; Guttman, 1998) is one of the most common drought indices that have been widely used in the United States. It is based on anomalies in the supply and demand concept of the water balance equation. Input data include precipitation, temperature, and local antecedent soil moisture conditions. To account for regional differences, the input data are standardised so that it is possible to make comparisons of the index at different locations, irrespective of the differences in the amount of rainfall at the different locations. The PDSI is, however, limited in use as a drought monitoring tool and should be used with caution, especially given the fact that it was developed specifically for the United States (Kogan, 1995). Some of the limitations of PDSI include the fact that the index is exclusive to monitoring agricultural droughts and it cannot adequately address long-term hydrological droughts. With this index, runoff is underestimated due the fact that the natural lag between rainfall and runoff is not considered. The index responds slowly to developing drought conditions such that drought conditions may still reflect even after the conditions have improved. Moreover, a considerable amount of meteorological data is required and the computation of the index is complex (Hayes et al., 1999; Smakhtin and Hughes, 2004).

The Standardised Precipitation Index (SPI), (McKee et al., 1993) was developed in an attempt to address some of the limitations of PDSI and other drought indices. The SPI gives a good and reliable estimate of the magnitude, intensity and spatial extent of droughts; it is the number of standard deviations by which the observed precipitation deviates from the long-term mean for a normally distributed random variable. It is not a drought prediction tool, but can be used to define and monitor droughts. The index captures the severity of dry and wet spells and quantifies the precipitation anomalies as a single numeric value. When precipitation is above the mean value, then SPI is positive and if precipitation falls below the mean value, the SPI is negative. Unlike other drought indices, SPI is less cumbersome to use because it only requires a single input data series of long term precipitation (Smakhtin and Hughes, 2004). The fundamental strength of SPI over other indices is its versatility of use at different time scales (3, 6, 12 and 24 months) and thus, various types of drought can be monitored (meteorological, agricultural and hydrological). Because it is based on normalised data, the SPI is spatially invariant and droughts can be used in different regions (Guttman, 1998).

The SPI has been widely used in different regions of the world. Manatsa et al. (2010) used the SPI to analyse different aspects of agricultural droughts in Zimbabwe, while Rouault and Richard (2003) examined the intensity and spatial extent of droughts in South Africa using SPI. Bordi et al. (2001a; b) used the SPI as a tool to reconstruct historical drought events at regional and large scales in Italy. Vicente-Serrano (2006) analysed the spatial drought patterns in Europe, and, in India, Sharma et al. (2009) monitored drought using the SPI. Giddings and Soto (2005) derived SPI zones for Mexico. Hayes et al. (1999) demonstrated that the SPI can be used operationally as a regional drought watch system in the United States; in their results the SPI was able to identify the onset and severity of the 1996 drought in the United States at least a month ahead of the PDSI. However, the SPI has its own drawbacks that must be considered when it is used. The quality of the SPI result can only be as good as the input data (Tirivarambo and Hughes, 2011), therefore, in data scarce areas, such as in Africa, the SPI result may be fraught with inconsistencies and this introduces some uncertainties in the mitigation process. Because of the nature of a normal distribution, the SPI gives severe and extreme droughts as occurring at the same frequency in different spatial locations over a long period; it is not able to distinguish those areas that are more prone to droughts from those that are not (Hayes et al. 1999).

2.6 Climate change and water resources

Climate change is one of the most important environmental issues facing the world today. The United Nations Framework Convention on Climate Change (UN, 1992) states that climate change is a direct and indirect consequence of human activities that alter the global atmosphere and it adds to the natural climate variability observed over long time periods. With technological advancement, humans have improved their lifestyles and they have tended to demand more of improved services such as transportation, industry and energy. Agriculture and urbanisation have increased likewise. These human-induced services and activities alter the composition of the global climate system by emitting excessive amounts of greenhouse gases that cause additional warming of the global climate (Karl and Trenberth, 2003) and consequently, a shift in the water balance of the hydrological cycle. The processes that drive climate change, its characteristics and threats are summarised in Figure 2.6.

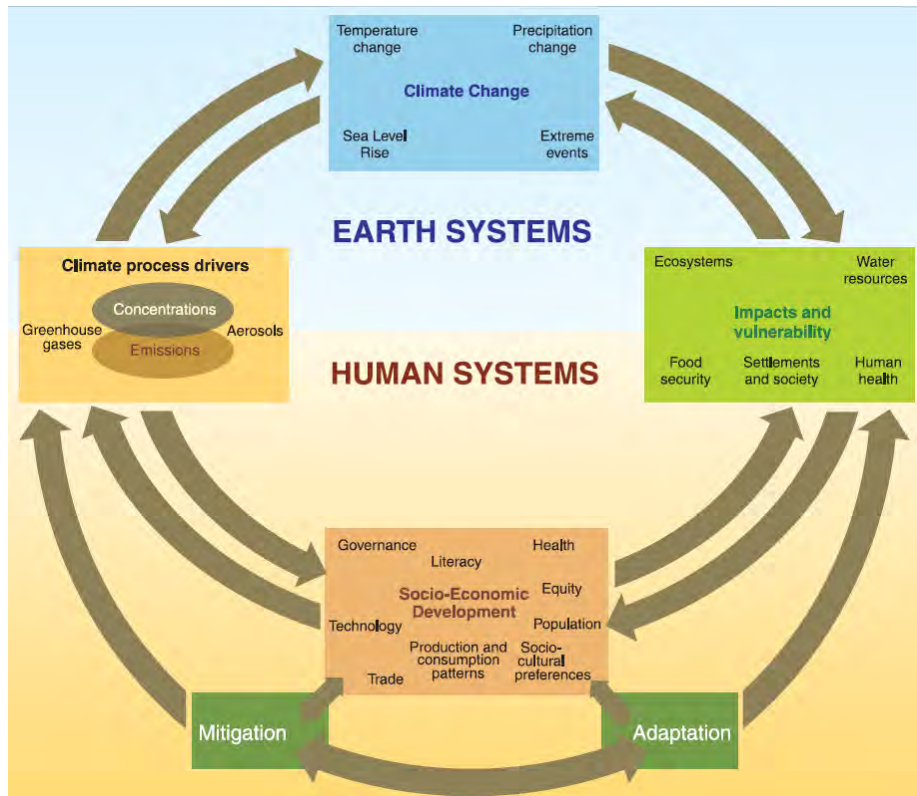


Figure 2.6 Schematic of climatic impacts and responses to anthropogenic drivers and their linkages (source: IPCC, 2007)

It is projected that a warming climate will provide more energy to accelerate and intensify the hydrological cycle, and in uncertain ways, the frequency and timing of flood and drought events may be altered (Nijssen et al., 2001; Milly et al., 2002; Scott et al., 2004). In considering global water resources, it remains quite difficult to attribute change in events such as precipitation and droughts to climate change in isolation of natural variability because both factors interact and contribute towards the development of such events (Allen and Ingram, 2000). Determining the impacts of climate change on water resources is also made difficult by the availability of short hydrological records, direct human influences and the effects of catchment physical properties (Nemec and Schaake 1982). A number of studies have been carried out worldwide to assess the effect of greenhouse gas concentrations (particularly CO₂) on future precipitation and temperatures. So far the assessment of climate change impacts has relied on the use of Global Atmospheric General Circulation Models (GCMs).

2.6.1 General Circulation Models (GCMs)

GCMs are dynamic three dimensional representations of the processes occurring in the atmosphere, on the land surface and on oceans and seas (Jacob and van der Hurk, 2009). Based on coupled land-atmosphere-ocean interactions, and through the use of well known physical principles and different parameterisations, GCMs simulate the response of the earth's climate system to the current and future greenhouse gas concentrations (Xu, 1999a; Christensen et al., 2007). The effect of manmade activities on the global climate system has been transformed or represented through green house concentrations and to date much of the work on climate impact assessment has been carried out by the IPCC (Solomon et al., 2007). When used as input forcing to hydrological models, the GCM predicted climate signal can be transformed into hydrological variables at regional and local scales and this renders the GCMs important as one of the precursors to impact assessments.

Emission Scenarios: Quantifying the global impacts of climate change in the future is bound to encounter some uncertainties mainly due to the fact that we hardly know how the climate is going to be like in the future, and if the climate does change we are not sure exactly by how much the change will be and whether it will be a positive or negative change. It would seem that no methods are yet in place to provide reliable estimations of the changing climate. Climate

scenarios have thus been used as a means of assessing the sensitivity of the global system to climatic changes. It should be noted, however, that emission scenarios are not necessarily used as predictors of climate change but serve to explore the uncertainties emanating from lack of an indepth understanding of the impacts of future developments on the complex global climatic processes (Parry and Carter, 1998). Currently a set of emission scenarios has been published by the Intergovernmental Panel on Climate Change and are found in the Special Report on Emission Scenarios (SRES, Nakićenović and Swart, 2000). Four groups of scenarios with different story lines (Figure 2.7), derived from assumed key drivers of emissions (socioeconomic development, demographic and technological change), are in use and these are: A₁ and B₁, whose focal point is on globalisation and which project a future in which regions are almost the same; A₂ and B₂, focussing on regional, local socio-economic, and environmental development in different regions in the future (Van Vuuren and O’Neill, 2006). These scenarios are transformed into greenhouse gas concentrations which are then used to project the climatic responses within the GCMs (Giorgi, 2005). It should, however, be noted that due to uncertainty, the use of a single climate change scenario may be inadequate, particularly in view of formulating the appropriate responses to adaptation and mitigation (Hulme and Brown, 1998; New et al., 2000).

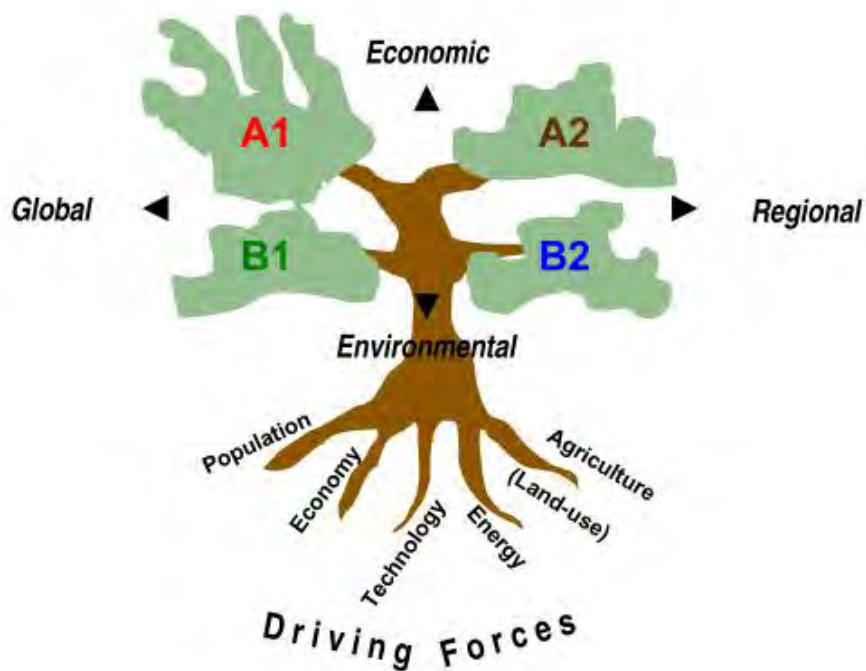


Figure 2.7 The four IPCC SRES scenarios (source: Nakićenović et al., 2000)

2.6.2 Downscaling

GCMs are the most widely used tool in the prediction of climate change to date and they are capable of reasonably good predictions at continental and hemispherical scales. However, GCMs have a coarse spatial resolution (~ 100s of km or 2.5° grid cells), which falls short of adequately representing the climate dynamics at local scales (Carter et al., 1994; Salathe, 2003), yet, societal problems (e.g. water resources) and most of the water management decisions (policy, technical or infrastructural) are region-specific (Zhang et al., 2007). To circumvent the scale problem, which in a way is a form of GCM uncertainty, regionalisation or downscaling methods (Giorgi and Means, 1991) have been employed, which involve taking coarse resolution GCM outputs and transforming them to a local scale, i.e. “bringing them down to earth” (Jones et al., 2005). Downscaling methods have proven a good remedy for doing away with the scale disparities between the large scale GCM projections and the finer scale regional or local response units (Giorgi et al., 2001; Wilby, 2007). Two basic approaches to downscaling have been used, namely, statistical downscaling, and dynamical downscaling.

Statistical downscaling: Statistical downscaling (Hewitson and Crane, 1996; Fowler et al., 2007) relies on an observed relationship between the large scale global climatic processes and the quantities of locally observed climatic variables, such as temperature and precipitation. The relationship is then merged onto the GCM output to generate the localised or regionalised climate change signals. Statistical downscaling has been widely used in Africa compared to dynamical downscaling (e.g. Brown et al., 2008; Conway and Hulme, 1996; Yates and Strzepek, 1998; Hewittson and Crane (2006). It is a better option than dynamical downscaling in situations where low cost and rapid assessments of climate change impacts are required (Wilby et al., 2002). The method is also preferred in instances where estimation of variables at point locations is required for model input or for decision making purposes. However, statistical downscaling has a major drawback in that it uses the principle of stationarity in which there is invariance of the stochastic parameters, even under a changed climate, which may, in fact, cease to hold if the climate does change (Xu, 1999; Jacob and van der Hurk, 2009).

Dynamical downscaling: In dynamical downscaling, a fine-scale regional climate model which provides more detailed physiographic information is nested into a coarse resolution GCM

(Cubasch et al., 1995; Jones et al., 1995) as shown in Figure 2.8. The aim is to extract local scale information from the large scale information that is contained in the GCMs. Lateral boundary conditions and sea surface temperatures from the GCM are forced onto a regional climate model (RCM), or a limited-area model (LAM). High resolution regional climate models simulate climate features dynamically at finer scales (10–50 km or $\sim 0.5^\circ$ latitude and longitude), using the temporal variation of atmospheric conditions at the boundary of a specified domain. GCM simulated variables, such as surface pressure, wind, temperature and vapour are superimposed at various levels onto the boundary of the RCM at different vertical and horizontal levels (Xu, 1999; Wilby, 2007). The RCM then manipulates the information so that the model, through its algorithms, generates patterns of climate change differing from those of the ‘host’ GCM.

Dynamic downscaling has an advantage over statistical downscaling in that it places more emphasis on local feedback processes and there is a coherent downscaling of the variables, unlike in the statistical method where there is an independent relationship between the observed and simulated variables. In dynamical downscaling, topographic features, including land use and vegetation, are well incorporated (Brown et al., 2008). However, one major drawback is that this method is computationally and resource intensive and it is quite laborious and almost impossible to carry out multi-decadal simulations with different GCMs, or multiple emission scenarios. Also, the output from dynamical downscaling is sensitive to the choice of the initial conditions (Wilby, 2000). The limitations of dynamical downscaling have been widely discussed in the literature (e.g. Wilby and Wigley, 1997; Murphy, 2000; Hay and Clark, 2003; Christensen et al., 2004; Wood et al., 2004; Fowler and Kilsby, 2007). Some researchers, for example, Brown et al. (2008), have reported that it is easier and more efficient to work with statistical downscaling than with dynamical downscaling. Although the scale issue is resolved through downscaling, uncertainty still abounds in the downscaling activity, starting from the choice and nature of the GCM and extending to lack of knowledge as to what the local level impacts of climate change are likely to be (Wilby, 2007).

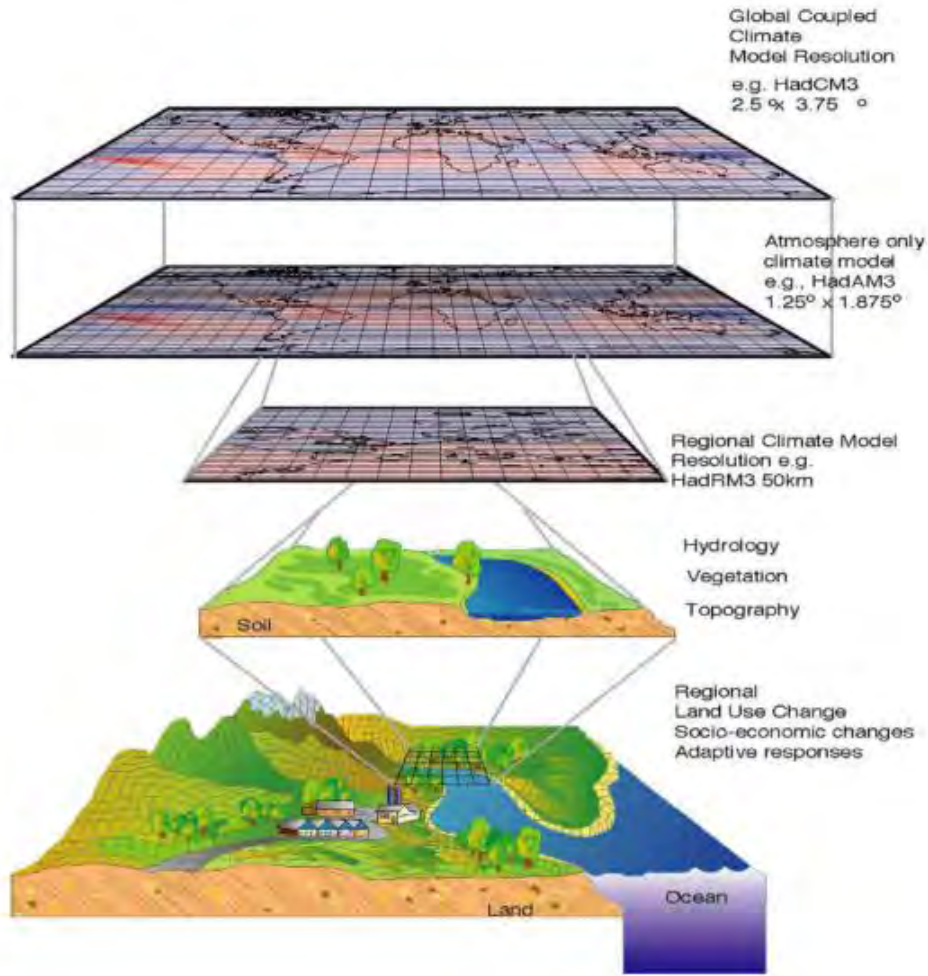


Figure 2.8 Dynamical downscaling (source: World Climate Programme, 2007)

2.6.3 Observed trends in global temperature and precipitation

Changes in global temperature: Throughout the history of the earth, the global climate has changed considerably due to a change in its driving forces (land-ocean-atmosphere interactions). However, according to the IPCC (2001b), the rate of change in climate during the 20th century was more than in the previous years. It is indicated that there has been a trend of significant changes in climatic variables across the globe and that these changes are likely to amplify historical climate variability and to increase the extent, intensity and frequency of occurrence of extreme flood and drought events in the future. For example average global surface temperatures increased by 0.6°C during the past 100 years, and these changes are attributed to human-induced climate change. Using a linear trend for the global surface temperatures, Trenberth et al. (2007) also report that the temperatures increased by 0.74°C (confidence interval 0.56-0.92) between the

periods 1850 to 2005. Figure 2.9 shows that the rate of change of temperature increased markedly since 1955, with a bigger margin for the 25 years starting 1981. Webster et al. (2005) also observed that during the last half of the 20th century, sea surface temperatures increased by 0.25-0.5°C and this led to an average rise in global mean sea levels of 1.8 mm per year (IPCC, 2007). Although solar radiation is the main driver of climate, some studies (e.g. Lockwood and Frohlich, 2007; 2008) concur that changes in temperature after 1985 were largely due to anthropogenic activities that increased the atmospheric greenhouse gas concentration.

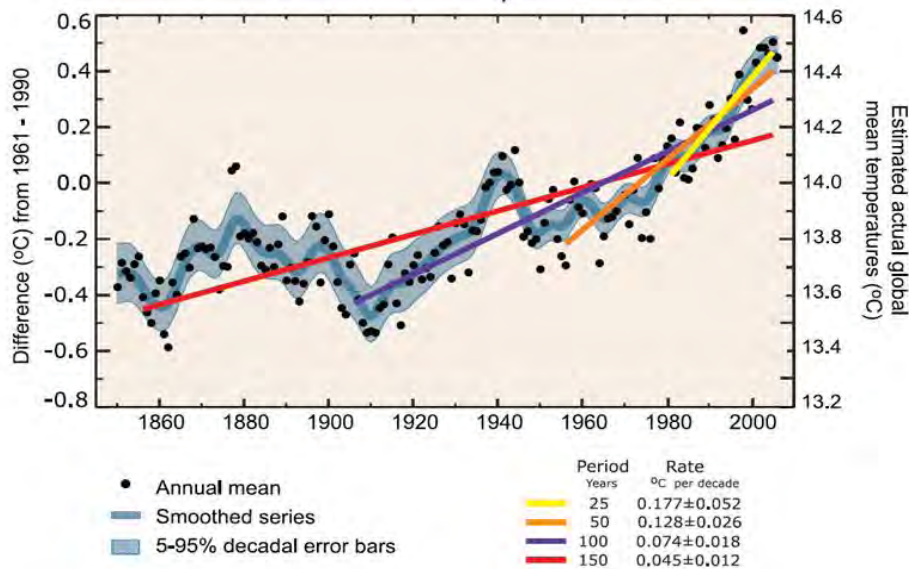


Figure 2.9 Global annual mean temperature with linear trend lines for the 1981-2005, 1956-2005, 1906-2005, and 1856-2005 (source: Trenberth et al., 2007)

Observed trends in global precipitation: Although widely varying in space and time, global precipitation has shown a rising trend since the beginning of the 20th century, and has risen by 2% since then (IPCC, 2001b). In spite of the irregular trends in precipitation during the period 1901 to 2005, there was a significant increase in precipitation over North and South America, northern Europe and northern and central Asia, while reduced precipitation was observed over the Mediterranean, southern Africa and in some areas of southern Asia (Trenberth et al., 2007). The same observations also indicate that drought periods have been on the rise since the 1970s especially in the tropical regions of the world.

2.7 Impacts of climate variability and climate change in the Zambezi basin

About 70% of the population in the Zambezi basin survives on rainfed subsistence agriculture, at the same time, agriculture contributes about 35% of the basin's GDP (UNEP, 2006). Almost a third of the basin population lives in drought-prone areas and is vulnerable to impacts of droughts (Pandey et al., 2007). Out of the total hydroelectricity generated in the region, about 75% comes from the Zambezi River (Euroconsult, 2007; Flint, 2006). Given the fact the basin's climate is already highly variable; climate change could add more pressure on the water resources. At the same time, increased uncertainty and shifting crop water requirements caused by possible changes in the timing and distribution of rainfall events will adversely impact agricultural productivity, food security and hydroelectricity generation in the Zambezi basin. Some previous studies have been conducted to investigate the effect of climate variability and climate change in the Zambezi basin. Farquharson and Sutcliffe (1998), Jury and Gwanzantini (2002), Kampata et al. (2008) and Mazvimavi (2010) investigated the trends in rainfall and streamflows during the past century and concluded that the trends were insignificant and that the basin's hydrological resources were sensitive to interannual variations in climate. The most critical impacts of climate variability in the basin have been felt through droughts, floods and cyclones.

Evidence of climate variability in the basin during the past century is shown through the significant variations in rainfall and lake levels of Lake Malawi (Figure 2.9, Calder et al., 1995), in flow variations at Victoria Falls (Mazvimavi and Wolski, 2006) and in changes in mean and extreme precipitation over southern Africa (Shongwe et al., 2009). A series of droughts between 1981 and 1992 resulted in the water level of Lake Kariba dropping by 11.6m, which had a severe impact on the dam's capacity to generate electricity (SADC, 2007). ENSO is cited as the major cause of the severe flood and drought events that have occurred in the basin (Thiaw et al., 1999, SARDC, 2010). Some of the recent extreme events that are linked to ENSO include; the severe droughts of 1946/47, 1965/66, 1972/73, 1982/83, 1986/87, 1991/92, 1993/94 and 2001/2002, 2004/5 and 2007. Floods have also occurred in 1957/58, 2000, 2003, 2006/2007, 2007/2008 and these floods have been linked to cyclonic events, for example, the Cyclone Eline induced floods of 1999-2000 that caused a lot of damage in Mozambique (Chenje and Johnson, 1994; WMO, 2000). Droughts have also imposed severe impacts on the region's food security, following the

1994/95 drought, the region experienced a 35% decline in cereal harvests and a 42% reduction in maize yields compared to the previous season (SADC, 1996).

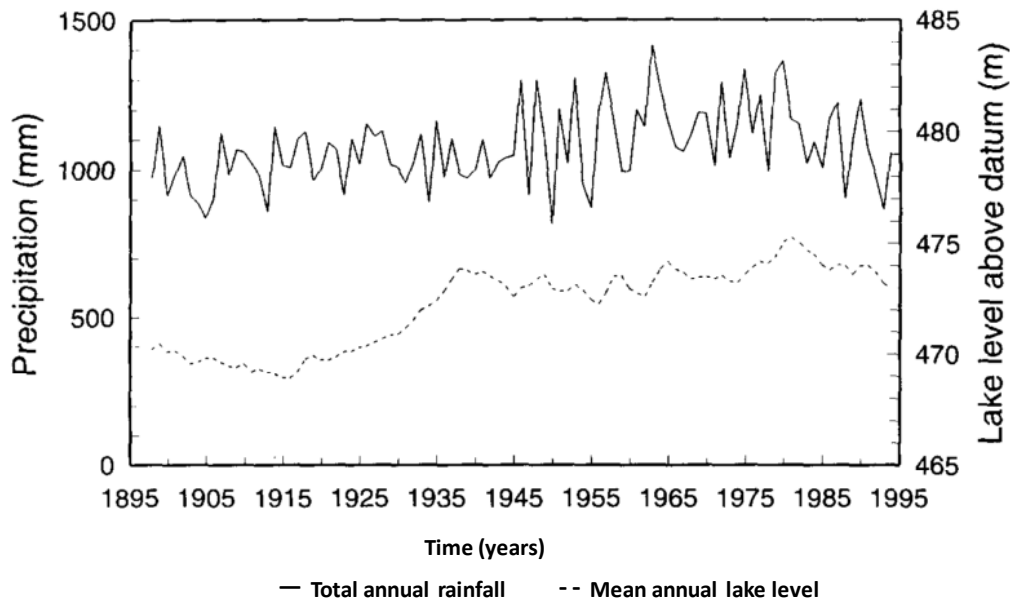


Figure 2.10 Annual rainfall and lake levels for Lake Malawi for the period 1896-1994. (source: Calder et al., 1995).

2.8 Application of models in water resources management

Worldwide there is an ever increasing demand for reliable water supplies for domestic, agricultural and industrial uses. As economies develop changes occur in lifestyles which have resulted in people demanding more water as they improve their standards of living, and as populations grow water resources are put under more pressure. In addition there has been an increased demand from the ecological community for hydrological regimes that can sustain a healthy and diverse ecosystem and where possible minimize the occurrence of floods and droughts (Loucks et al., 2005). Hydropower which happens to be one of the major sources of energy in most parts of the world also requires that certain critical water levels be maintained in the reservoirs. All these demands which often are in conflict with each other are a responsibility of and a challenge to the water manager who has to ensure that ecological, social and economic values are preserved in the decision making processes (Jakeman and Letcher, 2003). More threats are imposed on the water management process due to uncertainties in the availability of water supplies resulting from climatic variability, climate change and land use changes. The

question of how, when and by how much continues to haunt water managers as they try to manage and integrate the water resource systems under conditions of uncertainty and as they attempt to build confidence in the decisions that they make for the future management of water resources (Loucks et al., 2005). For example, if projects are developed too early resources may be wasted if these projects are not utilized until later. At the same time if the projects are developed at a later stage there may be risks of water shortages in the event that the climatic conditions suddenly turn out to be drier than expected.

A variety of approaches which range from the traditional to the modern day technology-based approaches are available to assist the water manager in making decisions. The traditional methods are based on what the decision makers believe, or expect to happen and are largely guided by the principle of stationarity (Mearns et al., 2010), whereby, the past climatic conditions and their statistics are postulated to remain the same and where variability is not expected to increase in the future, this method is largely qualitative in nature. However, this principle is now challenged by the potential for changes and uncertainties in the future climates and focus has shifted to a range of dynamic climates which can also be quantitatively assessed through models (Lempert and Collins, 2007). This has been made possible by improved model development and increased availability of spatial databases. To formulate a comprehensive decision making plan in view of climate change, Lempert et al. (2006) suggested a robust decision making framework which incorporates both the traditional methods and model optimization. It was also recognised by many in the scientific field (e.g. Lam and Swayne, 1993) that the plethora of problems facing the decision making process in managing water resources required an extensive set of decision support systems that could support a number of possible future outcomes and that could integrate various aspects such as changes in land uses, water quality and quantity as well as changes in demand as necessitated by socio-economic shifts. Computer based decision support systems with tools that represent the various capabilities as required for the integrated management of water resources are now in common use.

2.8.1 Decision support systems in water resources management

A model can generally be defined as a simplified representation of the real world system; it consists of algorithms embedded in a computer program and of parameters representing

properties that remain constant under certain conditions (Hesse et al., 2008; Wheater, 2008). When the models are put into computer code, their underlying assumptions become more explicit and an environment is created for integrating different types of models (Jakeman and Letcher, 2003), for example a runoff simulation model can be linked to a water yield model. When these models are embedded in computer software programmes it is possible to run a variety of water resource scenarios and to assess and quantify the outcomes which can then be used for decision making, thus creating a decision support system. An illustration of the common components of a support system is given in Figure 2.11. Reynolds et al. (1996) describe decision support systems as having an interactive modelling interface which allows easy data entry and control of the model operations while at the same time providing spatial display functionalities. On the other hand, Jewitt and Gorgens (2000) describe decision support systems as software systems that enable integrated management through the incorporation of three forms of information/processes which include; information on the state of the environment or the catchment, modelling of the system and evaluating outcomes or plans. Parker et al. (2002) also describe five basic models that can be integrated into a decision support system as:

- i. data models that are representative of measurements and experiments
- ii. qualitative conceptual models that describe the verbal or visual interpretation of systems and processes
- iii. quantitative numerical models that represent the qualitative models
- iv. mathematical descriptions and models that are used to analyse and interpret the outcome of the quantitative models and
- v. decision making models that transform the results and knowledge gained into action.

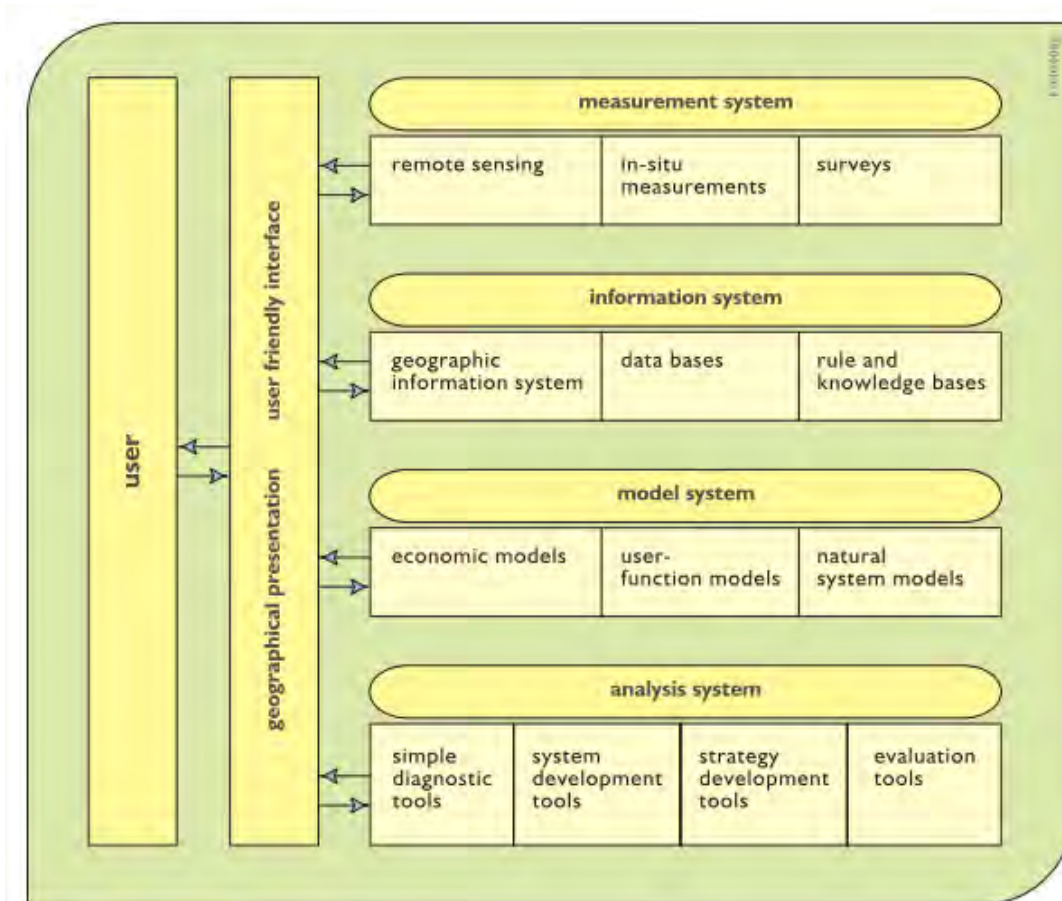


Figure 2.11 Common components of a decision support system (source: Loucks et al., 2005)

2.8.2 Types of water resource systems for decision making

A number of models are now available for decision support in water resources management. These models make it possible for decision makers to assess, in an integrated manner, the use and management of water resources (Jakeman and Letcher, 2003). The most common model classes (Cap-Net, 2009) include:

- hydrological models which mainly focus on quantifying and understanding how water flows through a catchment in response to hydrological perturbations, they attempt to capture the most important land-atmosphere interactions of the hydrological cycle.
- hydrodynamic models that can simulate river channel dynamics such as the flood inundation extent and water levels.
- water yield or water resource management models which assess the long term water resources yield based on some operation rules and also allocate the available water .

The Soil Water Assessment Tool, SWAT (Arnold et al., 1998) is among the common hydrological simulation models. SWAT consists of modules that simulate, among other things, rainfall-run-off processes, irrigated agriculture processes, and point and non-point watershed dynamics. The MIKE SHE hydrological model developed by the Danish Hydraulic Institute (DHI) is also common in simulating the major land processes of the hydrological cycle. The HEC hydrological model provided by the United States Army Corp of Engineers Hydrologic Engineering Centre is common for simulating the hydrology of dendritic catchment systems. Some of the hydrological models that simulate the surface-groundwater interactions include the HYMOS model developed by the Delft Hydraulics Laboratory and the modified Pitman Ground Water model (Pitman, 1973; Hughes et al., 2006). Examples of hydrodynamic models include the DHI products of MIKE21 and MIKE3 which can simulate the hydraulics, sedimentation and water quality in rivers. The DELFT 3D and the HEC-RAS models also fall under the category of hydrodynamic models which, from a climate change perspective can be applied in the mapping and forecasting of floods and in simulating the changes in sea level (Cap-Net, 2009). Some of the water planning and operation models include; the WEAP model (Raskin et al., 2001), RiverWare (Zagona et al., 2001), MIKE-BASIN (Danish Hydraulic Institute, 1997), RIBASIM (Delft Hydraulics, 2004) and the AQUATOOL (Andreu et al., 1991) models.

2.8.3 Software packages as decision support tools

For a model to function efficiently, it must be incorporated into a computer software package. The use of software is aimed at allowing the modeller to run the different scenarios and also provides a means of assessing, quantifying and communicating the various modelling outcomes (Loucks et al., 2005). Some of the features required of software that can handle the decision support systems (Jewitt and Gorgens, 2000) include:

- facilities for data input, editing and data visualisation
- user friendly model operation and interactive assessment of the problem
- the capability to display and analyse spatial data through geographic information systems
- provision of expert help for the user to understand how problems may be solved and what are the better options
- provision of a means of communicating and sharing the outcomes

- model reuse and integration of a number of models that may be required to solve a particular problem.

GIS is increasingly becoming a useful tool in decision support systems for water resource management. Among the most commonly used GIS tools is the Environmental Systems Research Institute's (ESRI) spatial analyst software package. These tools provide maps which show the location, spatial distribution and the linkages or relationships between the spatial objects. The information is stored in databases which are linked to the model through data access functionalities. A number of software packages are available to support water resources modelling. One such software is the Spatial Time Series and Information Modelling, SPATSIM (Hughes and Forsyth, 2006) which has been used widely in southern Africa. The GIS Viewer programme, WQ2000 (Herold, 2003) has also been used in South Africa.

2.9 Hydrological modelling

Hydrological models are simple mathematical representations of the complex and interlinked dynamic and nonlinear transformation of climate variables (e.g. precipitation, temperature and evaporation) into hydrological outputs such as runoff, soil moisture and groundwater content (Gleick, 1986; Beven, 1989; Xu, 1999; New et al., 2000). A hydrological model has also been described simply as an entity within a boundary that receives water and, together with other internally operating inputs, a net output (runoff) is produced (Killingtveit and Saelthun, 1995). In hydrological modelling, catchment scale processes which include infiltration, soil-water redistribution, evaporation, transpiration, snowmelt, surface, subsurface and groundwater flows are considered together with the process-based equations that are premised on well known scientific principles (Hesse et al., 2008; Wheater, 2008). Understanding the hydrological processes that take place within a catchment is a prerequisite in formulating a hydrological model. Figure 2.12 illustrates the steps involved in the formulation of a hydrological model. The steps start from understanding the catchment responses to hydrological input variables, schematising the hydrological processes, formulating mathematical representations of the perceived processes, and finally developing algorithms in computer programs that also encompass parameter values and constraints.

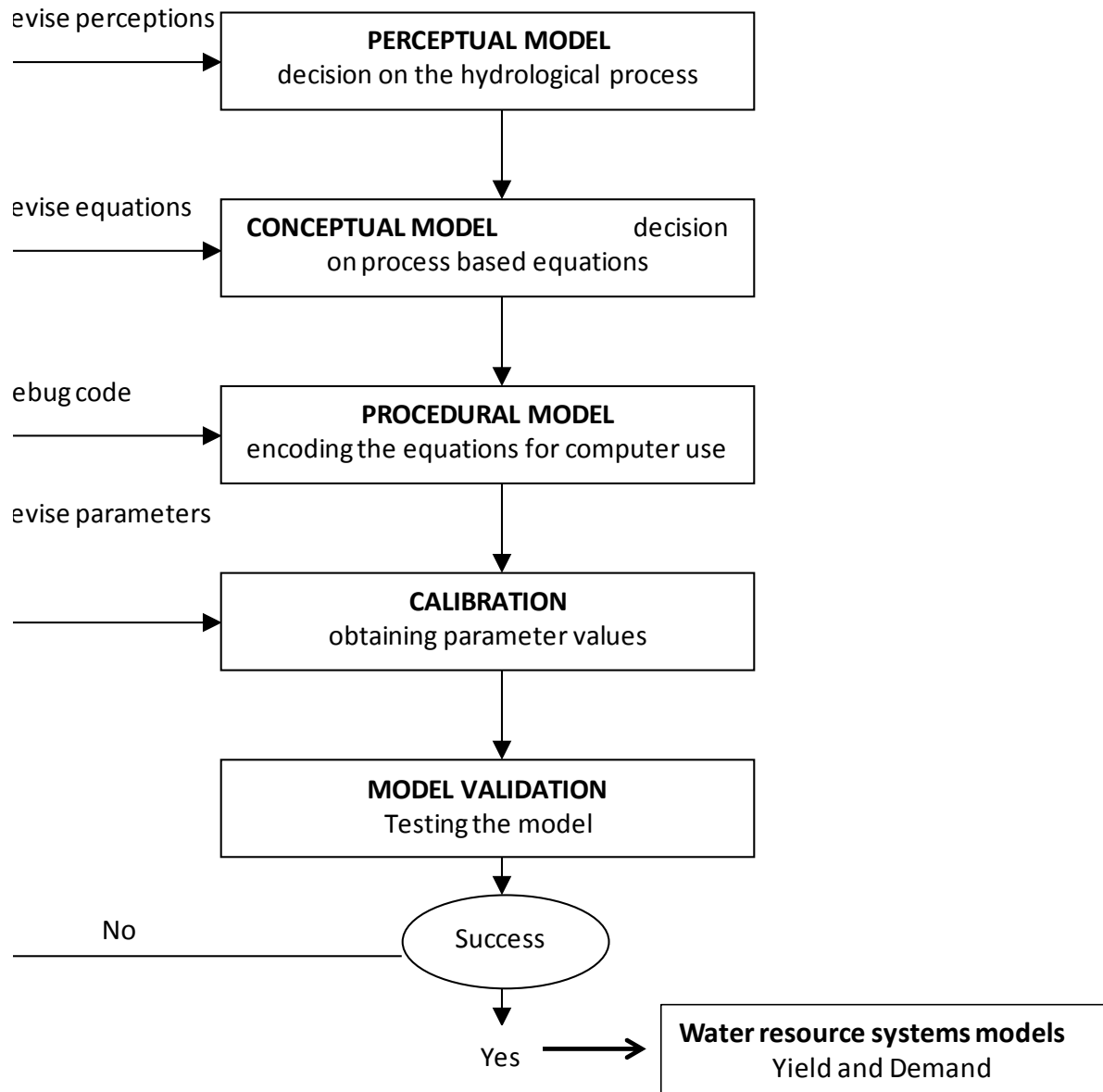


Figure 32.12 Schematic of the steps involved in the formulation of hydrological models (modified from Beven, 2005)

2.9.1 Uses of hydrological models

Hydrological models were initially developed for the purpose of assessing catchment response to different hydrological conditions (Xu and Singh, 1998) but current developmental trends have resulted in the models also being used for a variety of purposes (Xu and Singh, 2004) which include the evaluation of the spatial and temporal distribution of water supplies, assessing the hydrological impacts of climate change and land use changes, the reconstruction of a catchment's hydrological regime, generating runoff records for ungauged catchments, predicting

water resources system yield and in the derivation and classification of regions based on climate and hydrology. Because it is also impractical to obtain an adequate number of point measurements to effectively represent a catchment, hydrological models assume great importance in providing the information required for quantifying and assessing the water resources in a catchment (Hughes, 2004a).

2.9.2 Types of hydrological models

For a long time hydrological models have been used to simulate rainfall-runoff processes, initially representing a simplistic, stochastic and conceptual overview of the land processes and later on, with increased computer power, more complex physically based deterministic models were developed founded on the use of mathematical equations to represent all the basic processes involved in the conversion of rainfall to runoff (Beven and Freer, 2001; Liu and Gupta, 2007). Although complex in nature, Hughes (1995) reports that physically based deterministic models may not succeed in the predictive estimation of water resources due to among other reasons, poor model representations of the catchment processes and failure to represent spatial variability of runoff in response to rainfall. A wide range of hydrological models are now in existence, and clearly the choice of which model to use is guided by the nature and scale of the problem, catchment characteristics, and the type of data available. The level of complexity in the conceptualisations of the real world processes generally distinguishes the model types (Jewitt and Gorgens, 2000). In addition to stochastic and deterministic models, models can also be classified into discrete and continuous where discrete models are those that focus on single events, while continuous models focus on simulating long continuous time series. Models can also be referred to as lumped or distributed wherein, the lumped models assume homogeneity in basin properties of the catchment being modelled and the distributed models account for heterogeneity. In principle, the choice of a hydrological model is guided by the particular area of application, i.e. the spatio-temporal scale of the problem, the nature and objective of the problem, availability of data and the type of catchment under consideration (Wheater et al., 1993). Since there is a wide range of models it is appropriate to consider them in terms of different forms of complexity (Hughes, 2004a):

- **model complexity:** refers to how well the model can represent the catchment hydrological responses, resulting in simple models which make use of a few parameters and complex models which have a large parameter space and attempt to explicitly represent the individual catchment processes. However according to Hughes (2004a) complex models are resource intensive and time consuming since they require a large amount of data compared to simple models.

- **spatial complexity:** this category includes simple lumped models which use averaged climate variables as input data and do not consider the spatial variability over the catchment. Such models may be considered adequate for small catchments but not for large catchments which have a large variation in input parameters in space (Madsen, 2003). Complex spatially distributed models are designed to account for spatial variation in the parameters, inputs, and outputs over individual sub-catchments (Beven, 2005, Yadav et al., 2007). They are ideal for application in areas that have high climatic variability such as in Africa (Hulme et al., 2001). However, the requirement of large input parameter datasets complicates the calibration process and uncertainty can be increased (Hughes, 1995; Brown et al., 2008) if sufficient data are not available.

- **temporal complexity:** model complexity can also be expressed in terms of the time step that is used. Some models use coarser monthly time steps while some use finer time steps that can range from days to minutes (Xu and Singh, 2004)). It is always important to define the appropriate temporal and spatial scales at which the model should be run as well as discretising the model to the appropriate time steps and both scales should be such that they provide the required level of detail.

2.9.3 Parameter estimation approaches

Quantitative prediction of hydrological variables is required for operational purposes in any water resource management systems. Since hydrological models are simplified mathematical representations of the catchment scale processes, some of the parameters cannot be measured directly to provide meaningful representations of the basin properties (Winsemius et al., 2006; B'ardossy, 2007). If the parameters are not correct then they may not be useful for the quantitative approximation of the water resources for management purposes and this may therefore defeat the purpose of hydrological modelling. Beven (2005) states that even physically

based models require some form of calibration since field measurements are usually taken at a scale that is smaller than the modelling scale thus making it difficult to obtain values for all the parameters. For reliable predictions the parameters must be estimated using measurements of the inputs (e.g. rainfall, evapotranspiration) and outputs (e.g. runoff and soil moisture) through a calibration procedure. During calibration the parameters can be adjusted manually or automatically until a parameter set that represents a behavioural response between the simulated and observed hydrological (input-output) responses is obtained (Gupta et al., 1998; Kuczera et al., 2006; Zhang et al., 2009). For poorly gauged and ungauged catchments the calibration process becomes difficult due to unreliable and inconsistent data, or because of a complete lack observed data against which the simulated parameters can be evaluated (Vrugt et al., 2005).

Because of the challenge of estimating runoff from ungauged catchments and under uncertain conditions, hydrologists have been compelled to look for alternatives by which the water resource yield in ungauged basins can be estimated. In a bid to improve the quantification of water resources in ungauged catchments, concerned hydrologists, through the International Association of Hydrological Sciences (IAHS), undertook a major international initiative (Sivapalan et al., 2003), declaring 2003-2012 a Decade on Prediction in Ungauged Basins (PUB). The main initiative of PUB is to account for and reduce predictive uncertainty in ungauged and poorly gauged basins. Another initiative was taken through an international research project, Model Parameter Estimation Experiment (MOPEX) which was launched in 1996 aiming to better resolve parameter uncertainty in hydrological modelling particularly in ungauged catchments (Boughton and Chiew, 2007). Although many advances have been made, PUB still remains a challenge, since more work has to be done in estimating parameters for ungauged catchments and in developing countries the problem is compounded by diminishing measurement networks (Hughes, 1997) and in some cases, old data sets which are difficult to reconcile (Winsemius et al., 2008). Despite these challenges hydrologists are still expected to come up with realistic estimates of water resources in ungauged catchments for purposes of planning and management. Two alternative methods by which hydrological predictions (through parameter estimation) can be carried out in the ungauged basins have been employed. These are the parameter regionalisation method and the *a priori* method of estimating parameters from field observations (Hughes, 2006; Kapangaziwiri, 2008; Hughes et al., 2011a).

Parameter Regionalisation: The process of regionalising parameters is undertaken through the extrapolation of calibrated parameters of the gauged catchments to the ungauged catchments (Kokkonen et al., 2003; Hundecha and Bárdossy, 2004; Wagener and Wheeler, 2006). These parameters are obtained by calibrating the catchment model against observed data and the method is based on the assumptions that catchments with similar characteristics exhibit the same hydrological behaviour and thus parameters can be generalized to the ungauged catchments (Parajka et al., 2005). In addition spatial proximity can be used in which it is assumed that neighbouring catchments have the same hydrological behaviour (Bárdossy, 2007; Randrianasolo et al., 2011). A number of regionalisation approaches are available (see Kim and Kaluaracchi, 2008), of which various statistical methods of regression are the commonly used method. These statistical methods make use of regression relationships between attributes of a number of gauged basins and optimized model parameters (Boughton and Chiew, 2007) which are then transferred to the ungauged basins. Despite being one of the few methods of assigning parameters to ungauged catchments some studies (e.g. Wagener and Wheeler, 2006) indicate that there are uncertainties involved in transferring parameters. There are also uncertainties associated with the model calibration process even before the parameters are transferred through the regionalisation process. These uncertainties are dealt with in the next section but they include:

- input data uncertainty: where it is possible that the rainfall-runoff relationships may not be adequately represented in the observed data probably due to errors in the input climatic data (Gupta et al., 1998),
- parameter uncertainty (Kuczera and Mroczkowski, 1998) and equifinality (Beven and Freer, 2001; Beven, 2006), resulting in low confidence in linking calibrated parameters to ungauged catchment characteristics (Winsemius, 2009),
- model structural uncertainty and questions about how well a model represents reality (Masden, 2003) and
- the need to calibrate the regionalized parameters against some observed data (Franks, 2007), which may not be available in data sparse regions like southern Africa (Hughes, 2004a).

The fact that there are no available data with which to constrain the predictive uncertainty (Kapangaziwiri, 2008) also increases the hydrological model uncertainties in ungauged basins. When looking at the similarity in characteristics between the gauged and ungauged catchments due regard is also given to the climate and physical basin properties such as soil and vegetation types, relief and geology. This means that the regionalisation method may be limited to small catchments or to those catchments that are in very close proximity as there might be some marked heterogeneity and variability between the basin characteristics if the catchments are too widely spaced which may increase the predictive uncertainty (Bardossy 2007).

A priori parameter estimation: This is a direct approach which makes use of the physical basin properties to estimate the catchment parameters for both the gauged and ungauged catchments (Kapangaziwiri 2008; Kapangaziwiri and Hughes, 2008). The parameter values are fixed based on experience and knowledge of the catchment physical properties or on values obtained from the literature. Unlike in the regionalization method where parameter equations are derived from the gauged catchment characteristics, *a priori* parameter estimation derives the parameter equations independently using a conceptual interpretation of the model structure as guided by hydrological principles and thereby assigning a physical meaning to the parameters (Kapangaziwiri and Hughes, 2008). Although there are uncertainties associated with the *a priori* method of estimating parameters, the uncertainties are at least expected to be different from those generated in regional parameterization (Hughes et al., 2011b) as hydroclimatic variability is reduced by focusing on specific physical basin properties for each catchment. Furthermore Kapangaziwiri (2008) states that there is less ambiguity in estimating parameters directly from physical basin properties than estimating the parameters based on calibration against an observed runoff signal. This is because different catchments may exhibit the same runoff pattern yet they possess different physical basin attributes. Nevertheless uncertainties may be encountered with the *a priori* parameter estimation method if the spatial detail of the physical basin properties is too coarse (Hughes et al., 2011a). To achieve some degree of reliability in the *a priori* estimation method, Ao et al. (2006) recommend that direct physical meanings should be assigned to the parameters, sufficient and relevant physical basin property data should be available, adequate relationships should be established between these data and the parameters and there should be methods (GIS techniques) of linking the relationships to the basin.

Regionalisation of constraints on catchment hydrological responses: In view of the fact that there is predictive uncertainty in the parameter estimation approaches based on regression relationships and on *a priori* estimation and in a bid to reduce uncertainty in hydrological modelling, Yadav et al. (2007) devised an approach whereby the regional response of a catchment to hydrological processes is estimated within an uncertainty framework. This framework makes use of regionalized streamflow indices to independently constrain the catchment's hydrological response to a behavioural set of possible outputs. The indices are those hydrological response features that are characteristic of a catchment and can be derived from variables such as rainfall, evapotranspiration and streamflow (Shamir et al., 2005). The regionalisation of constraints approach derives its strength from the fact that the catchment's response characteristics are not directly linked to the model structure. The procedure for regionalising the constraints (Yadav et al., 2007) involves deriving the response characteristics, applying regression methods to derive relationships between the response characteristics and the physical basin characteristics and estimating the uncertainty range of the indices (parameters) for ungauged catchments. The parameter ranges can be used within a hydrological model with a Monte Carlo sampling framework, which randomly selects an ensemble set of parameters from a distribution of the constrained parameter space. For use in water resources assessments in southern Africa, a generic uncertainty framework (Kapangaziwiri et al., 2009) has been developed which is based on *a priori* parameter estimation and the principles of regionalisation of constraints.

2.9.4 Uncertainty in hydrological modelling

Obtaining exact answers or solutions to any problem or phenomenon is the most ideal situation in any field of study. However, the complex hydrological dynamics, temporal shifting of the physical domains, climatic variability and data issues have rendered hydrology an uncertain discipline and this has also led to predictive uncertainty in hydrological modelling (Smith, 2002; Beven, 2005; McWilliams, 2007; Knutti, 2008). Hulme and Carter (1999) have singled out two categories of uncertainty as either 'incomplete' knowledge or 'unknowable' knowledge. Incomplete knowledge is due to lack of knowledge or poor understanding of the underlying physical processes, and to lack of resources with which to undertake impact assessments. Unknowable knowledge is caused by the inherent unpredictability of the global climate system,

and the difficulty to predict future socio-economic scenarios in a deterministic manner (Giorgi and Francisco, 2000). There are three common sources of uncertainty in hydrological modelling namely model structure uncertainty, input-output data uncertainty and uncertainty in the estimation of parameters.

Model structure uncertainty: Hydrological models are based on assumptions and simplified representations of the processes that take place in the real world system and always be associated with some degree of uncertainty (Hughes et al., 2011a). The complexity of the underlying hydrological processes has resulted in poor or insufficient knowledge of the processes and consequently the use of inappropriate assumptions for model conceptualisation and mathematical formulations (Sorooshian and Gupta, 1985; Liu and Gupta, 2007). Another compounding factor stems from the manner in which the spatial and temporal discretisations are mathematically represented (Refsgaard et al., 2007; Beven et al., 2008; Smith et al., 2008).

Input data uncertainty: Input data uncertainty arises from errors in measuring the climatic variables (rainfall, evaporation) and in the observed streamflow (for the gauged catchments). Input data deficiencies arising from limited and infrequent monitoring, sparse and diminishing measuring networks as well as short time series (Wagener and Gupta 2005, Vrugt et al, 2008) also contribute to uncertainty, this situation is particularly common in developing regions such as southern Africa (Hughes et al., 2008).

Model parameter uncertainty: Parameter uncertainty arises from the manner in which the parameters are estimated either through regionalization or *a priori* methods (Neuman, 2003; Liu and Gupta, 2007). Reliance on observed data for calibration unavoidably introduces input data uncertainty (Hughes et al., 2011b) and according to Knutti (2008), parameter uncertainty arises if the values used in the parameterisations are not adequately constrained by the observed evidence. Equifinality (Beven, 2006) also contributes to uncertainty in the regionalisation of parameters, while the lack of appropriate physical basin property data suggests that both regionalisation approaches, as well as *a priori* parameter estimation method will be highly uncertain.

2.9.5 Dealing with uncertainty in hydrological modelling

Although hydrological modelling has been used for a long time, Refsgaard et al. (2007) state that most of the modelling studies carried out in the past have neglected uncertainty or treated it as an ‘end of pipe’ analysis. Water resources have often been managed under unknown and unquantified uncertain conditions in the past. The reasons for not having embraced uncertainty are clearly outlined by Pappenberger and Beven (2006) who also state that although it is difficult to understand the concept of uncertainty most decision makers are eager to embrace the potential risks linked to uncertainty. With increased computer use and with improvements in understanding of processes, modellers have now realized that associated uncertainties must be rigorously assessed if hydrological models are to gain full recognition in public usage and if the future predictions are to provide meaningful information for the decision making process (Benke et al., 2011). The rapid trend of global development and the anticipated changes in the global climate, both of which are uncertain, also impress upon the need to incorporate predictive uncertainty as an integral part of the modelling process (Neuman, 2003, Refsgaard et al. 2005; Wagener and Gupta, 2005). To allow for flexibility in managing risk throughout the decision making process the trend has been to work within a certain range of uncertainty (Hughes et al., 2008). Vrugt et al. (2005) singled out three aspects that are required to address predictive uncertainty in hydrological modelling namely, understanding of the uncertainty and its causes, quantifying and reducing the uncertainty. Before attempting to deal with the uncertainty a ‘Code of Practice’ (Pappenberger and Beven, 2006) is necessary in which uncertainty analysis should be considered as an extension of the existing modelling practices and the concepts of uncertainty must be explicitly communicated to the end users (decision makers and managers). In terms of risk in decision making, water managers should therefore be positioned to understand and translate the predicted uncertainties into risk management.

Reduction of uncertainty in hydrological modelling has been carried out through a number of approaches (Benke et al., 2011) which result in the conditioning of the model parameters within some acceptable uncertainty boundaries (Shrestha et al., 2009). A variety of uncertainty analysis frameworks (e.g. Beven and Binley, 1992; Thiemann et al., 2001; Neuman, 2003; Vrugt, 2003a; b; Wagener et al., 2003; Wagener and Kollat, 2007) have been developed to deal with the uncertainty problem. It is noted, however, that these methods are not able to address all the three

major sources of hydrological uncertainty i.e. input, structural and parameter errors (Liu and Gupta, 2007). In an attempt to deal with all the three basic forms of hydrological model uncertainty, methods of prediction based on probability distributions and combined with some data assimilation techniques have been devised. These methods mainly compute the uncertainty through a probability distribution function which is calculated using a probabilistic rather than a deterministic approach (e.g. Kavetski et al., 2006). Rather than a single optimized prediction, the uncertainty framework is based on the prior estimation of the model parameters and a parameter distribution type (e.g. normal or uniform distribution) is determined, which in turn is used to generate a large number of possible parameter sets (Kapangaziwiri et al., 2009). A choice of the most suitable model structure is made and the different parameter sets are forced onto the hydrological model to generate ensembles of predicted flows through random and independent sampling techniques such as the Monte Carlo approach. The regional responses to hydrology (the ensemble model outputs) are constrained and then used as input to water yield models (Liu and Gupta, 2007). The method is capable of providing responses to a range of the climates that are likely to occur in the future (Johnson and Weaver, 2009). One such framework has been developed for application in southern Africa (Hughes et al., 2011b).

2.9.6 Hydrological modelling in southern Africa

Hydrological forecasting models have been used to estimate water resources availability and for impact assessments in southern Africa (Hughes, 2004a), but lack of hydro-meteorological data and the problem of ungauged basins have not made the process easy. There is a general consensus that a lack of high quality observations hinders the progression of arid zone hydrology (Pilgrim et al., 1988). Southern Africa is faced with a problem of diminishing monitoring networks whose data are sparse and of poor quality (short time series, missing data and sometimes, unreliable) and difficult to access. Lack of resources, shifting priorities especially on the political front and war in some countries have resulted in some recording networks going unmonitored for a prolonged time period. Hughes (2004a) reports that hydrological modelling in the southern African region is hampered by poor understanding of some of the underlying catchment hydrological processes, such as surface-groundwater interactions and channel transmission losses.

A number of models, most of them of the conceptual type, have been applied in southern Africa. The type of models used in the region has been influenced by region-specific needs which are mainly estimating basin water resource availability and impact assessments (Hughes, 2004a). The Pitman model (Pitman, 1973; Hughes, 1997; 2004b), a conceptual and semi-distributed model, is one of the most widely used models in southern Africa. Some of the recent applications of the model include: Mazvimavi (2003) for estimating flow characteristics in ungauged catchments in Zimbabwe; Mwela (2004) and Ndiritu (2009) for assessing water resource availability in the Kafue basin; Hughes et al. (2006) for the regional calibration for the Okavango basin; Kapangaziwiri (2008) for estimating parameters for a wide range of selected basins in the region; Sawunyama (2008) for estimating uncertainty in water resources assessment in South Africa; Hughes et al. (2011a) for assessing the impacts of climate change on the Okavango river and Kapangaziwiri (2010) for an uncertainty analysis in selected basins in the region. Hughes (2004b) has also cited a large number of references in which the model has been applied. The ACRU (Agricultural Catchments Research Unit) model (Schulze, 1986; 1994), a conceptual and physically-based daily time-step multilayer soil-accounting model, has been widely used in South Africa. Among some of the other models that have been used in the region are: the Variable Time Interval (VTI) model (Hughes and Sami, 1994), the Namrom model, which is designed specifically for use in the Namibian basins (de Bruine et al., 1993), the HBV model (SMHI, 2000; Love et al., 2010) and the Global Water Availability Assessment (GWAVA) model (Meigh et al., 1999).

2.10 Modelling the hydrological responses to climate change

Future climatic changes as predicted by the various models included in the IPCC (2001c) reports will have important consequences on regional water resources (Chiew et al., 2009) and on many aspects of human survival ranging from water supply, health, food security and energy. In view of these threats and to ensure sustainable water resources for the future there is need to understand and quantify the hydrological responses to these potential climate changes (Kundzewicz et al., 2007). Understanding the impacts of climate change will also assist in developing appropriate adaptation and mitigation measures that will safeguard the well being of the population and ecosystems. What is required is a framework in which to conceptualise and investigate the relationship between climate change and water resources. The resulting impacts

can be quantified by coupling a calibrated hydrological model to the outputs of downscaled GCMs (Gleick, 1989). Coupling the two models will ensure that solutions to climate-induced water resource problems are generated at a level appropriate to the local catchment scale. Using the large scale GCM derived climate on its own will only produce very coarse information which does not assist the decision making process. Several studies have been carried out on the use of GCMs in quantifying the possible impacts of climate change on water resources (e.g. Nash and Gleick, 1993a;b; Christensen et al., 2004; Graham et al., 2007; Kundzewicz et al., 2007; Bates et al., 2008; Arnell, 2011). The basic steps followed in evaluating the hydrological impacts of climate change are outlined (Xu, 1999; Gleick, 2000):

- Determine the parameters of a hydrological model in the study catchment using historical climatic inputs (where possible) of precipitation and evaporation and observed river flow for model validation.
- Making use of GCM model simulations to derive estimates of regional climatic variables such as temperature, precipitation and evapotranspiration.
- Downscaling from the large scale GCMs to local or basin scale.
- Forcing the GCM-predicted climate scenarios onto a calibrated hydrological model to produce estimates of runoff and other hydrological variables under a changed climate.
- Assessing the impacts of the climate induced hydrological changes on various water resource systems by forcing the climate adjusted hydrological data onto water use or water yield models (CapNet, 2009; Hughes et al. 2011a) and then comparing the current and the future water resource availability.

2.10.1 GCM uncertainty in predicting climate

Predicting the future climate using GCMs goes through a series of steps which start from using assumptions to determine the future some emission scenarios (Nakicenovic, 2000), transforming the scenarios into future greenhouse gas concentrations and downscaling the GCMs before they can be used in impact assessments. All these processes are linked to some uncertainties of which three major sources of uncertainty are identified, namely, model configuration, internal model variability and the stochastic nature of natural forcings in the future (Giorgi, 2005). Generally uncertainty arises from the fact that no model can be able to fully represent any specified system

(Smith 2002, McWilliams, 2007, Knutti, 2008). Incomplete knowledge of the physics of the climatic processes and on the sources and sinks of greenhouse gases (Hulme and Carter, 1999; New et al., 2000) also compound the GCM uncertainty. The nonlinearity of the climate system's response to various forcings such as solar radiation and volcanic eruptions also makes it difficult to develop appropriate sets of the process equations that are required for the models (New, 1999; Rial et al., 2004). The nature and intensity of future greenhouse gas concentrations will mainly be guided by future decisions that will be made by the relevant authorities and individuals, the rate of uptake of alternative energy sources and the growth in population and socio-economic advancement. It is quite impossible to predict and attach any exact figures to the socio-economic conditions, the extent of development and the demographics in the future, making it difficult to know exactly the quantity of greenhouse gases and how they will affect the future climate (Chiew et al., 1995; Giorgi and Francisco, 2000).

According to Brown et al. (2008), GCMs are insensitive to very short time scales and as such it might be misleading to use them to predict interannual climate variability, especially the variability linked to ENSO. The GCM capability is also limited to predicting mean values of the climate variables rather than high order statistics such as variability. Important hydrological processes such as precipitation occur at shorter time scales that cannot be resolved by the GCMs. Although GCM downscaling is used to reduce uncertainty, the exact relationship between large-scale climate data and the smaller-scale dynamics on the ground may not be well established and therefore false linkages may be created especially in relation to local scale dynamics (Gleick, 2000). The fact that GCMs operate better at large scale spatial and atmospheric dynamics than at the smaller scale surface dynamics means that the models are limited in their ability to incorporate and reproduce important aspects of the hydrologic cycle, thus making them generally more skilful in predicting variables such as temperature than precipitation (Solomon et al., 2007).

2.10.2 Uncertainty in assessing the hydrological impacts of climate change

Although significant progress has been achieved in predicting the impacts of a changing climate on future water resources, there remains considerable uncertainty in quantifying the associated impacts. Uncertainty occurs mainly as a result of limited knowledge and the assumptions made in some of the hydrological and climatic processes as well as the fact that the models are

attempting to simulate highly complex systems (Mitchell and Hulme, 1999). The uncertainties associated with both the hydrological models and the GCMs have been outlined in the preceding sections. These uncertainties are propagated throughout the entire process of quantifying the hydrological impacts of climate change (Viner, 2003; Wilby, 2005; Stainforth et al., 2007). A cascade of the uncertainties is illustrated in Figure 2.13.

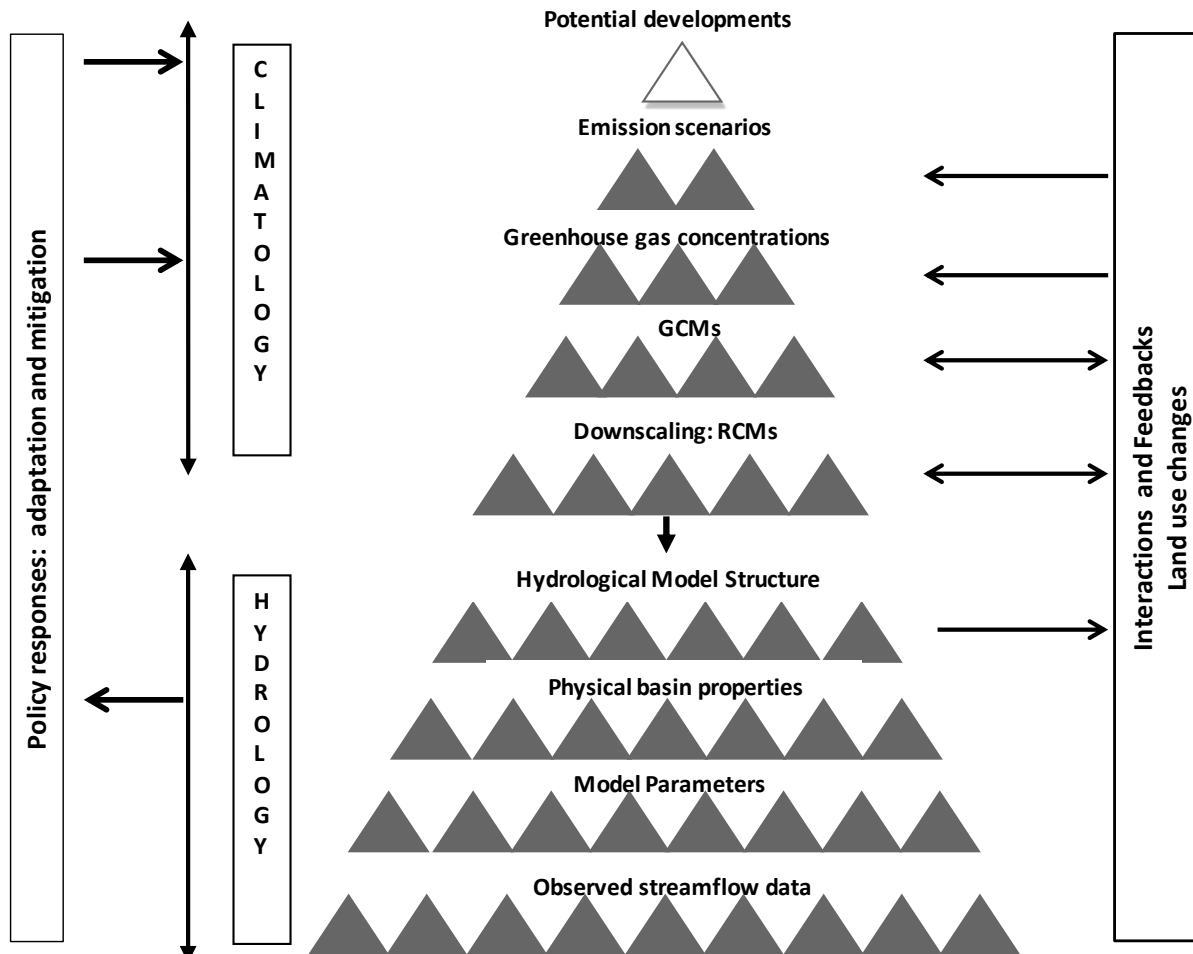


Figure 2.13 Cascading uncertainty in quantifying the hydrological impacts of climate change (modified from Mearns et al, 2001).

It is now clear that even though GCMs are the best tool so far available for predicting future climate, uncertainty renders them incapable of fully representing the hydrological responses of climate change, especially at regional or local scales (Ludwig et al., 2009b). Despite the fact that uncertainties emanate from both the GCMs and the hydrological models, comparative studies of

the sources of uncertainty show that GCMs are responsible for most of the uncertainties in the prediction of hydrological impacts of climate change (Wilby and Harris, 2006; Brown et al., 2008; Kay et al., 2009). Cascading uncertainty, if unaccounted for will hinder the formation of appropriate options for adaptation at the basin scale (Minville et al., 2008). To date, many studies have assessed the uncertainty between climate forcing and hydrological responses in various catchments (e.g. Hughes et al., 2011a; Kingston and Taylor, 2010, Kingston et al., 2010; Singh et al., 2010; Thorne, 2010; Todd et al., 2010; Arnell, 2011; Nobrega et al, 2011; Xu et al.; 2011). It has been realised (Gudmundsson et al., 2012) that different models present different results (e.g. % bias and differences in performance of different models. This also constitutes a major source of uncertainty which can not only be dealt with by making use of multiple climate models but by also incorporating a framework that can be able to account for the uncertainty (Haddeland et al., 2011). It is therefore necessary to incorporate the uncertainty framework into the modelling process if the uncertainties in modelling the hydrological responses to climate change are to be accounted for.

2.11 Summary of key aspects

The aim of this chapter was to review the current literature which is relevant to water resources development, under the context of climate variability and climate change. Globally climates are known to be variable at continental and regional scales and this variability has been translated to water resources. Southern Africa in particular, is characterised by high levels of variability at different temporal and spatial scales and these have resulted in recurrent flood and drought events. Variability arises normally from natural fluctuations in climatic variables and the associated feedback processes. Knowledge of the causes and patterns of variability is important as it forms a basis upon which future water resource management plans can be made. A variety of methods are available in the literature for assessing trends in variability, these range from simple statistical methods to the more complex approaches such as the Mann-Kendall test and spectral analysis methods. The success of these methods is, however, dependent on the quality of the time series data available to make such assessments. Apart from natural causes, fluctuations can be amplified through increased greenhouse gas emissions that result from human activities. To date GCMs are the most common means of predicting changes in global climate.

Impact predictions are very important for planning, designing and managing water resources. In terms of climate change and water resources, GCMs have been coupled to hydrological models in order to quantify the hydrological impacts of climate change. A variety of models are available for decision support in water resources management. These models focus either on understanding and quantifying the flow responses in a catchment or on allocating the available water to various uses. While acknowledging the increasingly important role that modelling has played in the planning and management of water resources it must also be acknowledged that there will always be uncertainty in the modelling approaches of both the hydrological models and the GCMs. Some of the uncertainties include the inherent limitation of models to represent the real world, the assumptions made, data limitations and socio-economic factors. Previously uncertainty has been treated as an 'end of pipe' process but with the increasingly threatening impacts of a changing climate, uncertainty needs to be acknowledged and quantified so that the process of decision making can be better informed. The need for appropriate decision making tools is also emphasized in order to allow the water manager to make effective decisions and to enable effective communication among stakeholders. This has been made possible by improvements in computer technology and the availability of spatial databases that allow for interactive and integrated water resources assessments.

To enable sustainable management of water resources at the catchment scale, it is important, therefore, to look at how historical variability in climate will change in the future, but the success will depend on the tools that are available to carry out the assessments and on data availability especially given the fact that the southern African region is characterised by limitations in climate and hydrological data.

CHAPTER 3 STUDY AREA AND AVAILABLE DATA

3.1 The Zambezi River Basin

Covering an area of about 1 360 000 km² and located between latitudes 8°S-20°S and longitudes 16.5°E-36°E, the Zambezi is the fourth largest river basin in Africa. The Zambezi River runs for a total length of 2 750 km from source to its mouth in the Indian Ocean. Much of the basin's drainage area is within south-central Africa and there are eight countries riparian to the basin namely; Angola, Botswana, Malawi, Mozambique, Namibia, Tanzania, Zambia and Zimbabwe. About 30 million people reside in the basin and a majority of them are fully dependent on the basin's natural resources for survival (Chenje, 2000). Figure 3.1 shows the location of the Zambezi basin while Table 1 presents the basin area occupied by and the population of each country.

Table 3.1 Basin countries, area and population details

| Country | Country area in basin | | Basin population | |
|------------|-----------------------|------|------------------|------|
| | km ² | % | millions | % |
| Angola | 247 484 | 18.2 | 0.477 | 1.5 |
| Botswana | 38 074 | 2.8 | 0.013 | 0.04 |
| Malawi | 104 705 | 7.7 | 9.28 | 30.1 |
| Mozambique | 155 017 | 11.4 | 3.836 | 12.4 |
| Namibia | 16 318 | 1.2 | 0.05 | 0.2 |
| Tanzania | 27 196 | 2 | 1.282 | 4.2 |
| Zambia | 553 438 | 40.7 | 6.452 | 20.9 |
| Zimbabwe | 217 568 | 16 | 9.452 | 30.6 |
| Totals | 1 359 800 | 100 | 30.842 | 100 |

(source: Euroconsult, 2007)

The Zambezi River rises about 1 450 m above sea level in Kalene Hills on the Central African Plateau in northwest Zambia. The river traverses an S-shape over a distance of about 2 700 km from its source to the mouth in the Indian Ocean (ZACPRO, 1998; Beilfuss and dos Santos, 2001). From the source in western Zambia, the river flows westwards into Angola where it captures runoff from the Luena River and other tributaries. The river then flows southwards back into the western province of Zambia where it is intercepted by its two largest head water tributaries; from the east, the Kabompo in Zambia (catchment area in excess of 70 000 km²) and

serve the Kafue Gorge Hydroelectric scheme. Further in a north easterly direction the river is joined by the Luangwa River after which it flows through a flat flood plain area before entering Mozambique through Cahora Bassa dam. The river then flows south-eastwards and is joined by the Shire river before emptying into the Indian Ocean. The Shire River connects Lake Malawi to the Zambezi River. The Zambezi basin is traditionally divided into three parts; the Upper Zambezi from the headwaters to upstream of Victoria Falls, the Middle Zambezi from Victoria Falls to Cahora Bassa which includes the Kafue catchment and the Lower Zambezi from downstream of Cahora Bassa to the Indian Ocean (Tilmant et al, 2010). For this study the basin is sub-divided into sub-basins as shown in Figure 3.2 while catchments are the gauged and ungauged sub-divisions within the sub-basins (Figure 3.3).

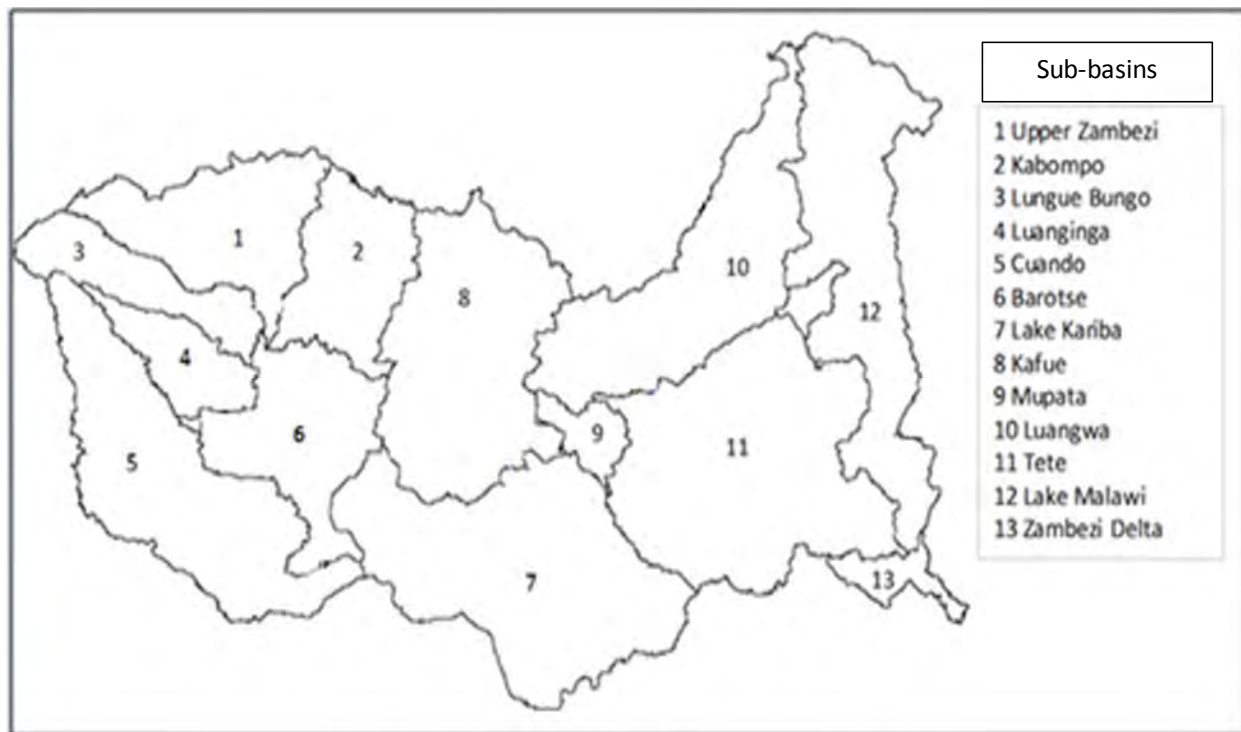


Figure 3.2 Sub-basins of the Zambezi



Figure 3.3 Catchments of the Zambezi basin (source: GRDC, 2007, HYDRO1K, 2001)

3.1.1 Geology and topography

Achaean Craton rocks which consist mainly of a granitic terrain intruded by various greenstone belts, dolerite dykes and sills are the dominant underlying rocks in the Zambezi River basin. A large portion in the central part of the basin is overlain by Karoo rocks which have been intruded by crystalline cretaceous rocks that were formed through metamorphosis of sedimentary deposits. These rocks are composed of shale, sandstones and conglomerates. Most of the valleys in the basin are lined with sedimentary deposits. The eastern part of the basin, which comprises mainly of Lake Malawi, Luangwa and Lusemfwā catchments lies within the East African Rift Valley (Chenje, 2000). The Copperbelt area of Zambia in the north is surfaced with quartzite sandstones (Mendelsohn, 1961). A distinct variation in topography is evident in the basin as shown in Figure 3.4. The catchment elevation ranges from 1 000 metres above mean sea level (amsl) in the west (in Angola), to over 2 500 amsl in the east along the Lake Malawi Rift Valley and to sea level at the river's mouth in Mozambique (Ashton et al., 2001). Between Lake Malawi and the Luangwa rifts, the highly elevated Nyika and Viphya plateaux demarcate the border between Zambia and Malawi. In the north eastern part of the basin, the Livingstone Mountains

mark the border with Tanzania. The Muchinga escarpment also marks the western part of the Luangwa Rift valley. An undulating terrain with low hills and escarpments formed by outcrops of quartzite, granites, schists and gneisses marks the central part of the basin. The Upper Zambezi catchment (from source to upstream of Victoria Falls) is a relatively broad valley of a moderate gradient. From upstream of Victoria Falls to Lake Kariba the basin is underlain by the super Karoo basalts and here the river flows into a deep narrow gorge. In the Middle Zambezi, the gradient is quite low and it steepens at Cahora Bassa where the river flows through some narrow gorges as it enters the broad shallow valley in the lower reaches of the basin. In the Lower Zambezi portion of the catchment (downstream of Tete in Mozambique) the river flows in a flat bottomed valley where it joins the Shire River before reaching the delta at the coast. Due to the marked variations in elevation across the basin there exists a large potential for hydropower generation (Chenje, 2000; Ashton et al., 2001; Euroconsult, 2007).

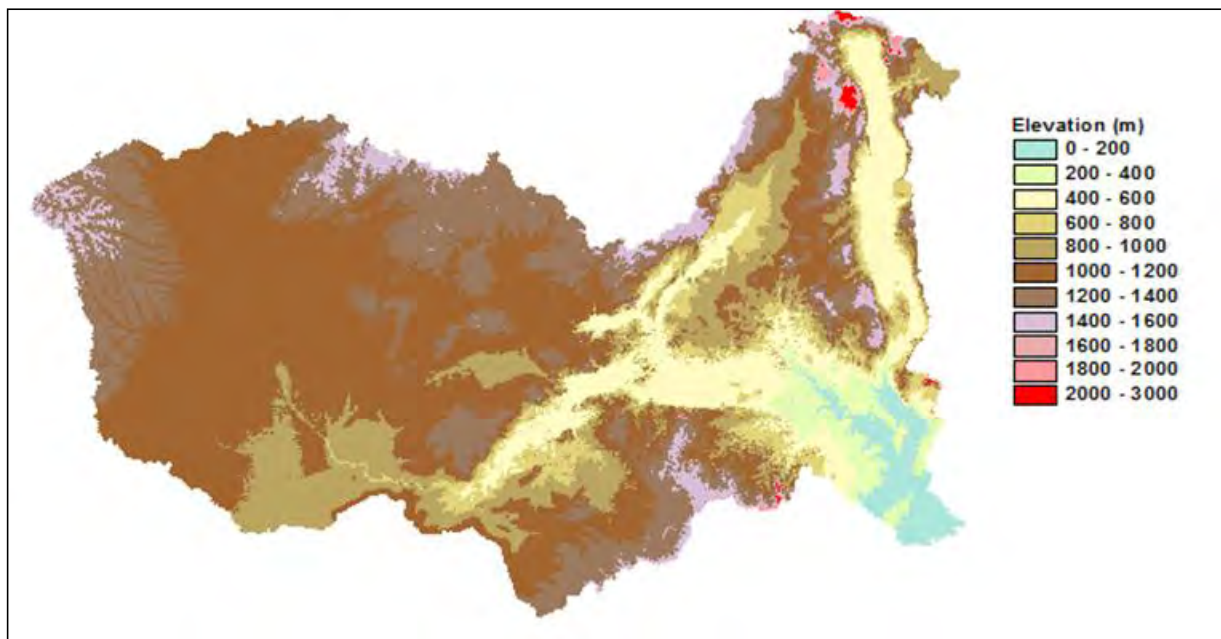


Figure 3.4 Zambezi basin topography (source: <http://edcdaac.usgs.gov/gtopo30/hydro>)

3.1.2 Soils

Figure 3.5 depicts the different soil types that are found in the Zambezi basin. The soil data are downloaded from the Digital Soil Map of the World produced by the Land and Water Development Division of the Food and Agriculture Organisation (FAO, 2003). The dominant soil types in the basin are ferrasols (tropical red soils) which are acidic and leached tropical soils

of low fertility (Ashton et al., 2001). High quality vertisols (black cotton soils) are found in many parts of the basin and these soils are good for agriculture. Much of the western part of the basin is covered by deep layers of wind-blown Kalahari sands which are overlain with ferrasols, arenosols and gleysols as shown in Figure 3.3. These Kalahari sands are very permeable such that surface runoff is minimal in this part of the basin (Bastiaansen, 1990). In the valleys of the Middle Zambezi soils are mostly alluvial or colluvial types and they are quite good for agriculture. A variety of soils are found in the lower Zambezi and they range from sandy to sandy loams that overly some red ferralitic soils, these are amongst the most fertile soils in the basin. Deep sandy loams are found in the Lake Malawi catchment and they are extremely fertile. Vertisols that overlie basalt and mudstone or shale formations are found in the floodplain areas of Kafue and Barotseland. Dambo soils are dominant in Angola, Malawi, Zambia and some parts of Zimbabwe. These soils are hydromorphic, with high clay content, blocky in nature and highly susceptible to swelling and shrinking in wet and dry conditions respectively. Sparsely distributed sodic soils are found in areas whose underlying parent rock has high sodium content and these soils have been subjected to severe mechanical weathering.

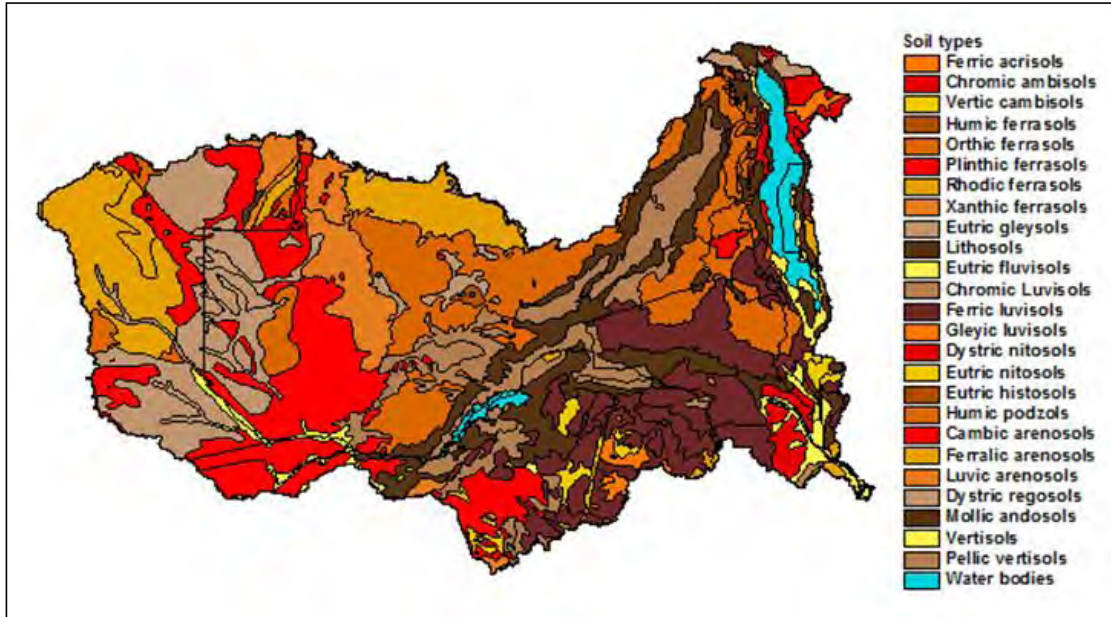


Figure 3.5 Dominant soil types in the Zambezi River basin (source: FAO, 2003, <http://www.fao.org/ag/agl/agll/key2soil.stm>)

3.1.3 Land cover

Land cover and land uses have an impact on water resources since they play an important role in the conversion of rainfall to runoff. The processes of infiltration, evapotranspiration and surface runoff all depend on the type of land use and cover. The sediment load of rivers and their water quality are also affected by predominant land cover and land uses. About 15.4% of the basin area is under agriculture; about 71% is open land (usually savannah, grassland or woodland) on which shifting cultivation occasionally takes place. Forests take up about 5.6% of the basin area whilst about 7.7% of the area includes water bodies of various forms (Chenje, 2000). The predominant natural vegetation type in the basin is Savanna (Figure 3.6) while dense forests and woody Savannas are common in the north-western part of the basin. Large areas of cropland are present particularly in the middle and in some lower areas of the basin. A number of floodplains and swamps exist in the basin and these mainly act as evaporating pans resulting in substantial loss of the basin's annual precipitation. About 65% of the total annual precipitation is lost to evaporation over the Barotse and Chobe flood plains before passing over Victoria Falls (Salecwicz, 1995). A summary of the sub-basin characteristics is provided in Table 3.6

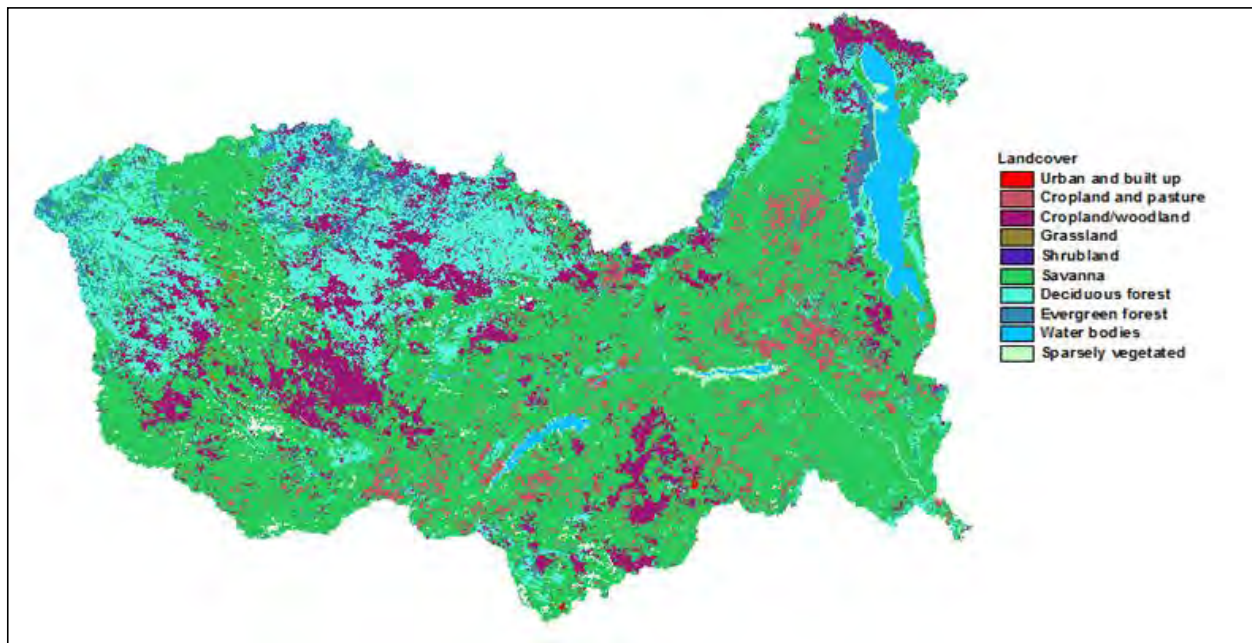


Figure 3.6 Land use in the Zambezi River basin (source: GLC2000 database, <http://www-gem.jrc.it/glc2000>)

3.1.4 Climate

The arid to semi arid climate of the Zambezi basin is influenced by the Congo air masses and prevailing wind systems, including tropical cyclones from the Indian Ocean. The basin has three distinct seasons; a cool and dry season (April to August), a warm and dry season (September to October), and a warm and wet season (November to March). In southern Africa temperatures vary according to altitude. There is a relatively small variation of mean monthly temperatures. The months of June and July are the coldest while October and November are the warmest months in the region. The hottest temperatures (19-31°C) are recorded during the early Austral Summer months and lowest temperatures (<13-23°C) during the cool, dry winter months (Ashton et al., 2001). High temperatures are the main cause of the variable and elevated evaporation rates across the basin. The potential evapotranspiration amounts are variable across the basin and range from average annual amounts of 1 600 mm to 2 500 mm based on the class A evaporation pans and using a standard coefficient of 0.9 (Beilfuss and dos Santos, 2001).

The Zambezi basin rainfall is largely influenced by the ITCZ which moves over the basin from October until April (Chenje, 2000), thereby concentrating the rainfall during the months of December to March. Seasonal variability in rainfall is therefore controlled by the position of the ITCZ as it moves between the north and south latitudes. The ITCZ is a convergence of the South East Trade Winds of the Indian Ocean that cover Mozambique and Zimbabwe, the North East Monsoon that covers the east African coast and the Congo Air-mass which is a monsoonal air flow across west Africa covering the Zambezi basin from a north-easterly direction. In the Zambezi basin, the wet season starts from around August when the ITCZ advances southwards from the north inducing some convective rains south of the equator. The amount of rainfall received in various parts of the basin is governed by the position of the ITCZ. At the start of the rain season around September-October, rainfall is higher in the northern parts of the basin (Tanzania) and by January higher rainfall amounts are received in the southernmost parts of the basin. In October, northern Angola receives rainfall as the ITCZ continues on its southward journey. By November the ITCZ is fully established in the south and most parts of the basin receive rainfall. In January the ITCZ is in the southernmost part of the basin and by April it is displaced far to the north. When the dry season starts in May, the ITCZ moves northwards and reaches the topmost position in July after which it reverses direction and October marks the end

of the dry season. In contrast to the ITCZ, another system called the Botswana High often has a tendency to push the ITCZ away from its sphere of influence resulting in droughts across the region (Chenje & Johnson 1996). There is only one rainy season per year extending from October through to April and the timing varies slightly depending on location. Based on the Climate Research Unit (CRU, Mitchell and Jones, 2005) estimates the mean annual rainfall in the basin is about 950 mm but there is a relatively high degree of spatial variability (Figure 3.7). Less rainfall is received in the south while the northern areas receive more rainfall. The driest areas of the basin include Southern Zimbabwe and some parts of Mozambique, these areas receive annual rainfall as low as 500 mm. Northern Zambia, central Angola and some areas in the Lake Malawi catchment are among the wettest areas in the basin and can receive annual rainfall as high as 1 400 mm (Nakayama, 2003). In a normal year, the north and south regions receive an annual average rainfall of 1 200 mm and 600 mm respectively (New et al., 2002). In dry years the annual rainfall amount can be as low as 400 mm while in the very wet years the annual rainfall can be as high as 2 000 mm, however, a gradual decrease in basin rainfall since the 1960s has been noted by some studies (Chaguta, 2007).

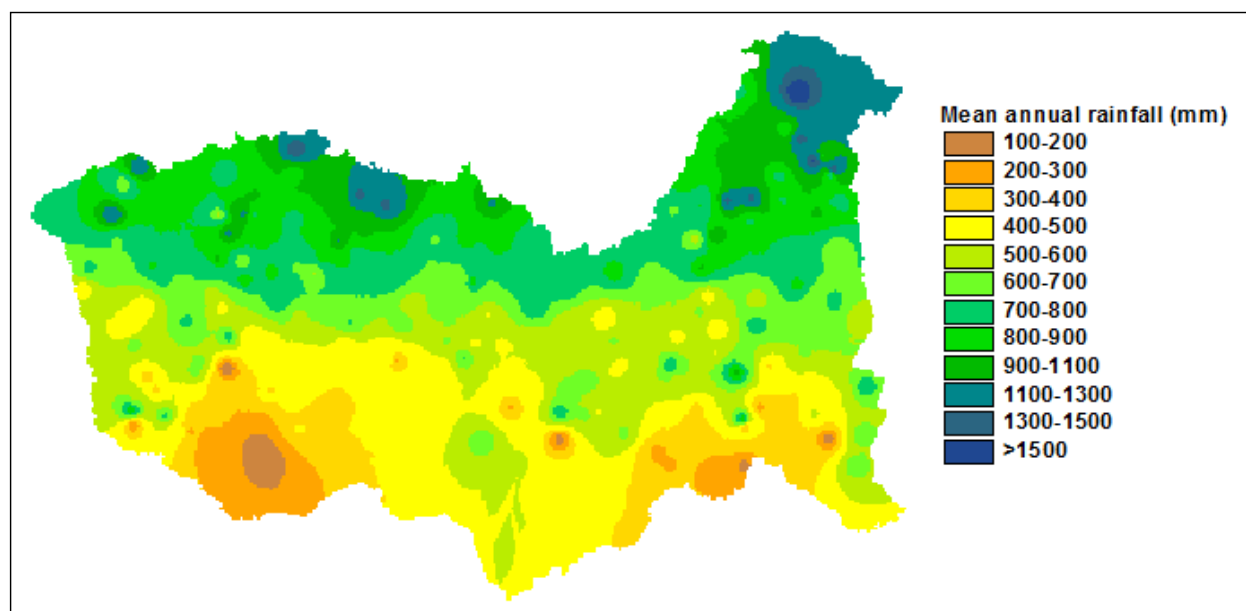


Figure 3.7 Mean annual rainfall (1961-1990) in the Zambezi River basin (source: SADC, 2007, GHCN v2 database)

Variability, Floods and Droughts

Although the occurrence of rainfall is seasonal, with wet summers and dry winters, the basin is characterised by high levels temporal variability in rainfall at the annual and decadal scales. Year to year variability in rainfall as well as recurrent droughts have adversely impacted the basin's water resources, food security, energy and human and ecosystems survival (SARDC, 2007). Droughts have caused a lot of suffering particularly in a basin where most livelihoods depend on rainfed agriculture. In the past, extensive droughts have occurred during the years 1946-47, 1965-66, 1972-73, 1981-83, 1986-87, 1991-92, 1994-95, 2001-02, 2004-05 and 2007 (Chibuye, 2008). As a result of these droughts, increasingly long dry spells and erratic occurrence of rainfall caused a drop in agricultural production in the basin. Energy production is also affected by the droughts, for example, between 1981 and 1992, the Lake Kariba levels dropped by 11.6 m (Figure 3.8) and this resulted in huge impacts on hydropower generation in the region (Muchinda et al., 2000). Relative to the 1993-94 season, the 1994-95 droughts resulted in a 35% decrease in cereal production in southern Africa, while the 2004-2005 droughts caused severe famine in the region (Nakayama et al., 2003).

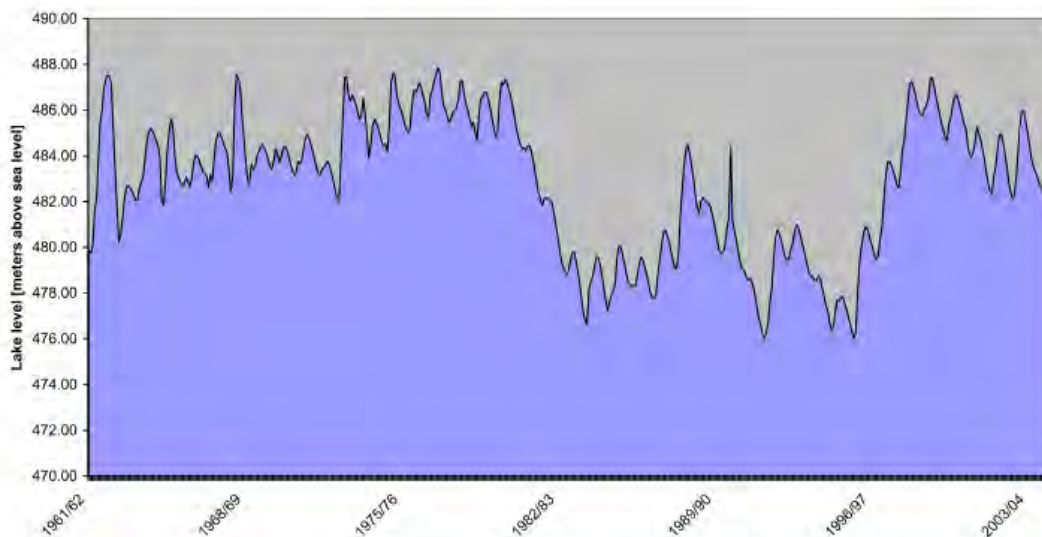


Figure 3.8 Lake Kariba water levels, 1961-2005 (source: Euroconsult, 2007)

The Zambezi basin has suffered severe consequences of cyclone induced floods in the recent past. The floods of 2000-01, 2005, 2007, 2008 (mainly due to Cyclone Eline and Cyclone Japhet) caused immense suffering and loss of life particularly in the downstream reaches.

According to United Nations statistics (Swain et al., 2011) on hydrological disasters (Table 3.2) the number of disastrous events emanating from floods and droughts in the Zambezi basin has increased in frequency and intensity over the last 30 years. A total of eight hydrological disasters were recorded between 1980 and 1989. The number of disasters increased to 77 between 2000 and 2009 and the most affected countries were Malawi and Mozambique.

Table 3.2 Hydrological disasters in the Zambezi basin since 1980 (source: Swain et al., 2011)

| Country | Number of events | | | Persons affected | | |
|------------|------------------|-----------|-----------|------------------|-----------|------------|
| | 1980-1989 | 1990-1999 | 2000-2009 | 1980-1989 | 1990-1999 | 2000-2009 |
| Angola | 1 | 0 | 19 | 100 000 | 0 | 783 328 |
| Botswana | 1 | 1 | 3 | 12 000 | 3 500 | 112 603 |
| Malawi | 2 | 6 | 15 | 6 000 | 417 000 | 1 159 276 |
| Mozambique | 3 | 3 | 15 | 1 000 000 | 470 000 | 6 212 111 |
| Namibia | 0 | 0 | 9 | 0 | 0 | 474 300 |
| Zambia | 1 | 1 | 11 | 800 000 | 1 300 000 | 2 398 816 |
| Zimbabwe | 0 | 1 | 5 | 0 | 0 | 265 000 |
| Total | 8 | 12 | 77 | 1 918 000 | 2 190 500 | 11 405 434 |

3.1.5 Runoff

The Zambezi and many of its tributaries are perennial rivers that portray seasonal cycles in high and low flows (Mazvimavi and Wolski, 2006). The river discharges an average of about 82 km³ (modified) per year into the Indian Ocean. Consumptive water uses take about 20% of the total runoff generated in the basin (Euroconsult, 2008). While many of the dams are mainly operated for hydropower generation and not abstraction, evaporation losses from reservoirs represent a significant part of the basin water budget. Estimates of water uses in the basin are presented in Table 3.3. Irrigated agriculture ranks second to evaporation in terms of water consumption but the amount is minimal given that irrigation only takes about 5% of the cultivated land in the basin. Water set aside to sustain the environment constitutes the environmental water uses.

Due to the spatial variation in rainfall, major contributors to the runoff are the northern sub-catchments (25%), the Kafue (9%), Luangwa (13%) and Shire (12%) rivers. The semi arid climate characteristics of the basin are responsible for the low runoff efficiency and high dryness

index and this is likely to increase the basin's vulnerability to climate change (Flint, 2006). Flows in the basin are extremely sensitive to small shifts in the rainfall regime such that interannual variability in precipitation has resulted in year to year variations in flow. In the upper reaches of the basin (see Figure 3.9) flow is almost natural as there is minimal impoundment or use by humans. However, hydropower reservoirs have altered the flow regime in the middle to lower reaches of the basin resulting in increased low flows while the peak flows have been reduced and delayed (Beilfuss and dos Santos, 2001). Reservoirs regulate runoff by altering the timing, magnitude, duration and frequency of flooding events. Figure 3.8 shows the major sub-catchments of the Zambezi and Table 3.4 presents the water balance for the Zambezi river basin based on gauged streamflows for the period 1969-1970 to 1993-1994. It is observed that the total basin area, based on total contribution from each country and on total contribution from the sub-basins differ slightly. The total area (per country basis) is 1 359 000 km² presented in Table 3.1 and the total area (per sub-basin contribution) as presented in Table 3.4 is 1 378 713 km². This difference indicates how difficult it is to estimate with precision, the areas of large basins.

Table 3.3 Water uses in the Zambezi basin (source Euroconsult, 2007)

| Use | Consumption (Mm ³) | % of total runoff |
|--------------------------|--------------------------------|-------------------|
| Total basin runoff | 103 224 | 100 |
| Rural | 24 | 0.02 |
| Urban | 175 | 0.17 |
| Industrial | 25 | 0.02 |
| Mining | 120 | 0.12 |
| Environmental | 1 202 | 1.16 |
| Irrigation | 1 478 | 1.43 |
| Livestock | 113 | 0.11 |
| Hydropower (evaporation) | 16 989 | 16.46 |
| Total | 20 126 | 19.49 |

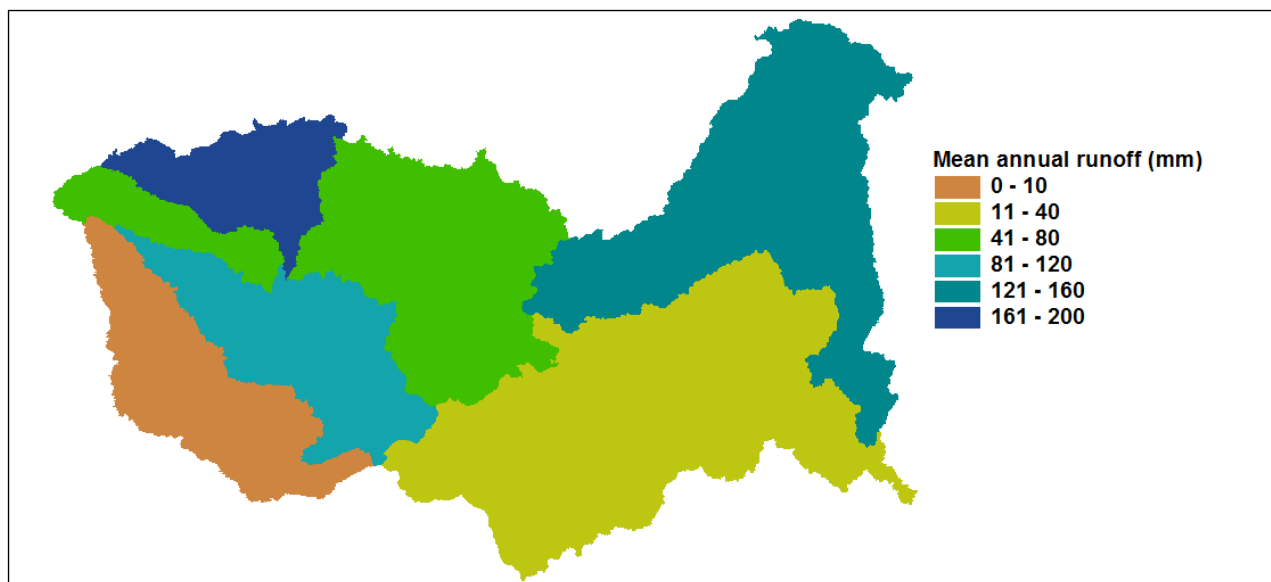


Figure 3.9 Zambezi basin mean annual runoff, 1970-1994 (modified from Euroconsult, 2007)

Table 3.4 Water balance for the Zambezi River sub-catchments based on mean annual rainfall and runoff for the period 1969-1970 to 1993-1994 (source: Euroconsult, 2007)

| Sub-catchment | Area (km) ² | Rainfall (mm/yr) | Runoff (mm/yr) | Evaporation (mm/yr) |
|---------------|------------------------|------------------|----------------|---------------------|
| Kabompo | 69 301 | 1 159 | 46 | 1 113 |
| Upper Zambezi | 90 359 | 1 225 | 211 | 1 014 |
| Lungue Bungo | 46 482 | 1 120 | 46 | 1 074 |
| Luanginga | 33 931 | 972 | 84 | 888 |
| Barotse | 118 994 | 840 | 84 | 756 |
| Cuando | 15 1465 | 760 | 7 | 753 |
| Kafue | 157 629 | 1 004 | 66 | 938 |
| Lake Kariba | 163 202 | 797 | 37 | 670 |
| Luangwa | 148 286 | 987 | 123 | 864 |
| Mupata | 19 552 | 793 | 40 | 753 |
| Lake Malawi | 158 043 | 1 157 | 130 | 1 027 |
| Tete | 197 816 | 903 | 40 | 863 |
| Zambezi Delta | 23 653 | 1 060 | 40 | 1020 |
| Total | 1 378 713 | 952 | 75 | 878 |

Two of the largest manmade lakes in the basin; Kariba dam (between the borders of Zambia and Zimbabwe) and the Cahora Bassa dam (in Mozambique) are found on the Zambezi River while smaller reservoirs, the Itzhezhi and the Kafue Gorge dams are found on the Kafue River. Other small reservoirs found in the basin include Lake Chivero and Lake Manyame on Manyame river in Zimbabwe. These reservoirs are heavily utilised for water supply and irrigation. The storage capacities and surface areas of these reservoirs are provided in Table 3.5. The Kafue River is the largest tributary of the Zambezi. The Kariba and Kafue gorge reservoirs regulate almost 90% of the flows in the middle Zambezi while the Cahora Bassa Dam controls much of the flow in the lower Zambezi. Lake Malawi, a large natural lake covering an area of 6 400km² and a volume of 8 400 km³ (Gandolfi et al., 1997) is also found within the basin and it provides inflow to the lower Shire River. Large areas of important wetlands are found in several areas of the Zambezi basin (Timberlake, 1998). These wetlands absorb and attenuate flows from upstream catchment areas and they slowly release water over a period of several months while at the same time maintaining flows during the dry winter months. In addition the wetlands provide some essential services for the basin communities ranging from pasture, fisheries and tourism. Such wetlands include; the Barotse flood plains, the Kafue Flats, the Lukanga swamps and the Chobe-Linyati swamps.



Figure 3.10 Kariba Dam (left) and Cahora Bassa Dam (right: source: Bourgeois et al., 2003)



Figure 3.11 Wetlands in the Zambezi Delta (left) and Kafue Flats (right: source: Bourgeois et al., 2003)

Table 3.5 Reservoirs and lakes in the Zambezi basin (source: Gandolfi et al., 1997)

| Reservoir/Lake | Surface area (km ²) | Storage capacity (km ³) |
|----------------|---------------------------------|-------------------------------------|
| Cahora Bassa | 2 739 | 55.8 |
| Kariba | 5 400 | 160 |
| Itezhitezhi | 392 | 6 |
| Kafue Gorge | 805 | 0.8 |

Table 3.6 Summary of sub-catchment characteristics (refer to Figure 3.8 for the location of sub-catchments, source: Ashton et al., 2001)

| Sub-catchment | Geology | Soils | Land use/ main activities |
|-------------------------|--|--|--|
| Kabompo | -Copper-rich sandstones, quartzites, arenites and conglomerates of the Copperbelt region | Deep, well-leached ferralitic soils. | Subsistence agriculture on floodplain levees along the rivers. |
| Upper Zambezi | -Predominantly sandstones and conglomerates of the Middle Zambezi basin and Archaean rocks of the Central African Craton in the headwaters | Deep, well-leached ferralitic soils Deep Kalahari sands | Subsistence agriculture on floodplain levees along the rivers. Small villages Administrative centres |
| Luanginga, Lungue Bungo | -Predominantly sandstones and conglomerates of the Middle Zambezi basin. | Deep ferralitic soils in upper headwaters | Subsistence agriculture on floodplain levees along the rivers. |

| | | | |
|---------------------------|---|--|--|
| | -Archaean rocks of the Central African Craton in the headwaters | Kalahari Sands over most of the lower reaches of the sub-catchment. | |
| Cuando | -Upper Karoo Batoka Basalt Formation -Archaean rocks of the Central African Craton in headwaters | Deep layer of Kalahari Sands covers most of the sub-catchment Rich alluvial soils on river terraces | Predominantly subsistence and floodplain agriculture, livestock and tourism -Small villages |
| Barotse | -Karoo Supergroup basalts and sandstones overlain with deposits of Kalahari Sands. | Alluvial soils and hydromorphic vertisols. Sandy-loam soils in small patches in the east. Deep, well-leached ferralitic soils in the high rainfall northern areas. | Subsistence agriculture Small towns and villages scattered throughout the sub-catchment. The Provincial capital, Mongu, Sesheke town |
| Lake Kariba sub-catchment | <i>Victoria Falls:</i> Upper Karoo Batoka Basalt Formation -Quartzites and associated rocks underlain by Karoo Supergroup sedimentary rocks and basalt. Deeply incised rocks formations <i>Manyame:</i> Zimbabwe Craton underlain by granites, Greenstone belt, Great Dyke. Dande Formation sediments underlie the northern area <i>Mupfure:</i> -Underlain by crystalline rocks of granitic terrain, -Midlands Greenstone belt, -Supergroup metasediments, gneisses, quartzites. -Great Dyke. Outlier of Upper | Kalahari Sands and very shallow, gravelly soils overlying the basalts. Very shallow gravelly soils Moderately deep sandy soils Moderately deep kaolinitic sandy to loamy sands -Very shallow gravelly soils shallow coarse grained sandy, kaolinitic soils -Deep kaolinitic clays -Moderately shallow to moderately deep sands slightly sodic in some places -Very shallow gravelly soils -Shallow to moderately shallow kaolinitic clays and loams | -Forestry and tourism Sparsely populated communal lands with subsistence farming, Commercial livestock Urban centre Commercial farming and communal lands Largely urban settlements Commercial farming, communal lands |

| | | | |
|---------|---|--|---|
| | <p>Karoo sediments</p> <p><i>Gwai</i></p> | <p>-Moderately shallow sands</p> <p>-Deep clays on the Great Dyke</p> <p>-Kalahari sands</p> <p>-Very shallow gravelly soils</p> <p>-Shallow to moderately shallow clays and loams</p> | <p>Communal and commercial farming lands</p> <p>Livestock farming</p> |
| Kafue | <p><i>Upper Kafue</i>: underlain by copper rich sandstones, quartzites, arenites and conglomerates of the Copperbelt region.</p> <p>-Large deposits of copper, cobalt and emerald bearing pegmatites</p> <p><i>Lower Kafue</i>: sedimentary and alluvial deposits underlain by Karoo basalts and sandstones</p> | <p>Deep well leached ferralitic soils</p> <p>Mostly alluvial soils and hydromorphic vertisols and well leached ferralitic soils in the northern area</p> | <p>Subsistence agriculture and mining. Informal settlements closer to the mines.</p> <p>Kafue, Blue Lagoon and Lochnivar National Parks. Rice and sugar cane cultivation on the floodplain, subsistence farming and pasture</p> |
| Mupata | <p>-Quartzites and associated rocks underlain by Karoo Supergroup sedimentary rocks and basalt.</p> <p>- Deeply incised rock formations</p> | <p>Very shallow gravelly soils</p> <p>Moderately deep sandy soils</p> <p>Moderately deep kaolinitic sands and loamy sands</p> | <p>Sparsely populated communal lands with subsistence farming,</p> <p>Commercial livestock</p> <p>Urban centre</p> <p>Large scale irrigated sugar at junction of Kafue and Zambezi rivers</p> |
| Luangwa | <p>-Quartzites, sandstones, granites, gneisses and underlain by sedimentary rocks.</p> <p>-Intrusions by small pegmatites</p> | <p>Moderately deep, well-leached ferralitic soils</p> <p>Moderately deep, sandy loams on areas underlain by limestone deposits</p> | <p>Sparsely populated communal lands with subsistence farming,</p> <p>Densely populated urban area with commercial crop and livestock farming</p> |
| Tete | <p><i>Mozambican side</i>:</p> <p>-Quartzites, sandstones, granites, gneisses and underlain by Karoo Supergroup sedimentary</p> | <p>Moderately deep, well-leached soils</p> <p>Shallow to moderately deep sandy soils</p> | <p>Sparsely populated communal lands with subsistence farming,</p> |

| | | | |
|-----------------------|--|--|--|
| | rocks. -Intrusions by small pegmatites and Greenstone formations <i>Zimbabwean side:</i> -Granites intruded by dolerites -Underlain by Zimbabwe Craton, and Zambezi mobile belt gneisses <i>Upper catchment:</i> Underlain with granites and Zambezi mobile belt gneisses, Upper Karoo Group, Dande Formation sediments | Moderately shallow to deep coarse grained kaolinitic sands and sandy loams Moderately deep granular clays Very shallow gravelly soils Moderately shallow coarse grained sandy kaolinitic soils Moderately shallow to moderately deep sands, sodic in some places | Commercial farming and communal lands Largely urban settlements Commercial farming and communal lands Largely urban settlements |
| Lake Malawi catchment | -Quartzites, sandstones, granites, gneisses and underlain by sedimentary rocks. -Intrusions by small Greenstone formations | Moderately deep to very deep, well leached ferralitic soils Moderately deep sandy soils and sandy loams Small areas of sodic soils | Densely populated communal and urban lands, extensive subsistence agriculture. Livestock farming, tourism on Lake Malawi, National parks. |
| Zambezi Delta | -Quartzites, sandstones, granites, gneisses and underlain by crystalline basement rocks | Moderately deep sandy soils Shallow sandy soils Deep deposits of alluvial soils on terraces | Sparsely populated areas with subsistence agriculture Commercial farming |

3.1.6 Water resource use and management

The Zambezi River basin is rich in natural resources and its waters are crucial to sustainable economic growth and poverty reduction in the region. Food security and the hydropower needs of the southern African region are mainly dependent on the existence of water in the Zambezi. Over 30 million people reside in the basin and most of them, particularly the rural majority who constitute about 70% of the basin population, depend on rainfed subsistence agriculture for their livelihoods (Chenje, 2000). Economic services such as fisheries, navigation, mining, agriculture, tourism and hydropower are derived from the river while the existing manufacturing industries are also heavily reliant on the basin waters. Agriculture, industry and mining account for 75% of

the water used in the basin. However, the uneven spread of rainfall in the basin has resulted in unequal distribution of the basin's water resources and this has often led to conflicts between member states (Ashton, 2000).

Two of the largest manmade lakes in Africa; Kariba and Cahora Bassa are the major sources of hydroelectric power in the basin. The Zambezi River provides about 75% of the basin's total hydropower (SARDC, 2007). The Itzehitezhi and the Kafue Gorge reservoirs are also important for providing power to some provinces in Zambia. In spite of the benefits derived from hydropower, the use of reservoirs to regulate flow has resulted in the alteration of the basin's hydrological regime. For example the constant flow delivered from Cahora Bassa without any regular flooding has reduced productivity for the fish industry and the extent of downstream floodplains has been reduced (Beilfuss and Brown, 2006). The river is also important in maintaining a rich and diverse natural environment which provides important environmental values and functions. The vast floodplains within the basin are used for ecosystems survival and livelihoods sustenance. Population expansion, developmental activities and the controlled flows in areas downstream of Kariba dam have greatly altered the basin's flow regimes and this has caused a decline in much of the basin's socioeconomic and ecological services including the carrying capacity of floodplains (Mazvimavi, 2008).

Several bilateral agreements and multilateral political arrangements are in place for the management of the Zambezi basin waters. Among the arrangements are the Zambezi River Authority (ZRA), which was founded in 1987, the Southern African Development Community (SADC) Protocol on Shared Watercourse Systems, concluded in 2000 and the Agreement on the Establishment of the Zambezi Watercourse Commission (ZAMCOM) which was signed in 2004. The ZRA is a bilateral agreement between Zambia and Zimbabwe and is responsible for managing Lake Kariba reservoir and allocating water for hydroelectricity generation in both countries. In addition ZRA manages telemetric stations that are important in operating Kariba Dam (ZRA, 2009). The SADC Protocol, to which all eight riparian countries are signatories, provides guidelines and a platform for managing the shared water resources and resolving conflicts arising from the development and use of the water. It also promotes regional cooperation and collaboration among the SADC countries. In 1987, the Zambezi River Basin Action Plan (ZACPLAN) was developed by SADC, the purpose of which was to formulate

sustainable plans for the management of water resources and their environment through a number of assigned projects (Beck and Bernauer, 2010). Under the Zambezi Action Plan Project 6 (ZACPRO 6) a number of agreements have been signed to ensure integrated and sustainable management of the basin waters. The project embraces all the relevant stakeholders from the local communities to large scale entities such as commercial agriculture, mining and hydropower. ZAMCOM falls under ZACPLAN and consists of a Council of Ministers responsible for ultimate decisions in basin management, a Technical Committee whose role is to provide technical advice to the Council of Ministers and the Secretariat responsible for the day to day running of ZAMCOM's programmes and projects (Euroconsult, 2007). Although each of the basin countries has specific governance structures which are responsible for the management of water resources, the key function of ZAMCOM is to create a regional and centralized information system which will allow all members access to basin-wide information, particularly regarding floods. Six countries are required to ratify the agreement in order to consolidate the basin-wide management of water. ZAMCOM became operational in 2011 after ratification by six of the eight basin countries, of which the two countries that have failed to ratify are still bound by the agreement. Other objectives of ZAMCOM include promoting equitable and reasonable utilisation, efficient management and sustainable development of the water resources of the Zambezi Watercourse (SADC, 2011).

Institutional frameworks differ between the riparian countries, these differences and the lack of adequate institutional structures (Kirchoff and Bulkley, 2008) may be the cause of conflict and challenges met in effectively managing the transboundary water resources and they could be one reason for the delayed ratification of ZAMCOM. Robust and coordinated national and international governance structures are required to promote the development of the basin's water resources and to prevent conflicts between the riparian states. Now that ZAMCOM is operational the question remains whether the coordinated management of the Zambezi basin will be beneficial to all the riparian states and their environments.

3.2 Sources of data

This study makes use of three main types of data which are rainfall, runoff and potential evaporation. Maize yield data are also used to assess the regional droughts in the Zambezi basin.

It should be noted that there are limitations in climate and hydrological data for the Zambezi basin mainly because the basin is data sparse, with deteriorating gauging networks and inadequate financial and human resources to maintain a constant data collection system (Euroconsult, 2007). Due to the data limitations this research has largely relied on global data sets.

Rainfall data: For change and variability analysis, some gauged monthly rainfall data was obtained from local sources (local data). These data consist of varying record lengths and most of the records are either short or have extensive periods of missing data. Only those stations with records longer than 30 years and with minimal gaps were selected for use in this study. These stations were selected to be as representative of the whole basin as possible. Information on the local rainfall stations used in this study is presented in Table 3.7. Due to the past civil war Angola does not have any gauged stations and stations in Mozambique have very low and apparently anomalous annual values (<300mm/year) which were considered erroneous and were therefore discarded. It was however difficult to obtain a consistent time period for all the local stations therefore various periods of observation are used based on the available record period for a particular station. Locations of the local rainfall stations together with the CRU rainfall grids are presented in Figure 3.12.

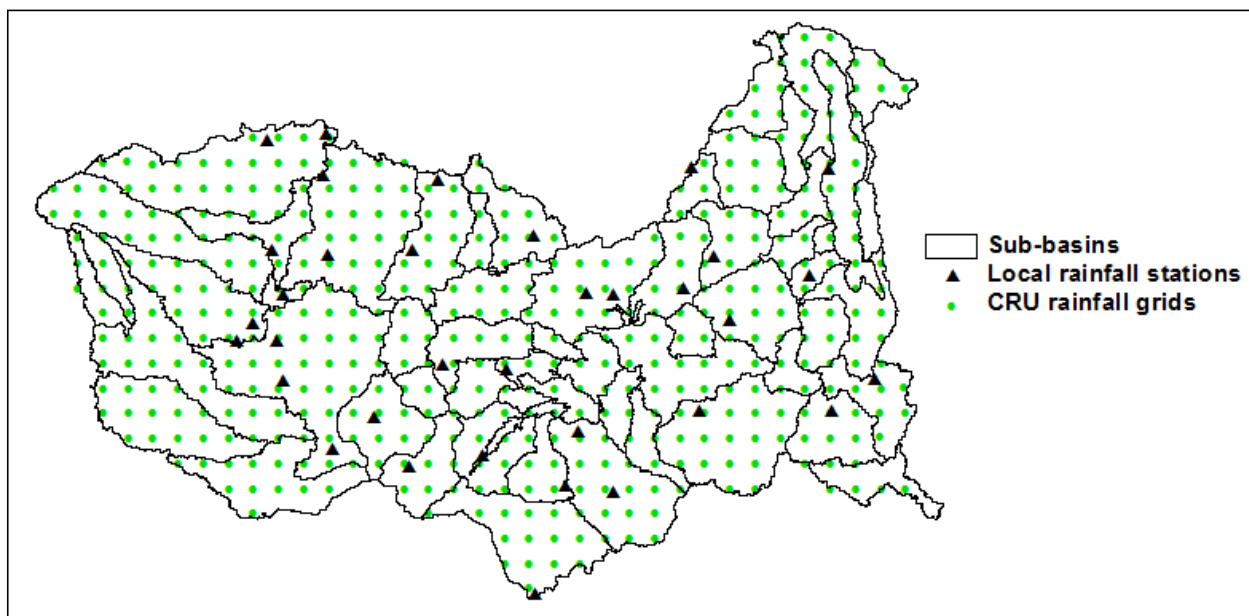


Figure 3.12 CRU rainfall grids and local rainfall stations

Table 3.7 ID and location of local rainfall stations (selected based on record length and fewer missing data)

| Sub-basin | Station ID | Sub-basin | Record | Latitude | Longitude | Altitude(m) |
|----------------------|------------|------------|---------|----------|-----------|-------------|
| Kabompo | 20519 | Kabompo | 1926-72 | -12.00 | 24.12 | 1 075 |
| Upper Zambezi | 82134 | Zambezi 12 | 1917-94 | -13.50 | 23.10 | 1078 |
| | 204446 | Luena | 1927-83 | -11.18 | 24.18 | 1432 |
| | 1847 | Zambezi 12 | 1946-87 | -14.40 | 23.29 | - |
| Luanginga | 204258 | Luanginga | 1917-75 | -14.95 | 22.70 | 984 |
| | 83528 | Luanginga | 1956-87 | -15.30 | 22.40 | - |
| Barotse | 3539 | Zambezi 10 | 1931-94 | -16.10 | 23.30 | 1027 |
| | 24140 | Zambezi 11 | 1904-98 | -15.20 | 23.20 | 1053 |
| | 3749 | Zambezi 10 | 1908-77 | -17.45 | 24.30 | 1021 |
| | 21160 | Zambezi 9 | 1938-83 | -16.83 | 25.13 | - |
| Lake Kariba | 21554 | Zambezi 8 | 1904-98 | -17.82 | 25.82 | 724 |
| | 112 | Mapfure | 1911-92 | -17.11 | 29.20 | - |
| | 214 | Sengwa | 1912-84 | -18.21 | 28.93 | 1160 |
| | 127 | Mazowe | 1962-93 | -16.71 | 31.58 | - |
| | 949 | Zambezi 7 | 1943-82 | -17.6 | 27.29 | - |
| | 201 | Gwai | 1930-90 | -20.35 | 28.33 | 1370 |
| Kafue | 205931 | Lunga | 1910-88 | -13.50 | 25.90 | 1324 |
| | 83110 | Lunga | 1906-94 | -12.10 | 26.40 | - |
| | 20428 | Lufwanyama | 1906-64 | -13.20 | 28.29 | 12158 |
| | 25629 | Kafue 2 | 1919-87 | -15.80 | 26.50 | 1001 |
| | 1201 | Kafue1 | 1916-86 | -15.87 | 27.76 | 978 |
| Luangwa | 23759 | Lusemfwa | 1915-63 | -14.37 | 29.37 | 1131 |
| | 91533 | Lusemfwa | 1925-87 | -14.40 | 29.89 | 518 |
| | 2318 | Luangwa1 | 1919-83 | -14.25 | 31.28 | 1033 |
| | 24853 | Luangwa2 | 1920-83 | -13.62 | 31.90 | 1028 |
| | 24319 | Munyamadzi | 1919-83 | -11.85 | 31.45 | 1466 |
| Lake Malawi | 8800356 | Chire | 1912-79 | -16.08 | 35.12 | - |
| | 8801322 | Lake Nyasa | 1905-71 | -11.87 | 34.18 | - |
| | 8802453 | Lilongwe | 1919-81 | -13.99 | 33.80 | - |

Since the rainfall gauging networks in the Zambezi basin are sparse and some of them do not have any recorded data while some areas are not gauged at all, an alternative rainfall data set (CRU TS2.1) was obtained from the Climate Research Unit of the University of East Anglia (Mitchell and Jones, 2005). CRU TS2.1 is a global data set consisting of 0.5° latitude-longitude grids of monthly time series of climate variables for the period 1901-2002. This data set is a compilation of local data which are homogenised through an iterative procedure. Reference time

series are used to correct any heterogeneity in the station records. The corrected data are then merged with an existing database and converted to anomalies which are used to construct the climate grids. The advantage of this data set is that it has a finer resolution compared to other globally available data sources, it has no missing data gaps and is of a long time period and thus the data are capable of providing consistent information across various locations. This data set also provides an opportunity for hydrological modelling in data scarce areas. The CRU data are used for the larger part of the study which constitutes hydrological modelling, climate change and drought assessment.

To assess the reliability of the rainfall data sets, long-term mean monthly CRU and locally observed rainfall data were correlated. Thirty (30) local rainfall gauging stations that are representative of the various sub-basins and their nearest CRU grid points were selected and correlations between the two different data sets were obtained using the Pearson's correlation coefficient. Figure 3.13 and Table 3.8 show the correlation results which are a combination of all the stations used in the analysis and averaged to represent a composite result for the entire basin for the various months of the year. Except for the month of January the correlations between the two data sets are in good agreement as indicated by the correlation coefficients ($R^2 > 0.6$ for all and 0.543 for December). The poor correlation for the month of January can be attributed to an over estimation of the maximum monthly rainfall by the CRU method (294 mm versus 101 mm). The wide scatter for the months of December to February may be a result of over estimation of the minimum monthly rainfall by CRU. The relationship between the two data sets is generally stronger for the dry season months compared to the wet season months. Most of the data points lie within the 95% confidence band and overall the relationships are assumed to be reasonably good to provide confidence in the use of the CRU TS2.1 rainfall data set.

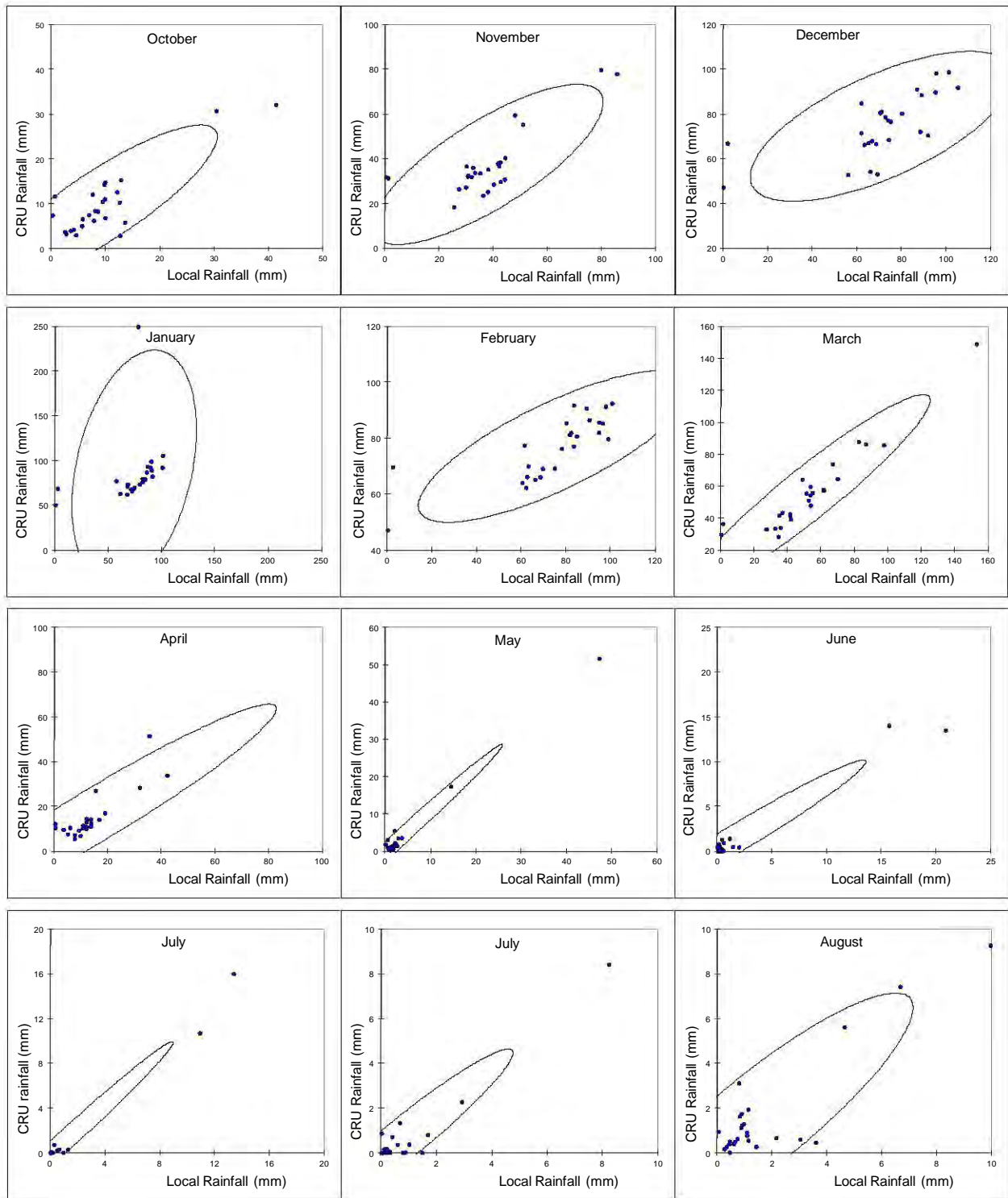


Figure 43.13 Comparison of CRU TS2.1 rainfall data and local rainfall data (based on long-term mean monthly rainfall for various stations and averaged for the whole basin, lines show 95% confidence bounds)

Table 3.8 Comparison of CRU and local rainfall data

| Month | Minimum (mm/month) | | Maximum (mm/month) | | Mean (mm/month) | | Standard deviation | | R ² |
|-----------|--------------------|-----|--------------------|-----|-----------------|-----|--------------------|-----|----------------|
| | Local | CRU | Local | CRU | Local | CRU | Local | CRU | |
| October | 0 | 3 | 41 | 32 | 10 | 10 | 9 | 7 | 0.733 |
| November | 0 | 19 | 86 | 80 | 38 | 38 | 17 | 15 | 0.606 |
| December | 0 | 47 | 105 | 99 | 71 | 75 | 24 | 14 | 0.543 |
| January | 0 | 50 | 101 | 294 | 74 | 92 | 24 | 54 | 0.323 |
| February | 0 | 47 | 101 | 92 | 75 | 77 | 25 | 11 | 0.610 |
| March | 0 | 28 | 153 | 149 | 53 | 56 | 30 | 25 | 0.892 |
| April | 0 | 6 | 142 | 102 | 18 | 18 | 27 | 19 | 0.919 |
| May | 0 | 0 | 47 | 52 | 4 | 4 | 9 | 10 | 0.988 |
| June | 0 | 0 | 21 | 14 | 2 | 1 | 5 | 4 | 0.959 |
| July | 0 | 0 | 13 | 16 | 1 | 1 | 3 | 4 | 0.983 |
| August | 0 | 0 | 8 | 8 | 1 | 1 | 2 | 2 | 0.918 |
| September | 0 | 0 | 10 | 9 | 2 | 2 | 2 | 2 | 0.781 |

Streamflow data: The most important climate variables required as input for the calibration of hydrological models are precipitation and potential evaporation (which can be in the form of temperature data). In order to assess the performance of any hydrological model, observed streamflow data are also required. Runoff data were provided by the Global Runoff Data Center (GRDC, 2003). It should be noted that due to the highly ungauged nature of the Zambezi River basin it was quite difficult to find stations that are adequately representative, except for the Victoria Falls station and the Kafue stations. Despite this discrepancy, stations were selected based on the length of time series, minimal number of missing values and catchment representativeness. Stations at the outlet of the defined catchment (Figure 3.9) were preferred although in some cases gauging stations within the catchment were used depending on the available data since most of them do not have any data (due to dysfunctional gauging networks) or their data are of poor quality, in terms of missing data and total record length. The Kafue basin was found to have a relatively high number of good quality stations and these have been selected for the purposes of hydrological modelling. In some cases data from local sources if of good quality were also used. The study mainly focused on gauging stations that are on the mainstream of the Zambezi while those stations on the tributaries with some relatively good data were also

utilised. The runoff stations used in this study are presented in Figure 3.14 and the station IDs and location are given in Table 3.9.

Potential evapotranspiration: Although there are pan evaporation data in some areas of the basin, these data are not sufficient and they are too sparse to be used for a basinwide analysis. Potential evaporation data (1961-1990) for the various sub-basins were downloaded from the International Water Management Institute's (IWMI, 2009) World Climate portal. These data are based on the Penman-Montieth evapotranspiration estimates which compute the evaporation from open water surfaces using the climate records of sunshine, temperature, humidity and wind speed (Allen et al., 1998).

Maize yield data: The maize yield data used for regional drought analysis were downloaded from the Food and Agricultural Organisation Statistics Division (FAO, 2012). The database consists of maize yield, and maize production data as well as the areas harvested.

Table 3.9 Identification and location of runoff stations

| Sub-basin | Station ID | River | Area (km ²) | Record period | Latitude | Longitude |
|---------------|------------|-----------|-------------------------|---------------|----------|-----------|
| Upper Zambezi | 1591002 | Zambezi | 21944 | 1989-2003 | -14.4 | 23.2 |
| Kabompo | 1591200 | Kabompo | 65792 | 1976-1979 | -14.0 | 23.6 |
| Luanginga | 1591820 | Luanginga | 34621 | 1958-1997 | -15.0 | 22.7 |
| Barotse | 1291100 | Zambezi | 334000 | 1964-2005 | -17.5 | 24.3 |
| Lake Kariba | ZGP25 | Zambezi | 360683 | 1924-2006 | -17.8 | 26.0 |
| | A22 | Gwai | 21000 | 1955-1984 | -18.4 | 27.0 |
| | 1491580 | Mapfure | 5180 | 1950-1978 | -18.1 | 30.2 |
| Kafue | 4560 | Lunga | 35061 | 1959-2000 | -14.0 | 26.4 |
| | 1591406 | Kafue | 23065 | 1953-1991 | -13.7 | 27.6 |
| | 1591405 | Kafue | 18207 | 1953-1992 | -14.4 | 27.0 |
| | 1591404 | Kafue | 95053 | 1977-2001 | -14.9 | 25.9 |
| | 1591403 | Kafue | 105672 | 1977-2002 | -15.8 | 26.0 |
| | 1591440 | Kafue | 8782 | 1970-1999 | -13.8 | 27.4 |
| | 470800 | Kafue | 152 810 | 1971-2000 | -15.9 | 28.5 |
| Luangwa | G.E. Rd | Luangwa | 143885 | 1930-1990 | -14.9 | 30.2 |
| Tete | 1891500 | Zambezi | 940000 | 1951-2008 | -16.1 | 33.6 |
| | D6 | Mazowe | 4000 | 1948-1991 | -17.6 | 31.6 |
| | 1491700 | Manyame | 7900 | 1964-1986 | -16.9 | 30.4 |
| Lake Malawi | 1992640 | L. Malawi | 6634 | 1974-1996 | -13.8 | 34.3 |
| | 1992480 | Lilongwe | 10645 | 1957-1982 | -12.8 | 34.2 |

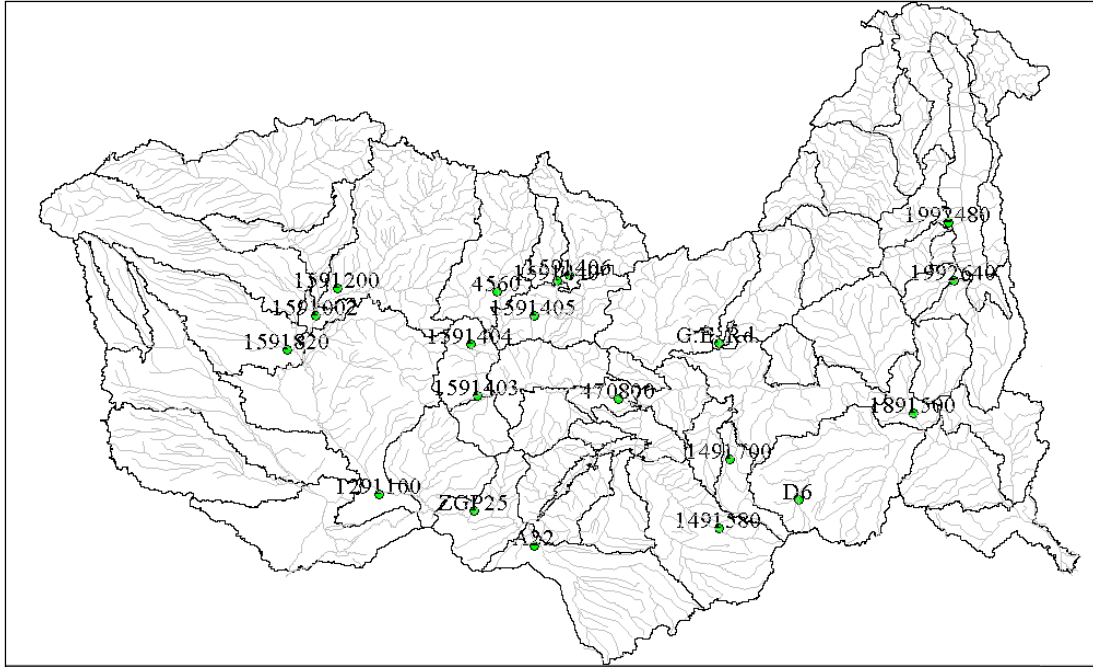


Figure 3.14 Runoff stations used in the study

CHAPTER 4 METHODOLOGICAL APPROACHES

4.1 Introduction

This chapter provides an outline of the various methods used in this study. The methodology consists of five main components; (i) generating catchment averaged rainfall, (ii) analysing historical variability, (iii) application of the Pitman rainfall-runoff model for the Zambezi River basin and simulating runoff and soil moisture storage, (iv) regional drought analysis based on rainfall and simulated soil moisture conditions and relationships with food security and (v) predicting future climate and hydrological responses to climate change. In order to address the set objectives, a variety of methods which mainly involve statistical techniques are applied.

4.2 SPATSIM - Spatial and Time Series Information Modelling

This study focuses on variability, drought analysis, rainfall-runoff modelling and modelling the hydrological impacts of climate change on water resources. Most of these processes have been facilitated using the data storage, analysis and modelling facilities in SPATSIM, a Spatial and Time Series Information Modelling software package. A brief summary of the facilities and options that are available in SPATSIM and how they were used to achieve the aims of the study is described.

The SPATSIM software was developed at the Institute for Water Research at Rhodes University (Hughes and Forsyth, 2006). This software was developed out of the need to improve the efficiency of the application of hydrological and water resource simulation models. It was also developed as an improvement to the HYMAS software which had no GIS functionality and was mainly used to manage the flow of input and output data to different hydrological models (Hughes et al., 1994). The software is intended to provide tools for managing and manipulating data, setting up and running hydrological models, as well as analysing and interpreting data. SPATSIM has a GIS spatial interface linked to a flexible database of attribute information and supported by a comprehensive range of data display and analysis facilities. A brief description of SPATSIM is given below and reference can be made to (Hughes and Forsyth 2006) for more detail.

The software was developed using the Delphi programming language. ESRI Map Objects is used to provide a spatial data interface for links to different types of information. All attribute information pertaining to spatial elements (point, line or polygon) is stored in Paradox data tables with generic structures. Spatial data are accessed through shapefiles and four data dictionaries, while other information relating to specific spatial elements is accessed through linked database tables. Shapefiles are created externally, through GIS facilities such as ArcView or ArcMap before adding them to SPATSIM. Four data dictionaries are used in SPATSIM to manage access to attribute information. Dictionary 1 contains references to all shapefiles that are used as well as the unique field identifiers. Dictionary 2 consists of references to the SPATSIM attributes and their data types. Data dictionary 3 specifies where to find attribute-linked information in the SPATSIM database tables and dictionary 4 links the records in the spatial data with the records in the SPATSIM attribute data tables for all the attributes. Eight types of attribute data can be stored in the SPATSIM generic database. The attribute types range from short text, real and integer single numbers, time series, graphics, tables (array) and memo information. Some of the variables specified in the time series data include the variable type and units, the start and end data of the series, the number of records and missing data codes. The memo type enables the storage of large amounts of formatted text data and can be used for notes and metadata.

4.2.1 SPATSIM components

Figure 4.1 provides the main SPATSIM screen which consists of six menu items: features, attribute, data exchange, procedure, application and the help facility. The 'Features' menu item is used to manage the display and content of spatial information, mainly consisting of shapefiles containing polygons, lines or points. It is also possible to add non-vector graphics images such as maps and Google Earth images to the visual display.

The 'Attribute' menu item is used to create or delete attributes, import or export data to the attributes or edit the attribute information. Figures 4.2 and 4.3 illustrate some of the procedures for importing text files with various formats to the time series attributes. It is possible to import a large number of files associated with data for many different spatial elements (polygons or points, for example) to be connected to a single attribute. There are similar bulk import options available for the other attribute types, such as text, single real or integer numbers and array types.

The array type of attribute is a generic type that allows storage of 1 or 2 dimensional tables. Each array attribute has a defined template that indicates how many rows and columns as well as defining what the rows and columns represent. Figure 4.4 illustrates this using an example of a 1-dimensional array type (parameters of a model) and a 2-dimensional array type (seasonal distribution and water uses).

Procedures are internal data processing methods in SPATSIM. Examples include the generation of catchment averaged rainfall data using an inverse distance weighting procedure and generating tables that summarise various annual and monthly statistics from time series data. Of greater relevance to this study, SPATSIM also provides a drought index generation option from which a variety of drought indices and index tables are generated from monthly rainfall data (Smakhtin and Hughes, 2004).

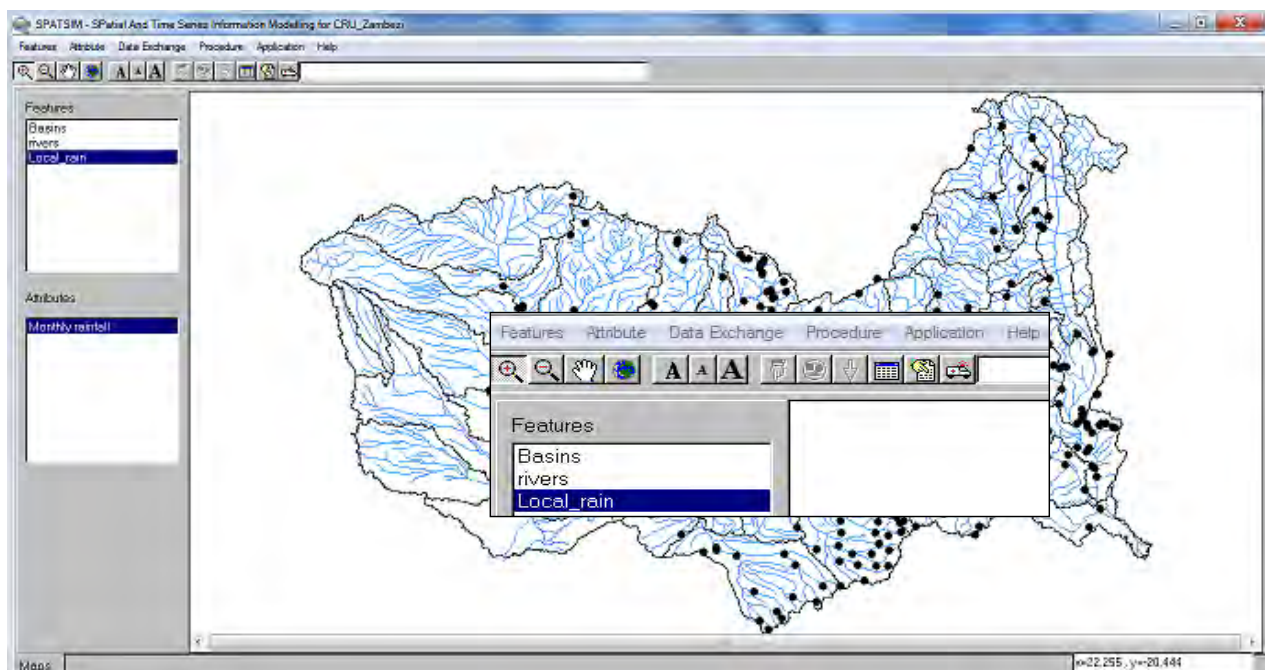


Figure 4.1 SPATSIM main screen (insert: menu options)

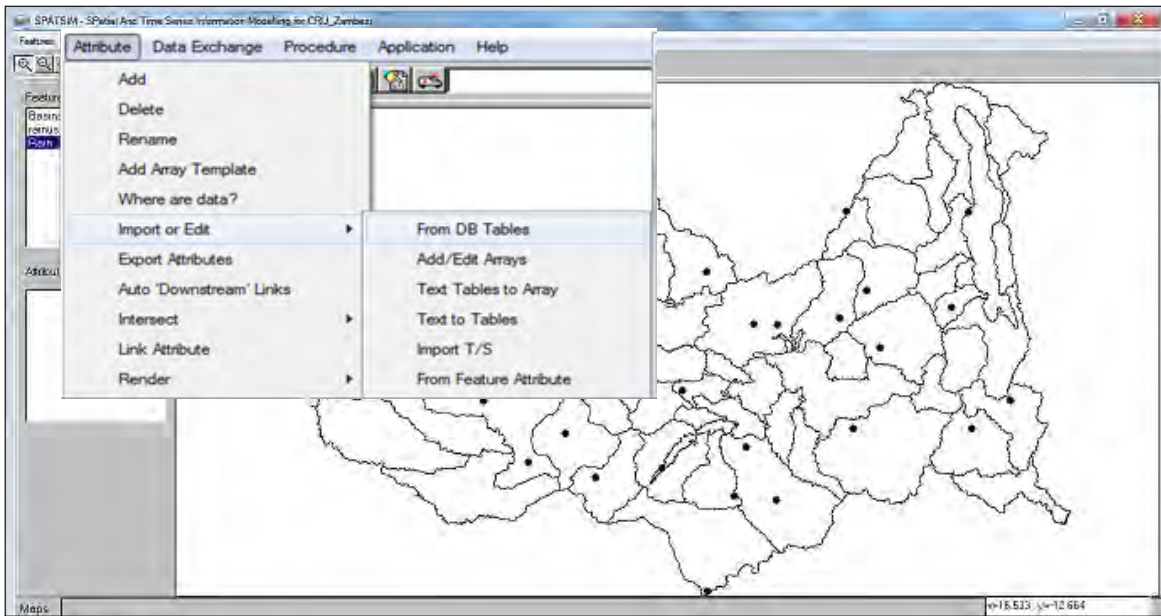


Figure 4.2 Selecting data the import item under the attribute menu



Figure 4.3 Selecting data and specifying the variable type to be imported

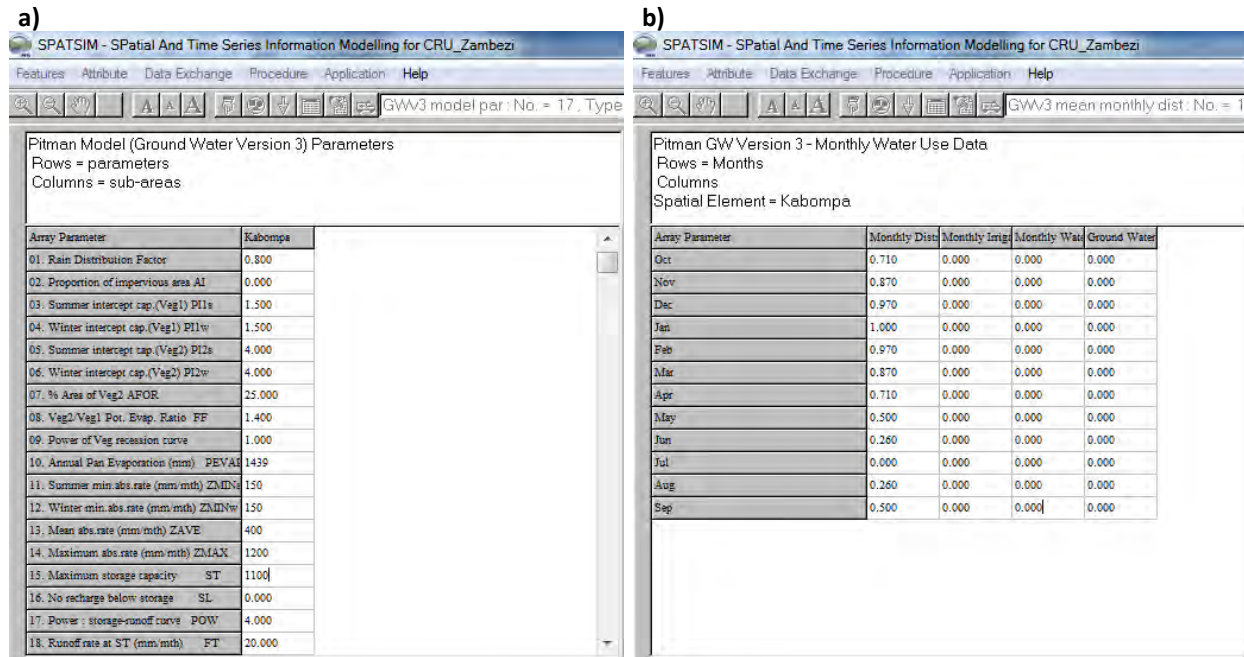


Figure 4.4 Example of (a) 1-dimensional and (b) 2-dimensional arrays in SPATSIM

4.2.2 Generation of catchment averaged rainfall in SPATSIM

Water resources assessments on a regional scale are better carried out using catchment averaged rainfall, which provides an average rainfall amount for a set of point data within the catchment. In performing a regional analysis, catchment averaged rainfall has an advantage over point data in that local variabilities associated with specific stations are eliminated (2000; WMO, 2000). In this study catchment averaged rainfall, R , is generated in SPATSIM using the CRU rainfall grids and applying an inverse distance weighting (IDW, Shepard, 1968; Wilk et al., 2006) method and is given as:

$$R = \frac{\sum R_i}{\sum \frac{1}{d_i^2}} \quad 4.1$$

where, R is the estimated rainfall for a specific area (polygon), R_i is the rainfall at a sample point, i , and d is the distance between the centroid of the area and the sampled point.

The IDW method is based on the assumption that the interpolating surface should be influenced most by the nearby points and less by the more distant points. The interpolated areal rainfall is a weighted average of the point rainfall and it is calculated by examining surrounding data points

that lie within a user-defined search radius. Some or all of the data points can be used in the interpolation process. The interpolating surface is a weighted average of the scatter points and the weight assigned to each scatter point diminishes as the distance from the interpolation point (centroid of the area) to the scatter point increases.

Weighted average rainfall data is generated from point rainfall data using the ‘Procedure’ -> ‘Point to Area’ menu item. Polygons whose average rainfall is to be calculated are selected either automatically by allowing SPATSIM to select a catchment and its upstream linkages or by choosing all catchments within the current SPATSIM view area. The user can determine the maximum number of gauges to be used in the interpolation process as well as the maximum search radius (Figure 4.5). If missing data are present within the maximum number of gauges that are closest to the catchment centroid then additional gauges will be used as long as they are within the search radius. There are additional weighting options that can be used (for example, gridded median monthly values) but these have not been applied in this study.

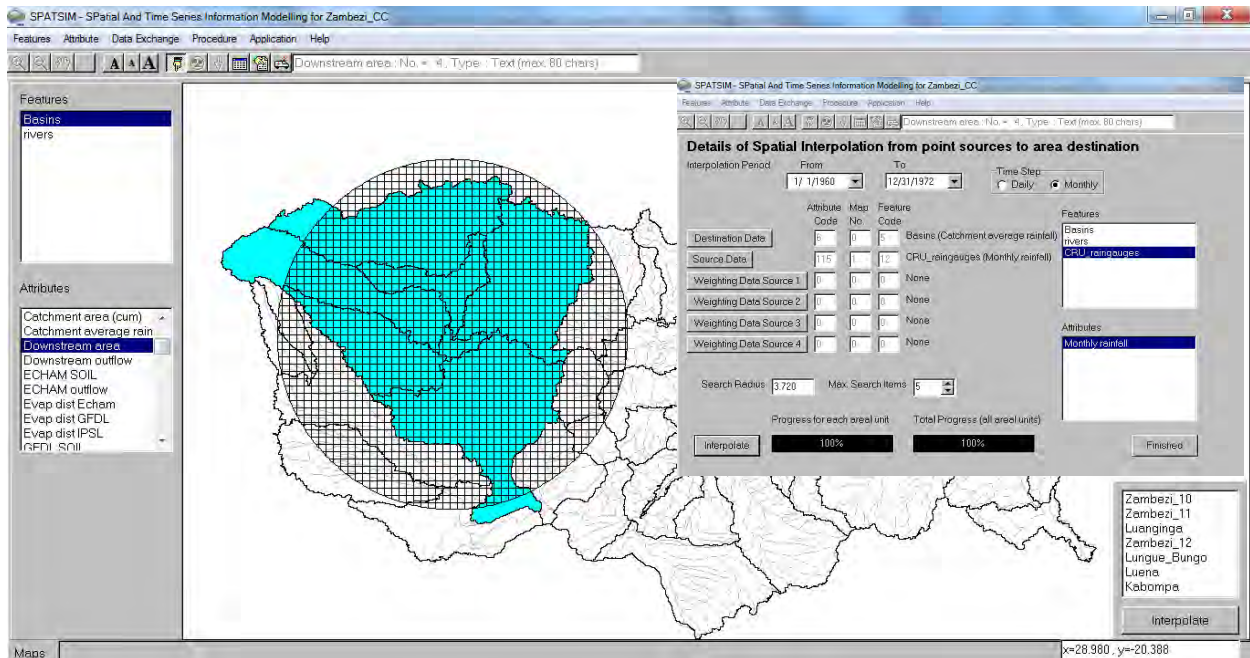


Figure 4.5 Selection of sub-catchments, search radius, interpolation period and time step to be used for interpolation.

4.2.3 Drought analysis routines in SPATSIM

Several drought analysis methods are available in SPATSIM (see Figure 6.5) but this study makes use of the SPI method. The Standardised Precipitation Index (SPI) method was developed by Mckee et al. (1993). It transforms precipitation into normalised numerical values that can be used to define and compare drought conditions in different areas. Its main advantage is that it can be calculated over different time scales and can therefore distinguish between droughts of different durations and for different seasons. SPI is the number of standard deviations by which the cumulative precipitation over the specified duration deviates from the long-term mean for a normally distributed random variable and it is defined by the equation:

$$\text{SPI} = \frac{x_i - \bar{x}}{\sigma} \quad 4.2$$

where, x_i is the precipitation of the selected period during the year i , \bar{x} and σ are the mean and standard deviation for the selected period.

The SPI is derived from time series of accumulated monthly rainfall values. The SPATSIM drought analysis routines were developed in partnership with the International Water Management Institute (IWMI; Smakhtin and Hughes, 2004) to provide a comprehensive set of drought assessment tools for relatively data sparse regions. While many of the rainfall drought analysis methods that are available are typically applied using daily data (e.g. Palmer, 1968; Zelenhasic and Salvai, 1987; Byun and Wilhite, 1999), monthly rainfall data are more readily available in developing countries. While SPATSIM provides facilities for estimating several rainfall-based drought indices, the focus in this study has been on the SPI. In SPATSIM the SPI is obtained by normalising the accumulated time series of rainfall values using the Box-Cox transformation (Smakhtin and Hughes, 2004). The λ parameter of the Box-Cox transformation is optimised in SPATSIM using an automated procedure based on selecting the λ value that minimises skewness of the transformed data. The Box-Cox transformation is defined as:

$$y = \frac{y^\lambda - 1}{\lambda}, \quad \text{if } \lambda \neq 0 \quad 4.3$$

$$y = \ln(y), \quad \text{if } \lambda = 0$$

where y , is the response variable or the accumulated rainfall and λ is the transformation parameter.

In SPATSIM the SPI can be generated for multiple time scales and for different durations. It can be calculated using an annual value based on a selected starting month and on a defined group of months e.g. if the start month is January and the duration is 3 months, 4 SPI values will be generated per year (SPI3, for the JFM, AMJ, JAS, OND, where the letters represent the months starting from January). Similarly if the duration is 6 months (SPI6) then 2 SPI values will be generated per year (ONDJFM and AMJJAS). It is also possible to generate single annual SPI values with the starting month and a defined duration specified, e.g. if the start month is October and the duration 3 months the SPI (SPI3, OND) will be based on rainfall that is accumulated for 3 months starting from October while the rainfall for the other months is ignored.

There are various ways by which the droughts can be classified and for this study the drought conditions are categorised using the classification scheme as shown in Table 4.1. Positive SPI values indicate above average precipitation while negative values indicate below average precipitation. A drought event occurs when the SPI is less than -1 and ends when the category changes to near normal.

Table 4.1 SPI categories and drought classes

| SPI values | Category |
|----------------|----------------|
| ≥ 2.00 | Extremely wet |
| 1.5 to 1.99 | Very wet |
| 1.00 to 1.49 | Moderately wet |
| -0.99 to 0.99 | Near normal |
| -1.00 to -1.49 | Moderately dry |
| -1.5 to -1.99 | Severely dry |
| ≤ -2 | Extremely dry |

Generation of SPI in SPATSIM: SPI values can be generated for any monthly time series through a SPATSIM procedure using the method of Smakhtin and Hughes (2004, 2006). In order to assess seasonal variability, the SPI is generated for the planting and growing seasons which spread through October to December (OND) for the planting season and from January (JFM) for the growing season, 6 monthly SPIs are also explored. A number of routines are involved in the generation and analysis of SPI values within SPATSIM and these include:

- i. The generation of catchment averaged rainfall. This method has already been outlined in Section 4.1.2. Drought indices require a complete rainfall time series with no missing data and the process of filling any gaps is catered for during the averaging of catchment rainfall.
- ii. Using the averaged catchment rainfall, the SPI is generated by making use of the Drought Indices Procedure in SPATSIM. This procedure is summarised in Figure 4.6.

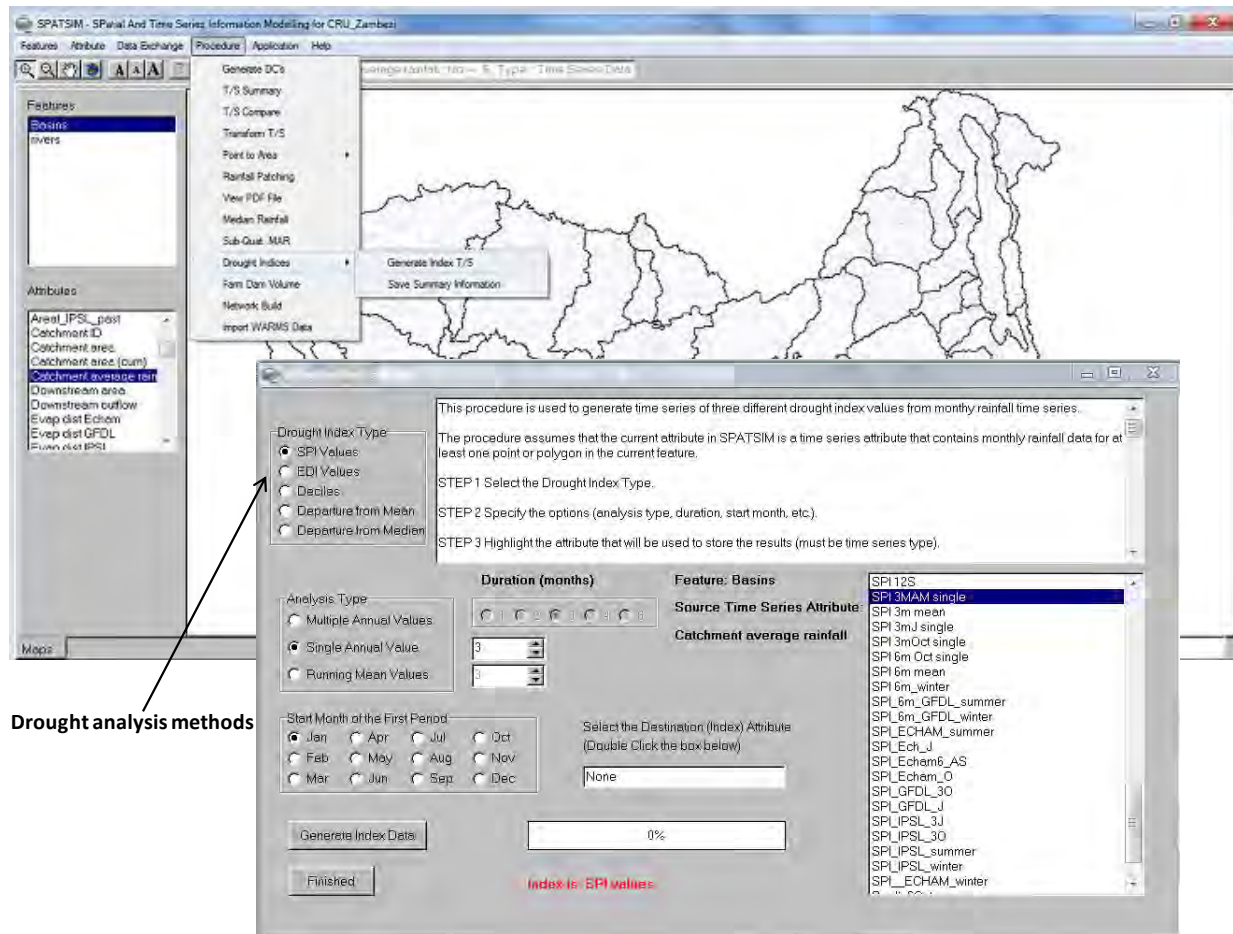


Figure 4.6 Procedure for generating and saving time series SPI

iii. The full time series of the SPI can be graphically visualised using the TSOFT facility which is a generic time series data display and analysis tool in SPATSIM (see Figure 4.7).

iv) A sample of the drought indices for all the spatial elements of a map (sub-basins for example) can be stored in an array attribute to facilitate rendering the map based on the index values for catchments in a specific year (see Figure 4.8).

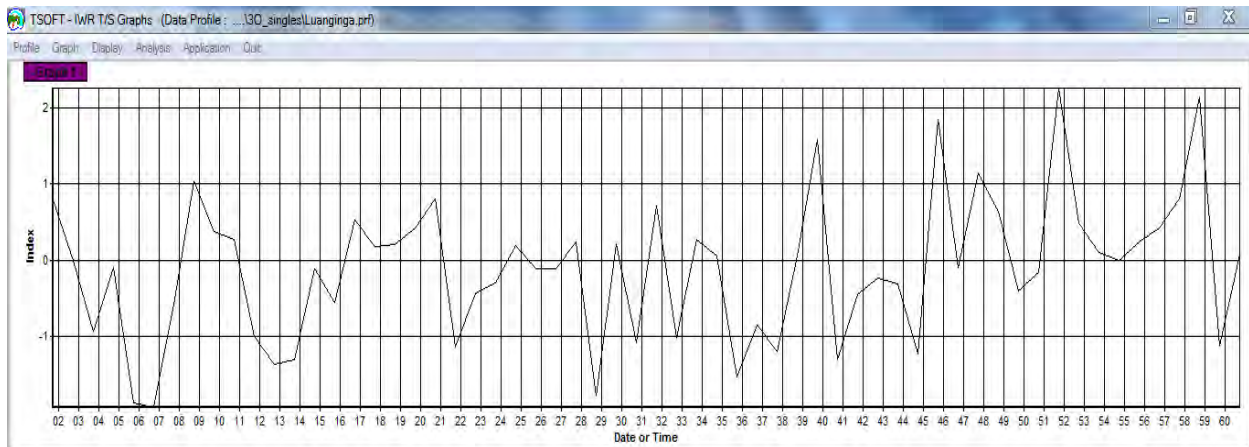


Figure 4.7 Time series of SPI plotted in TSOFT

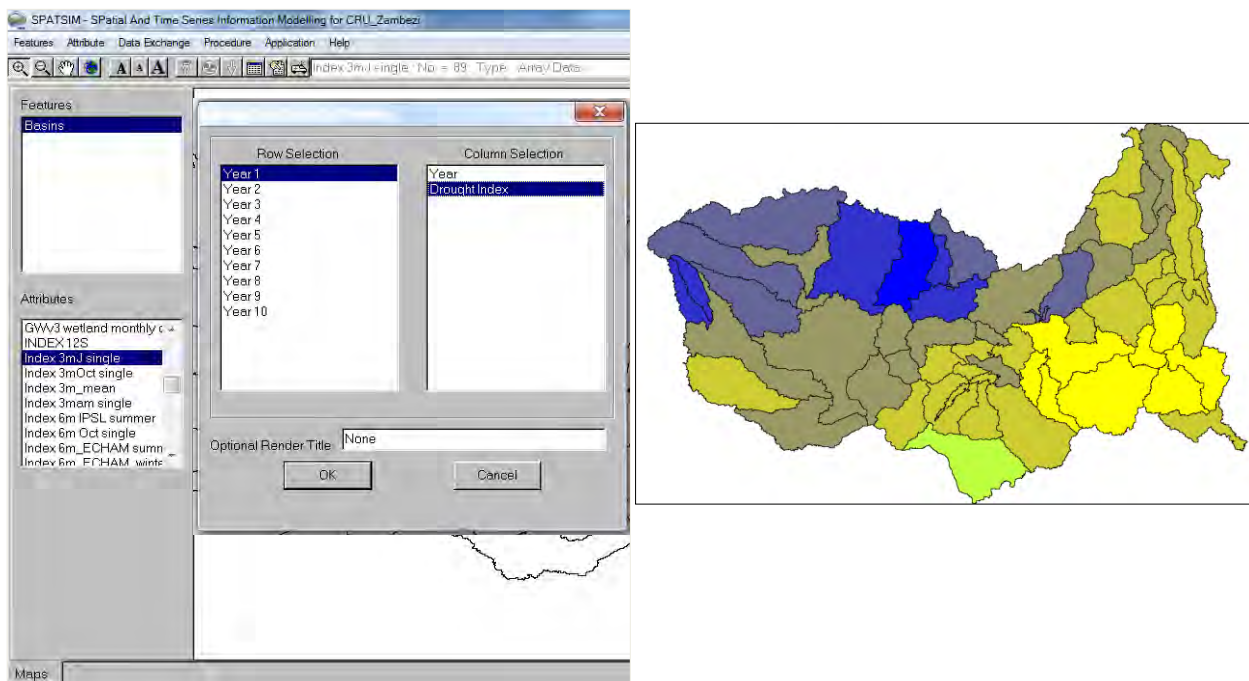


Figure 4.8 Starting the render process and generating maps in SPATSIM

4.2.4 Applications - External linkages to SPATSIM

External models or data analysis programmes that are developed outside SPATSIM can be linked in various ways to data stored within the database. A variety of applications are available and these include, TSOFT, (Hughes and Forsyth, 2006). TSOFT can be used to display multiple time series data and, in association with rainfall-runoff modelling, it can be used to visually compare the observed and the simulated time series (Figure 4.9). A number of standard analysis

methods such as seasonal distributions, flow duration curves and scatter plots are also provided in TSOFT. Statistical relationships and objective functions can also be calculated within the scatter plot option (Figure 4.10).

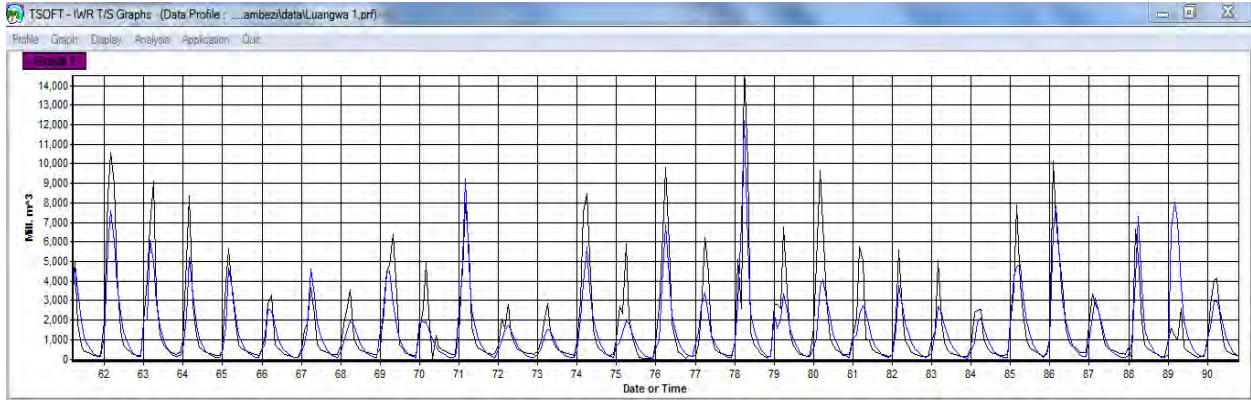


Figure 4.9 Comparison of simulated and observed time series data in TSOFT

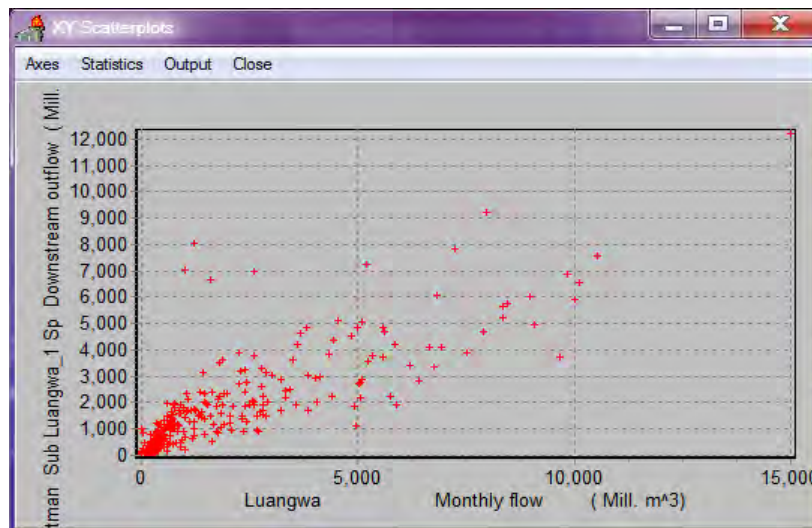


Figure 4.10 TSOFT scatter plot display of simulated versus observed streamflow

A wide range of models are also available to link with SPATSIM, which facilitates data exchanges between the models and the SPATSIM attribute database. These models include general hydrology and data analysis models, rainfall-runoff models which include the modified Pitman model (Hughes et al., 2006) that has been used in this study, water resource systems models, flood models and environmental flow requirement models.

4.3 The Pitman model

The Pitman model (Pitman, 1973) is a conceptual semi-distributed monthly time-step rainfall runoff model. The model consists of conceptual tank type storages (interception, soil moisture and groundwater) that are linked by functions to represent hydrological processes at the catchment scale. The main inputs to the model are a time series of monthly rainfall and monthly distributions of potential evaporation. Catchment area is also a necessary requirement for the model. Originally developed by Pitman (1973), the model has since undergone some modifications that are meant to account for challenges in data availability and to better quantify hydrological processes at the catchment level. In this study, a modified version of the Pitman model (Hughes et al., 2006) is used. The new version still maintains a large part of the original model structure as developed by Pitman (1973) but with additions of other components and functionalities. A more explicit representation of the ground water and surface water interactions as well as reservoir and wetland water balance functions have also been added (Hughes 1997, 2004b). During the process of modifying the model, an attempt was also made to ensure that some of the model components would be well adapted to the southern Africa context (Hughes et al., 2000; 2006). Such modifications included the consideration of channel losses in semi-arid basins and the incorporation of a channel routing component, especially for large river basins. A semi distributed approach is implemented in the revised version, where, sub-catchments are modelled independently with their own sets of parameters and input rainfall and evaporation data. Because of its ability to represent real catchment responses to runoff in southern Africa, the model has been widely applied to water resources assessment in the region (e.g. Hughes, 1997; Mazvimavi, 2003; Mwelwa, 2004; Hughes et al., 2006; Kapangaziwiri and Hughes, 2008; Sawunyama, 2008; Ndiritu, 2009; Hughes et al, 2010).

4.3.1 Structure and parameters of the modified Pitman model

This section gives a brief discussion of the Pitman model while in depth descriptions of the model can be found in various literature sources (e.g. Mwelwa, 2004; Hughes et al, 2006). A full description of the current version of the model and its algorithms can be found in Kapangaziwiri (2008). The main structure representing the model (with modifications) is given in Figure 4.11 while the model parameters including the reservoir parameters are presented in Table 4.2.

Manmade abstractions are also accounted for in the modified version of the model. A provision is made for direct abstractions and it is also possible for the abstracted water to be returned back to the channel. A new wetland function was also developed during the course of this study, partly as a response to the identified needs in the Zambezi basin and in other basins that also contain wetlands. The function was formulated based on the previous methods by Bailey and Pitman (WR2005) for the Kafue catchment and has been added as part of the reservoir model component. In Figure 4.11 the wetland function becomes an optional replacement for the reservoir model component. The Pitman model components are generally classified into surface processes, subsurface processes, groundwater storage and discharge processes, routing processes and water use activities.

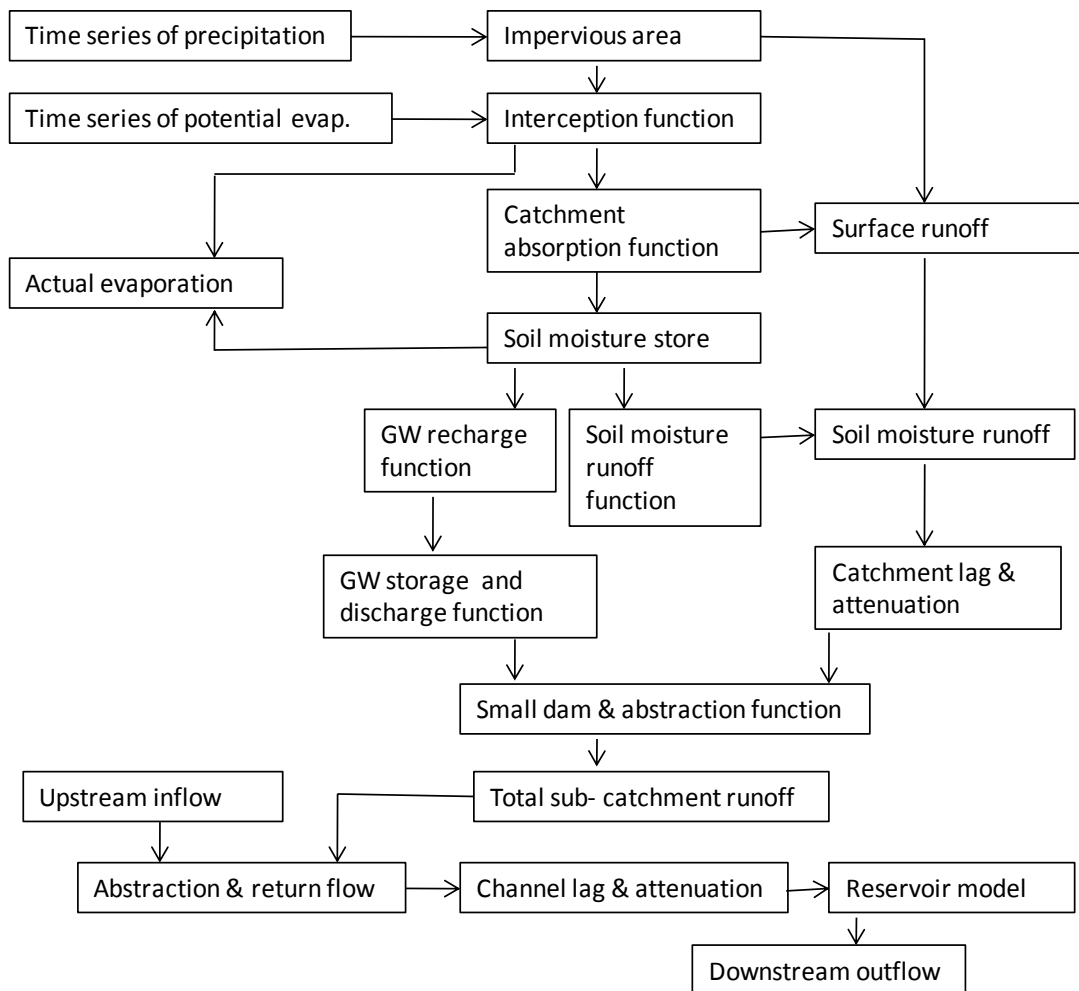


Figure 4.11 Schematic of the main components of the Pitman model (Source: Hughes et al., 2006)

Table 4.2 Pitman model, reservoir and wetland model parameters

| Parameter | Units | Parameter description. |
|--------------------------|---------------------------------|--|
| RDF | | Rainfall distribution factor |
| AI | Fraction | Impervious fraction of the sub-basin |
| PI1 and PI2 | mm | Interception storage for two vegetation types |
| AFOR | % | % area of sub-basin under vegetation type 2 |
| FF | Fraction | Ratio of potential evaporation rate for Veg2 relative to Veg1 |
| PEVAP | mm y ⁻¹ | Annual potential evaporation (typically based on S-pan values) |
| ZMIN | mm month ⁻¹ | Minimum sub-basin absorption rate |
| ZAVE | mm month ⁻¹ | Mean sub-basin absorption rate |
| ZMAX | mm month ⁻¹ | Maximum sub-basin absorption rate |
| ST | Mm | Maximum moisture storage capacity |
| SL | Mm | Minimum moisture storage below which no GW recharge occurs |
| POW | | Power of moisture storage-runoff equation |
| FT | mm month ⁻¹ | Runoff from moisture storage at full capacity (ST) |
| GPOW | | Power of moisture storage-GW recharge equation |
| GW | mm month ⁻¹ | Maximum groundwater recharge at full capacity (ST) |
| RSF | % | Controls the riparian evaporation losses from GW storage |
| R | | Evaporation-moisture storage relationship parameter |
| TL | Months | Lag of surface and soil moisture runoff |
| CL | Months | Channel routing coefficient |
| D.Density | km km ⁻² | Drainage density |
| T | m ² d ⁻¹ | Groundwater transmissivity |
| S | Fraction | Groundwater storativity |
| GW Slope | Fraction | Initial groundwater gradient |
| Optional reservoir model | | |
| A,B | | Parameters in non-linear area-volume relationship |
| ResCap | Mm ³ | Reservoir capacity |
| DEAD | % | Dead storage |
| INIT | % | Initial storage |
| Res 1-5 | % | Reserve supply levels (% full capacity) |
| ABS | Mm ³ y ⁻¹ | Annual abstraction volume |
| COMP | Mm ³ y ⁻¹ | Annual compensation flow volume |
| Optional wetland model | | |
| RWV | Mm ³ | Residual wetland volume |
| WV | Mm ³ | Initial wetland volume |
| QCAP | Mm ³ | Channel capacity for spillage |
| RFF, AA & BB | Mm ³ | Return flow factor, scale & power in the return flow equation. |
| CSF | Fraction | Channel spill factor |

Rainfall distribution function: A rainfall distribution function (RDF) is used to distribute the monthly rainfall depths into four periods. According to Hughes et al. (2006), lower RDF values represent a more even spread of rainfall and the impact is more prominent with higher total rainfalls. In the original Pitman model this parameter was fixed at a value of 1.28 but in this study it was varied between 0.8 and 1.0, partly based on the values used by Mwelwa (2004) for the Kafue basin.

Interception parameters: Before precipitation reaches the ground surface, it is intercepted by vegetation. This interception is dealt with in the model through two interception storage parameters PI1 and PI2 (for vegetation types 1 and 2). In any given month, the amount of rainfall intercepted is derived from the relationship between the parameter PI and rainfall depth and any demands from potential evaporation can be partially satisfied by the interception storage. Vegetation types 1 and 2 are frequently treated as natural and plantation vegetation, although in the model the two can be used to represent any two dominant types of vegetation in the catchment. A parameter AFOR is also specified and it represents the proportion of the catchment area that is under vegetation type 2. In previous applications of the model in southern African conditions, the parameters PI1 and PI2 have been assumed to be fixed at 1.5 mm and 4 mm respectively (Kapangaziwiri, 2008) and these values have also been adopted in this study.

Surface runoff parameters: Three sources of surface runoff are defined in the model, namely runoff from impermeable surfaces, infiltration excess and moisture storage excess. The absorption capacity of the basin in response to different rainfall rates is controlled through three surface runoff parameters ZMIN, ZMAX and ZAVE. These parameters are measured in mm month⁻¹ and they describe the shape of a triangular distribution which determines the amount of rainfall that can be absorbed at rates that vary from a minimum to a maximum value. ZMIN varies seasonally and a parameter, ZAVE, is used to allow for an asymmetric triangular distribution. A parameter AI represents the proportion of the basin that is impermeable and it is used in calculating runoff from the impervious surface.

Soil moisture storage and runoff parameters: As infiltration increases, the soil moisture storage also increases. The parameter ST (mm) represents the maximum value of the soil moisture storage. The soil moisture is, however, depleted through evaporation, interflow and recharge to

ground water. All moisture storages above the groundwater are represented in the model by the parameter ST. A non-linear relationship is assumed between interflow runoff and soil moisture storage, this relationship being controlled by a power function, POW. The interflow runoff rate at a storage of ST is defined by the parameter FT, the maximum rate (mm month^{-1}) of interflow runoff. If ST is exceeded in any month, the excess also contributes to runoff (saturation excess runoff).

Evapotranspiration from the soil moisture store: A parameter, R, is used to define the relationship between the ratio of actual evapotranspiration to potential evapotranspiration and the current level of soil moisture storage. R varies between 0 and 1 ($0 \leq R \leq 1$). More effective evapotranspiration loss is achieved at low values of R and this would be normally associated with deep rooted vegetation. Evapotranspiration losses are expected to be different between the two vegetation types and a parameter FF is used as an evapotranspiration scaling factor for vegetation type 2.

Groundwater recharge parameters: The parameters SL, GW and GPOW are used to define the groundwater recharge function. In the PitmanGW version, the parameter GW is used to define the maximum groundwater recharge rate. GPOW defines the power of the relationship between the current soil moisture store and recharge through which the recharge at different moisture levels can be quantified (GW and GPOW are the recharge equivalents of FT and POW in the interflow runoff function).

Groundwater discharge parameters: The groundwater response processes are defined through a composite set of parameters namely, drainage density (DDENS), transmissivity (T), storativity (S), regional groundwater slope (GW slope) and the riparian strip factor. Drainage density (km km^{-2}) is defined as the ratio of total channel length to the basin area. Transmissivity (m^2d^{-1}) is a product of the thickness of the saturated aquifer and its permeability. Storativity refers to the aquifer's capacity to hold water. GW slope represents the regional groundwater gradient that influences the drainage from an upstream to a downstream sub-basin. The riparian strip factor (RSF,%) controls the evaporation losses from the groundwater storage through areas in the margins of the channel. RSF is represented as a percentage of the total slope element width over which the evapotranspiration process is active.

Routing parameters (TL and CL): The parameter TL is a sub-basin routing parameter which represents the runoff time lag as it relates to the surface and soil moisture runoff components. The Muskingum routing equation is used to define the lag parameters. The parameter CL is a channel routing parameter that is used for large basins where attenuation, even at the monthly scale is possible (Hughes et al., 2006).

The main reservoir parameters: A set of reservoir water balance model parameters has been incorporated into the Pitman model. The main inputs to the reservoir water balance are rainfall and inflow from the upstream catchments. The outputs include evaporation, abstractions, spills, environmental water requirements and compensation flow. Operating rules based on reduced requirements related to a decrease in reservoir storage are used for abstraction, compensation and environmental water requirements. The main requirements of the reservoir model are monthly distributions of normal drafts given as a fraction of the annual abstraction requirement (parameter ABS). ABS is given in million cubic meters ($m^3 \cdot 10^6$). Compensation flows are given as fractions of the annual compensation flow requirement, COMP ($m^3 \cdot 10^6$) and up to five reserve supply levels (RES 1-5) are used as monthly distributions of drafts and compensation flow. The reserve levels are given as a percentage of the reservoir's full capacity.

The wetland model: A wetland function was developed at the Institute for Water Research and incorporated into the modified Pitman model during the course of this study which was conducted in parallel with other studies on large basins in southern Africa (Tshimanga, 2012). In the previous applications of the model the reservoir component of the model was used to represent storage as a 'dummy dam' but it was realised that the wetland dynamics were not being adequately simulated. This development was shared between this project and parallel projects on the Congo and Okavango basins. In the Zambezi basin, the development was used to improve some previous work that had been reported on the Kafue flats (WRC, 2008). The new wetland component is designed to account for the water balance of natural lakes and wetlands. Important parameters in the wetland model include:

Local catchment area (km^2): the area directly contributing runoff to the wetland (as opposed to contribution from upstream via channel outflows). It is also used to represent the maximum possible area of inundation.

Residual wetland volume (RWV, $m^3 \cdot 10^6$): the nominal storage capacity for that part of the wetland which is permanently inundated and below which there are no return flows to the channel.

Initial wetland volume (WV, $m^3 \cdot 10^6$): the water stored on the wetland at the start the model run, typically dependent upon the seasons.

Channel capacity for spillage (QCAP, $m^3 \cdot 10^6$): the monthly threshold volume of the river channel below which there is no spillage onto the wetland.

Channel spill factor (fraction): the proportion of the flow volume above the channel threshold that spills onto the wetland. The spill fraction ranges between 0 and 1 depending on the situation. In the case of lakes, where the river channel flows directly into the lake, the channel spill factor would be set to 1 and the capacity for spillage to 0, this is to ensure that all of the flow enters the lake or reservoir.

Return Flow Factor (RFF): a fraction that is limited to a maximum value of 0.95 and which determines the amount of water from the wetland that is returned to the channel (RFV) and contributes to downstream outflow. The return flow volume is given as:

$$RFV = RFF * (WV - RWV) \quad 4.4$$

The relationship between wetland storage and return flow is given as:

$$RFF = AA * (WV/RWV)^{BB} * QCAP/Q \quad 4.5$$

where, AA is the return flow constant, BB is the power of the equation in a nonlinear relationship, Q is the flow into the river channel. The QCAP/Q part of the equation is designed to limit the return flow when the channel flow is high and spilling onto the wetland.

The area-volume relationship; is a nonlinear relationship presented by equation 4.6 and is used to determine evaporation losses from the wetland.

$$\text{Area (km}^2\text{)} = a \cdot (WV)^b \quad 4.6$$

where, a and b are empirical scaling (a) parameters and power (b). Losses from the wetland include the evaporative losses (mm) based on the current wetland inundation area and potential evapotranspiration and water use abstractions ($\text{m}^3 \cdot 10^6$) based on an annual demand and a seasonal distribution.

4.4 Setting up the Pitman model in SPATSIM

The Pitman model for the Zambezi River basin is set up in SPATSIM and the steps followed include creating the necessary features by loading shapefiles of all the relevant spatial elements which consist of the sub catchment polygons, raingauge and streamflow gauging station points and rivers (lines). Table 4.3 provides the attributes that are necessary for the model. The Pitman model can be run in SPATSIM either through the ordinary version which uses a single parameter set to perform manual calibrations or through the uncertainty version of the model where a range of parameter values (upper and lower bounds) are used to generate an ensemble of outputs. The Pitman model has been modified by incorporating an uncertainty framework to enable the assessment and quantification of the uncertainties in parameters and in the input climate data. The uncertainty framework (Hughes et al., 2010; 2011a) makes use of a range of parameter values which incorporate the lower and upper bounds and the probability distribution as inputs to the model. A Monte Carlo approach is used to sample the possible parameter space and an ensemble of output results. Independent sampling is applied to the parameters of each sub-catchment in the semi-distributed model. The sampling process is based on either a uniform distribution which requires input of the minimum and maximum values of the parameters or on a normal distribution in which case the mean parameter values and standard deviations are specified and all the samples are constrained within the minimum and maximum limits of the parameter values. The full time series of simulated flows for each ensemble are stored within the SPATSIM database and can be examined in detail using the normal SPATSIM utilities. In addition, two text files for each sub-catchment are generated which summarise the ensemble outputs. The first text file consists of all the parameter values and some summary statistics, including mean monthly flow, mean monthly recharge and the flows for three % points (10, 50 and 90) of the simulated flow duration curves. If observed data are available for a specific sub-catchment a set of objective functions are included for each ensemble. These are the percentage bias between the mean monthly flows (observed and simulated) and the Nash-Sutcliffe

coefficient of efficiency (Nash and Sutcliffe, 1970) based on the normal and transformed values. The transformed values are used to eliminate the large influence of high flows and to emphasise the role of low flows. The second text file consists of three time series defining the range of the ensemble outputs. For each month of the time series all of the ensemble values are sorted and the 5% (upper), 50% (median) and 95% (lower) exceeded values written to the output. If observed data are available, these are included in this second text file. The results for both the ordinary and the uncertainty versions of the model are examined through TSOFT which provides both graphic views of the results and the goodness of fit statistics.

Table 4.3 Required attributes for the Pitman model

| Type | Attribute | Description |
|--------------------|--------------------------------|--|
| Text | Catchment ID | Identifies each of the sub-catchments |
| Text | Downstream area | Identifies links between sub-catchments |
| Single real number | Catchment area | Specifies the area (km ²) for all the sub-catchments |
| Array | Catchment model parameters | Represents the rainfall-runoff model parameters |
| Array | Mean monthly evaporation | Monthly distribution data of potential evaporation |
| Array | Mean monthly distribution | Monthly distribution weights of rainfall |
| Time series | Catchment average rainfall | Required for all the sub-catchments. |
| Time series | Observed monthly flows | Observed flow for a sub-catchment |
| Time series | Downstream outflow | Simulated flow at the outlet of each sub-catchment |
| Array | Reservoir model parameters | Represents the parameters of the reservoir model. Required where a reservoir is to be simulated. |
| Array | Reservoir monthly distribution | Normal and reserve drafts and seasonal distributions for the annual compensation flow. |
| Array | Wetland parameters | Parameters of the wetland model and used if a wetland is to be simulated. |
| Array | Wetland monthly distribution | Monthly distribution of potential evaporation over the wetland and monthly distributions of abstractions |

Due to the problem of ungauged catchments and issues of data paucity, the Pitman model is calibrated for the Zambezi River basin only at those sub-basins that are gauged and whose data are of reasonably long time series and with few missing gaps. These sub-basins are mainly on the mainstream of the Zambezi River as well as at the outlet of the Luangwa sub-basin. In addition

the Kafue and its sub-basins are also calibrated; this is mainly because of the long and consistent time series data found within the basin. The Angolan part of the basin is highly ungauged and it is therefore not possible to calibrate the model in this region. The gauging stations that are used for the calibration are indicated in Figure 4.12 (see also Table 3.9).

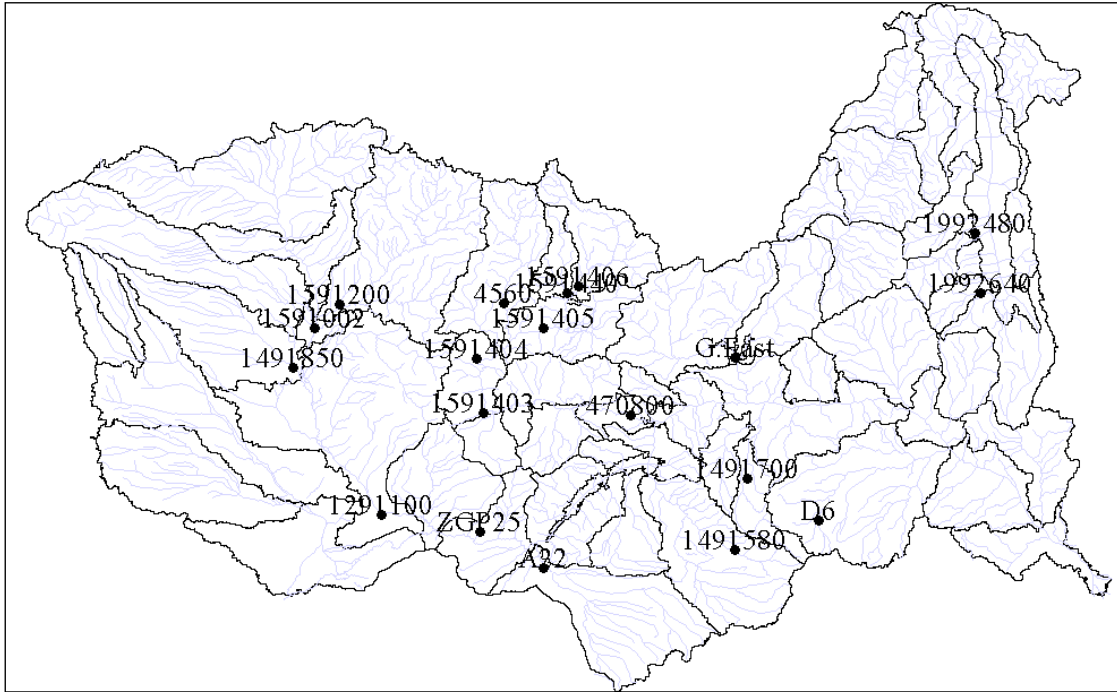


Figure 4.12 Flow stations used to calibrate the Zambezi River basin

4.5 Assessing the model performance

Various objective functions are used to assess the performance of the calibration process and these can be calculated in SPATSIM. They include the coefficient of determination R^2 which is described as the amount of variance in the observed data that is explained by the simulated data and is given as:

$$R^2 = \frac{[\sum (Q_o - \bar{Q}_o) * (Q_s - \bar{Q}_s)]^2}{[\sum (Q_o - \bar{Q}_o)^2 * (\sum (Q_s - \bar{Q}_s)^2)]} \quad 4.7$$

where, Q_o is the observed discharge, $Q_{o(m)}$ is the mean of the observed discharge and Q_s is the simulated discharge and $Q_{s(m)}$ is the mean of the simulated discharge. R^2 takes on values between 0 and 1 and a value of 1 indicates that the simulated value has incorporated all the variabilities in

the observed data, while a value of 0 shows a poor correlation of the variabilities. However, for hydrological purposes the R^2 function tends to be over sensitive to outliers and insensitive to the systematic differences between the observed and simulated values (Legates and McCabe, 1999). To circumvent this problem of systematic bias the Nash Sutcliffe coefficient of efficiency has become the commonly used statistic whose goodness of fit equation (Nash and Sutcliffe, 1970) is given below; its advantage is that it is sensitive to systematic error and therefore it is a better statistic than the R^2 value.

$$CE = 1 - [\sum (Q_o - Q_s)^2 / (Q_o - \overline{Q_o})^2] \quad 4.8$$

The Nash Sutcliffe efficiency measures the variance of the observed flows as explained by the model. An efficiency value of 1 implies a perfect match between the observed and simulated values, whereas values less than 0 indicate an undesirable outcome in which the observed mean is deemed to be a better predictor than the model. When used together, big differences between CE and R^2 are an indication of systematic errors. In assessing the performance, normal and log transformed values are used. The logarithmic transformation eliminates the large influence of high flows and emphasises the role of low flows. Also available as a measure of performance is the % bias (% MeanDiff) between the observed and simulated mean monthly flows. This function is given as:

$$\% \text{ MeanDiff} = 100 * [(\overline{Q_s} - \overline{Q_o}) / \overline{Q_o}] \quad 4.9$$

where, $\overline{Q_s}$ is the mean of the simulated monthly flow and $\overline{Q_o}$ is the observed mean monthly flow. A percentage difference of $\pm 5\%$ is considered to be a target for successful calibrations. Another measure that can be used is the % difference of standard deviations (%STD) between the mean monthly flows and it is given by the equation by the equation:

$$\% \text{ STD} = 100 * [(\text{STD}_s - \text{STD}_o) / \text{STD}_o] \quad 4.10$$

where, STD_s is the standard deviation of the simulated flows and STD_o is the standard deviation of the observed flows.

4.6 SPI, soil moisture and regional food security relationships

One of the objectives of this study is to explore the relationship between food security and drought conditions in the Zambezi basin. An assessment is carried out to establish the relationship between SPI and agricultural yield and between the agricultural yield and the soil moisture estimates that are simulated by the Pitman model. The study also examines whether the soil moisture estimates and SPI vary together and seeks to determine which of the two variables would be appropriate for defining droughts in the Zambezi basin.

4.6.1 Drought and food security relationships

The impact of drought on food security in the Zambezi basin is assessed through a correlation of the SPI with maize yield statistics and of the simulated soil moisture with maize yields. Maize is chosen because it is common to the basin countries. The crop production statistics are obtained from FAOSTAT (2012) and detrended crop yield data are used for the analysis. Apart from climate variability there are other factors that may affect crop yield. Such factors include economic, policy, management and technological improvements, a theoretical example showing the effect is given in Figure 4.13 (Gommes, 1999). The yield data therefore needs to be detrended in order to separate the climate related impacts and to enable the analysis of more frequent shifts that may be due to climate variability. The detrending process is also meant to remove long term changes but not short term variations. A relative detrended yield which incorporates factors other than climate is obtained to represent the deviation of the yield values from the long term trend while the absolute detrended yield represents a projection of the yield with respect to a current season.

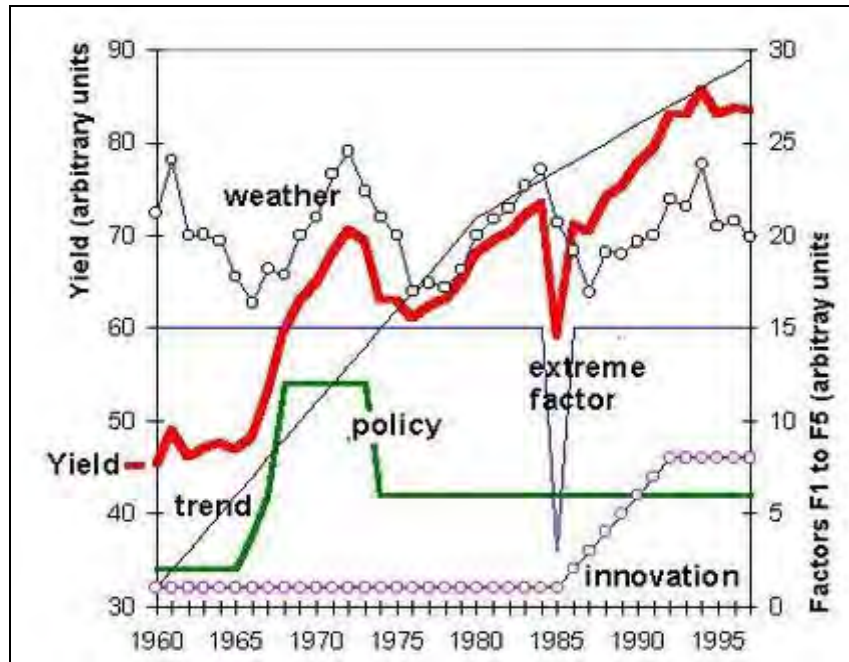


Figure 4.13 An example showing the impacts of various factors on agricultural yield-red line. (source: Gomme, 1999)

Detrending the maize yield

For n observed years, the first step in detrending involves calculating the predicted normal yield ($Y_{\text{predicted}_i}$) for each of the years, i , by fitting a regression curve through the observed yield data Y_i . The predicted yield is given as:

$$Y_{\text{predicted}_i} = A * \text{Year}_i + B \quad 4.11$$

Where, A and B are the slope and intercept of the yield data for n years respectively and i represents the i^{th} year in the series.

The detrended yield, Y_{DT_i} (absolute) is obtained as:

$$Y_{\text{DT}_i} = (Y_i - Y_{\text{predicted}_i}) + Y_{\text{predicted}_n} \quad 4.12$$

where $Y_i - Y_{\text{predicted}_i}$ represents the relative detrended yield. $Y_{\text{predicted}_n}$ is the yield forecasted for the last year of the record and gives an absolute detrended yield which is used for analysing the food security and drought relationships (Gomme and Hoefsloot, 1998). Figure 4.14 represents the detrending process in a graphical form.

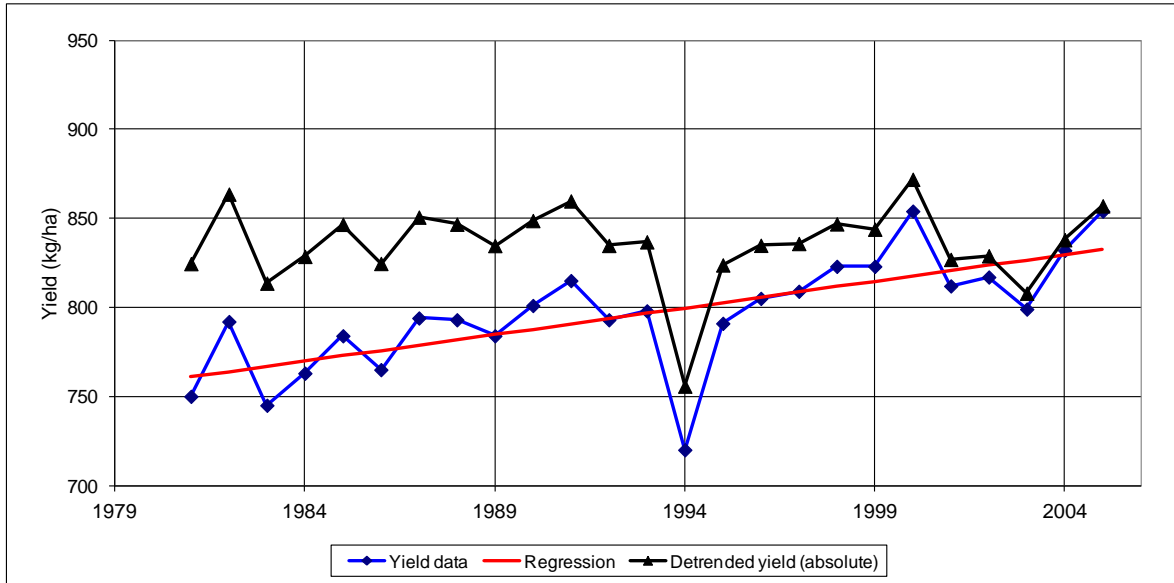


Figure 54.14 Graphical representation of the detrending process

4.6.2 SPI and soil moisture relationships

In addition to Pearson's correlation, the wavelet analysis method (Torrence and Compo, 1998) is performed to establish the correlation between SPI and soil moisture. This procedure is performed using online interactive wavelet plot software provided by the University of Colorado (<http://paos.colorado.edu/research/wavelets/>). Wavelet analysis is an extended method of Fourier spectral analysis (Torrence and Compo, 1998; Torrence and Webster, 1999) and the method has an advantage over other methods of correlation in that the output signal incorporates the time localisation of the frequencies by simultaneously decomposing the time series into time and frequency domains. This method provides information on the amplitude of any cyclic signal within a time series and on how the amplitude varies with time. The wavelet transform function, W_n , for a time series X with x_n values and a localised time index of n is defined as the inner product (convolution) of x_n with a wavelet scale, s , and a wavelet ψ_x and it is given by the equation:

$$W_n(s) = \sum_{n'}^{N-1} x_{n'} \psi_m * \left[\frac{n' - n \delta t}{s} \right] \quad 4.13$$

where, δt is the sampling period, N is the number of points in the time series (x) and $*$ denotes a complex conjugate. The Morlet wavelet is used in this study and it consists of complex exponential that is modulated by a Gaussian function ψ .

$$e^{i\omega t/s} e^{-t^2/(2s^2)}, \text{ where, } \omega \text{ is a nondimensional frequency and } s \text{ is the wavelet scale.}$$

A two dimensional wavelet power spectrum representing a measure of the time series variance of time for a certain period is then constructed by plotting the wavelet amplitude and phase (Figure 4.15). The x-axis shows the wavelet location in time and the y-axis gives the wavelet period in years. To test for significance in the peaks, a Fourier spectrum background is chosen while the global wavelet spectrum is chosen to test for the non-stationary changes in variance (Kestin et al., 1998). A chi-square distribution of the wavelet power spectrum about the global wavelet spectrum is then presented.

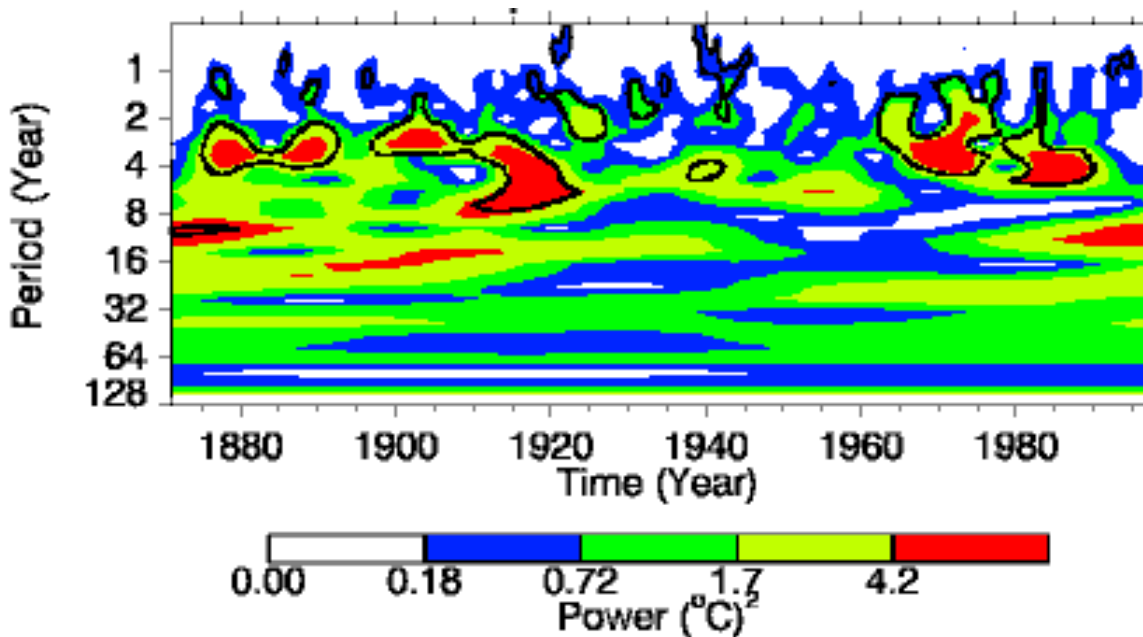


Figure 4.15 Example of Morlet Wavelet power spectrum showing El Niño activity (source: www.paos.colorado.edu/research/wavelets)

The Morlet wavelet function is used to smooth the global wavelet spectrum in a Fourier space. Figure 4.15 is an example of a wavelet spectrum showing the activity of El Niño with respect to global temperature between the years 1880-2000. The x -axis represents the wavelet location in time and the y -axis is the wavelet period in years. The red areas (in contours) indicate that high

El Niño activity occurred during 1880-1920 and from 1965 onwards while there was not much activity between 1920-1960. The figure also shows a larger power of the spectrum in the 2-7 year period indicating that El Niño events are predominated by 2-7 year cycles. Although not as frequent as the 2-7 year cycles there is also evidence of 16 year cycles of the events. Wavelet coherency is then used to establish the similarity or relationship between different time series (Tang and Piechota, 2009). This is done by identifying the frequency bands at which the time intervals of the two time series are related. Coherency is used in this study to determine how well the simulated soil moisture is represented relates to agricultural droughts (SPI) in the Zambezi basin. The coherency, R is given as:

$$R^2(s) = \frac{\left\langle s^{-1} W_n^{XY}(s) \right\rangle^2}{\left\langle s^{-1} |W_n^x(s)|^2 \right\rangle \left\langle s^{-1} |W_n^y(s)|^2 \right\rangle} \quad 4.14$$

where, $\langle \rangle$ indicates smoothing in both time and scale, $W_n^X(s)$ and $W_n^Y(s)$ represent the wavelet transforms of two time series X and Y. $W_n^{XY}(s)$ is the cross-wavelet spectrum of X and Y which is defined as:

$$W_n^{XY}(s) = W_n^X(s) W_n^{X*}(s) \quad 4.15$$

4.7 Methods of detecting trends and changes in hydrological variables

Detecting trends and changes in the historical time series of hydrological data is fundamental to informing what the future may be like and can therefore be used as a basis for water resources planning. It is also necessary to detect trends and patterns in historical hydrological events if the effect of climate change on hydrological systems is to be established. There are various ways in which change can occur in a time series. It can occur gradually (a trend), or abruptly (a step change) and it can also occur in a more complex form that may affect the mean, median, variance, autocorrelation, or almost any other aspect of the data (Kundzewicz and Robson, 2004). Other common properties of a time series include oscillations, seasonal effects and randomness. In order to determine variability and trends in climatology, it is recommended by WMO (2000) to use long term rainfall and runoff data of at least 30 years. Simple statistical parameters of the mean, standard deviation, coefficient of variation as well as running means are

used to characterise the rainfall and streamflow patterns in the Zambezi River basin. Non-parametric distribution free tests are the most commonly used methods as they make few assumptions, if any, about the distribution of the dependent variable in the population.

Simple regression analysis is used to determine rainfall-runoff relationships while the distribution-free Cumulative Sum test (CUSUM) together with bootstrapping are used for step change detection. Fourier transform spectral analysis is undertaken to investigate any cyclic behaviour within the long term time series. The Mann-Kendall test and Sen's slope estimator are used to detect for trends and magnitude of change. To enable comparison between and within different sets of data, anomalies are used and these are calculated as fractional deviations from the long term means of hydrological variables.

Several methods are available for the detection and quantification of significant trends. These include graphical methods whereby visual estimates of the trend are derived from the graphical plots, but with no quantifiable results. Regression and correlation analysis methods are important in trend analysis for establishing the variation in a dependent variable with the variation in the independent variable and for estimating the strength of the relationship between the two variables. Non-parametric tests such as the Mann- Kendall method (Mann, 1945) have an advantage over linear regression methods in that they are less affected by outliers. The Mann-Kendall method is a non-parametric test which seeks to determine trends through the existence, or non-existence, of slope which is then related or transformed to statistical parameters of evaluation (Mann, 1945). Sen's test estimates the magnitude of the slope or change and the confidence interval for the slope (Sen, 1968). Two parameters that are of importance are the significance level of the trend and the slope magnitude, which provides the direction and magnitude of the trend.

4.7.1 Tests for trends

Graphical methods make use of a visual estimate of the presence or absence of a trend but with no quantifiable results. Linear regression provides an estimate of the slope, confidence interval, and quantifies goodness of fit. It allows quantified estimates of the influence of multiple independent variables but does not handle missing data and may be greatly affected by outliers and cyclic data (Brauner, 2012). The Box-Jenkins Model method tests for trends in long term,

regularly spaced data, however, large data sets of constant temporal spacing are required (Box and Jenkins 1976).

The Mann-Kendall test: The Mann-Kendall test is a nonparametric rank-based method has been used in this study to detect the presence or absence of trends in linear and nonlinear time series data (Kendall, 1975). It has also been used widely in other studies (e.g. Ndiritu, 2005; Kampata et al., 2008; Karpauzos et al, 2010) to detect trends in rainfall, runoff and even in water quality variables. This approach is robust in the sense that it is capable of dealing with extremes and outliers and can also be applied to skewed variables and to non-normally distributed data (Hamed, 2008; Burns et al., 2007). A standard normal variate, Z and a test statistic, S , are used to estimate the significance of a trend slope of a linear trend model and $\text{var}(S)$ is the variance in S . Z is given as:

$$\begin{aligned} Z &= \frac{S - 1}{\sqrt{\text{var}(S)}} && \text{if } S > 0 \\ Z &= 0 && \text{if } S = 0 \\ Z &= \frac{S + 1}{\sqrt{\text{var}(S)}} && \text{if } S < 0 \end{aligned} \tag{4.16}$$

where S is presented by the equation:

$$S = \sum_{k=1}^{n-1} \sum_{j=k+1}^n \text{sgn}(x_j - x_k) \tag{4.17}$$

where, n represents the total number of elements in the time series. The sign function is given as:

$$\begin{aligned} \text{sgn}(x_j - x_k) &= 1 && \text{if } x_j - x_k > 0 \\ \text{sgn}(x_j - x_k) &= 0 && \text{if } x_j - x_k = 0 \\ \text{sgn}(x_j - x_k) &= -1 && \text{if } x_j - x_k < 0 \end{aligned}$$

A positive S value indicates that there is an upward trend while a negative value signifies a decreasing trend. Based on whether the calculated Z is greater or less than the critical Z -

statistic, the null hypothesis H_0 , which states that there is no trend in the data, is either rejected or accepted. The variance of S is calculated as:

$$\text{Var}(S) = \frac{1}{18} \left[n(n-1)(2n+5) - \sum_{p=1}^q t_p(t_p-1)(2t_p+5) \right] \quad 4.18$$

where, n is the number of data points, t_p is the number of ties for the p^{th} value and q is the number of tied values. A tie is a subset of the ordered data that comprises a sequence of the same value. $\sum t_p$ represents the summation over all ties.

Sen's method for the estimation of slope: Sen's test (Sen, 1968) is used to estimate the value and confidence interval for a trend and is normally used in conjunction with the Mann-Kendall's test. Time series of equally spaced data are required and the method makes no assumptions about the distribution of data, it is also not affected by outliers. In this method, slope is calculated as a measure of change with time and is given as:

$$Q_i = \frac{X_{i+t} - X_i}{t} \quad 4.19$$

where, Q_i is the slope between data points X_i and X_{i+t} and t is the time interval.

Sen's estimator of the slope, Q, is simply given by the median slope as:

$$Q = Q_{[(N+1)/2]} \quad \text{if } N \text{ is odd and} \quad 4.20$$

$$Q = (Q_{[N/2]} + Q_{[(N+2)/2]})/2 \quad \text{if } N \text{ is even} \quad 4.21$$

where, N is the number of calculated slopes

Sen's Method also allows determination of whether the median slope is statistically different from zero. To develop a confidence interval, the rank for the upper and lower confidence interval is estimated. The slopes corresponding to these ranks are used to define the actual confidence interval for Q. For a two-sided confidence interval about the median slope, the Zstatistic is first established for the required confidence level (e.g. $Z=1.96$ at 95% confidence interval). The variance, $\text{Var}(S)$ of the Mann-Kendall statistic is then calculated as given in equation 4.16.

The range of ranks for the specified confidence interval, C_α is estimated using the equation

$$C_\alpha = Z_{1-\alpha/2} * \sqrt{Var(S)} \quad 4.22$$

Using the value of C , the ranks of the lower ($M1$) and upper ($M2+1$) confidence limits are calculated using the following equations:

$$M1 = \frac{N - C_\alpha}{2}$$

$$M2 = \frac{N + C_\alpha}{2} \quad 4.23$$

The slope corresponding to the ranks $M1$ and $M2+1$ as the lower and upper confidence limits respectively is then calculated. This slope is defined as statistically significant if zero (for the selected confidence interval) does not lie between the upper and lower confidence limits.

4.7.2 Change point analysis

Change point analysis is used to determine whether a change has occurred within a time series and the method also detects the period when the change occurred. Change point analysis is also capable of estimating the significance of a change by providing confidence levels and confidence intervals. Various methods of detecting changes are available and these include; Pettitt's test (Pettitt, 1979), a robust rank-based method that tests for change in the median of a set of values, the Wilcoxon-Mann-Whitney test (Helsel & Hirsch, 1992), a rank-based method used to identify differences between two independent sample groups and the Kruskal-Wallis test (Siegel and Castellan, 1988) which is an alternative of the one-way analysis of variance if there are more than two variables to compare. This study makes use of the approach of Taylor (2000) to detect for changes in rainfall and streamflow time series. This method has been chosen because of its simplicity and also because a 'change point analyser' software tool (Taylor, 2000) is readily available for use. The advantage of using this method is that it is able to handle large amounts of data and it is also able to account for errors generated over time within the time series. The distribution-free CUSUM (cumulative sum) test is also a rank-based test that relies on the comparison of successive observations with the median of the time series. The method uses the maximum cumulative sum of the signs of the difference from the median as the test statistic series (Chiew & McMahon, 1993). In order to detect for change, the study applies a combination

of the Cumulative Summation (CUSUM) method and bootstrapping (Taylor, 2000; Parida et al., 2003). A CUSUM chart (Figure 4.16) is first generated. The CUSUM, C_{si} , for each data point A_i is given as:

$$C_{si} = C_{si-1} + (A_i - \bar{A}) \quad 4.24$$

where, S_{i-1} is the cumulative sum at the previous data point and the starting sum is set to zero. The CUSUM chart gives the picture of change through an analysis of the change of slope direction, where an increasing slope suggests periods where the values are consistently above the mean and a negative slope indicates values below the long term mean. If there was no systematic change in the mean values the, CUSUM is expected to fluctuate around zero (Taylor, 2000). In order to confirm the CUSUM changes, confidence levels are determined by performing a bootstrapping analysis. Bootstrapping is based on generating new data sets (resamples). The original data set is used as the distribution from which the resamples are chosen at random, with replacement (so that they can be chosen again). A large number of data sets are generated and a test statistic, in this study, an estimator of magnitude of change, C_{sdiff} , is calculated, and it is defined by the equation:

$$C_{sdiff} = C_{s \max} - C_{s \min} \quad 4.25$$

where, $C_{s \max}$ is the sum of the maximum values C_s of the data sets and $C_{s \min}$ is the sum of minimum C_s values of the data sets. The C_{sdiff} of the resamples are then ranked and the number of bootstraps for which C_{sdiff} is less than C_s (max-min) of the original data sample is calculated. If B , is the number of bootstraps and J is the number of bootstraps for which $C_{sdiff} < C_s$, then the confidence level is calculated as:

$$\text{Confidence level} = [100 * (J/B)] \% \quad 4.26$$

Typically, 90% or 95% confidence is required for a significant change to be identified. In order to obtain reliable significance level estimates, this study used 1 000 bootstraps for each sample.

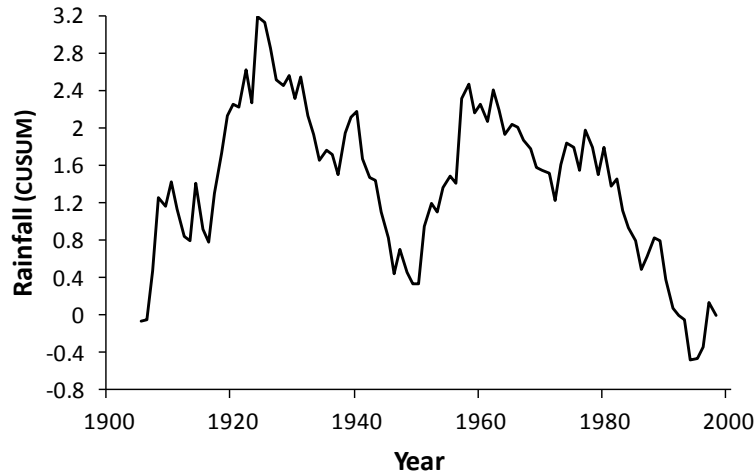


Figure 4.16 Example of a cumulative sum (CUSUM) plot (rainfall within the Barotse)

4.7.3 Spectral analysis

Spectral analysis is one of the methods that can be used to explore various kinds of periodic behaviour in time series under a frequency domain. The rationale behind spectral analysis is that a time series which is recorded at equal time intervals can be decomposed into a sum of trigonometric periodic functions with different frequencies, amplitudes and phases (Rauscher, 2001). Any periodicities in the time series are portrayed through spectral densities. Various forms of spectral analysis can be applied to seasonality studies. To establish the existence of cycles, this study uses the Fourier Transformation method which is included as part of the STATISTICA software package (StatSoft, Inc., 2009). Fourier analysis is a standard method for converting any time series data into its sine and cosine components which are then displayed in the form of a frequency spectrum. This method produces a series of spectra (spectral densities) or periodograms whose magnitude can be used to assess the presence of significant cycles (Shumway, 1988).

The Fourier series, X_i , is given as:

$$X_i = a_0/2 + \left(\sum_k \{a_k * \cos[2\pi f_k (t - 1)]\} + \{b_k * \sin[2\pi f_k (t - 1)]\} \right) \quad 4.27$$

where, X_i is the i^{th} element in the series. The frequency f_k is the number of cycles per unit time, a_0 , a_k (sine) and b_k (cosine) coefficients are the Fourier coefficients, which can be interpreted as regression coefficients that give the correlation between the cosine or sine function and the time

series data. For a number of observations in the time series, Q , successive frequencies are calculated as, k/Q , (for $k=0$ to $Q/2$). The period (p), given as, $1/f_k$, is the number of observations required to complete one cycle at frequency f_k .

The sine and cosine coefficients for a given time series are calculated as:

$$a_k = \frac{2}{Q} \sum_{t=1}^Q X_t \sin\left(\frac{2\pi p t}{Q}\right) \quad 4.28$$

$$b_k = \frac{2}{Q} \sum_{t=1}^Q X_t \cos\left(\frac{2\pi p t}{Q}\right) \quad 4.29$$

The magnitude of the spectrum (periodogram) is the basic measurement of the Fourier transformation (Rauscher, 2001). For each time series, the periodogram, I_k , is given by the equation:

$$I_k = \frac{Q}{2} \left(\sum_{f_i} a_k^2 + b_k^2 \right) \quad 4.30$$

Spectral densities on the other hand are derived from smoothed periodograms and they are used to represent frequency regions that are significant to the time series. Examples of periodogram and spectral density plots are presented in Figure 4.17 using the historical rainfall of a sub-basin in the Zambezi. The spectra show that the most predominant cycle to be 10 years based on the magnitude of the periodogram or the spectral density.

The standardised cumulative periodogram, C_k of a series X_i is given as:

$$C_k = \frac{\sum_{p=1}^j I_p}{Qs^2} \quad 4.31$$

where, s is the standard deviation of X_i and k is an integer value (1,2,...,Q/2-1). Two statistical tests, the Fisher's Kappa statistic and Bartlett's Kolmogorov-Smirnov test (Fuller, 1976) are used to test for white noise (background noise) in spectral analysis. The Bartlett's Kolmogorov-Smirnov test is used to test whether there is a significant difference between the observed

periodogram and that of white noise (whether the observed cycles are random or not). The Fisher's Kappa statistic indicates whether there is a significant difference between the largest periodogram value, I_k and the mean of all the periodograms.

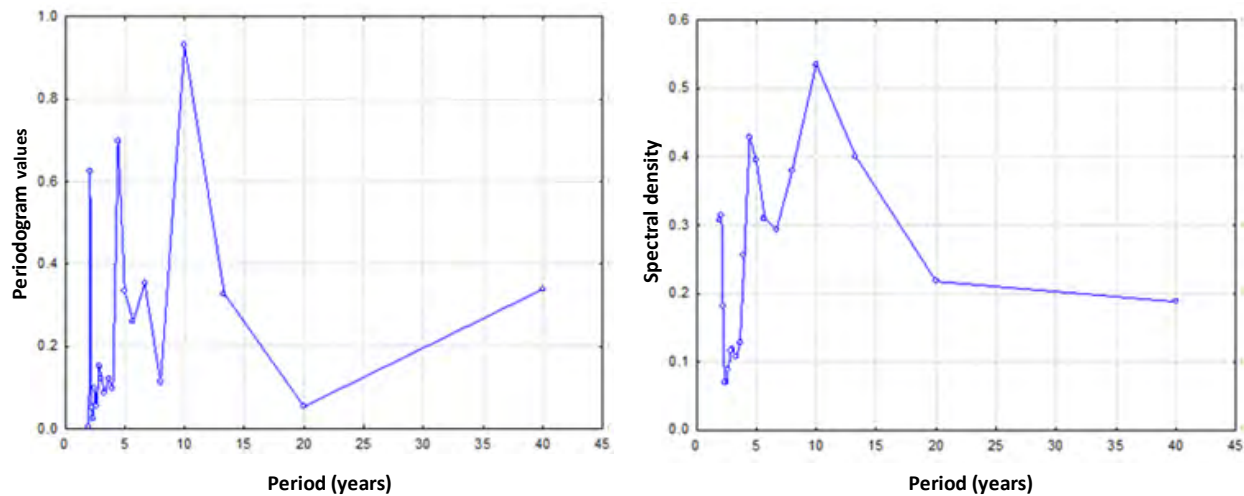


Figure 64.17 Illustration of a periodogram and spectral density (station 21554, Zambezi)

4.8 Scenarios for climate change

Quantifying the impacts of climate change based on hydrological data is frequently made difficult by the fact that available records are often very short. Challenges are also encountered in linking the data outputs of GCMs to the data input requirements of a basin scale hydrological model. However, it is still important that future climate change predictions be made for purposes of planning and for the sustainability of water resources.

To evaluate the climate change impacts on water resources in the Zambezi basin, three GCM model outputs are used to force the Pitman rainfall runoff model. These GCMs were downscaled by the Climate Systems Analysis Group (CSAG) at the University of Cape Town. Although the CSAG has to date downscaled a number of GCMs (≥ 10), only three GCMs; ECHAM, GFDL and IPSL were used in this study because they were the ones readily available and they also have extensive spatial coverage compared to the other GCMs that have been downscaled for the area of study. The CSAG datasets consist of daily rainfall, maximum and minimum temperatures for a baseline period (1961 to 2000), a near future (2046 to 2065) scenario and a far future (2081-2100) scenario. The GCMs are based on the SRES A2 emission scenario which represents high

population growth and less rapid economic development. The GCMs are empirically downscaled (Hewitson and Crane, 2006; Hewitson et al., 2005) to a 0.25° resolution (about 25km). The aim of empirical downscaling is to establish quantitative relationships between the global scale circulations and the local climate. The downscaling method used in this study (Hewitson and Crane, 2006) uses artificial neural networks to derive such relationships. Unlike the traditional empirical downscaling methods that rely on statistical relationships between the global circulations and the local climate characteristics and thus constrained by the assumptions of the statistical model, the artificial neural networks' method removes the constraints by deriving direct mathematical relationships between the global circulations and the local climate characteristics. In addition this method is able to capture some of the non-linear relationships that exist between the global and local climates. A summary of the three GCMs used in this study is given in Table 4.5. The models differ in spatial resolution, the processes they represent and they have different parameterisations. The points for which the downscaled GCM data are available are shown in Figure 4.18.

Table 4.4 Characteristics of the three GCMs availed for this study

| GCM | Institute | Country | Atmospheric resolution (lat/long) | Oceanic resolution (lat/long) | Reference |
|------------|--|----------------|--|--------------------------------------|-----------------------|
| ECHAM | Max Planck Institute for Meteorology | Germany | $1.9^\circ \times 1.9^\circ$ | $1.5^\circ \times 1.5^\circ$ | Roeckner et al., 1996 |
| GFDL | NOAA Geophysical Fluid Dynamics Laboratory | USA | $2.0^\circ \times 2.5^\circ$ | $0.3-1^\circ \times 1^\circ$ | Delworth et al., 2006 |
| IPSL | Institut Pierre Simon Laplace | France | $2.5^\circ \times 3.75^\circ$ | $2^\circ \times 2^\circ$ | IPSL 2005 |

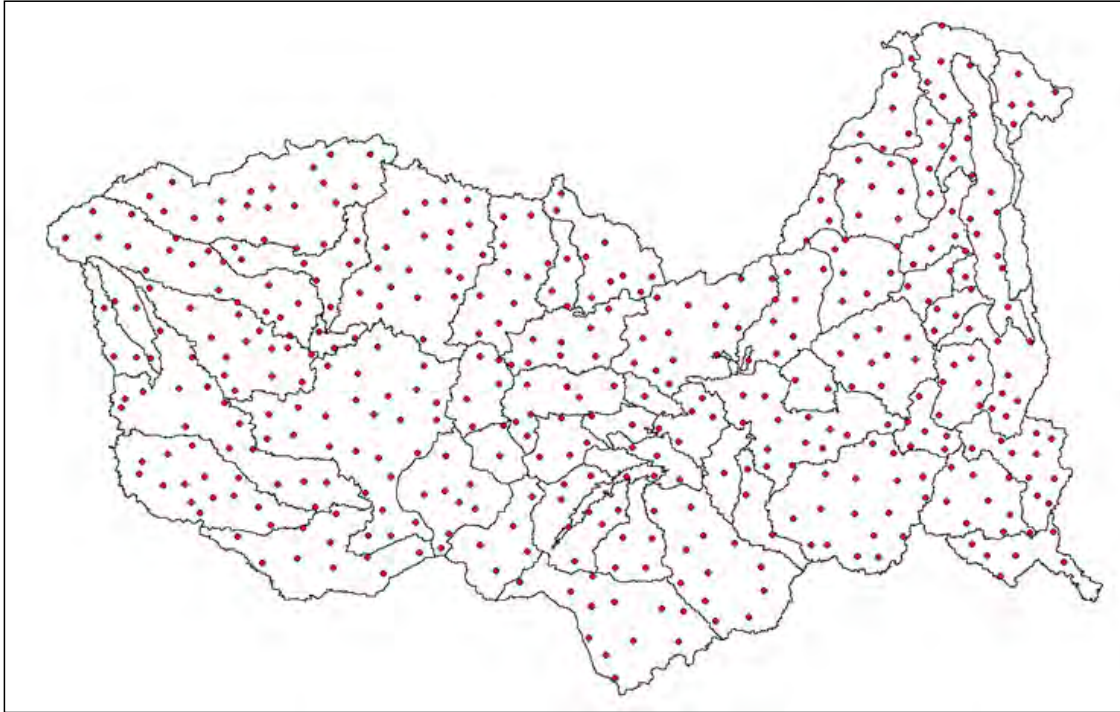


Figure 4.18 Downscaled GCM grid points used in this study

4.8.1 Bias correction

Typically a hydrological model used for climate change assessments will be calibrated using historical climate (rainfall and potential evaporation) data and the calibrations assessed using historical streamflow data. It is therefore essential that the future data used (outputs from the downscaled GCMs) represent changes relative to the historical climate as far as possible. In many cases the GCM outputs for the baseline period do not compare very well with the equivalent historical data (Figure 4.17). However, the historical and baseline GCM data need to have similar statistical and seasonal distribution properties if the future GCM data are to be compared with historical simulations otherwise the hydrological model simulations may produce meaningless results in terms of addressing real water resource problems (Wood et al., 2002; Chung et al, 2011; Kirono et al, 2011). Wood et al. (2004) also state that even though downscaling may reduce GCM uncertainty to some extent, it is still necessary to perform bias correction especially if the GCM model output is employed to drive a hydrological model. While it is possible to consider calibrating the model parameters using the baseline GCM output this could require separate calibrations for all GCMs. This option makes it difficult to compare results across GCMs. It is also not possible to apply this method if the observed streamflow data

do not correspond to the GCM baseline period of 1961 to 2000. The other option is to bias correct the GCM data based on comparisons between the observed historical data and the GCM baseline data. Figure 4.19 illustrates the bias in IPSL baseline rainfall with respect to historically observed CRU rainfall for a sub-basin in the Zambezi basin.

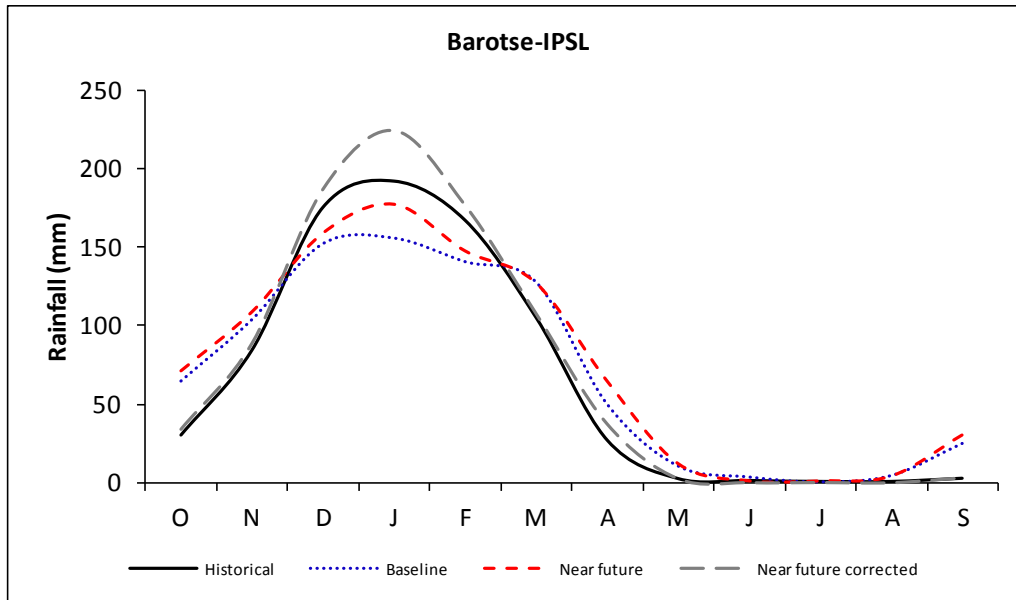


Figure 4.19 Bias in baseline precipitation with respect to historically observed precipitation

Bias correction for rainfall: In order to remove bias in the future rainfall estimates, future monthly rainfall totals are expressed as standard deviates of the baseline monthly rainfall distributions using a square root transformation (Hughes et al., 2012) and then rescaled using the historical data means and standard deviations. The square root transformation method has advantages over other methods of transformation in that it can be used to account for the positive skewness that is observed in the rainfall data while at the same time maintaining the seasonal pattern of the downscaled future rainfall. By compressing the upper end of a distribution more than the lower end of distribution, the square root transformation method has an effect of making positively skewed distributions resemble normal distributions and it also makes it possible to compare variances between different groups of data (Howell, 2007). However, it is possible that different transformations may be appropriate in different regions. The transformation method used in this study is adopted from Hughes et al. (2012) and it is outlined below:

$$FRC_{ijk} = (SWRM_j + SWRSD_j * (SFR_{ijk} - SBRM_{jk}) / SBRSD_{jk})^2 \quad 4.32$$

where:

$FRC_{i,j}$ = Future rainfall after correction for month i and calendar month j in the time series of GCM k.

$SFR_{i,j}$ = Square root transformed future rainfall for month i and calendar month j in the time series of GCM, k.

$SBRM_j$ = Mean of the square root transformed baseline rainfalls for GCM k and calendar month j.

$SBRSD_j$ = Standard deviation of the square root transformed baseline rainfalls for GCM k and calendar month j.

$SWRM_j$ = Mean of the square root transformed CRU rainfall for calendar month j.

$SWRSD_j$ = Standard deviation of the square root transformed CRU rainfalls for calendar month j.

The standard deviates are then rescaled using the distribution statistics of the historical rainfall data to obtain a corrected future rainfall time series. This process is aimed at ensuring that the baseline conditions are representative of the historical seasonality in rainfall while at the same time maintaining the differences between the baseline and future scenarios.

Bias correction for temperature and evaporation: Annual potential evaporation and fixed calendar month evaporation distributions are used as input to the Pitman rainfall-runoff model. There are various ways by which evaporation data can be derived from temperature data. Assumptions are made about other variables in order to calculate the evaporation demand, for example, the Penman method requires four meteorological parameters: air temperature, relative humidity, wind velocity, and net radiation. Although this method is considered to be the most reliable method and recommended by FAO as the standard against which other methods can be verified, it suffers from the fact that some of the parameters may not be available, especially in data sparse regions (Allen *et al.*, 1998). The Hargreaves equation (Hargreaves and Allen, 2003) is given as:

$$E_p = 0.0023 * S_0 (T + 17.8) * \sqrt{\delta t} \quad 4.33$$

where E_p is the potential evaporation, S_0 is the water equivalent of extraterrestrial radiation (mmd^{-1}), T is the mean monthly temperature ($^{\circ}\text{C}$) and δt is the difference between the maximum

and minimum mean monthly temperatures ($^{\circ}\text{C}$). This study, however, adopted a simple approach (Hughes et al., 2012) in which the maximum and minimum temperature GCM output data for the baseline and future climates were converted to a Hargreaves component (Equation 4.31):

$$\text{HC}_k = (\text{TMax}_k + \text{TMin}_k) / 2 \times \text{SQRT} (\text{TMax}_k - \text{TMin}_k) \quad 4.34$$

where, HC_k represents the temperature component of the Hargreaves equation for GCM k , calculated for baseline and future conditions. Tmax_k , Tmin_k are the daily maximum and minimum temperatures ($^{\circ}\text{C}$) which were converted to a monthly average value for a particular GCM. The Pitman model requires as input annual potential evaporation and seasonal distributions of the potential evaporation. Therefore to obtain the monthly evaporation data for the future period, the average percentage increase in the HC_k values for the baseline and the future conditions are calculated for each month of the year and the same increases are applied to the historical seasonal distributions used in the model calibration.

4.8.2 Modelling the impact of climate change on the Zambezi River basin

It is important for water resource managers to be to be aware of and to be prepared to deal with the impacts of climate change on the hydrology of river basins. Through moisture deficiencies and reduced runoff, drought affects many sectors of society. Reduced soil moisture leads to agricultural drought and reduced runoff may lead to water supply deficits. Population growth increases the demand for water while industry and irrigation also use a considerable amount of water in the basin. Any water deficits will therefore be most critical in drought periods and more than 70% of the population whose livelihoods rely on rainfed agriculture are bound to suffer more from the impacts of droughts. It is important to consider the impacts of drought under the context of a changing climate in the Zambezi basin. In this study the hydrological responses of the Zambezi basin to climate change are assessed. The variables considered include precipitation, streamflow, soil moisture, evaporation and droughts. Insufficient and poor records of runoff data and the absence of soil moisture data necessitated the use of hydrological modelling to generate runoff and soil moisture data for use in this study. The analysis methods (drought index and hydrological modelling) that were applied to the historical data are repeated using the bias corrected GCM output data for the near future period of 2046-2065.

CHAPTER 5 VARIABILITY IN RAINFALL AND STREAMFLOW

5.1 Introduction

Trend analysis studies are important as historical records of rainfall and streamflow have potential to be used as a basis for water resource planning and management strategies. Flood and drought events are common in the Zambezi basin and for purposes of water resource planning it is important to establish whether such events are a result of short term fluctuations in rainfall patterns or a result of long term changes in climate. Furthermore, the assessment of change and variability in trends becomes important given the current concerns about greenhouse gas induced climate change. It is also necessary to assess the spatial and temporal nature of change and climatic variability at a regional scale as it can guide the interpretation of future climates. This section aims to investigate the nature of historical variability in the Zambezi River basin and to establish trends and patterns in rainfall and runoff. Point (local) rainfall and runoff data as well as catchment averaged CRU rainfall data are used in order to determine hydrological variability in the Zambezi River basin. Representative rainfall and streamflow stations of reasonably long time series and with few missing data or minimal gaps are selected from each of the major drainage areas of the Zambezi River basin and are indicated in Figures 5.1 and 5.2.

To ensure statistical validity of results, WMO (2000) recommends the use of long term periods of rainfall and runoff data of at least 30 years and this was also one of the selection criteria for the stations under this study. Rainfall and runoff data are characterised according to the standard WMO periods of 1931-1960 and 1961-1990, subject to the length of the available time series particularly for the local data. An investigation is carried out to check for any abrupt changes, trends and cycles in the historical rainfall and runoff time series data. A number of statistical approaches are employed and these include simple statistics of the mean, standard deviation, coefficient of variation, rainfall-runoff coefficients as well as graphs and running means of 5, 10 and 20 years. Running means are used to smooth fluctuations in annual values and to identify any persistent trends of increasing or decreasing water availability. Step change detection is carried out using a combination of the distribution-free Cumulative Sum (CUSUM) test and bootstrapping (Taylor, 2000). The Mann-Kendall method and Sen's estimator of slope (Kendall,

1980; Sen, 1968) are used to determine the presence of trends in the time series. Fourier Spectral analysis (Shumway, 1988) is used to investigate the existence of cyclic behaviour. The time series data used in this study are normalised by the long term means over the periods of observation.

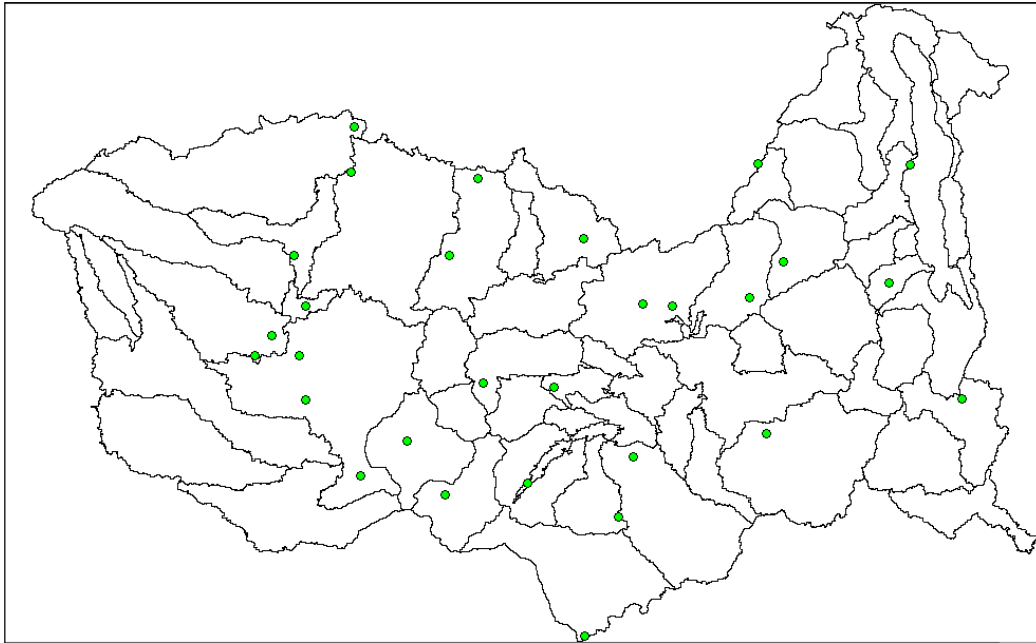


Figure 5.1 Rainfall stations used for variability analysis

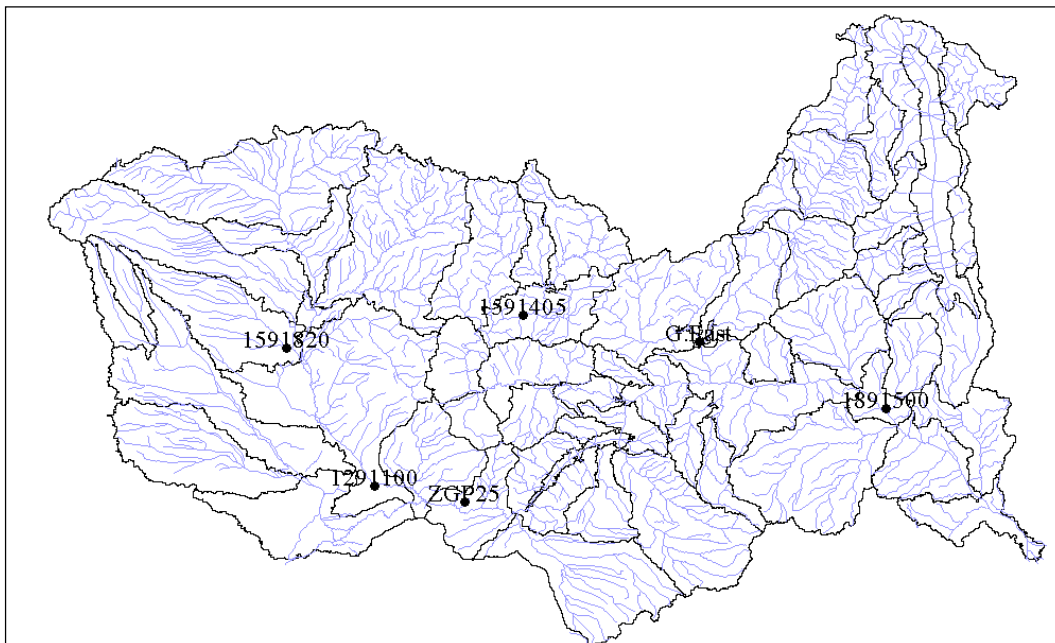


Figure 5.2 Streamflow gauging stations used for variability analysis

5.2 General characteristics of the rainfall time series

Table 5.1 shows the statistical parameters obtained for the local rainfall stations for the period 1931 to 1990 within which two time periods of 1931-1960 and 1961-1990 were used for the assessment. Substantial heterogeneity is exhibited within and between sub-basins. Annual rainfall across the Zambezi basin varies markedly, ranging from 500 to about 2 000 mm from the driest to the wetter parts of the basin.

Table 5.1 Statistical parameters for mean annual precipitation using local rainfall data

| Location | Station ID | 1931-1960 | | 1961-1990 | | Rainfall % change |
|---------------|------------|---------------|-----------|---------------|-----------|-------------------|
| | | Rainfall (mm) | CV (%) | Rainfall (mm) | CV (%) | |
| Kabompo | 20519 | 1337 | 15 | 1392 | 14 | 4 |
| Upper Zambezi | 204446 | 1487 | 15 | 1554 | 11 | 4 |
| | 82134 | 1060 | 18 | 1029 | 17 | -3 |
| Luanginga | 204258 | 949 | 25 | 845 | 21 | -11 |
| Barotse | 3749 | 701 | 33 | 714 | 31 | 2 |
| | 24140 | 981 | 19 | 928 | 20 | -5 |
| | 3539 | 840 | 26 | 718 | 24 | -15 |
| | 1847 | 996 | 18 | 977 | 24 | -4 |
| Lake Kariba | 21554 | 692 | 26 | 728 | 32 | 5 |
| | 21160 | 779 | 26 | 707 | 28 | -9 |
| | 112 | 819 | 31 | 786 | 31 | -4 |
| | 201 | 578 | 25 | 549 | 28 | -5 |
| Kafue | 25629 | 812 | 28 | 759 | 32 | -6 |
| | 1201 | 798 | 27 | 681 | 35 | -15 |
| Luangwa | 91533 | 921 | 20 | 902 | 19 | -2 |
| | 2318 | 974 | 20 | 952 | 21 | -2 |
| | 24853 | 874 | 20 | 1035 | 21 | 18 |
| Lake Malawi | 8801322 | 1934 | 27 | 1829 | 15 | -5 |
| | 8800356 | 1374 | 22 | 1261 | 24 | -8 |

Observations from local rainfall stations show that headstream areas exhibit higher rainfall than the low lying areas and these are exemplified by the Kabompo (20519), Upper Zambezi (204446) and the dry Gwai sub-basin (201) which is located in the Lake Kariba drainage area.

High altitude areas receive the highest rainfall in the basin as shown by station 8801322 which is found in the mountainous areas around the Lake Malawi catchment. Year to year variability is quite high in the basin as evidenced by the high annual coefficients of variation for the two time periods. Coefficients of variation based on the interannual mean rainfall range from 15 to 33% for the period 1931-1960 and from 11 to 35% during 1961-1990. Interannual variability tends to be more pronounced in the middle and lower parts of the basin (Barotse, Kariba, Kafue, Luangwa, Lake Malawi catchments) compared to the wetter headstream areas of the Upper Zambezi and the Kabompo. With the exception of headstream areas and the Luangwa basin, a decreasing rainfall trend of between -2 to -15% is observed in transition from the period 1931-1960 to 1961-1990. Changes in the headstream areas of Kabompo and Upper Zambezi sub-basins are stable between -3 to 4%. Between the two time periods, changes in rainfall are mixed with 72% of the stations falling in the decreasing category. Out of the 18 stations under observation, six show a considerable decrease in rainfall, a moderate decrease for four of the stations, a considerable increase for one station, moderate increase for three stations and almost no change for four of the stations. Apart from temporal variability, spatial variability is also evident whereby there is substantial variability within a sub-basin. Within the Kafue, Barotse, Kariba and Luangwa catchments changes from one location to another range between -2 to -15, -5 to 2, -10 to 5 and -2 to 18 respectively.

Table 5.2 provides the statistical parameters obtained from the catchment averaged CRU data. The observations made with the CRU data are consistent with those of the local rainfall stations in that the middle and lower areas of the basin portray higher variability compared to the headstream catchments. A generally decreasing rainfall pattern is observed between the two time periods of 1931-1960 and 1961-1990, while the changes are stable within the headstream catchments. As observed with point rainfall data, the coefficients of variation show that there is high variability in rainfall across the basin. These wide variations may be attributed to factors such as differences in topographic and climatic conditions. For example the Upper Zambezi catchment is characterised by a humid seasonal climate, while a semi arid seasonal climate predominates in the low lying southern areas.

Table 5.2 Statistical parameters for catchment averaged rainfall using CRU data

| Location | 1931-1960 | | 1961-1990 | | % change |
|-------------|---------------|--------|---------------|--------|----------|
| | Rainfall (mm) | CV (%) | Rainfall (mm) | CV (%) | |
| Luena | 1185 | 15 | 1209 | 11 | 2 |
| Kabompo | 1176 | 14 | 1154 | 14 | -2 |
| Barotse | 870 | 20 | 790 | 20 | -9 |
| Luanginga | 1001 | 16 | 914 | 16 | -9 |
| Kafue | 984 | 17 | 966 | 21 | -2 |
| Luangwa | 1005 | 26 | 992 | 17 | -1 |
| LunguBungu | 1130 | 14 | 1049 | 14 | -7 |
| Tete | 848 | 19 | 912 | 17 | 8 |
| Lake Kariba | 790 | 24 | 756 | 28 | -4 |
| Lake Malawi | 1250 | 15 | 1317 | 14 | 5 |
| Cuando | 845 | 19 | 779 | 22 | -8 |

5.2.1 Spatial analysis of rainfall variability across the Zambezi basin

To assess the variation of annual rainfall in space, stations were selected in a south easterly direction from the western part of the basin and the change in rainfall with distance was observed. Station 82134 located in the Upper Zambezi drainage area was taken as the reference point and distance was calculated between this station and the stations; 1847, 24140, 3539, 3749, 21554 and 201. The locations of these stations are presented in Table 5.3. Mean annual rainfall in the basin decreases with increasing distance in a south easterly direction as shown in Figure 5.3. Spatial variability is further expressed by the change in the coefficient of variation with distance. The coefficient of variation tends to increase in a south easterly direction which is generally from the headstream areas to the drier and low lying areas in the Zambezi basin. Once more it is observed that variability is higher in the drier areas of the basin. There is a general decrease in altitude from north to south across the basin and therefore the decrease in annual precipitation may be attributed in part to a change in relief and topography. Generally, the higher the altitude the more the precipitation received in the basin.

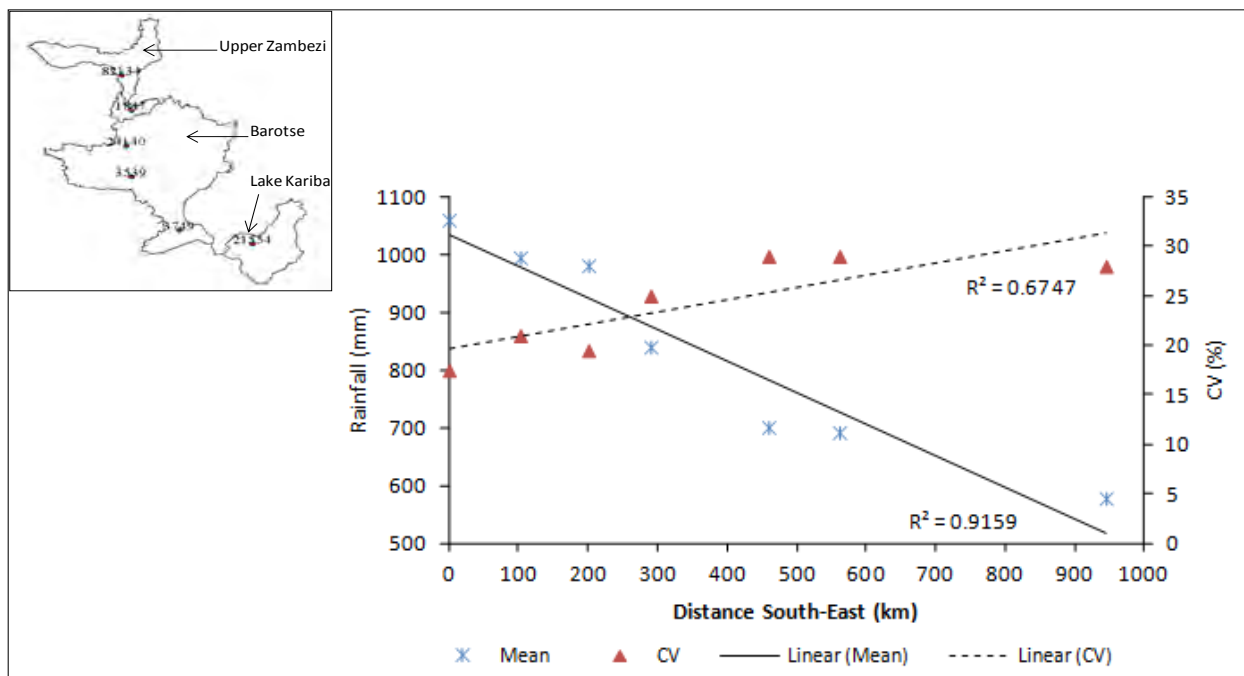


Figure 5.3 Spatial distribution of rainfall between example stations in the western part of the Zambezi basin. Insert (location of the stations used for analysis)

Table 5.3 Stations used for analysis of spatial variability in rainfall. The reference point is allocated a distance of 0 km

| Station | Latitude | Longitude | Distance (km) |
|---------|----------|-----------|---------------|
| 82134 | -13.50 | 23.10 | 0.00 |
| 1847 | -14.40 | 23.30 | 102.40 |
| 24140 | -15.20 | 23.20 | 200.40 |
| 3539 | -16.10 | 23.30 | 289.90 |
| 3749 | -17.45 | 24.30 | 459.50 |
| 21554 | -17.82 | 25.82 | 561.30 |
| 201 | -20.35 | 28.33 | 944.70 |

5.2.2 Inter-annual and decadal variability in rainfall in the Zambezi basin

Running means are used to smooth fluctuations in annual values and to allow any persistent trends between increases and reductions in rainfall to be more clearly identified. For this purpose variability in rainfall has been demonstrated using 5, 10 and 20 year running means. Long term rainfall patterns filtered with 5 year running means as well as the long term means for the two periods of 1931-1960 and 1961-1990 are shown in Figures 5.4a and b. The long term rainfall

patterns indicate that the 1920s and 1950s up to the 1980s received above average rainfall while the 1930s, 1940s, 1960s and the period after 1980 had below average rainfall. Figure 5.4 also compares the two means for the periods 1931-1960 and 1961-1990, where 70% of the stations under analysis show a generally decreasing pattern in the mean annual rainfall between the two time periods. These observations confirm the results obtained in sections 5.1.

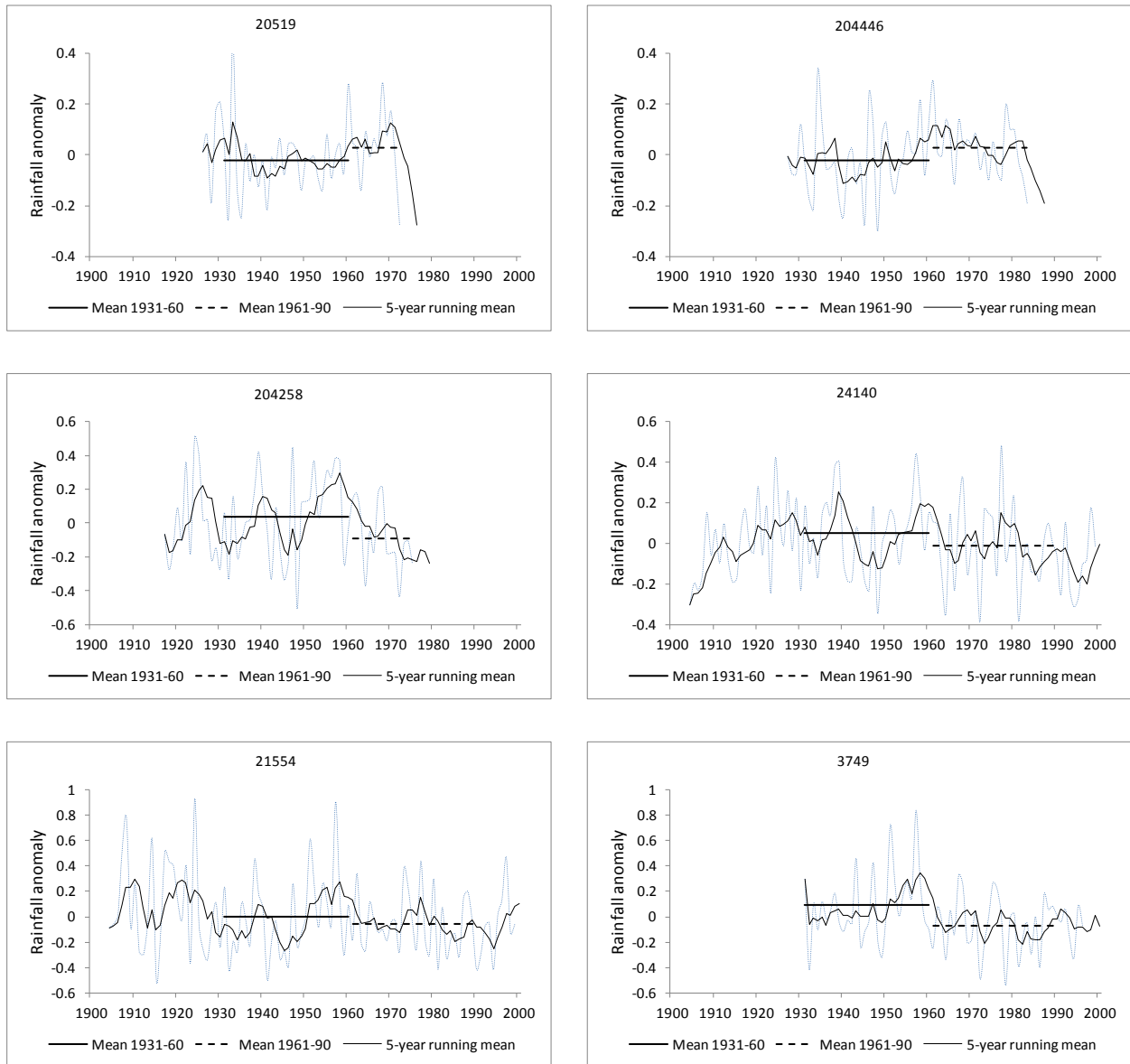


Figure 5.4a 5-year running trend in rainfall for example stations in the Zambezi River basin

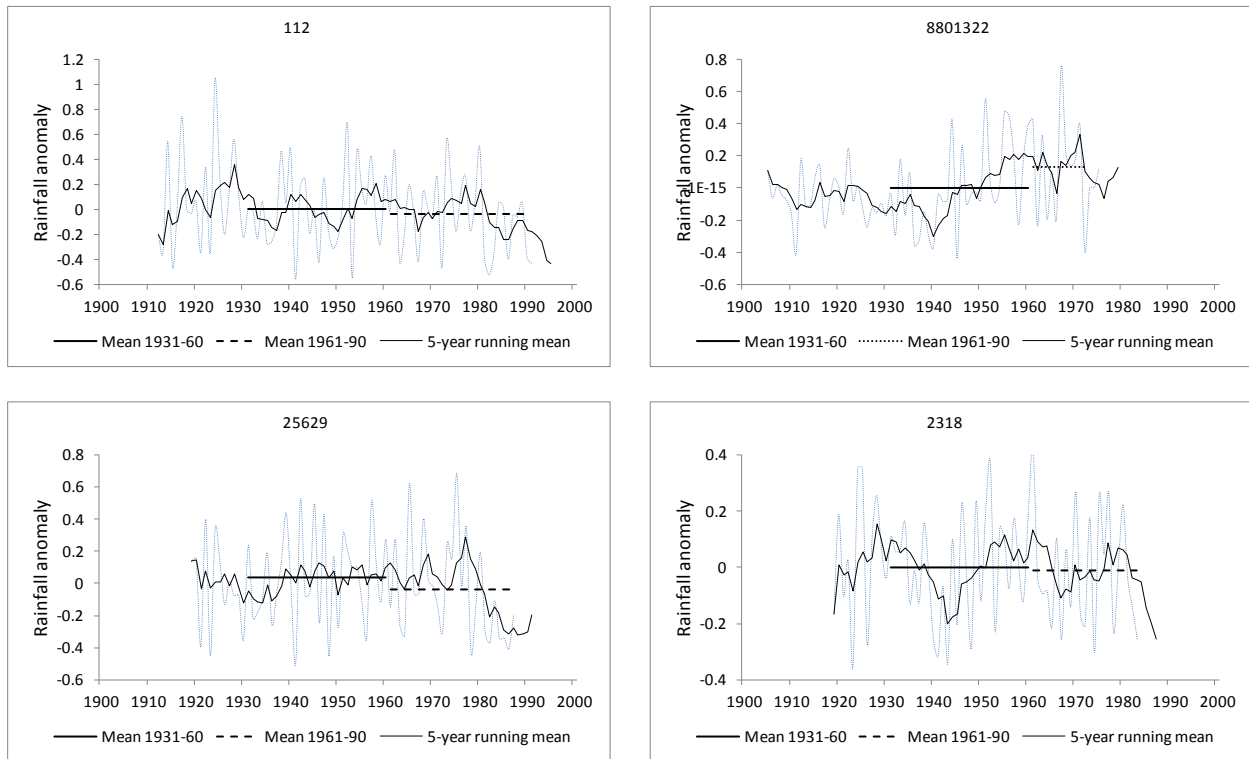


Figure 5.4b 5-year running trend in rainfall for example stations in the Zambezi River basin

Inspection of the graphs in Figures 5.4a and b suggests a 10 to 15 year cyclic pattern for the period under assessment, starting from the year 1915 and this occurrence is evident in most of the stations. Short term fluctuations about the long term mean are also observed within thin the long term cycles. Figures 5.5a and b illustrate the variability using 10 and 20-year running means. An alternating pattern of wet and dry cycles is observed. For the 10-year running means, 15 to 20-year cycles are more evident while 30 to 40-year cycles predominate for the 20-year running means. Patterns of increasing and decreasing rainfall with high variability within the wet and dry cycles are observed for most of the stations. The fact that most of the stations show a similar time series pattern gives a clear signal of regional homogeneity within the Zambezi River basin. It is evident that extended periods of wet and dry conditions have occurred in the Zambezi River basin and an analysis of decadal variability shows that these periods can extend for a period of 20 years or more. Despite the WMO limit of at least 30 years time series it is observed that the trends are more visible over a long time period indicating that the historical time series data of rainfall must be of reasonably long periods if the long term impacts of future changes in climate are to be clearly singled out from those purely emanating from historical climate

variability. The WMO limit, however, remains necessary to consider, especially in data sparse areas.

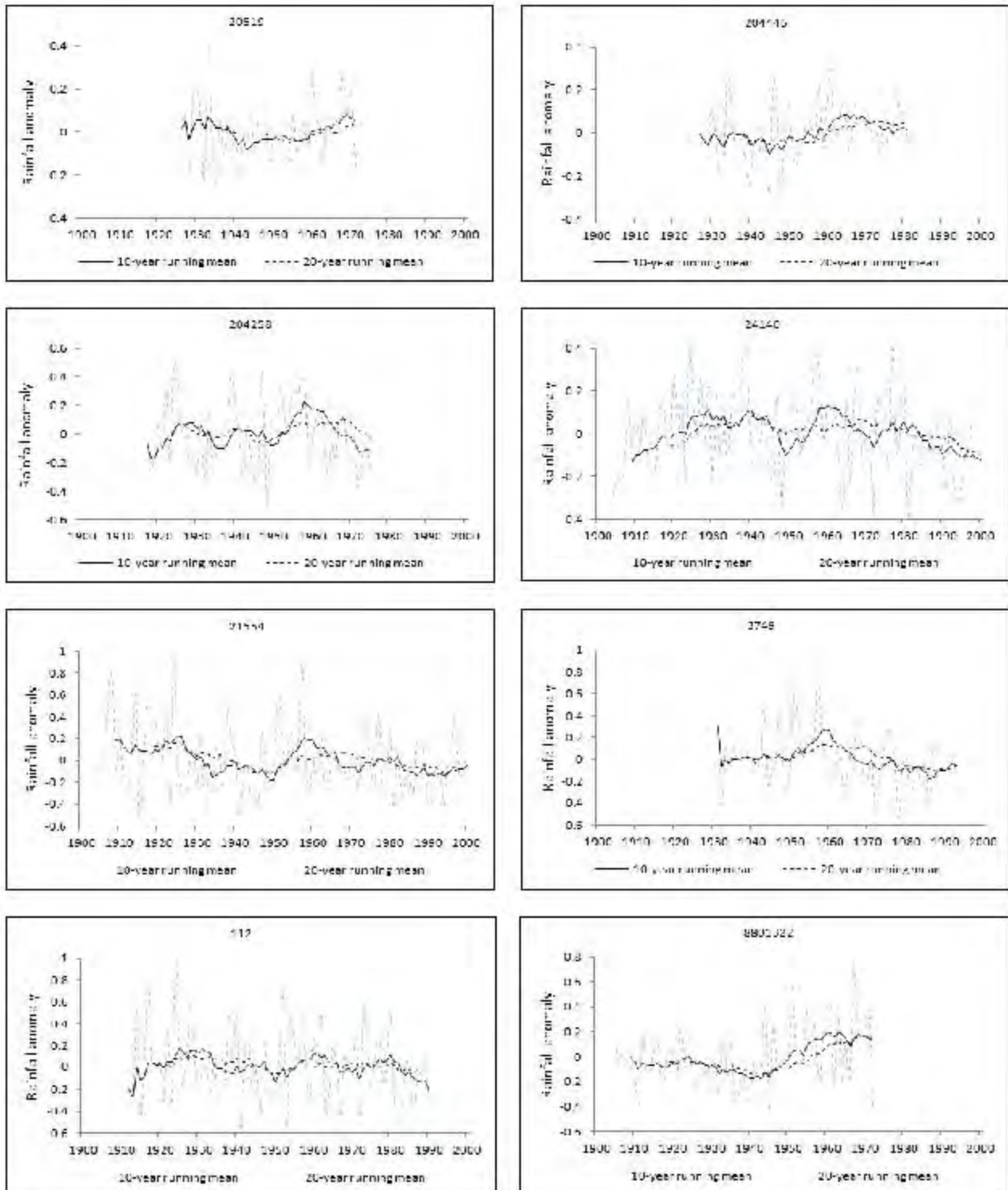


Figure 5.5a 10 and 20-year running trends in rainfall

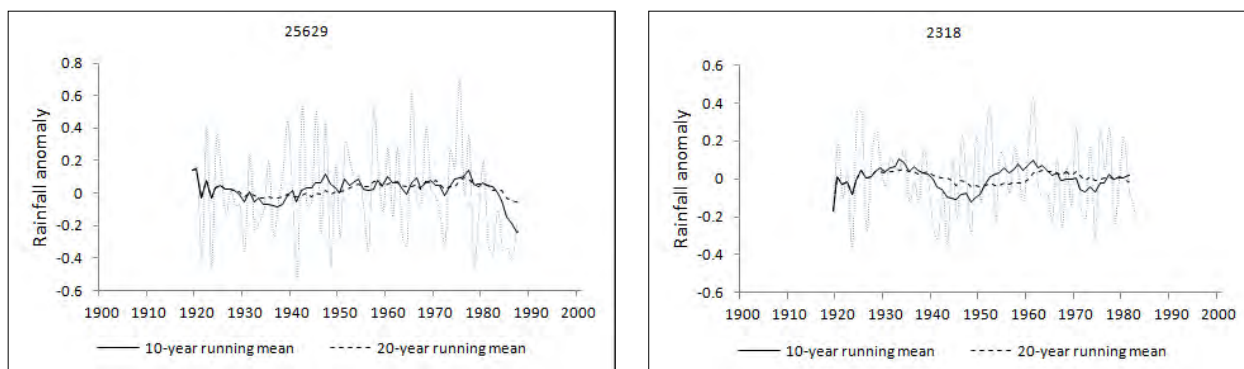


Figure 5.5b 10 and 20-year running trends in rainfall

5.2.3 Linear trend detection in mean annual precipitation

The Mann-Kendall test and Sen’s slope estimator are used to determine whether there is a significant linear trend in annual precipitation. The Mann-Kendall test is a non-parametric rank-based method which is used to detect the presence of trend in linear and nonlinear time series data. Sen’s test on the other hand estimates the magnitude of the trend slope (Q) and the confidence interval for the slope. Lower and upper confidence limits ($Q_{\min 95}$ and $Q_{\max 95}$) are used to test the significance of the slope at the 95% confidence interval. Q is then defined as statistically significant if zero does not lie between the upper and lower confidence limits. Trend analysis results using both tests based on raw rainfall data are presented in Table 5.4 and Figure 5.6.

Table 5.4 Rainfall trend statistics for Mann-Kendall’s and Sen’s test

| Location | Station ID | Period (years) | Mann-Kendall trend | | Sen's slope estimate | | |
|---------------|------------|----------------|-----------------------------|--------------|----------------------|---------------|---------------|
| | | | Z_{test} statistic | Significance | Q | $Q_{\min 95}$ | $Q_{\max 95}$ |
| Kabompo | 20519 | 47 | 1.00 | no | 2.00 | -1.64 | 6.59 |
| Upper Zambezi | 204446 | 57 | 1.12 | no | 2.33 | -1.59 | 4.89 |
| Luanginga | 204258 | 59 | -0.34 | no | -0.67 | -4.54 | 3.22 |
| Barotse | 24140 | 95 | -0.59 | no | -0.47 | -1.90 | 0.92 |
| Lake Kariba | 21554 | 95 | -1.14 | no | -0.91 | -2.65 | 0.57 |
| | 3749 | 64 | -1.55 | no | -1.96 | -4.69 | 0.53 |
| | 112 | 80 | -1.03 | no | -1.30 | -4.35 | 0.98 |
| Lake Malawi | 8801322 | 68 | 1.77 | no | 6.22 | -0.43 | 12.00 |
| Kafue | 25629 | 69 | -1.05 | no | -1.61 | -4.49 | 1.35 |
| Luangwa | 2318 | 65 | -0.54 | no | -0.78 | -3.86 | 2.01 |

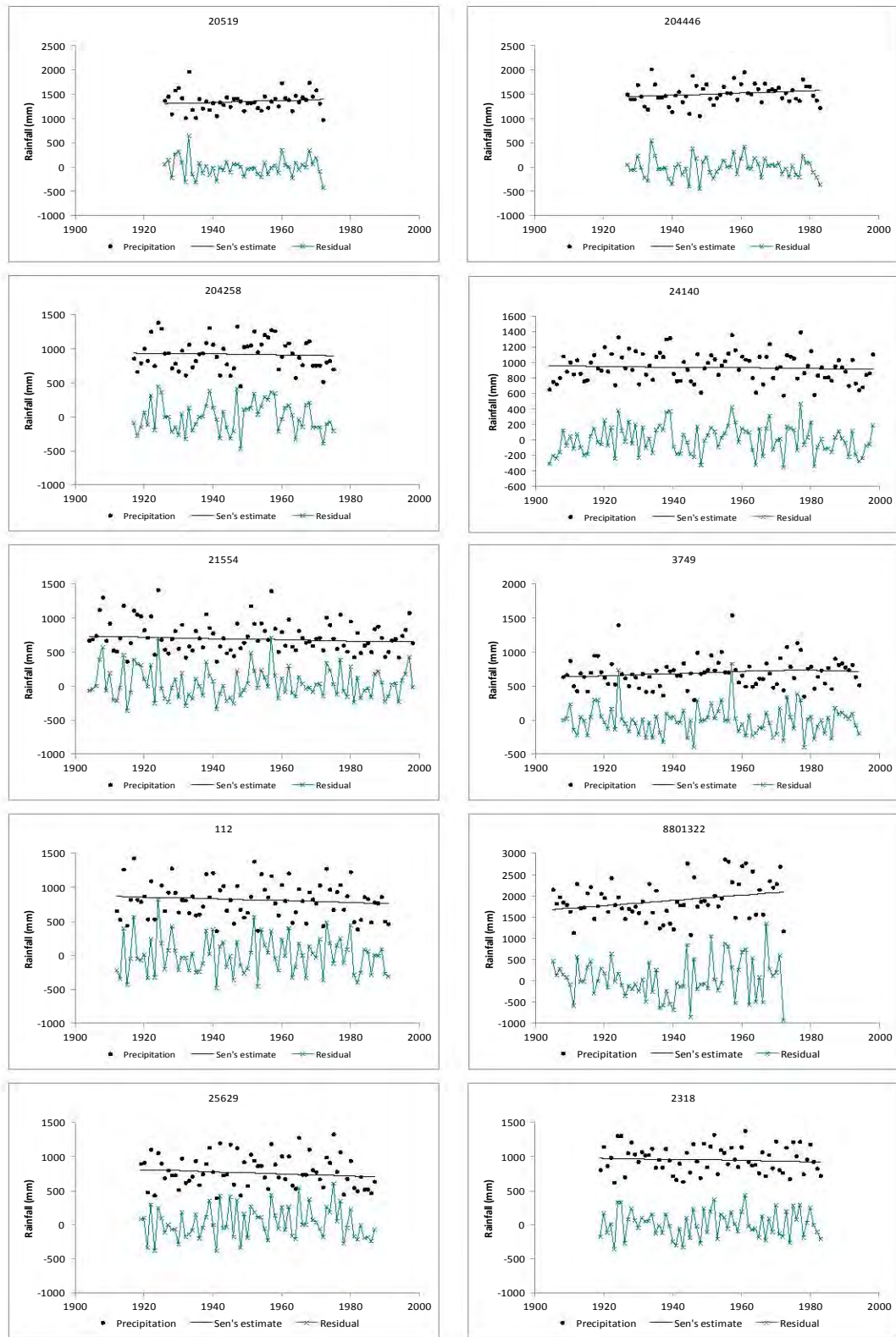


Figure 5.6 Sen's linear estimates of rainfall at example stations

5.2.4 Change point analysis in rainfall

The CUSUM test and the bootstrapping method are used to investigate the existence of step changes (shifts) in annual precipitation. CUSUM charts and distribution free plots for the annual precipitation time series are presented in Figures 5.7a and b. On the CUSUM plot, a positive slope indicates that the precipitation was above average during that time period whereas a negative slope indicates below average precipitation values. Any change in the direction of slope may represent a change in the time series but whether the change is significant or not has to be statistically proven. As observed in the previous sections, the CUSUM plots show the presence of cycles between the wet and dry periods. Generally the periods 1920-1930, 1950-1960 and 1970-1980 experienced above average rainfall while below average rainfall was received during the periods 1930-50 and 1960-70 and 1980-2000. Exceptions are noted for the Kabompo (20519), Upper Zambezi (204446), the Kafue (25629) and Lake Malawi (8801322) in which wet conditions were experienced during the 1960-1980 period. Although decadal cycles are evident in the CUSUM plots, there remains substantial variability in annual rainfall amounts within the cycle where relatively wet years occur in dry cycles, while dry years occur in wet cycles.

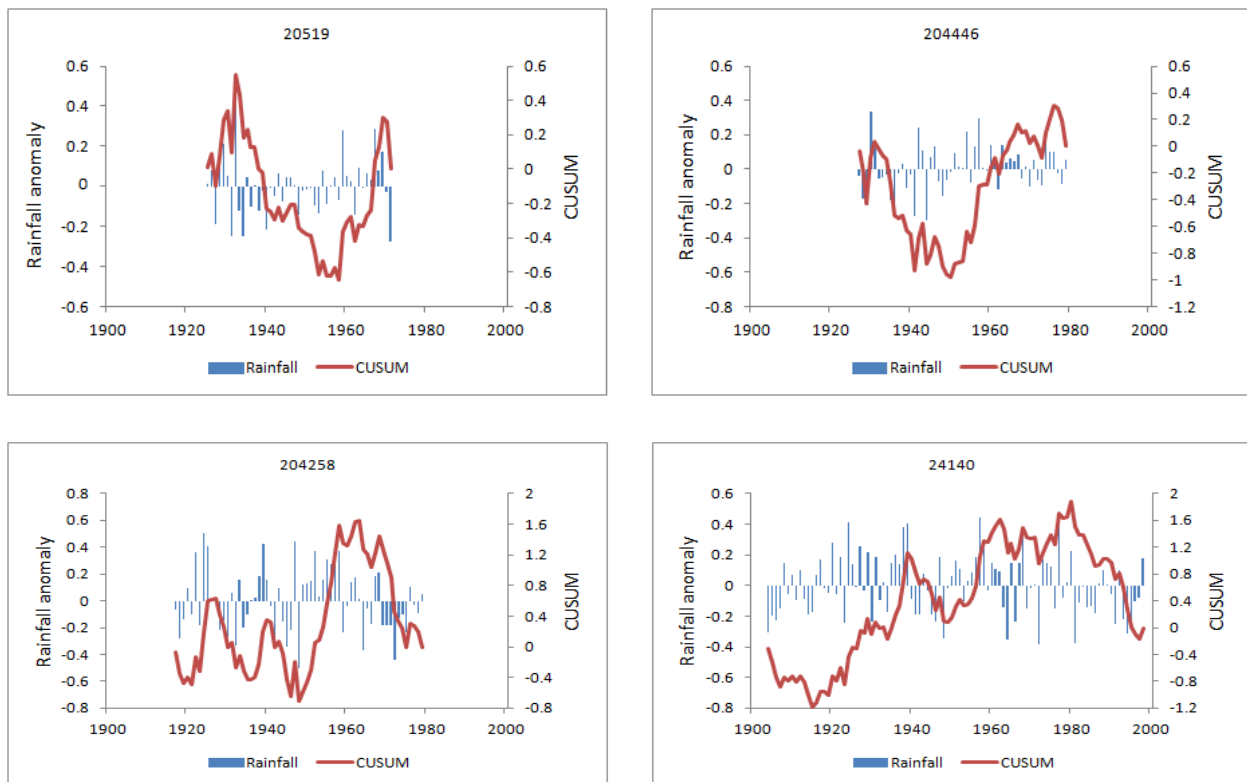


Figure 5.7a CUSUM and distribution plots of rainfall anomalies at example stations

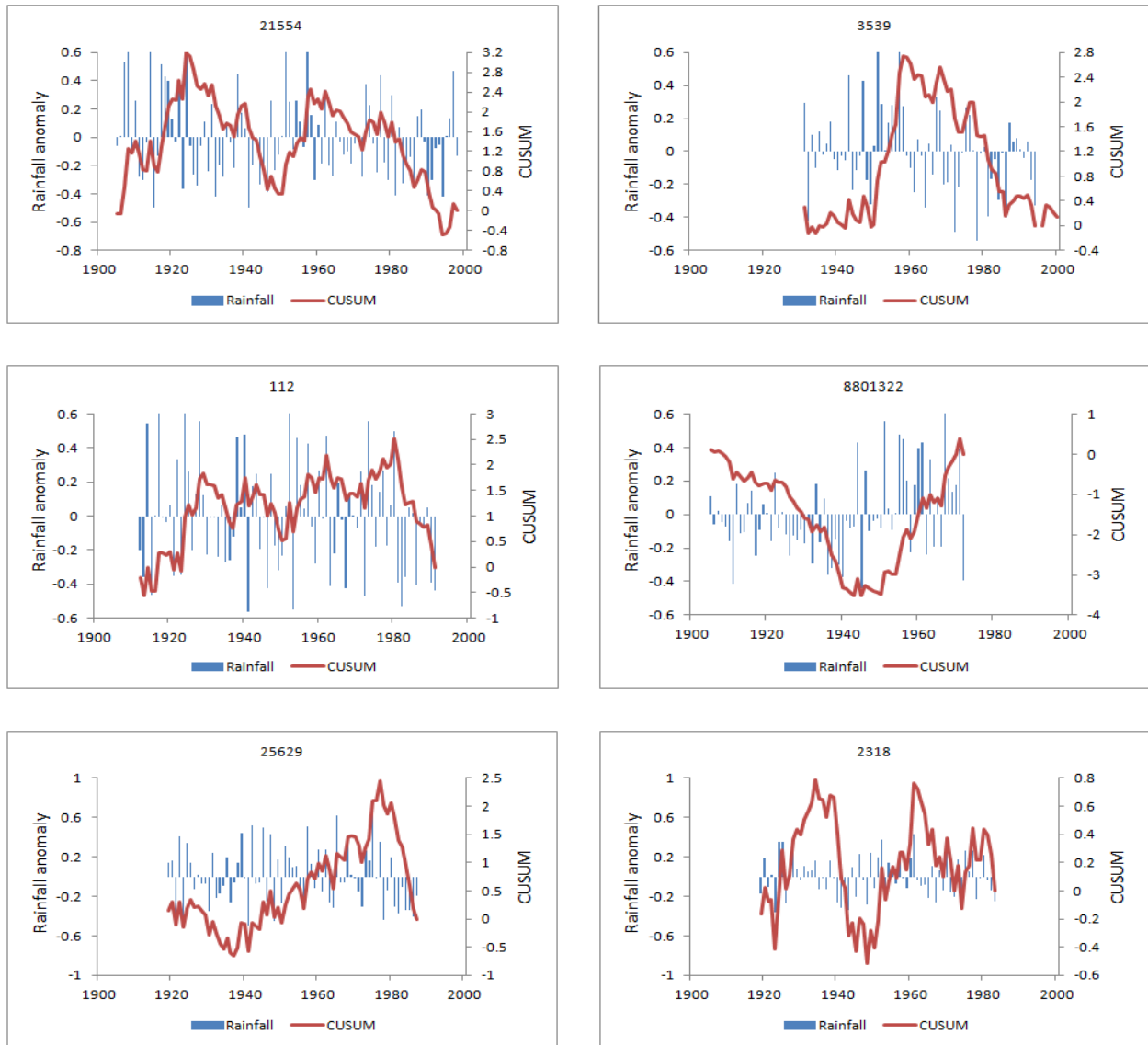


Figure 5.7b CUSUM and distribution plots of rainfall anomalies at example stations

Significant step changes are observed at stations 24140 in the Barotse and 8801322 in the Lake Malawi catchment and these are represented in Figure 5.8. Shaded backgrounds serve to show the steps of change in the two cases. There is 95% confidence that change started around the year 1951 at station 8801322 and around 1981 at station 24140. Also with 95% confidence it is shown that the respective changes occurred between the years 1945-1966 and 1971-1990 respectively.

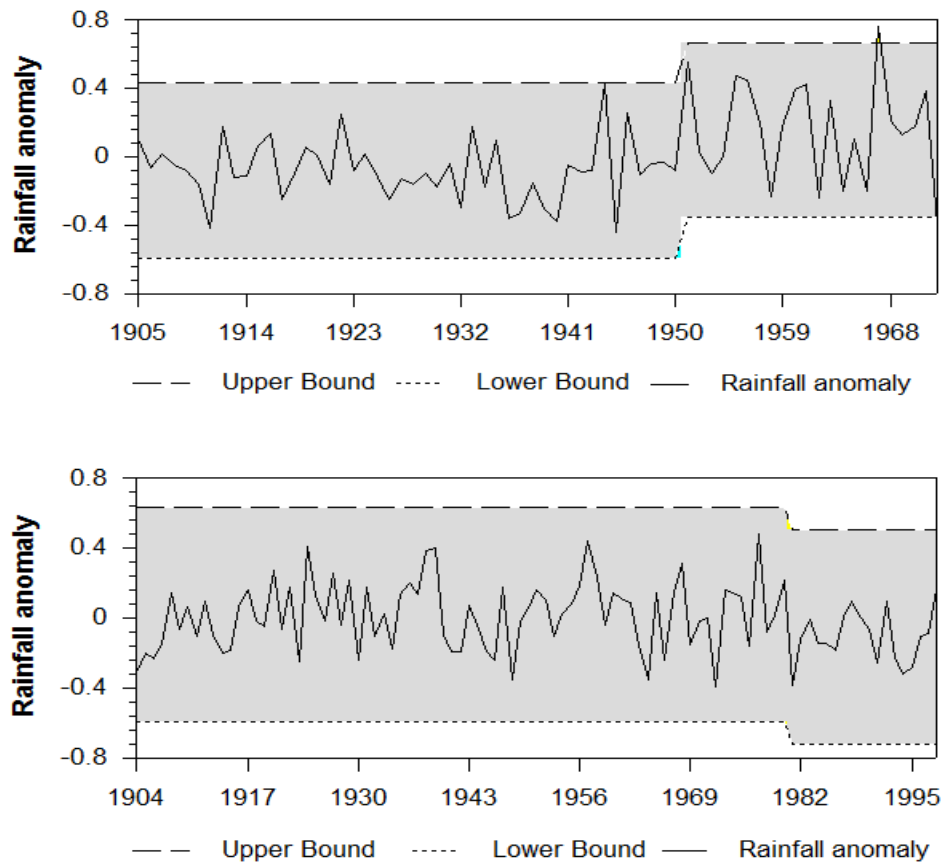


Figure 5.8 Significant step change at stations 8801322 (top) and 24140 (bottom) at 95 % confidence level

5.2.5 Detection of cyclic behaviour in rainfall time series

To further investigate possible periodicity, the rainfall time series data are analysed by single spectrum Fourier analysis using STATISTICA software (StatSoft, Inc., 2009). Smoothed periodograms representing the spectrum of cycles of different lengths for some example cases are depicted in Figures 5.9a and b. Apart from the 2-5 year cycles which are common to all the sub-basins, the spectrograms show the predominance of 7.5, 9 and 11-year cycles. Significant 14-year cycles are also evident in the Barotse (24140) and Lake Kariba (21554) where time series extend to 95 years. Due to the short length of the time series data (less than 100 years) that were available for this study, it is impossible to speculate on cycles longer than 15 years. In order to test for statistical significance of the cycles, two tests are performed and the results are presented in Table 5.5.

Table 5.5 Fisher's Kappa and Bartlett's Kolmogorov-Smirnov statistical tests for rainfall

| Sub-basin | Station | Fisher's Kappa | Bartlett's K-S |
|---------------|---------|----------------|----------------|
| Kabompo | 20519 | 3.84 | 0.19** |
| Upper Zambezi | 204446 | 4.25 | 0.15** |
| | 82134 | 3.88 | 0.19** |
| Luanginga | 204258 | 4.72 | 0.24** |
| | 24140 | 2.89 | 0.14** |
| Barotse | 21160 | 3.46 | 0.17** |
| | 3749 | 3.09 | 0.12** |
| | 3539 | 2.97 | 0.15** |
| Kariba | 21554 | 3.45 | 0.07** |
| Kafue | 25629 | 6.69* | 0.23** |
| | 112 | 4.51 | 0.19** |
| | 1201 | 5.01 | 0.12** |
| Luangwa | 24853 | 3.79 | 0.14** |
| | 2318 | 2.64 | 0.19** |
| | 91533 | 5.14 | 0.23** |
| L. Malawi | 8800356 | 3.81 | 0.16** |
| | 8801322 | 4.51 | 0.17** |

**Significance at 0.01 level

*Significance at 0.05 level

The Bartlett's Kolmogorov-Smirnov statistic determines whether the observed periodogram is distinct from white noise (randomness). For all the example cases, the Bartlett test statistics are significant at the 0.01 level, indicating that the cycles are not a result of random noise (or they are not a result of white noise). Fisher's Kappa statistic determines whether the most prominent period is statistically significant by establishing whether the largest periodogram value differs significantly from the mean of all the periodograms in the series. The Fisher's Kappa tests are not significant at the 0.05 level except for station 25629. In general white noise is rejected for the historical rainfall time series in the Zambezi basin, but the dominant cycles are not statistically significant.

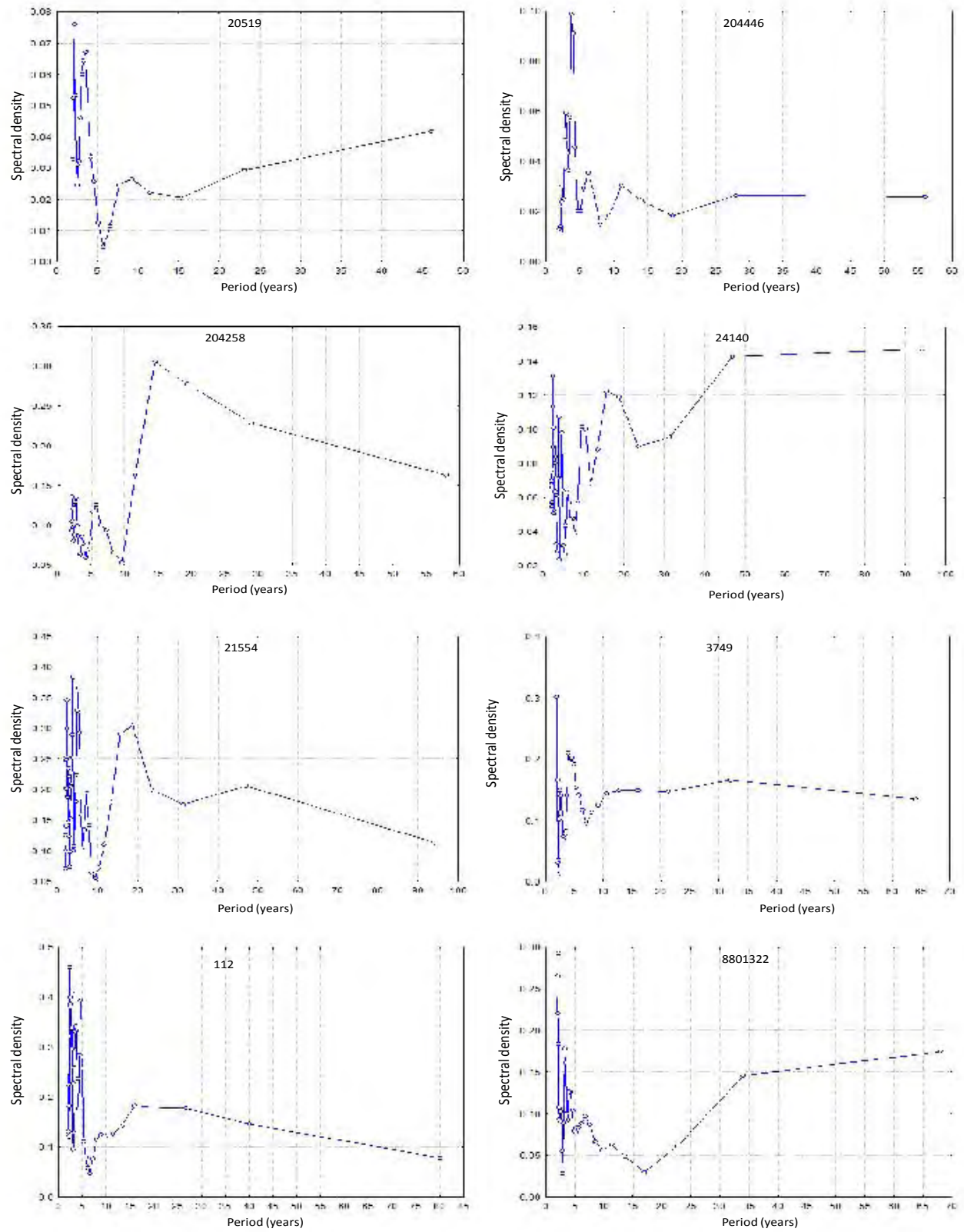


Figure 5.9a Rainfall spectral densities for example cases in the Zambezi River basin

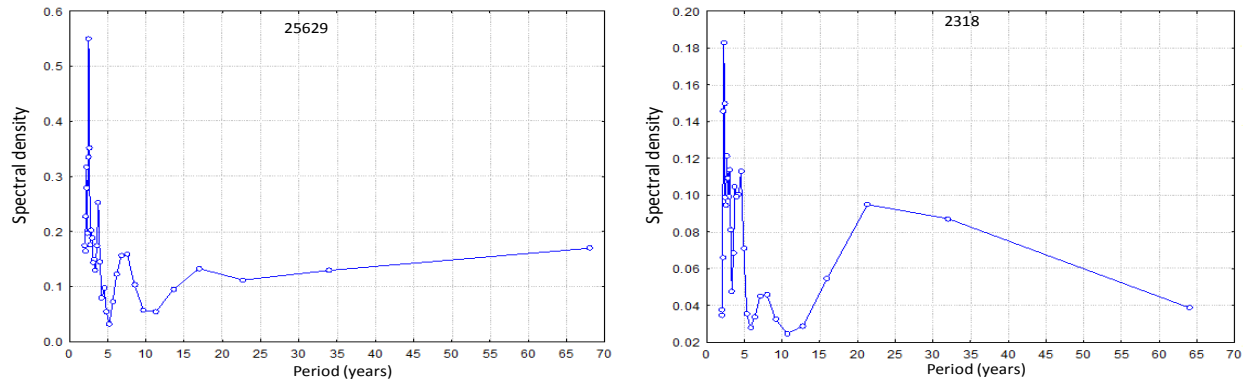


Figure 5.9b Rainfall spectral densities for example cases in the Zambezi River basin

5.2.6 Seasonality in rainfall distribution

Monthly rainfall distribution in the Zambezi basin is presented in Figure 5.10. Rainfall is higher in the headstream areas of Kabompo, Luanginga and Upper Zambezi with mean monthly rainfall amounts above 200 mm. The middle and lower lying areas of the basin such as the Barotse, Victoria Falls and Kafue have monthly averages below 200mm. There is pronounced variability in rainfall from one month to another and clearly there is a marked difference between the wet months of October to April and the dry months of May to September. The seasonal pattern remains the same for both the time scales of 1931-1960 and 1961-1990. However, a shift in seasonality towards the austral autumn is noted for the Lake Malawi drainage area (represented by station 8801322). While other areas are summer dominated, rainfall starts around the months of September-October, with amounts increasing gradually from October and peaking from December to February. In the Zambezi basin seasonal variability in rainfall is mainly influenced by the ITCZ. The movement of the ITCZ in the basin is such that at the start of the rainy season around late September more of the influence is in the north-eastern part of the basin (see Chapter 2 Section 2.2.2). The influence of the ITCZ increases towards the southern and central parts of the basin around late November to December and around February March the ITCZ exerts its maximum influence in the south-easternmost parts of the basin mainly dominated by the Lake Malawi drainage area, which explains why peak rainfall amounts are realised later in the austral summer for the Lake Malawi sub-basins.

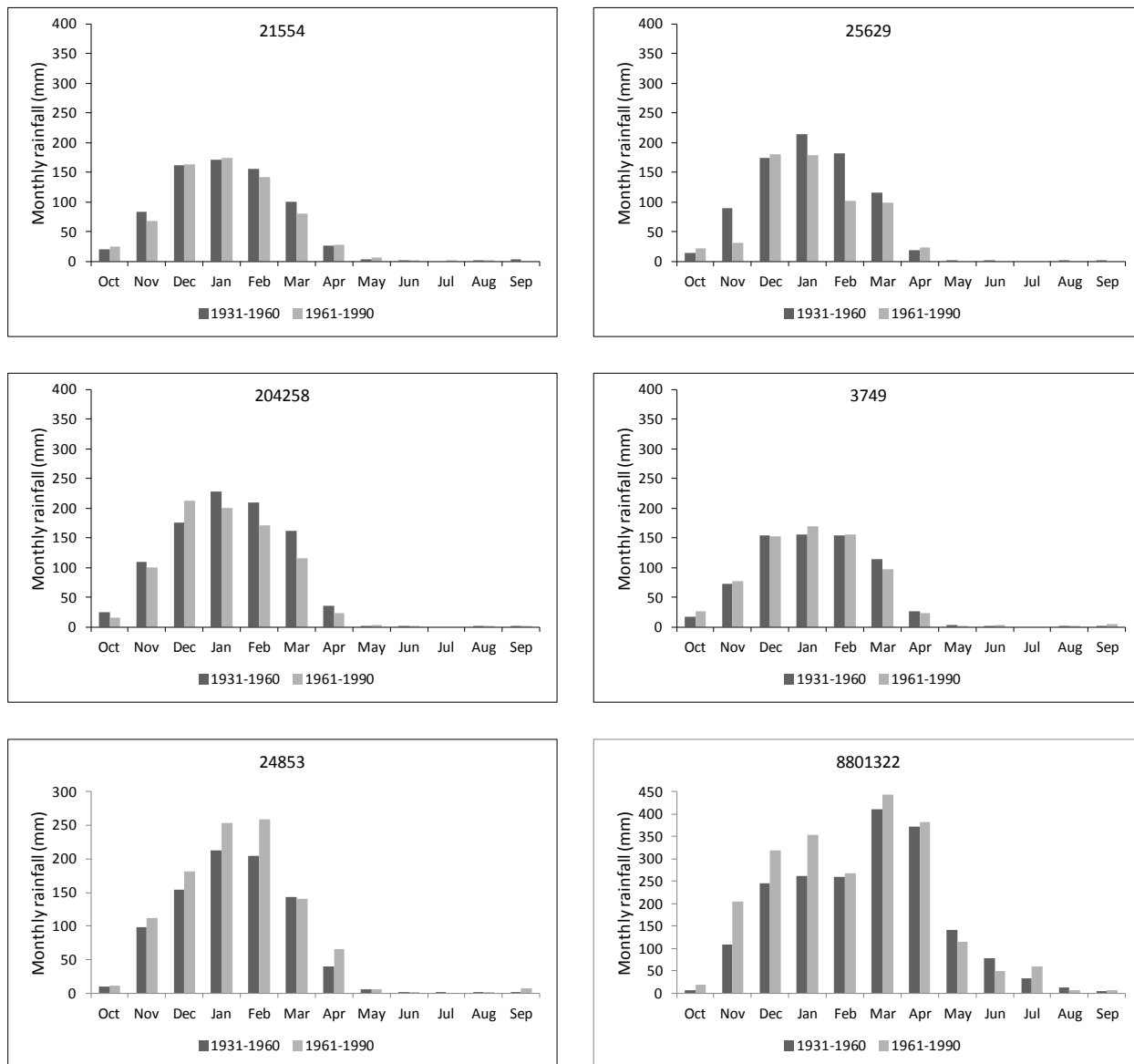


Figure 5.10 Seasonal rainfall distribution for example stations during the periods 1931-1960 and 1961-1990

5.3 General characteristics of the streamflow time series

Given the issue of data paucity in southern Africa, only a few streamflow gauging stations in the Zambezi basin have data of reasonable quality and time series length. Most of the stations have long periods of missing data and could not be used for this study. Of all the stations, ZGP25 at Victoria Falls in the lake Kariba catchment area was found to be of reasonably good quality, with no missing data and spanning 83 years starting from 1924 followed by the Great East Road

Bridge (G.E. Rd.) station in the Luangwa catchment whose time series span 60 years from 1930. In the Zambezi basin, various studies such as Jury and Gwanzantini (2002), Mazvimavi and Wolski (2006) and Conway et al. (2008) have adopted the Victoria Falls station as representing the Zambezi basin, an indication of the reliability of the consistent and long time series data available at the station. In this study the station ZGP25 has also been used in conjunction with other stations. Statistical parameters for river flow in the Zambezi River basin are given in Table 5.6. General observations on river flow indicate stability in flow at ZGP25 (1% change) while the G. E. Rd. station in Luangwa basin and station 1891500 at Matundo Cais in Tete province of Mozambique recorded a 13% increase and a 19% decrease in river flow, respectively, between the periods 1931-60 to 1961-90. Although it cannot be ascertained in this study, it is possible that the changes in flow regime at 18915000 were influenced by the construction of Kariba dam (1960s) and Cahora Bassa dam (1975). These results also show that upstream impacts particularly those from human activities have great potential of impacting the downstream flows, and if future developments are to be sustainable, it is necessary to have knowledge of how the hydrological regime can be affected by climatic and non-climatic changes such as land use change (Calder et al., 1995). Runoff coefficients given as the ratio of rainfall to runoff were also calculated using the local rainfall stations. Low runoff coefficients, which are typical of the semi arid climates of southern Africa where a very high evaporative potential exceeds the total rainfall amount received, are observed across the basin with values ranging between 12% and 15%.

It should be noted that apart from rainfall, streamflow is also impacted by other factors such as the basin physical properties (e.g. topography, soils, vegetation), catchment storage, antecedent moisture conditions, evaporation and the presence of wetlands (Kundzewicz et al, 2006). Tate et al. (2004) state that the presence of wetlands and other storages may result in delayed runoff responses. For example in the Zambezi basin the Barotse floodplain is well known to attenuate the runoff by 4 to 6 weeks and the peak discharge only reaches the catchment outlet in April or early May instead of February to March as expected in most parts of the north-western parts of the basin (Beilfuss and Santos, 2001). At the same it should be appreciated that data providing the necessary details on such factors as required for this study are hardly available for the Zambezi basin and as such the attribution of variability in streamflow may be hard to ascertain. Land use changes, catchment management and other human activities such as abstractions also

have potential to alter the runoff characteristics of a catchment, but according to Beilfuss and Santos (2001) and SADC (2007) the effects in the basin are negligible and are not likely to impact the runoff patterns in the future. Hydropower generation is the major activity that dominates the Zambezi waters. However, a considerable amount of water is lost through evaporation from the reservoirs. Also the presence of reservoirs such as the Cahora Bassa, Lake Kariba and Kafue Gorge for purposes of hydropower generation has potential to alter the runoff patterns particularly during releases in dry seasons and storage in extremely wet conditions. Rainfed agriculture is also another major basin activity upon which the survival of a larger part of the basin population as well as the basin economy are based but this kind of agriculture is not expected to impact on the nature of runoff in the basin.

Table 5.6 Statistical parameters for selected flow gauging stations in the Zambezi basin

| Sub-catchment | Station | Catchment area (km ²) | 1931-1960 | | | 1961-1990 | | | % change |
|---------------|----------|-----------------------------------|--------------------------|--------|--------|--------------------------|--------|--------|----------|
| | | | Flow (m ³ /s) | CV (%) | RC (%) | Flow (m ³ /s) | CV (%) | RC (%) | |
| Luanginga | 1591820 | 34621 | 776 | 34 | 14 | - | - | - | - |
| Barotse | 1291100 | 334000 | - | - | - | 1283 | 36 | 9 | - |
| Lake Kariba | ZGP25 | 360683 | 1178 | 33 | 15 | 1191 | 38 | 14 | 1 |
| Kafue | 1591405 | 59479 | - | - | - | 1440 | 47 | 15 | - |
| Luangwa | G.E. Rd. | 143885 | 539 | 49 | 12 | 609 | 44 | 12 | 13 |

CV: coefficient of variation, RC: runoff coefficient

5.3.1 Inter-annual and decadal variability in streamflow in the Zambezi basin

The temporal trends in streamflow at selected stations in the Zambezi basin are characterised using 5, 10 and 20-year running means. Figure 5.11 shows variability in streamflow using 5 year running means for selected stations in the basin. Below average flows were experienced across the basin during the 1930s and 1940s while the 1950 to 1980 period was characterised by above average flows and below average flows re-emerge after 1980. Despite the difference in the length of the time series data, a similar cyclical pattern in streamflow is evident between all the stations under study. This pattern is similar to that observed for the rainfall in the basin, with coinciding periods of the wet and dry years. The Victoria Falls station (ZGP25), whose time series is longer, indicates an upward shift after the year 2000. The long term mean between the periods 1931-1960 and 1961-1990 remains almost the same at station ZGP25 and an increase

between the two periods is seen at the G.E. Rd. station in the Luangwa sub-basin. The 10 and 20-year running trends in streamflow are shown in Figure 5.12. Similar patterns to the 5-year running means are observed whereby there is an alternation of wet and dry periods. The 1930s exhibit below average flow, the 1940s to 70s experienced above average flow and the 1980s were dry. For those stations (ZGP25, 18991500) whose data extend beyond the year 2000, the time series plots generally show an upward trend after 2000.

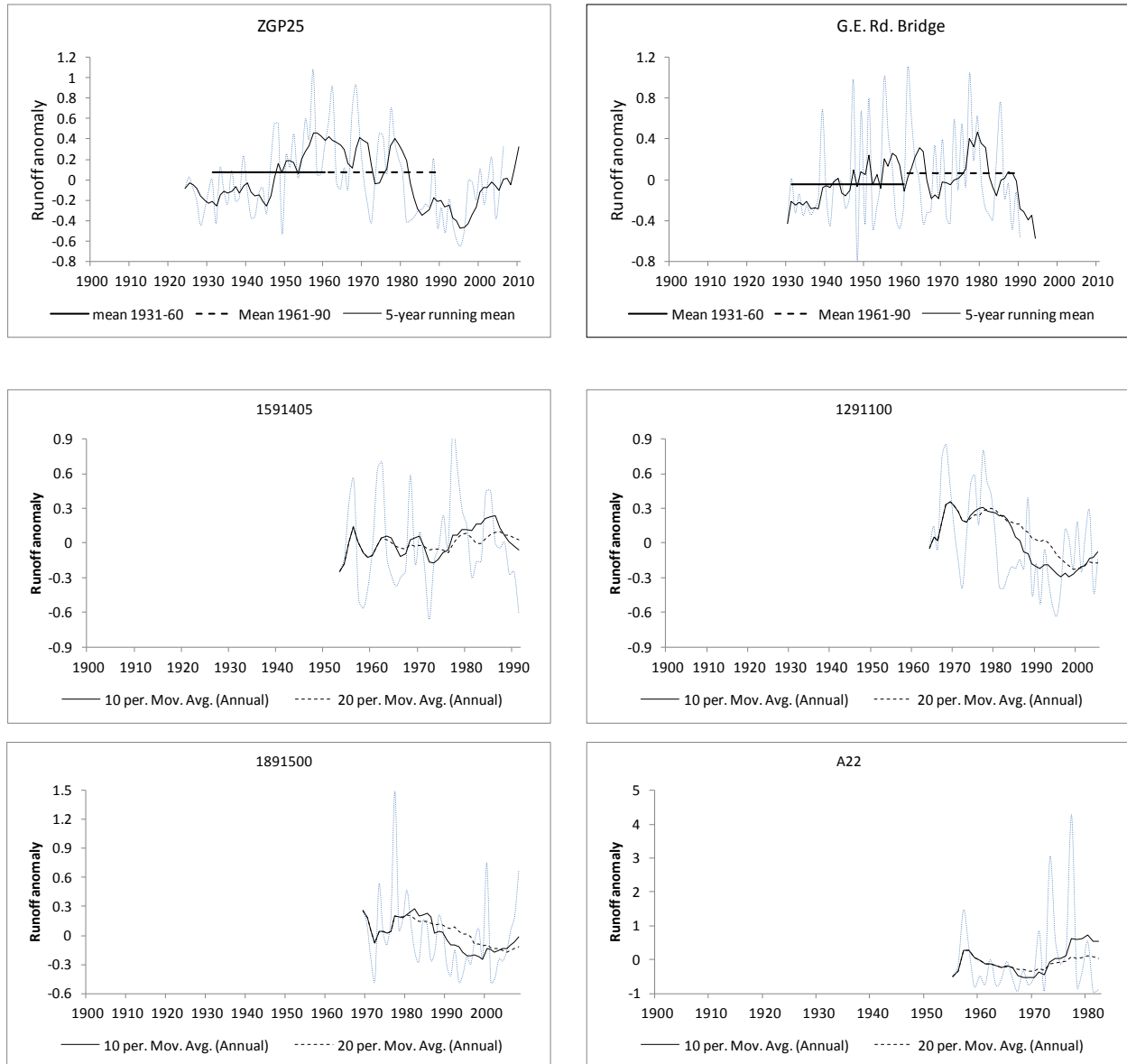


Figure 5.11 5-year running trends in streamflow for example cases in the Zambezi

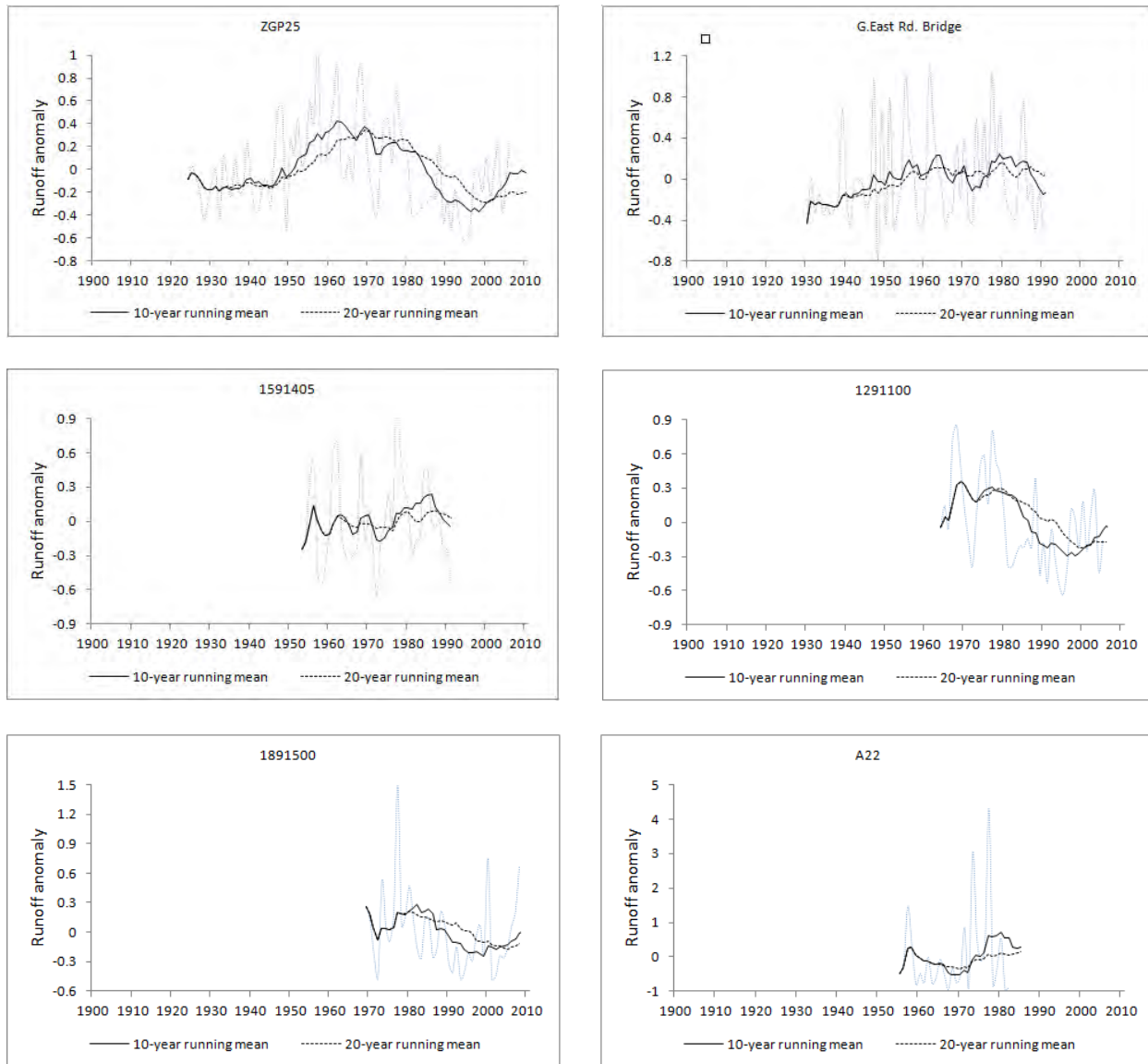


Figure 5.12 10 and 20-year running trends in streamflow for example cases in the Zambezi

The overlap of streamflow and rainfall fluctuations using 20-year running means is illustrated in Figure 5.13. Only the stations ZGP25 and G.E. Rd. are considered because they are the only ones with time series of streamflow that coincide with rainfall for a considerable length of time. For the other stations it was impossible to get a reasonably long overlapping time period. There is a match between the time of occurrence of the wet and dry conditions for the streamflow and rainfall time series. This observation is clear particularly for the Lake Kariba sub-basin at station ZGP25 where the time series of both streamflow and rainfall are longer. Due to data deficiencies,

a basin-wide overview cannot be made but it can be assumed from the observations made that there is similarity in the spatial and temporal variability of rainfall and streamflow.

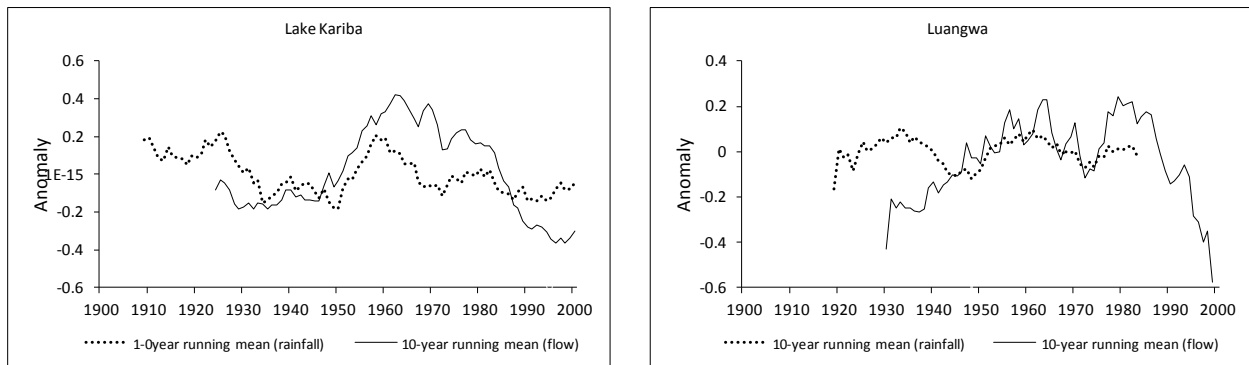


Figure 5.13 Variability of rainfall and streamflow

5.3.2 Linear trend detection in mean annual streamflow

Trends in streamflow are analysed by the Mann-Kendall test and the results are shown in Table 5.7 and Figure 5.14. With the exception of station 1291100 there are no statistically significant ($z=1.96$) trends in the streamflow time series for the example stations. Sen's slope estimator indicates a generally decreasing flow pattern for four out of the six stations under consideration. Slight increases in streamflow are observed in the Luangwa (G.E. Rd.) and the Kafue (1591405). The observed changes are consistent with the changes in rainfall in the respective sub-basins although not necessarily of the same magnitude. For the increasing flows, the rainfall patterns show a decreasing tendency (e.g. Luangwa) during the period of assessment. That there is no coincidence in the magnitude or direction of change between rainfall and streamflow points to the fact that streamflow responses are nonlinear largely as a result of the influence of the other factors that have were stated in Section 5.2.

Table 5.7 Mann-Kendall and Sen's tests for trends in streamflow

| Station ID | Period (years) | Mann-Kendall trend | | Sen's slope estimate | | |
|------------|----------------|--------------------|--------------|----------------------|---------------------|---------------------|
| | | Z-test statistic | Significance | Q | Q _{min} 95 | Q _{max} 95 |
| ZGP25 | 83 | -0.8 | no | -1.5 | -4.92 | 2.31 |
| 1291100 | 42 | -2.62 | yes | -40 | -66.53 | -10.42 |
| 1591405 | 39 | 0.56 | no | 1.27 | -3.92 | 5.79 |
| G. E. Rd. | 62 | 0.7 | no | 1.15 | -1.6 | 4.73 |
| 1891500 | 40 | -1.53 | no | -35.21 | -82.18 | 7.82 |
| A22 | 28 | -0.18 | no | -0.17 | -1.87 | 2.62 |

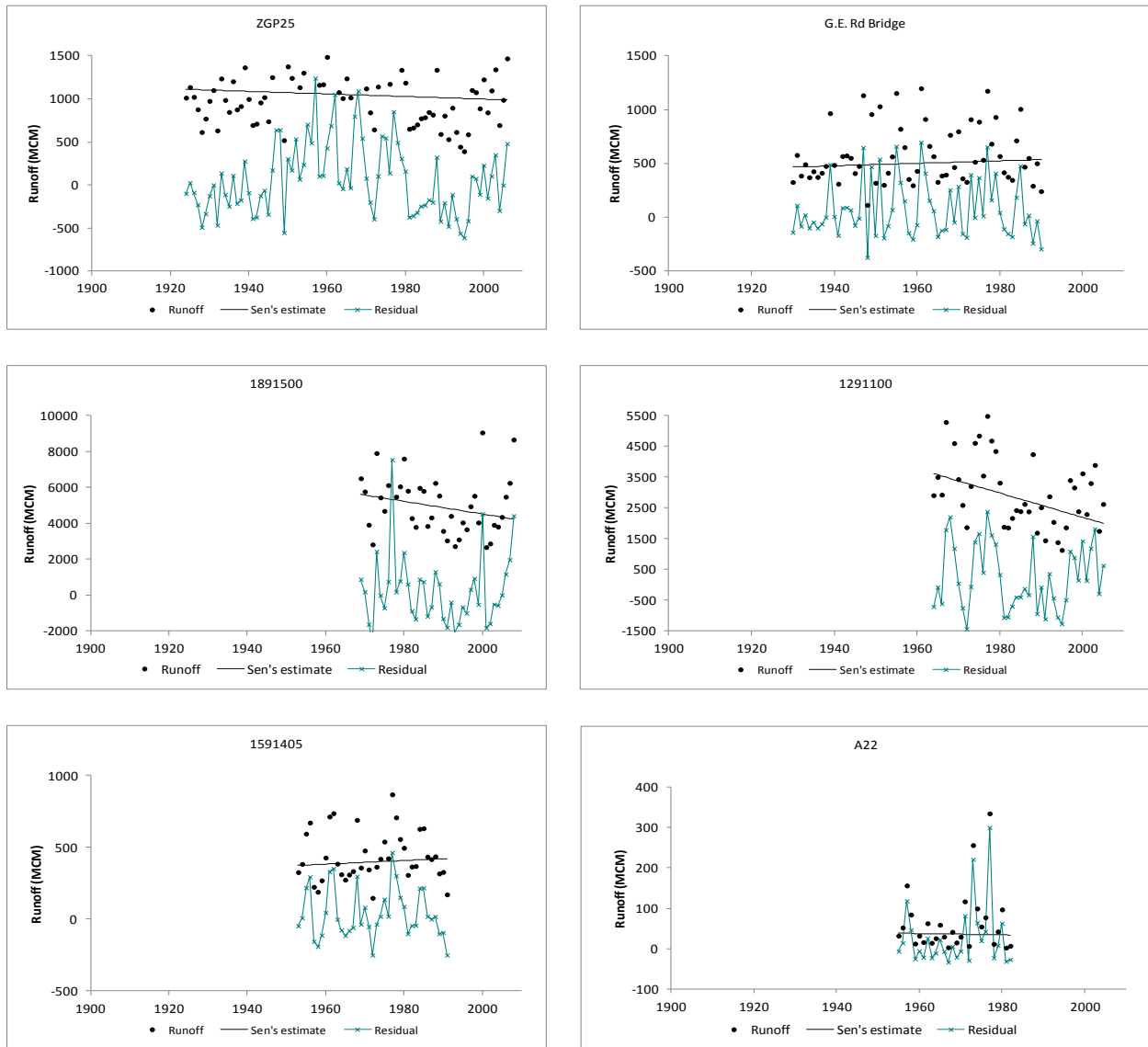


Figure 5.14 Sen's linear estimates of streamflow at example stations

5.3.3 Change point analysis in streamflow

Change point analysis was carried out to detect for any a changes in the stream flow time series. The CUSUM results given in Figure 5.15 show extended wet and dry periods. The periods 1920-1940 and 1980-2000 were dry while wet periods were experienced during 1940-1980. The alternation of wet and dry periods suggests cyclic patterns in the streamflow. Substantial variability is evident in the annual streamflows where wet spells occur within an extended dry season and dry spells also occur in an extended wet period. These observations are consistent with the rainfall patterns in Section 5.1.4.

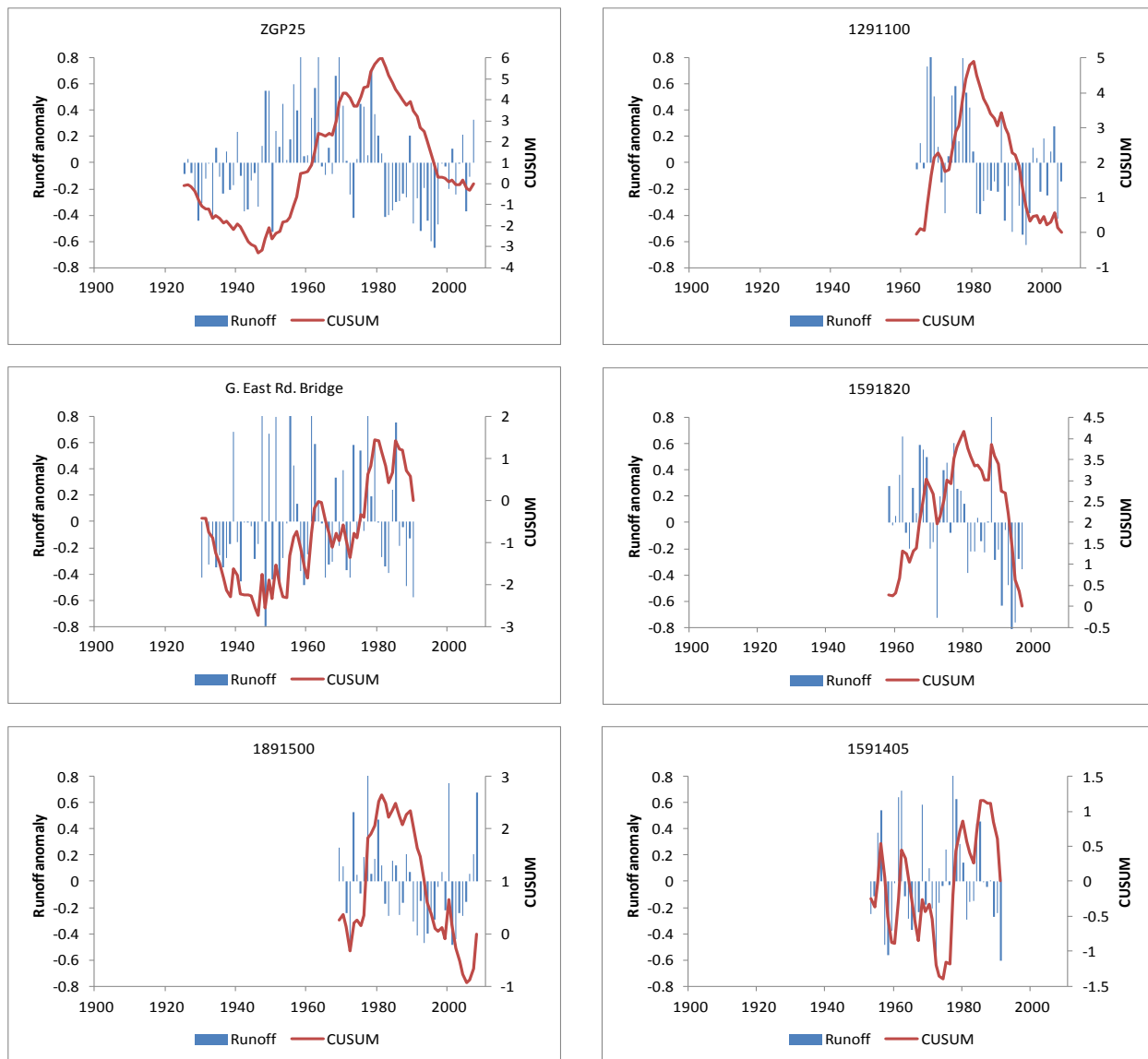


Figure 5.15 CUSUM and distribution plots of streamflow anomalies at example stations

Tests on the distribution free time series indicate significant changes to have occurred in the Lake Kariba catchment area at Victoria Falls (ZGP25) and in the Barotse (1291100) are shown in Figure 5.16. The statistics of the step changes are presented in Table 5.8. For the Victoria Falls station, three significant step changes are estimated to have occurred in 1946, 1981 and in 1997 and these occurred at 87%, 100% and 97% confidence levels respectively. A negative shift indicating a decrease in streamflow occurred in 1981 while the 1946 and 1997 shifts were positive indicating an increase in streamflow. Although the time series is limited, the shift in 1997 suggests conditions to have turned wet in the early 2000s. Three estimated step changes are observed at station 1291100 (Barotse). The first change which indicates decreasing flows was in

1971 and detected with 92% confidence. The second change was in 1974 with increased flow and detected with 93% confidence. The third step change was in 1980 with decreased flows and detected with 100% confidence. The Victoria Falls catchment is immediately downstream of the Barotse although separated by an area of about 200 000 km². Judging from the large area of separation between the two stations it is likely that a common development might have caused the changes around 1980-81 and these changes might have been basinwide but this cannot be substantiated due to insufficient data. That the changes in 1946, 1971, 1974 and 1997 are not common to both sub-catchments may be explained by the fact that in change analysis, the location of the point of change is largely determined by the length of the time series. Therefore two different time series may not necessarily experience changes at the same time even if those points are in the same region. Also if the time series data are short it may be difficult to detect some of the changes that may have occurred and as such no conclusions can be drawn on the changes that may have occurred in the basin.

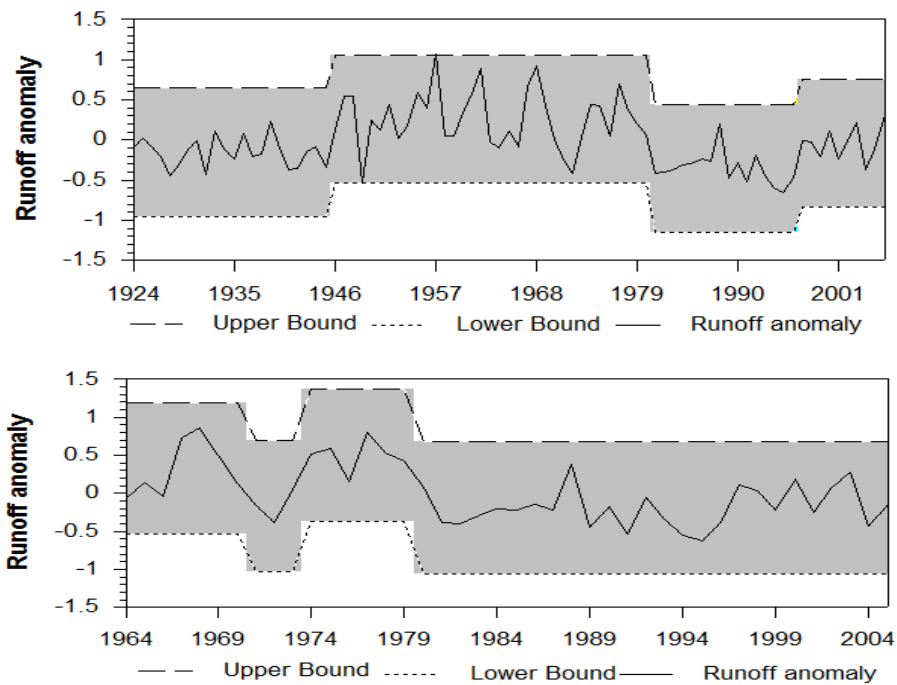


Figure 5.16 Significant step changes at ZGP25 and 1291100

Table 5.8 Step change statistics for stations ZGP25 and 1291100

| Station | Year | Confidence interval | Confidence level |
|---------|------|---------------------|------------------|
| ZGP25 | 1946 | 1940, 1949) | 87% |
| | 1981 | (1971, 1983) | 100% |
| | 1997 | (1991, 2001) | 97% |
| 1291100 | 1971 | (1965, 1972) | 92% |
| | 1974 | (1974, 1975) | 93% |
| | 1980 | (1979, 1982) | 100% |

5.3.4 Detection of cyclic behaviour in streamflow

Single spectrum Fourier analysis is applied to detect for any cycles in the mean annual streamflow. For the six stations under analysis, Table 5.9 presents the Fisher's Kappa and Bartlett's Kolmogorov-Smirnov statistical tests of significance while Figure 5.17 shows the spectral densities of the prominent peaks in the streamflow time series.

Table 5.9 Fisher's Kappa and Bartlett's Kolmogorov-Smirnov tests for streamflow

| Sub-basin | Station | Fisher's Kappa | Bartlett's K-S | Significant cycle (years) |
|-------------|----------|----------------|----------------|---------------------------|
| Lake Kariba | ZGP25 | 11.55** | 0.35** | 10.25 |
| Luangwa | G.E. Rd. | 5.25** | 0.63** | 7.50 |
| Tete | 1891500 | 4.35** | 0.21* | 10.00 |
| Barotse | 1291100 | 4.84** | 0.38** | 10.50 |
| Kafue | 1591405 | 7.27** | 0.43** | 7.60 |
| Luanginga | 1591820 | 3.66 | 0.28 | - |

** significance at 0.01 level

* significance at 0.1 level.

Except for the Luanginga sub-basin, the Fisher's Kappa test shows that the spectrograms are not random and the Bartlett's Kolmogorov-Smirnov results show some statistically significant 7.5 and 10-year cycles. Because of the short (< 100 years) time series data which are of insufficient length to represent longer time cycles with some degree of statistical confidence, cycles longer than 15 years are not considered in this study.

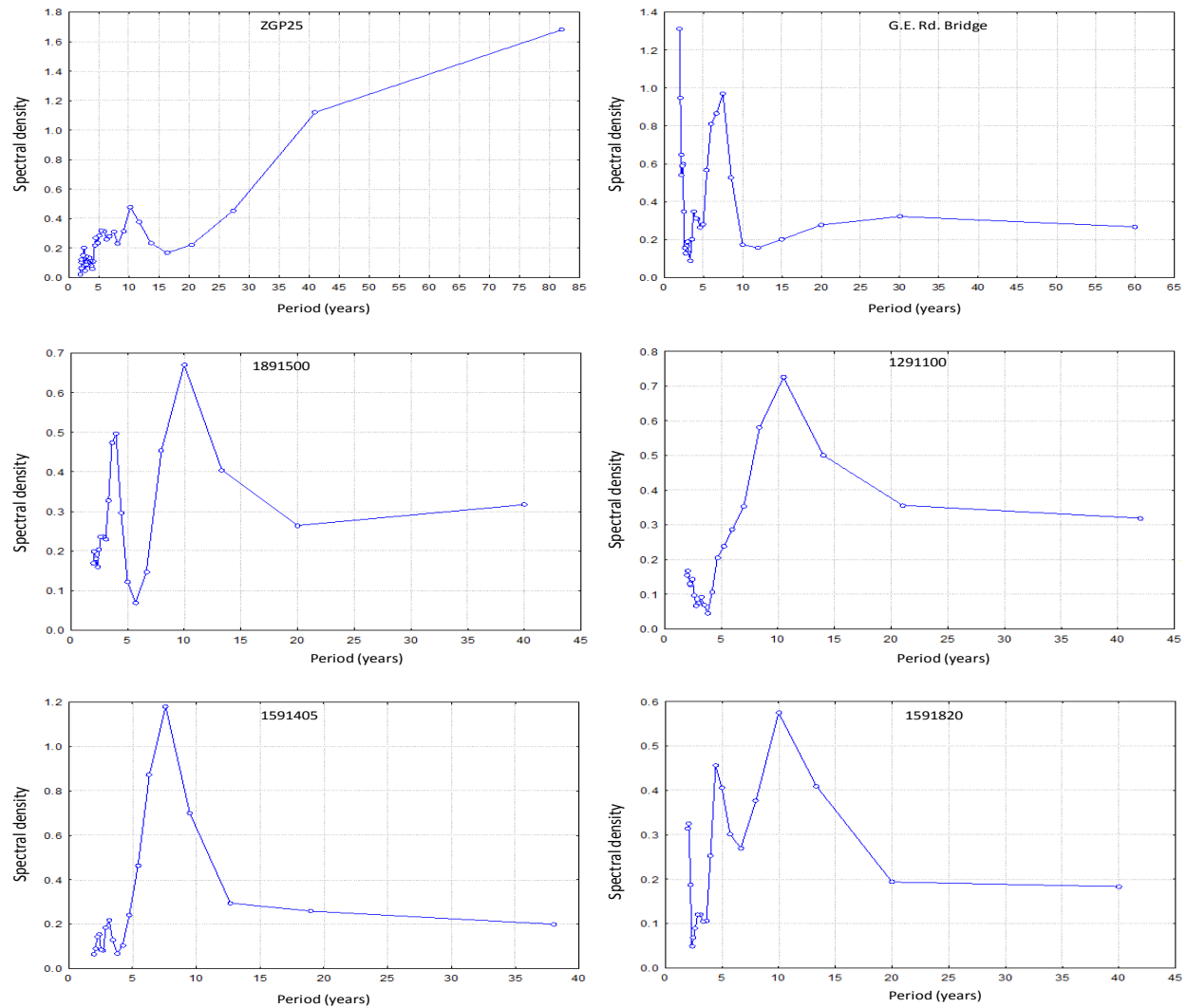


Figure 5.17 Streamflow spectral densities for case examples in the Zambezi

5.3.5 Seasonality in streamflow distribution

Monthly streamflow distribution in the Zambezi basin is presented in Figure 5.18. The observations reveal that the streamflow peaks in different months in moving from upstream to downstream. These streamflow variations can be attributed to the catchment storage and attenuation effects which tend to increase with distance from upstream to downstream. For 1291100 which is found in the Barotse further delays are attributable to the detention of water in the flood plains and this has also caused a delay in the peak flow at the downstream ZGP25 station at Victoria Falls catchment which is only attained later in May. The monthly distributions at 1891500 are higher even for the dry season months compared to the other stations, this is attributable to the presence of the Cahora Bassa reservoir upstream of the gauging station.

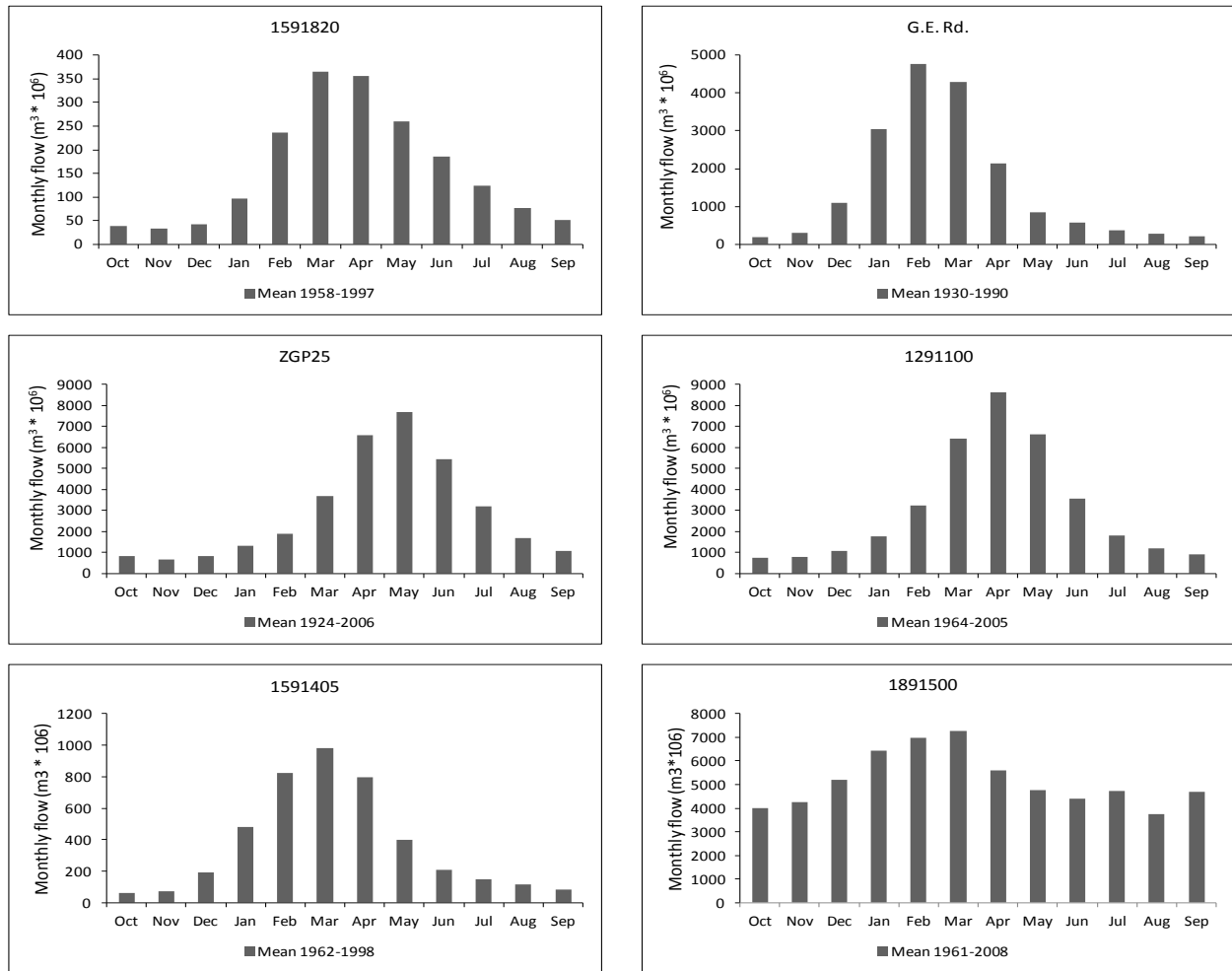


Figure 5.18 Mean monthly streamflow distribution

5.4 Discussion and conclusion

Extreme phases of climatic variability are associated with warm and cold conditions as well as with wet and dry conditions. These conditions have significant impacts on the environment and society and in some cases they are associated with disasters arising from extreme flood and drought events. At the same time hydrologists and water resource planners rely on the temporal and spatial scales of historical variability in rainfall and streamflow to evaluate hydrological and water management projects. In order to avoid the negative impacts of climatic variability, especially those caused by rainfall variability on the availability of water, it is necessary that the options for managing water resources be seen in the context of climatic variability. For this to be possible it is necessary to have knowledge of the historically observed variabilities as it can be used to understand the future hydrological conditions of the basin and to provide better options

for the water resource planners. In cases where variability in climate is well understood, and the results are reliable, the data may be extended to display future trends upon which adaptive management strategies can be developed.

In determining trends and patterns in historical data, the scale of observation and the density of gauging stations together with the length and quality of the time series data have significant influence on the nature of the outcome. Lack of long time series and good quality data will always be a setback when determining historical trends in climate and will result in unreliable outcomes which may not be useful in attempting to minimize the impacts of variability. In this study, the identification and quantification of hydrological variability in the Zambezi basin was hindered by data limitations. The available data are either of short time series or of poor quality with missing gaps, and in addition, some of the areas are not gauged making it very difficult to generate a comprehensive regional overview of the basin's variability. It is also difficult to determine long term trends and cycles from short time series data and this may result in insufficient information being generated to inform decision making in planning for the future water resources. Lack of properly documented information to quantify the effects of land use changes and other human-induced activities is also another drawback to the accurate quantification of hydrological variability in the Zambezi basin.

This chapter reflects on the complexity of the relationship between water resources and climate and highlights the implications of variability for water resources management. The series of tests carried out reflected the high spatial and temporal variability in rainfall and streamflow across the Zambezi basin. Further analysis of the historical time series data revealed an alternation between wet and dry conditions in the basin during the twentieth century. Short term seasonal to annual fluctuations were observed within the long term interdecadal cycles while at the same time it was noted that the nature of the cycles could be impacted significantly by the nature of the historical data. Both the long and short term fluctuations in rainfall and streamflow have consequent long and short term effects on the availability of water, but unlike the long term fluctuations, the short term fluctuations tend to be complex in nature and they have significant impacts on water supply which may require some prompt action. It is clear from the research findings that variability between the wet and dry years has remained relatively stable with respect to natural climatic variations and these observations suggest that there is little evidence of

climate change. The cycles observed in the historical time series of rainfall data in the Zambezi basin were noted to be not background noise (white noise) interference but they were not statistically significant implying some random fluctuations in the rainfall pattern. Despite the insignificant rainfall cycles, statistically significant cycles (7.5 years and 10 years) were observed in the streamflow time series and these were of a similar pattern and duration to those of the statistically insignificant rainfall cycles. Since streamflow is driven to a large extent by rainfall variability it is possible that the absence of statistically significant rainfall cycles may not be random but that the variability in rainfall is not consistent with the internal feedbacks that give rise to the interannual correlations within the climate system (Wolski et al., 2011).

Despite the influence of rainfall on streamflow, the higher coefficients of variation in streamflow compared to those in rainfall indicate the nonlinear response of runoff to rainfall. Statistically insignificant trends were observed in the historical rainfall and streamflow time series but over 70% of the sub-basins that were considered showed a generally decreasing pattern of rainfall and streamflow with time up to the end of the 20th century. Although there were signs of shifting towards wetter conditions after the year 2000 (e.g. Victoria Falls, ZGP25), this observation could not be ascertained for the entire basin due to shorter time series data most of which do not go beyond the year 2000. The decreasing runoff pattern can be attributed to some extent to the decreasing rainfall volumes received in a sub-basin during the same period since there are no strong indications of changes over time associated with water resource developments. This is largely because most of the developments in the basin are associated with non-consumptive uses, particularly hydropower generation. Decreasing rainfall patterns will also affect the streamflow and this may have adverse impacts on rainfed agriculture, water supply and the environment. If this decreasing pattern continues it may result in more dry periods which may extend into the future suggesting that water resources management should be implemented in such a manner that the deficits are accounted for while at the same time attempting to meet the demands of a growing basin population. Only two out of the ten stations under consideration revealed some statistically significant step changes in rainfall. It should be noted that in change analysis, the location of the point of change depends on the length of the time series, and as such, two different time series will not necessarily have changes occurring at the same time even if those points are in the same region. In addition the availability of short time series data may prevent

the detection of some of the changes that could have occurred across the basin and therefore no conclusions were drawn on the changes that could have occurred in the basin.

Several studies (e.g. Meehl, 1993; Mason 1995; Jury et al., 1999; Reason and Mulenga, 1999; Hulme et al., 2001) have confirmed the large increase in interannual rainfall variability over the southern African region and ENSO events are cited as the primary cause of climatic anomalies. In particular the warm El Niño events have been linked with past historical droughts in the region. Due to global teleconnections ENSO events have an influence over the basin through associated changes in SSTs over the tropical Indian Ocean. Variability in the region is also attributed to Tropical Temperate Troughs which have a large influence in rainfall variability over southern Zambia, Zimbabwe and most of the central parts of the basin (Washington and Todd, 1999). Although exploring the relationships between the rainfall variability in the Zambezi basin and the southern oscillation index (SOI) and SSTs was, beyond this study, such relationships have the potential to improve the understanding of variability in the basin.

Despite the difficulties encountered in detecting variability in the Zambezi basin, mainly due to data paucity, the results of this study impress upon the need to acknowledge that there is marked temporal and spatial variability in the historical records of rainfall and streamflow and that knowledge of the historical variability has important consequences for the management of variability and risk in water resource systems. In a basin, long term management plans are guided by the dynamic nature of water resources which is largely driven by climate variability. In view of the high variability in rainfall and streamflow there is need for flexible management systems that are able to accommodate the variability and therefore reduce the risks that occur as a result of over or under-estimation of the wet and dry events. For this to be successful there should be adequate knowledge and reliable estimates of the historical trends of rainfall and runoff. Although the study revealed interannual and interdecadal variability in rainfall and streamflow records, limited data may make it impossible to determine the return of the critical flood and drought events in the long term and in the absence of reliable information it may be difficult to formulate any adaptive measures with respect to climate variability. Nonetheless, the available records and the observed characteristics of variability in the Zambezi can still serve as a guide to decision making in water resource plans for the basin.

CHAPTER 6 HYDROLOGICAL MODEL CALIBRATION FOR THE ZAMBEZI BASIN

6.1 Introduction

Understanding the catchment hydrological processes and responses to change in climatic variables is crucial for water resources management and future planning. Hydrological models are usually used for the purpose of water resources assessment with regard to current and future conditions of environmental change. Before running a model it is necessary to gain an understanding of the catchment scale hydrological responses in relation to the physical basin properties and how these responses are interpreted in the model. It is therefore important to ensure that there is enough information on the physical basin properties that can be used to inform the model calibration. Primary catchment information can be used to constrain the model parameter space as well as reducing equifinality whereby different parameter sets can result in similar model outputs causing non-identifiability of the parameters (Wagener et al., 2003; Hughes et al., 2010). This information can be obtained from the modeller's experience and the understanding of the basin as well as from past studies in the basin. However, depending on the level of detail, such information, if insufficient, can result in inadequate conceptualisation of the processes thus generating an inadequate set of parameters which leads to parameter uncertainty. In large basins such as the Zambezi, the application of hydrological models is frequently faced with issues of uncertainty due to lack of data, heterogeneity and variability that occur at different scales.

This chapter presents the results of the Pitman model calibration for the Zambezi basin. The model makes use of 18 parameters to quantify the main hydrological processes at the basin scale. It has been identified that this large number of parameters is a major cause of equifinality (Hughes et al., 2010) and this problem is expected to be more pronounced in large basins such as the Zambezi where there is not enough data to constrain the model predictions. It is therefore important that the model parameters be derived from a sound conceptual understanding of the basin processes so as to minimise uncertainty in model predictions. The calibration of the Pitman model within SPATSIM is typically achieved through 'trial and error' manual calibration until a behavioural parameter set is obtained. This process is subjective, which may introduce

uncertainties in the modelling process. Although the SPATSIM facility does not include any methods for automatic calibration, the uncertainty version of the Pitman model is used in this study to explore the parameter space and to guide the calibration process for the Zambezi basin.

6.2 The calibration approach

The procedures used to establish the Pitman model for the Zambezi basin are outlined below and Figure 6.1 is a flow chart to illustrate the process.

- i. Assign the initial ranges (minimum and maximum) of model parameters using prior knowledge of the basin processes and guided by physical basin property information.
- ii. Use Monte Carlo sampling to generate ensembles from the total parameter space using the uncertainty version of the model.
- iii. Use statistical objective functions to select the behavioural (Beven, 2006) parameter set.
- iv. Refine the behavioural parameter set using manual calibration to establish the parameters for the gauged catchments.

The information used to determine the initial values of the parameters and their ranges included soil types (FAO, 2003), topography, geology and vegetation from the USGS-NASA databases (<http://edcdaac.usgs.gov/data>). Although the scale of the FAO soils is relatively coarse (1: 5 000 000), the information obtained is valuable in providing a baseline indication of the soil types in a given area and it was considered a good starting point to the calibration process. Other physical basin information was obtained from previous studies in the basin such as Mazvimavi (2003) for some of the sub-basins that lie in Zimbabwe, Mwelwa (2004) and Ndiritu (2009) for the Kafue basin in Zambia, Winsemius et al. (2006) for the Luangwa basin, Kumambala (2010) for the Lake Malawi catchment and Ashton et al. (2001) for some general physical property data that cover most parts of the Zambezi basin.

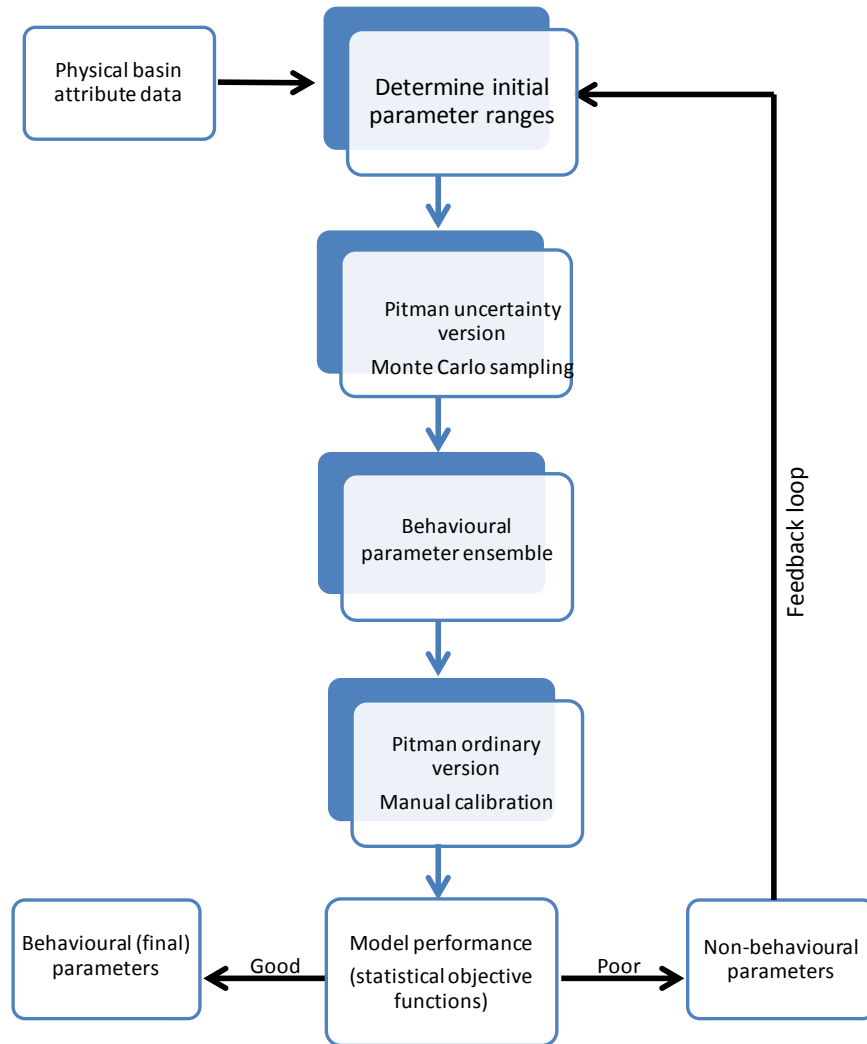


Figure 6.1 Schematic of the hydrological modelling process for the Zambezi basin

6.2.1 Assigning the initial parameter ranges

Given the limitations of available physical property data, a subjective ‘rule based’ approach was undertaken in order to assign and constrain the initial parameter ranges for the sub-basins. Based on some of the established calibration principles for the Pitman model (e.g. Hughes, 1995; 1997), the conceptual understanding of the model parameters and a qualitative interpretation of the physical basin characteristics (Kapangaziwiri, 2008), it was possible to derive the initial ranges of the model parameters (Tables 6.1 and 6.2) for the sub-basins (Upper Zambezi, Luanginga, Barotse, Kafue, Lake Kariba, Luangwa and Lake Malawi) of the Zambezi. Based on literature, the following parameters were assigned fixed values, PI1 (1.5), PI2 (4), SL (0), CL (0), TL (0.25), and GPOW (3). Each sub-basin was also assigned fixed AFOR and PEVAP parameter

values which are unique for each sub-basin. The RDF parameter was fixed at 0.8 for the most upstream sub-basins including the Kafue (Mwelwa, 2004) and varied (0.6 to 1.0) for the drier sub-basins such as Gwai and Mupfure, bearing in mind that lower rainfall amounts are likely to be more concentrated in fewer days over the month while an even spread across the month is expected for high rainfall amounts.

The main model parameters ZMIN, ZAVE, ZMAX, ST, POW, FT, GW and R are guided by the physical interpretation of the parameters and on the following calibration principles:

- Large differences in the ZMIN and ZMAX values are expected in basins which have a large variation in soil properties.
- Both ZMIN and ZMAX are assigned higher values for coarse textured and well drained soils (sands) while low values are assigned to soils of a finer texture (clays and loams).
- Arid basins with thin soils are expected to have low infiltration capacities and therefore low values of ZMIN and ZMAX.
- The ST parameter is largely guided by the moisture holding capacity of the soil in the saturated and unsaturated zones. Geological formations that are easily weathered result in deep soils and high ST values are expected for such soils while low values are assigned to areas with thin soils.
- The soil moisture runoff parameter (FT) is partly guided by soil characteristics. FT is also influenced by topography whereby the runoff rate is increased in areas of steeper gradients. High FT values are therefore assigned for high gradients and high relief areas. This is because slope is a good indicator of the kinetic energy available in moving the water towards the downstream outlet.
- GW is guided by the moisture state ST, soil texture and structure and the underlying geology. Fracturing and secondary weathering also have a major role to play in the movement of water to the groundwater aquifer.
- The R parameter is associated with the relationship between soil moisture and evapotranspiration. Low values are expected in areas of deep rooted vegetation (bushland forest) while high values are expected in areas of less dense vegetation (grassland and savanna).

The physical basin characteristics of the various catchment areas described in Chapter 3, are briefly outlined below and were used to inform the initial parameter ranges. The initial parameter ranges for the various sub-basins are presented in Tables 6.1 and 6.2.

Upper Zambezi and Barotse

The Upper Zambezi drainage area includes the Kabompo, Luanginga, Lungue Bungo and all areas upstream of the Barotse. The mean annual rainfall received in the upper reaches is above 1 300 mm and below 1 000 mm in the downstream areas. Deep layers of wind-blown Kalahari sands which are overlain with deep ferralitic soils cover much of this drainage area. High values of the soil moisture storage parameter (ST) that reflect the high storage capacity of the deep Kalahari sands are assigned and the initial parameters range between 800 and 1500 mm. The area is characterised by an elevation ranging from about 1 000 to 1500 m above mean sea level (amsl). Land use includes subsistence farming and small village settlements with minimal developmental activities which have resulted in almost no water withdrawals in this part of the basin. The area is made up of dense and deeply rooted natural vegetation suggesting high ZMIN (100 to 200 mm/month) and ZMAX (800 to 1 500 mm/month) parameters that indicate high permeability and high absorptive capacity of the soils. The initial ranges of the parameters are shown in Table 6.1. The Barotse receives mean annual rainfall of 500 to 800 mm and has an elevation extending from 1 200 to about 800 m amsl in the floodplain. It is an extensive area of marshland and its soils tend to be a mixture of the Kalahari sands and sandy loams and not as deep as in the upper catchments. A moderately high soil moisture storage capacity is assumed with the initial ST parameter ranging between 600 and 1 500 mm. The initial parameter ranges (minimum and maximum) are presented in Table 6.2.

Kafue

The sub-basins considered under the Kafue drainage area include Lufwanyama, Luswishi, Lunga, Kafue 4 (Lukanga swamps), Kafue 3 (Itezhitezhi) and Kafue 1 (Kafue Flats). The Kafue drainage area receives a mean annual rainfall of 1 050 mm and its elevation extends from about 1 400 m amsl in the upper lying areas to 1200 m amsl in the middle of the sub-basin down to 800 m amsl in the low lying Kafue Flats area (Kafue 1 sub-basin). The soils are well drained moderately deep to deep sandy soils which have high absorption rates such that ST is high and

the initial parameter values range between 1 000 and 1 500 mm. As a result of high rainfall amounts, extensive vegetative cover and high drainage capacity, the drainage area is also characterised by high absorption rates. The initial parameter ranges of ZMIN and ZMAX are 100-200 and 900-1400 mm/month respectively and are shown in Table 6.1.

Lake Kariba

Compared to the rest of the Zambezi basin, the Lake Kariba drainage area receives less rainfall with mean annual values between 500 and 700 mm. Catchments found in this area include, Zambezi 8 as well as Gwai and Mupfure. There is a wide variation in topography which extends from about 1 400 m amsl in the southernmost areas to about 400 m amsl in the area dominated by Lake Kariba. The Zambezi 8 catchment consists of deep Kalahari Sands which suggest high ST values ranging between 600 and 1 800 mm. This catchment is dominated by dense natural vegetation for conservation purposes implying high ZMIN (100 to 200 mm/month) and ZMAX (800 to 1200 mm/month). The Gwai and Mupfure catchments are dominated by Kalahari Sands and very shallow gravelly soils resulting in a lower ST ranging between 400 and 1000 mm. Due to prevailing dry conditions the antecedent soil moisture conditions are low, with sparse vegetation, resulting in low initial values of the ZMIN parameter (20 to 100 mm/month). The initial parameter ranges for these sub-basins are presented in Table 6.2.

Tete

The Tete drainage area experiences a mean annual rainfall amount of 500 mm to 900 mm. The area is made up of quite a low elevation (about 400 m amsl) at Cahora Bassa where the river flows through some narrow gorges as it enters the broad shallow valley in the lower reaches of the basin. Although located in Zimbabwe, the Manyame and Mazowe catchments drain into the Tete sub-basin of Mozambique. These catchments are considered since the sub-basins on the Mozambican side do not have sufficient data that can be used for modelling. The Manyame soils are generally gravelly and coarse grained sands on granite while the Mazowe sub-basin is characterised by shallow to moderately deep sandy soils with clays on granite and dolerite. The initial ST parameter range (400 to 800 mm) is therefore lower compared to the Kalahari Sand dominated areas. Some portions in the southernmost part of Mazowe have an elevation above 2 000 m amsl but the elevation gradually decreases to about 400 m amsl in the downstream

direction. The Manyame catchment ranges in elevation from around 1 500 m amsl in the upstream areas to about 800 m amsl in the downstream area. The vegetation is moderately dense and not very deeply rooted suggesting low ZMIN (10 to 100 mm/month) and ZMAX (600 to 1 200 mm/month) values.

Luangwa and Lake Malawi

The Luangwa drainage area is an extension of the African Rift valley, with steep slopes in the upstream areas and tributaries that drain a steep escarpment. The mean annual rainfall is around 1 000 mm and can be greater than 1 000 mm in the high north eastern areas. The altitude varies from 400 to 1 600 m amsl. The steep slopes suggest high FT and the range of initial parameters is between 50 and 150 mm/month. The initial ST parameter range (400 to 1 000 mm) reflects the moderately deep sandy loams that are predominant in the sub-basin. The Namitete is a catchment of the Lake Malawi drainage area and receives a mean annual rainfall of 900 to 1 000 mm. Most of the gauging stations in Lake Malawi have very poor data and only the Namitete has reasonably good quality data that could be used for calibration. A large part of the sub-basin is on a plateau which falls steeply towards Lake Malawi from an elevation of about 1 400 to 600 m amsl. Soils in this sub-basin are moderately deep sandy loams on compact and heavy textured ferralitic subsoil such that the initial range of ST is set at 400 to 800 mm.

Table 6.1 Initial parameter ranges for example catchments of the Zambezi

| Parameter | Catchment | | | | | | | | | | | | | | | | | |
|-----------|-----------|-------|-----------|-------|------------|-------|------------|-------|-------|-------|----------|-------|---------|------|---------|-------|---------|------|
| | Kabompo | | Luanginga | | Zambezi 12 | | Lufwanyama | | Lunga | | Luswishi | | Kafue 4 | | Kafue 3 | | Kafue 1 | |
| | Min | Max | Min | Max | Min | Max | Min | Max | Min | Max | Min | Max | Min | Max | Min | Max | Min | Max |
| ZMIN | 100 | 200 | 100 | 200 | 100 | 200 | 100 | 200 | 100 | 200 | 100 | 200 | 100 | 200 | 100 | 200 | 100 | 200 |
| ZMAX | 800 | 1500 | 800 | 1500 | 800 | 1500 | 900 | 1400 | 900 | 1400 | 900 | 1400 | 900 | 1400 | 900 | 1400 | 900 | 1400 |
| ST | 800 | 1500 | 800 | 1500 | 600 | 1500 | 1000 | 1500 | 1000 | 1500 | 500 | 5000 | 1000 | 1500 | 1000 | 1500 | 1000 | 1500 |
| POW | 1.5 | 6 | 2 | 5 | 3 | 6 | 1.5 | 4 | 2 | 5 | 2 | 10 | 2 | 6 | 3 | 6 | 2 | 8 |
| FT | 10 | 50 | 10 | 50 | 5 | 50 | 20 | 70 | 10 | 30 | 10 | 30 | 20 | 80 | 5 | 30 | 10 | 30 |
| GW | 5 | 50 | 5 | 30 | 5 | 35 | 5 | 10 | 3 | 15 | 3 | 10 | 5 | 15 | 5 | 15 | 5 | 15 |
| R | 0.2 | 0.8 | 0.3 | 0.8 | 0.3 | 0.8 | 0.2 | 0.5 | 0.2 | 0.5 | 0.25 | 0.8 | 0.2 | 0.6 | 0.2 | 0.5 | 0.2 | 0.8 |
| D.DENS | 0.2 | 0.5 | 0.3 | 0.6 | 0.3 | 0.7 | 0.2 | 0.4 | 0.2 | 0.6 | 0.2 | 0.7 | 0.2 | 0.4 | 0.2 | 0.6 | 0.2 | 0.6 |
| T | 5 | 100 | 10 | 80 | 10 | 70 | 10 | 250 | 0.5 | 40 | 10 | 50 | 15 | 60 | 3 | 20 | 20 | 80 |
| S | 0.001 | 0.005 | 0.001 | 0.005 | 0.001 | 0.008 | 0.001 | 0.008 | 0.001 | 0.005 | 0.001 | 0.008 | 0.001 | 0.01 | 0.001 | 0.009 | 0.001 | 0.01 |
| GW slope | 0.001 | 0.01 | 0.001 | 0.005 | 0.001 | 0.005 | 0.001 | 0.01 | 0.001 | 0.005 | 0.001 | 0.005 | 0.001 | 0.01 | 0.001 | 0.01 | 0.001 | 0.01 |
| RSF | 0.2 | 0.8 | 0.2 | 0.8 | 0.2 | 1 | 0.2 | 0.6 | 0.2 | 0.5 | 0.2 | 0.5 | 0.2 | 0.8 | 0.3 | 0.8 | 0.2 | 0.6 |

*Fixed parameters AFOR: unique values for the sub-basins, RDF: 0.8, SL: 0, CL: 0, PI1: 1.5, PI2:4, TL: 0.25, GPOW: 3

Table 6.2 Initial parameter ranges for example catchments of the Zambezi

| Parameter | Sub- basin | | | | | | | | | | | | | | | |
|-----------|------------|-------|-----------|-------|-------|-------|---------|-------|---------|-------|--------|-------|----------|------|----------|------|
| | Zambezi 10 | | Zambezi 8 | | Gwai | | Mupfure | | Manyame | | Mazowe | | *Luangwa | | Namitete | |
| | Min | Max | Min | Max | Min | Max | Min | Max | Min | Max | Min | Max | Min | Max | Min | Max |
| RDF | 0.7 | 0.9 | 0.7 | 0.9 | 0.6 | 1 | 0.7 | 1 | 0.6 | 0.9 | 0.6 | 0.9 | 0.6 | 0.8 | 0.7 | 0.9 |
| ZMIN | 100 | 200 | 100 | 200 | 20 | 100 | 20 | 100 | 10 | 90 | 10 | 90 | 50 | 200 | 100 | 200 |
| ZMAX | 800 | 1200 | 800 | 1200 | 800 | 1200 | 600 | 1200 | 600 | 1200 | 600 | 1200 | 500 | 1000 | 500 | 1000 |
| ST | 600 | 1500 | 1000 | 1800 | 400 | 1000 | 400 | 1000 | 400 | 800 | 400 | 800 | 400 | 1000 | 400 | 800 |
| POW | 1.5 | 6 | 2 | 6 | 3 | 5 | 3 | 5 | 2 | 6 | 2 | 6 | 2 | 6 | 2 | 6 |
| FT | 10 | 100 | 10 | 60 | 5 | 20 | 5 | 20 | 5 | 50 | 5 | 50 | 50 | 150 | 10 | 50 |
| GW | 5 | 30 | 5 | 30 | 2 | 20 | 2 | 20 | 5 | 20 | 5 | 20 | 10 | 30 | 2 | 20 |
| R | 0.2 | 0.8 | 0.2 | 0.6 | 0.3 | 0.8 | 0.3 | 0.5 | 0.3 | 0.8 | 0.3 | 0.8 | 0.2 | 0.8 | 0.2 | 0.8 |
| D.DENS | 0.2 | 0.7 | 0.2 | 0.6 | 0.2 | 0.4 | 0.2 | 0.4 | 0.2 | 0.9 | 0.2 | 0.9 | 0.4 | 1.8 | 0.2 | 1.5 |
| T | 15 | 100 | 15 | 80 | 10 | 80 | 10 | 80 | 0 | 50 | 0 | 50 | 0 | 40 | 0 | 50 |
| S | 0.001 | 0.005 | 0.001 | 0.003 | 0.001 | 0.003 | 0.001 | 0.005 | 0.001 | 0.005 | 0.001 | 0.005 | 0.001 | 0.01 | 0.001 | 0.01 |
| GW slope | 0.001 | 0.01 | 0.001 | 0.01 | 0.001 | 0.01 | 0.001 | 0.01 | 0.001 | 0.01 | 0.001 | 0.01 | 0.001 | 0.01 | 0.001 | 0.01 |
| RSF | 0.3 | 0.8 | 0.3 | 0.8 | 0.3 | 0.5 | 0.3 | 0.5 | 0.3 | 0.8 | 0.3 | 0.8 | 0.3 | 0.8 | 0.3 | 0.8 |

*Fixed parameters AFOR: unique values for the sub-basins, SL: 0, CL: 0, P11: 1.5, P12:4, TL: 0.25, GPOW: 3

* The Luangwa has been calibrated for the entire sub-catchment and not for the individual sub-basins

6.2.2 Generating the parameter space using the uncertainty version of the Pitman model

Using the previously generated minimum and maximum parameter ranges as input, the second step employs the uncertainty version of the Pitman model which uses a Monte-Carlo sampling approach (as described in Chapter 4) to explore the parameter space. While it is possible that a number of equally acceptable parameter sets may be generated, the behavioural (Beven, 2006) ensembles which are used to inform the manual calibration process are selected based on the model performance using statistical objective functions including, the percentage bias (PBIAS) and the Nash-Sutcliffe coefficient of efficiency (CE) for both transformed and log transformed data. Due to subjectivity and the non-reliability of the observed data which are mainly affected by measurement errors and the fact that we do not know what the data actually represent in terms of developments that exist within a sub-basin (Hughes et al, 2011b), an acceptable model performance was regarded as that in which $CE(Q) > 0.5$, $CE(\ln Q) > 0.5$ and $10\% \geq PBIAS \geq -10\%$. Q represents the untransformed flows while $\ln(Q)$ represents the log transformed flows. Using the UN1 text file generated by the uncertainty version of the model, the ensembles are ranked in order of model performance and the results demonstrate the issue of equifinality where a number of behavioural parameter sets are obtained for each uncertainty run. For example, using the performance criteria given above, a total of 525 ensembles out of 5 000 ensemble show behavioural performance for the Kabompo and 549 for Zambezi 10, while Zambezi 12, Gwai and Luangwa have behavioural ensembles amounting to 242, 154 and 255 respectively.

Although some parameters show equally performing values over a larger parameter space making it difficult to identify the optimum parameters, the scatter plots in Figure 6.2 show that some parameters (e.g. GW, ST, ZMAX, FT, POW) are identifiable and with distinct range of optimum parameter values at high CE values. These identifiable parameter values can be used to inform the manual calibration process. For example the optimum GW value required to reproduce the observed flows is identifiable at around 10 mm month^{-1} for Kabompo while ST is identifiable at values generally higher than 1 100 mm.

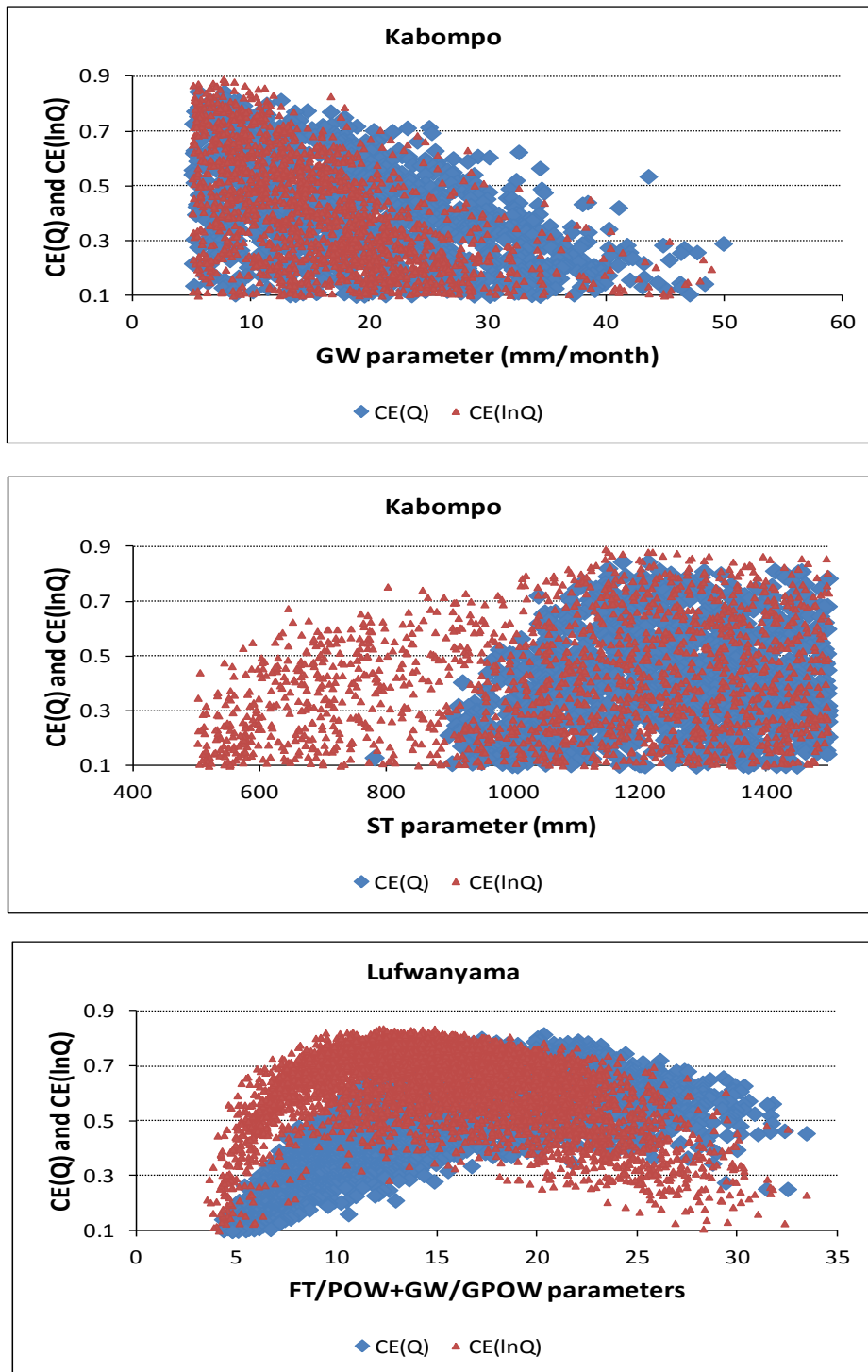


Figure 6.2 Scatter-plots of the variation of the coefficients of efficiency against GW, ST and FT/POW+GW/GPOW parameter values

The scatter plots can also be used to show interactions between parameters and the model performance over different parameter ranges. When combined GW and FT show more distinct

optimum values than considered separately. The lower graph in Figure 6.2 illustrates the effects for combinations of the soil moisture storage (FT and POW) and groundwater recharge (GW and GPOW) parameters. All of these parameters interact to generate the simulated low flow response and are not individually identifiable. Figure 6.2 can be used to guide the selection of a behavioural value of FT, given that the other parameters (GW, POW and GOW) have been fixed. However, the lower graph in Figure 6.2 illustrates that the range of behavioural combined parameter values is different if the two objective functions $CE(Q)$ and $CE(\ln Q)$ are considered. This suggests that further information is required to identify behavioural values for both soil moisture drainage and groundwater recharge function parameters. However, this information will not always be available.

In many cases there are several ungauged sub-basins above a gauging station used to assess the performance of the ensemble outputs. It will always be difficult to assess whether the differences in parameter values within the upstream sub-basins are totally appropriate and behavioural. However, using the physical basin properties to establish the initial parameter uncertainty range helps to ensure that the responses of the ungauged sub-basins have been appropriately simulated when the model is satisfactorily calibrated against the gauged sub-basin. While further detailed assessments of the quantitative limits between basin properties and model parameters are recommended, they were beyond the scope of this project. To improve the calibrations in the gauged sub-basins, the most behavioural parameter ensemble is chosen to inform the manual calibration process. The identifiable model parameters are manually adjusted where necessary while the other parameters are assigned fixed values using the optimum ensemble parameters or values derived from literature. Figure 6.3 represents the various sub-basins of the Zambezi as well as the gauging stations that were used for calibration and the final calibration results are presented in Section 6.3.

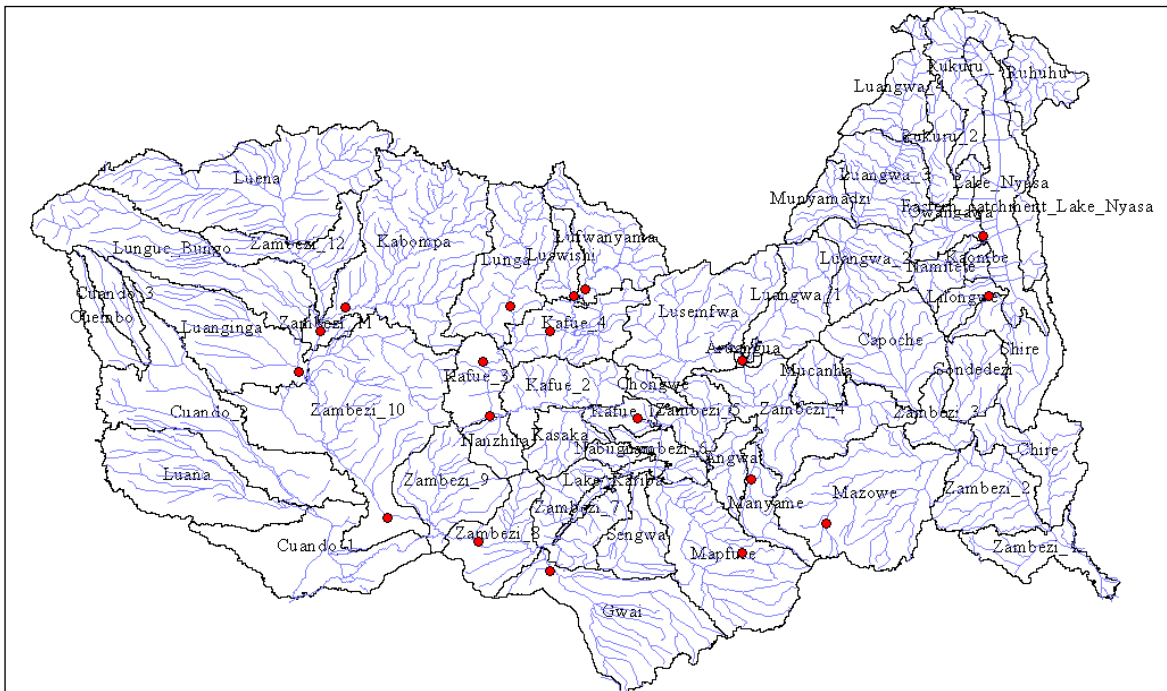


Figure 6.3 Flow gauging stations used for calibrations

6.3 Calibration results

This section presents the results of the model calibration process. It should be noted that there was no common simulation period and that simulations were based on the time series available at the different flow gauging stations. Table 6.3 summarises the model performance for the calibrations in the various sub-basins. In presenting the results, two types of data are used; the normal and natural log transformed. Log transformed values have an advantage of being less influenced by extremes while the normal values can be strongly influenced by high flows. The streamflow hydrographs and flow duration curves obtained from the calibrations are also presented in Figures 6.4 to 6.10. It should be noted, however that the results in Table 6.3 were simulated with natural parts of the model when there are substantial impacts (e.g. irrigation and water supply). It is possible that such impacts also contribute to the percent bias between the observed and simulated values.

Table 6.3 Summary statistics of streamflows based on untransformed and transformed data

| Catchments | Station | Months | Normal | | Ln values | | % bias | |
|------------|----------|--------|----------------|-------|----------------|-------|--------|------|
| | | | R ² | CE | R ² | CE | Normal | Ln |
| Kabompo | 1591002 | 48 | 0.72 | 0.71 | 0.84 | 0.82 | 3.4 | 1.8 |
| Luanginga | 1591820 | 383 | 0.715 | 0.714 | 0.684 | 0.662 | -1.3 | 3.1 |
| Zambezi 12 | 1591200 | 90 | 0.72 | 0.7 | 0.8 | 0.77 | 8.1 | 1.4 |
| Zambezi 10 | 1291100 | 324 | 0.763 | 0.761 | 0.838 | 0.828 | -0.9 | 1.1 |
| Lufwanyama | 1591406 | 335 | 0.769 | 0.768 | 0.84 | 0.834 | -2.3 | 1.2 |
| Luswishi | 1591440 | 164 | 0.584 | 0.559 | 0.727 | 0.725 | -4.2 | 0.8 |
| Lunga | 4560 | 430 | 0.556 | 0.55 | 0.721 | 0.717 | -8.2 | 0.7 |
| Kafue 4 | 1591405 | 343 | 0.765 | 0.749 | 0.83 | 0.793 | 8.5 | 3.8 |
| Kafue 3 | 1591404 | 156 | 0.678 | 0.662 | 0.593 | 0.55 | -7.9 | -0.6 |
| Kafue 1 | 470800 | 156 | 0.804 | 0.796 | 0.723 | 0.712 | -1.6 | 1 |
| Zambezi 8 | ZGP25 | 360 | 0.774 | 0.747 | 0.855 | 0.797 | -1.5 | 0.1 |
| Gwai | A22 | 329 | 0.537 | 0.438 | 0.61 | 0.593 | -4.8 | 6.2 |
| Mupfure | 1491580 | 351 | 0.516 | 0.51 | 0.662 | 0.613 | 1.9 | 11.1 |
| Manyame | 1491700 | 268 | 0.622 | 0.489 | 0.538 | 0.503 | 4 | 5.9 |
| Mazowe | D6 | 121 | 0.63 | 0.585 | 0.735 | 0.669 | 2.6 | -2.1 |
| Luangwa | G.E. Rd. | 372 | 0.723 | 0.721 | 0.757 | 0.735 | 0.1 | 1 |
| Namitete | 1992480 | 295 | 0.592 | 0.537 | 0.664 | 0.633 | -0.8 | 4.7 |

Upper Zambezi and the Barotse

The final calibration parameters for the Kabompo, Luanginga, Zambezi 12 and Zambezi 10 are presented in Table 6.4. Reasonably good simulations (Table 6.3) were achieved for the low and high flows as indicated by the coefficients of determination (R^2) and the coefficient of efficiency (CE) whose values are both above 0.6. The high ST which is above 1 000 mm is indicative of the deep Kalahari sands that dominate the area and the high absorption rate parameters (ZMIN and ZMAX) reflect the highly permeable nature of these soils. Compared to the upstream catchments, the predominant soils in the Barotse (Zambezi 10) are Kalahari sands and sandy loams which are not as deep as in the upper catchments. These soils, in addition to the area being extensively occupied by marshland, result in a moderately high soil moisture storage capacity (900 mm) and lower absorption rate parameters which are indicative of the less deeply rooted vegetation that is characteristic of swampy areas. The low POW value of 2.5 for the Zambezi 10 as compared to the upstream catchments suggests differences in conditions of wetness in a drainage area that is made up of a mixture of dryland and wetlands. Although a value of zero has

normally been assumed for the channel routing parameter, CL, this parameter has been calibrated at a value of 0.15 in order to obtain a good calibration. This observation could reflect an attenuation effect of the Barotse wetlands. The wetland function was also applied to the Barotse wetlands but the results were not very different from those calibrated without the wetland function.

Table 6.4 Calibrated parameters for upstream catchments

| Parameter | Kabompa | Luanginga | Zambezi 12 | Zambezi 10 |
|-----------|---------|-----------|------------|------------|
| RDF | 0.8 | 0.8 | 0.7 | 0.8 |
| PI1 | 1.5 | 1.5 | 1.5 | 1.5 |
| PI2 | 4 | 4 | 4 | 4 |
| AFOR | 25 | 20 | 40 | 10 |
| PEVAP | 1439 | 1515 | 1452 | 1564 |
| ZMIN | 150 | 180 | 200 | 100 |
| ZMAX | 1200 | 1200 | 1300 | 1000 |
| ST | 1100 | 1250 | 1500 | 900 |
| POW | 4 | 4 | 4 | 3 |
| FT | 20 | 22 | 5 | 70 |
| GW | 8 | 10 | 3 | 45 |
| R | 0.3 | 0.4 | 0.5 | 0.5 |
| TL | 0.25 | 0.25 | 0.25 | 0.25 |
| CL | 0 | 0 | 0 | 0.15 |
| GPOW | 3 | 3 | 3 | 2 |
| D.DENS | 0.3 | 0.5 | 0.3 | 0.5 |
| T | 40 | 30 | 8 | 30 |
| S | 0.001 | 0.001 | 0.008 | 0.005 |
| GW slope | 0.001 | 0.005 | 0.001 | 0.005 |
| RSF | 0.4 | 0.4 | 0.5 | 0.2 |

The time series plots and flow duration curves are presented in Figure 6.4. The low flow extremes are well simulated while the medium flows are slightly over-simulated and the extremely high flows are slightly under-simulated, but all within the acceptable behavioural range ($\pm 5\%$) of the percentage bias. The percent differences between the means of observed and simulated flows range from -0.9% to 3.4% for both untransformed and transformed flows, the only exception is the Zambezi 12 sub-basin with a bias 8.1% for the untransformed flows.

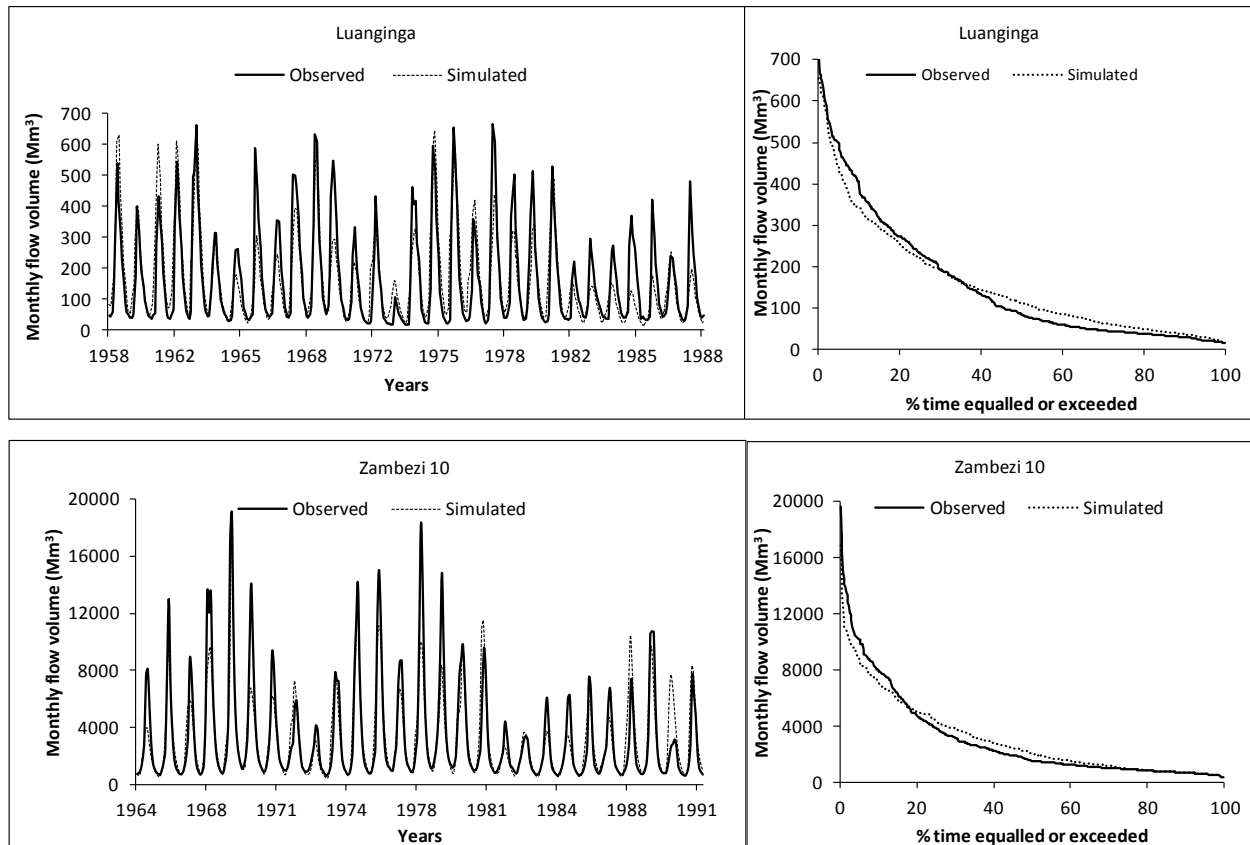


Figure 6.4 Observed and simulated monthly streamflows for Luanginga and Zambezi 10

Kafue

The Kafue Flats (Kafue 1) and the Lukanga swamps (Kafue 4) are modelled as natural reservoirs using the new wetland function of the model while the Itezhtezhi Dam (Kafue 3) is modelled using the reservoir component of the Pitman model. Some of the data for allocating the reservoir parameters were adopted from the water rights instituted by the Zambia Electricity Supply Corporation (ZESCO; World Bank, 2010), which include a freshet of $300 \text{ m}^3\text{s}^{-1}$ to be released from the Itezhtezhi every year over a period of 4 weeks in order to maintain the ecological balance of the Kafue Flats, a minimum release of $15 \text{ m}^3\text{s}^{-1}$ for other uses and a minimum flow of $25 \text{ m}^3\text{s}^{-1}$ to be maintained at all times. The final calibrated parameters for the Kafue basin are presented in Table 6.5 while the wetland and reservoir parameters are shown in Table 6.6. The calibration statistics (Table 6.3) indicate good simulations where both the R^2 and CE values are generally above 0.7, with the exception of Lunga and Luswishi where it was difficult to obtain good wet season calibrations. The low objective performance functions for the transformed values ($R^2 = 0.593$ and $CE = 0.55$) for the Itezhtezhi could be attributed to the fact

that the model applied in this study is based on a fixed operating rule while in reality the reservoir operation rules are not fixed and change depending on the amount of available water and the water uses.

Table 6.5 Calibrated parameters for the Kafue

| Sub-basin | Kafue | | | | | |
|-----------|------------|---------|----------|---------|---------|---------|
| Parameter | Lufwanyama | Lunga | Luswishi | Kafue 4 | Kafue 3 | Kafue 1 |
| RDF | 0.8 | 0.8 | 0.8 | 0.8 | 0.8 | 0.8 |
| PI1 | 1.5 | 1.5 | 1.5 | 1.5 | 1.5 | 1.5 |
| PI2 | 4 | 4 | 4 | 4 | 4 | 4 |
| AFOR | 25 | 30 | 35 | 20 | 20 | 5 |
| PEVAP | 1470 | 1533 | 1464 | 1510 | 1576 | 1617 |
| ZMIN | 200 | 200 | 200 | 200 | 100 | 200 |
| ZMAX | 1200 | 1334.88 | 1200 | 1200 | 1200 | 1200 |
| ST | 1200 | 1400 | 1500 | 1200 | 1000 | 800 |
| POW | 4 | 4 | 4.5 | 4 | 3.6 | 3 |
| FT | 50 | 20 | 20 | 60 | 10 | 50 |
| GW | 10 | 4 | 5 | 10 | 60 | 20 |
| R | 0.3 | 0.3 | 0.4 | 0.3 | 0.3 | 0.2 |
| TL | 0.25 | 0.25 | 0.25 | 0.25 | 0.25 | 0.25 |
| CL | 0 | 0 | 0 | 0 | 0 | 0 |
| GPOW | 3 | 3 | 3 | 3 | 3 | 3 |
| D.DENS | 0.5 | 0.5 | 0.3 | 0.3 | 0.5 | 0.4 |
| T | 50 | 5 | 28 | 70 | 7 | 50 |
| S | 0.008 | 0.005 | 0.001 | 0.001 | 0.002 | 0.001 |
| GW slope | 0.005 | 0.01 | 0.01 | 0.01 | 0.01 | 0.01 |
| RSF | 0.6 | 0.3 | 0.4 | 0.3 | 0.4 | 0.2 |

Table 6.6 Wetland and reservoir parameters for a) Kafue 1, b) Kafue 4 and c) Kafue 3

| Wetland parameter | (a) | (b) | Reservoir parameter | (c) |
|---|--------|-------|---|------|
| Local catchment area (km ²) | 15 000 | 5 000 | Reservoir Capacity (MCM) | 5700 |
| Residual Wetland storage (MCM) | 2 200 | 2 500 | Dead Storage (% Capacity) | 10 |
| Initial Storage (MCM) | 4 500 | 6000 | Initial Storage (% Capacity) | 100 |
| A in Area(m ²) = A*Volume(m ³) ^B | 40 | 10 | A in Area(m ²) = A * Vol (m ³) ^B | 0.9 |
| B in Area(m ²) = A*Volume(m ³) ^B | 0.85 | 0.8 | B in Area(m ²) = A * Vol (m ³) ^B | 0.2 |
| Channel capacity for spillage (MCM) | 450 | 600 | Annual Abstraction (MCM) | 466 |
| Channel Spill Factor (Fraction) | 0.8 | 0.7 | Annual Compensation Flow MCM) | 725 |
| AA in (Ret.Flow = AA*(Vol/RWS) ^{BB}) | 0.6 | 0.9 | | |
| BB in (Ret.Flow = A*(Vol/RWS) ^{BB}) | 0.5 | 0.8 | | |

Figures 6.5a and b illustrate the streamflow hydrographs and the flow duration curves for example sub-basins of the Kafue. The results for the Kafue Flats and the Lukanga swamps show an improvement from the results that had earlier been obtained without the wetland function (Mwelwa, 2004). Although the reservoir and the wetland models were applied, it was quite difficult to maintain a balance in the high flow components of the duration curve. Attempts to reduce the over-simulations in very high flows resulted in a worse under-simulation at lower flows (Figure 6.5b). Part of this problem could be related to uncertainties in the observed high flow measurements, but without more data this cannot be confirmed.

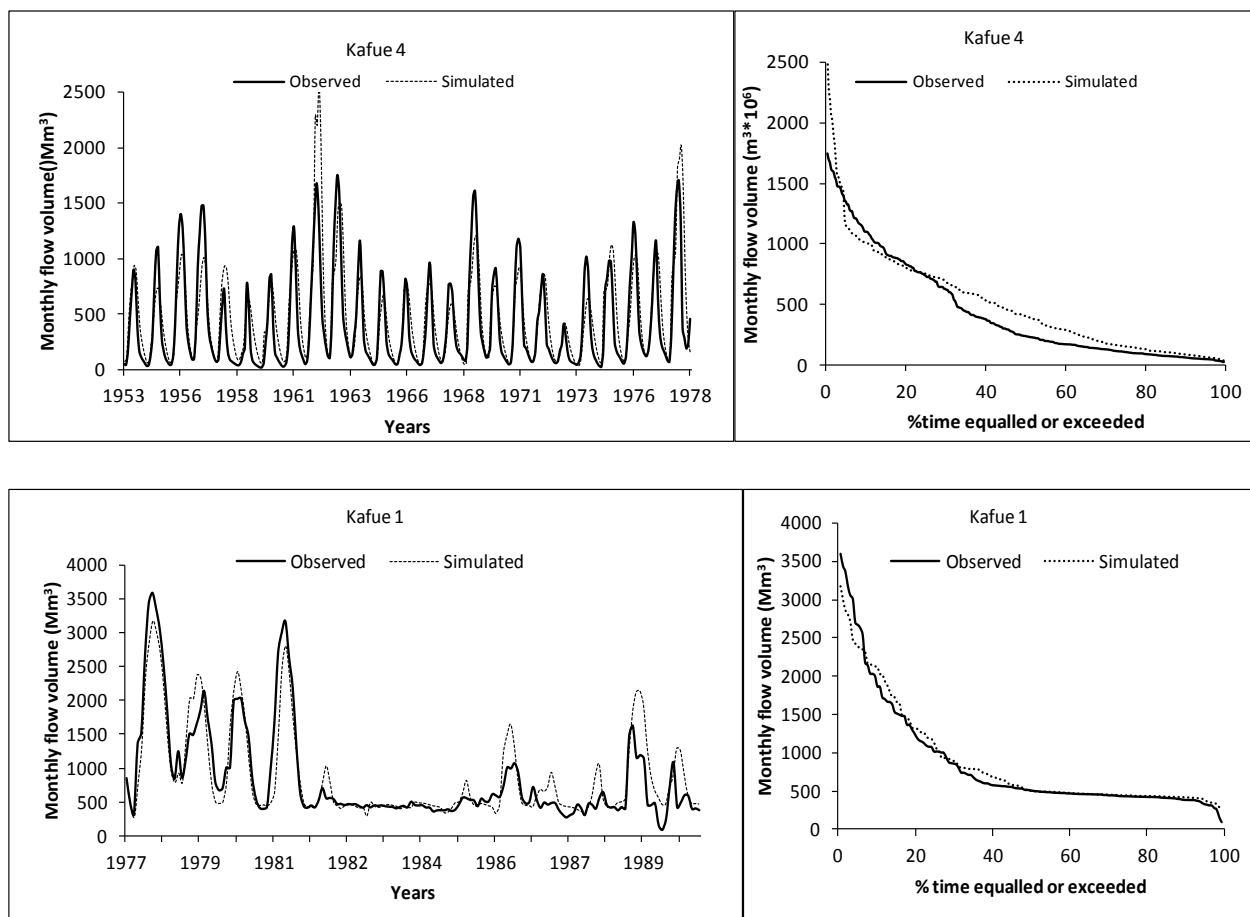


Figure 6.5a Observed and simulated monthly streamflows for Kafue 4 and Kafue 1

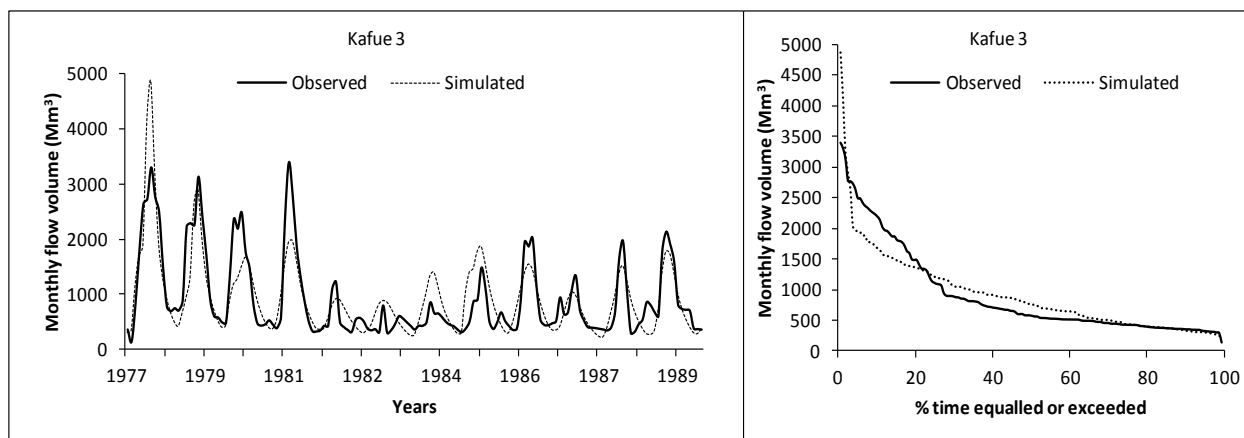


Figure 6.5b Observed and simulated monthly streamflows for Kafue 3

Lake Kariba

The final calibration parameters for the Lake Kariba catchments are presented in Table 6.7. The Zambezi 8 catchment which constitutes a larger part of Victoria Falls consists of deep Kalahari sands which resulted in a very high ST (1 900mm). This sub-basin is dominated by dense natural vegetation for conservation purposes and has high ZMIN (200 mm/month) and ZMAX (1400 mm/month) values. Due to the size of the catchment (516 878 km²), the parameter CL is used at a value of 0.2 suggesting attenuation of flow from this large area. This sub-basin is directly downstream of the Barotse where the CL parameter value is 0.15. The use of this parameter suggests that the flow is attenuated especially in the large sub-basins that are found in the western part of the Zambezi basin. The Gwai and Mupfure catchments are dominated by Kalahari sands and very shallow gravelly soils resulting in lower ST values of 500 and 800 mm respectively. These sub-basins are located in the dry and low rainfall (500 to 700 mm) areas of the basin. The prevailing dry conditions result in low antecedent soil moisture conditions, with sparse and moderately dense vegetation requiring low ZMIN and ZMAX values compared to the upstream sub-basins. Unlike the Zambezi 8 catchment, POW is lower indicating mixed soil characteristics that represent variable conditions of wetness. Overall the calibrated parameters reflect the marked variation in physiographic characteristics of the Lake Kariba drainage area which result in most of the runoff being generated from the northern sub-basins than from the dry southern areas such as the Gwai.

Table 6.7 Calibrated parameters for Lake Kariba, Tete, Luangwa and Lake Malawi

| Sub-basin Parameter | Lake Kariba | | | Tete | Luangwa | L. Malawi | |
|------------------------|-------------|-------|---------|---------|---------|-----------|----------|
| | Zambezi 8 | Gwai | Mapfure | Manyame | Mazowe | Luangwa | Namitete |
| RDF | 0.7 | 0.73 | 0.7 | 0.8 | 0.8 | 0.8 | 0.8 |
| PI1 | 2 | 1.5 | 1.5 | 1.5 | 1.5 | 1.5 | 1.5 |
| PI2 | 5 | 4 | 4 | 4 | 4 | 4 | 4 |
| AFOR | 80 | 30 | 40 | 30 | 40 | 25 | 20 |
| PEVAP | 1583 | 1619 | 1562 | 1445.58 | 1524 | 1685 | 1532.1 |
| ZMIN | 200 | 60 | 70 | 50 | 20 | 100 | 100 |
| ZMAX | 1400 | 1000 | 1000 | 900 | 1000 | 600 | 1000 |
| ST | 1900 | 520 | 800 | 530 | 350 | 600 | 630 |
| POW | 6 | 4 | 4 | 4 | 3 | 3 | 4 |
| FT | 5 | 5 | 7 | 12 | 28 | 92 | 15 |
| GW | 3 | 2 | 3 | 5 | 18 | 38 | 8 |
| R | 0.2 | 0.4 | 0.5 | 0.5 | 0.5 | 0.4 | 0.4 |
| TL | 0.25 | 0.25 | 0.25 | 0.25 | 0.25 | 0.25 | 0.25 |
| CL | 0.15 | 0 | 0 | 0 | 0 | 0 | 0 |
| GPOW | 3.5 | 3 | 3 | 2 | 3 | 3 | 3 |
| D.DENS | 0.3 | 0.3 | 0.25 | 0.3 | 0.8 | 0.7 | 0.8 |
| T | 2 | 20 | 20 | 10 | 40 | 15 | 60 |
| S | 0.005 | 0.001 | 0.001 | 0.005 | 0.001 | 0.008 | 0.005 |
| GW slope | 0.01 | 0.005 | 0.005 | 0.001 | 0.01 | 0.001 | 0.01 |
| RSF | 0.3 | 0.4 | 0.4 | 0.5 | 0.4 | 0.6 | 0.4 |

The calibration results (Table 6.3 and Figure 6.6) show a good fit between the observed and simulated values for the Zambezi 8 catchment while the results are moderate for Gwai (CE: 0.438 and 0.593 for transformed and untransformed flows respectively) and for Mupfure (CE: 0.51 and 0.613 for transformed and untransformed flows respectively). In both cases the dry season flows are over-simulated. These results highlight the sensitivity of streamflows to the nature of the input data which most frequently are inadequate in defining the spatial and temporal variations in the climate conditions. The flow duration curves indicate that extremely dry conditions or zero flow periods are expected more than 50% of the times in these drier areas of the Zambezi basin.

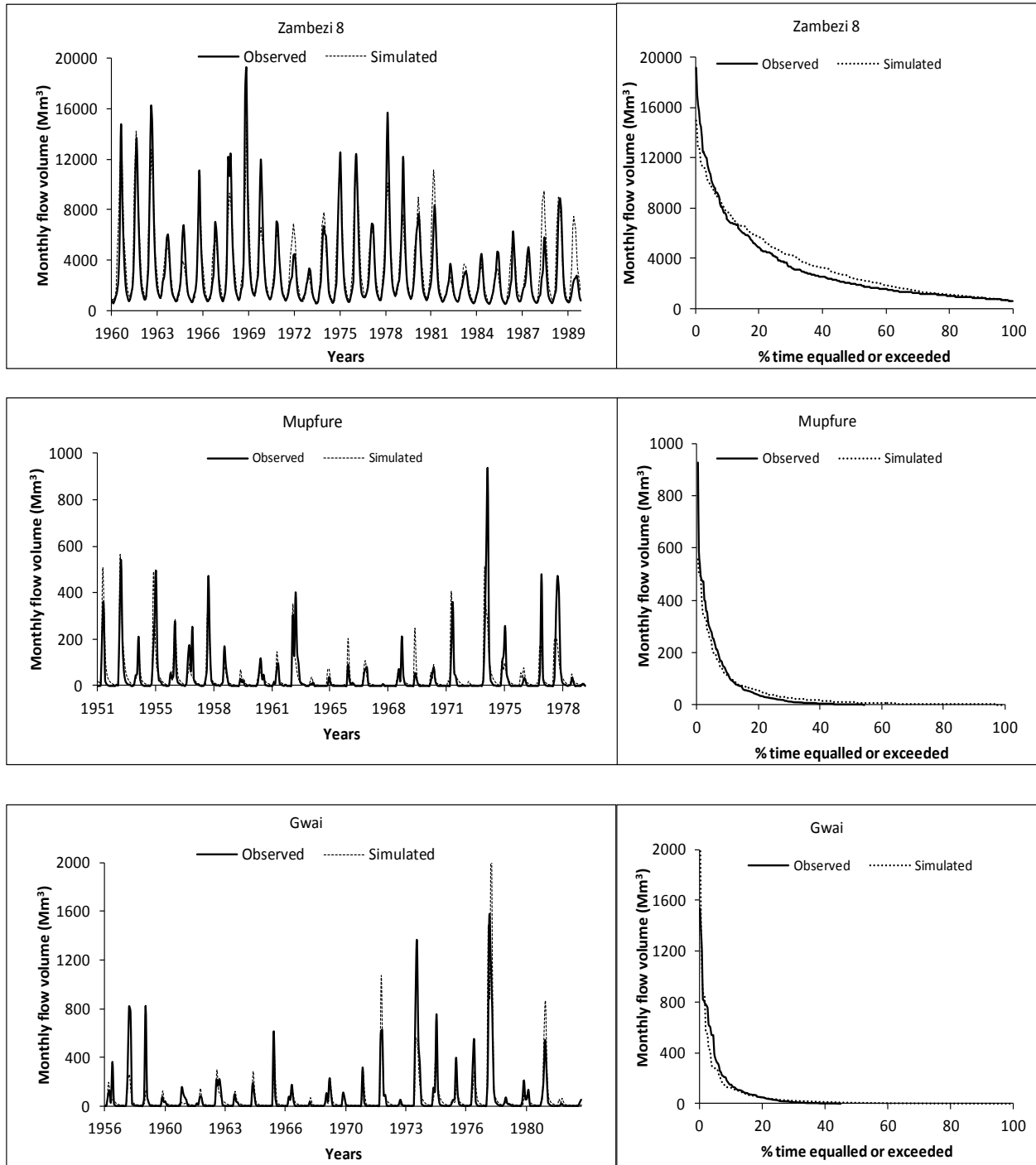


Figure 6.6 Observed and simulated monthly streamflows for catchments in Lake Kariba

Tete

The Mazowe and Manyame catchments represent the Tete drainage area. The calibrated ST values of 500 mm and 350 mm (Table 6.7) for Manyame and Mazowe respectively reflect that

the soil moisture storage capacity is not as high as in the wet upstream areas such as the Kabompo and the Kafue. Calibration plots of the observed and simulated flows for these catchments are presented in Figure 6.7. The performance of the model for both sub-basins is shown in Table 6.3, with CE: 0.489 and 0.503 untransformed and transformed values respectively for the Manyame catchment. The CE values for the untransformed and transformed flows are 0.59 and 0.67 respectively for Mazowe. The fact that the model performance is lower than in the wet upstream catchments reflects the sensitivity of streamflows in semi-arid catchments to the amount of rainfall and to the nature of the input data.

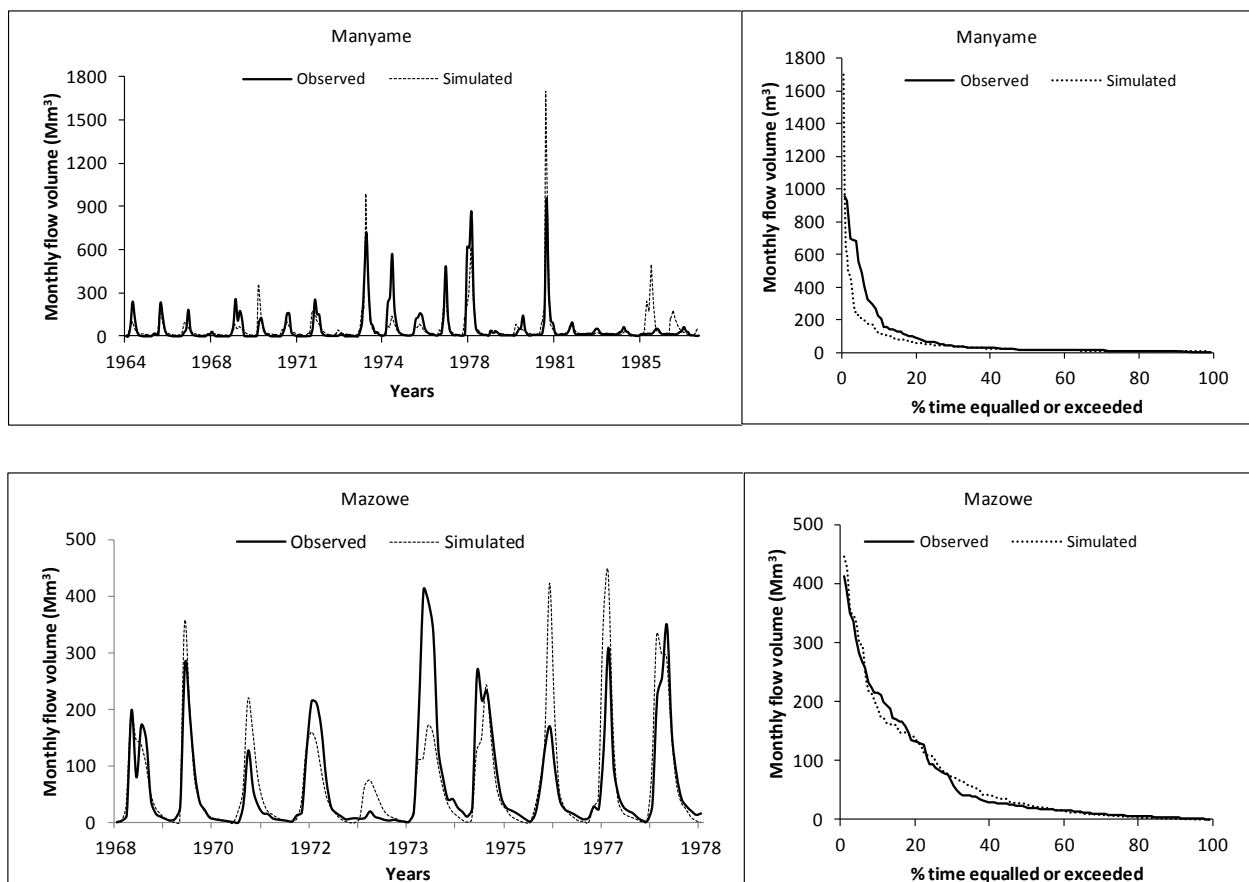


Figure 6.7 Observed and simulated monthly streamflows for Manyame and Mazowe

Luangwa and Lake Malawi

The Luangwa is a headwater catchment and characterised by a high mean annual rainfall of 1 000 mm as well as a large surface drainage area (142 832 km²). Steep gradients extending almost entirely from the upstream towards the downstream area require a high FT parameter value

(92mm month⁻¹) and although the catchment area is big, there is reduced attenuation effects compared to the other large sub-basins such as the Barotse and Lake Kariba. Much of the area, especially along the mainstream, is protected for conservation purposes resulting in well preserved soils that require moderately high surface absorption parameters. These conditions make it possible for a substantial amount of runoff to be generated from this drainage area. The final calibrated parameters for the Luangwa and Namitete are presented in Table 6.7. The Namitete is a small (8 176 km²) catchment of the Lake Malawi drainage area and is used in this study because the data are of reasonably good quality compared to other sub-basins in the drainage area. Because much of the sub-basin is a plateau, the FT (15 mm month⁻¹) parameter is not as high as that of the Luangwa. The calibration plots for the Luangwa drainage area and the Namitete catchment are depicted in Figure 6.8. Successful calibration was obtained for the Luangwa as indicated by the R² and CE values which are both above 0.7 (Table 6.3). The calibration experience for the Namitete was the same as in other dry catchments such as the Gwai and Mupfure where it is possible that the poor input rainfall data made it difficult to obtain a good fit between the observed and simulated flows and this is particularly so for the high flows where the R² and CE values are 0.592 and 0.537, respectively versus the values for the transformed data of 0.664 and 0.633, respectively. The general problem with high flows as observed in most parts of the basin may also be attributed to the quality of the observed data and the equations that are used to quantify the flows once the maximum gauge capacity is exceeded.

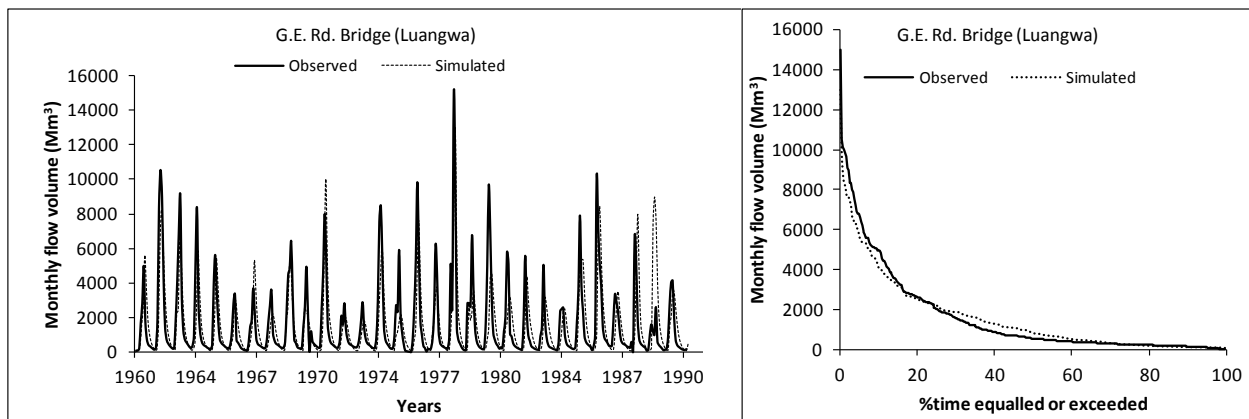


Figure 6.8a Observed and simulated monthly streamflows for Luangwa

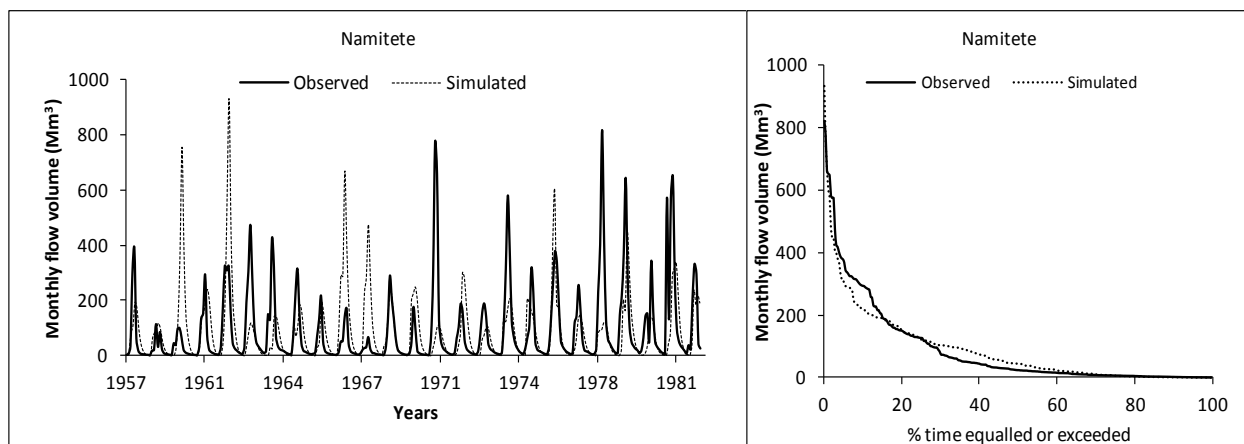


Figure 6.8b Observed and simulated monthly streamflows for Namitete

Model validation

It is necessary to test whether the calibrated model will perform well with other time periods outside the calibration time series. Validation was carried out using only those stations with a reasonably long time series that could be split to enable both calibration and validation. The validation results are presented in Table 6.8 and Figure 6.9.

Table 6.8 Validation and calibration statistics for example sub-basins

| Catchment | Period | Months | Normal | | Ln values | | % bias mean monthly | |
|------------|-------------|--------|----------------|-------|----------------|-------|---------------------|------|
| | | | R ² | CE | R ² | CE | Normal | Ln |
| Lufwanyama | Calibration | 335 | 0.769 | 0.768 | 0.840 | 0.834 | -2.3 | 1.2 |
| | Validation | 104 | 0.688 | 0.672 | 0.824 | 0.748 | 9.8 | 5.7 |
| Zambezi 8 | Calibration | 360 | 0.774 | 0.747 | 0.855 | 0.797 | -1.5 | 0.1 |
| | Validation | 141 | 0.703 | 0.687 | 0.67 | 0.654 | 6.2 | 3.3 |
| Zambezi 10 | Calibration | 324 | 0.763 | 0.761 | 0.838 | 0.828 | -0.9 | 1.1 |
| | Validation | 132 | 0.786 | 0.692 | 0.827 | 0.685 | 6.5 | 6.4 |
| Kafue 4 | Calibration | 343 | 0.743 | 0.735 | 0.808 | 0.763 | 0.3 | 3.6 |
| | Validation | 112 | 0.752 | 0.743 | 0.839 | 0.835 | -6.5 | -0.3 |
| Luangwa | Calibration | 372 | 0.723 | 0.721 | 0.757 | 0.735 | 0.1 | 1.0 |
| | Validation | 120 | 0.612 | 0.600 | 0.606 | 0.599 | -4.3 | 4.9 |

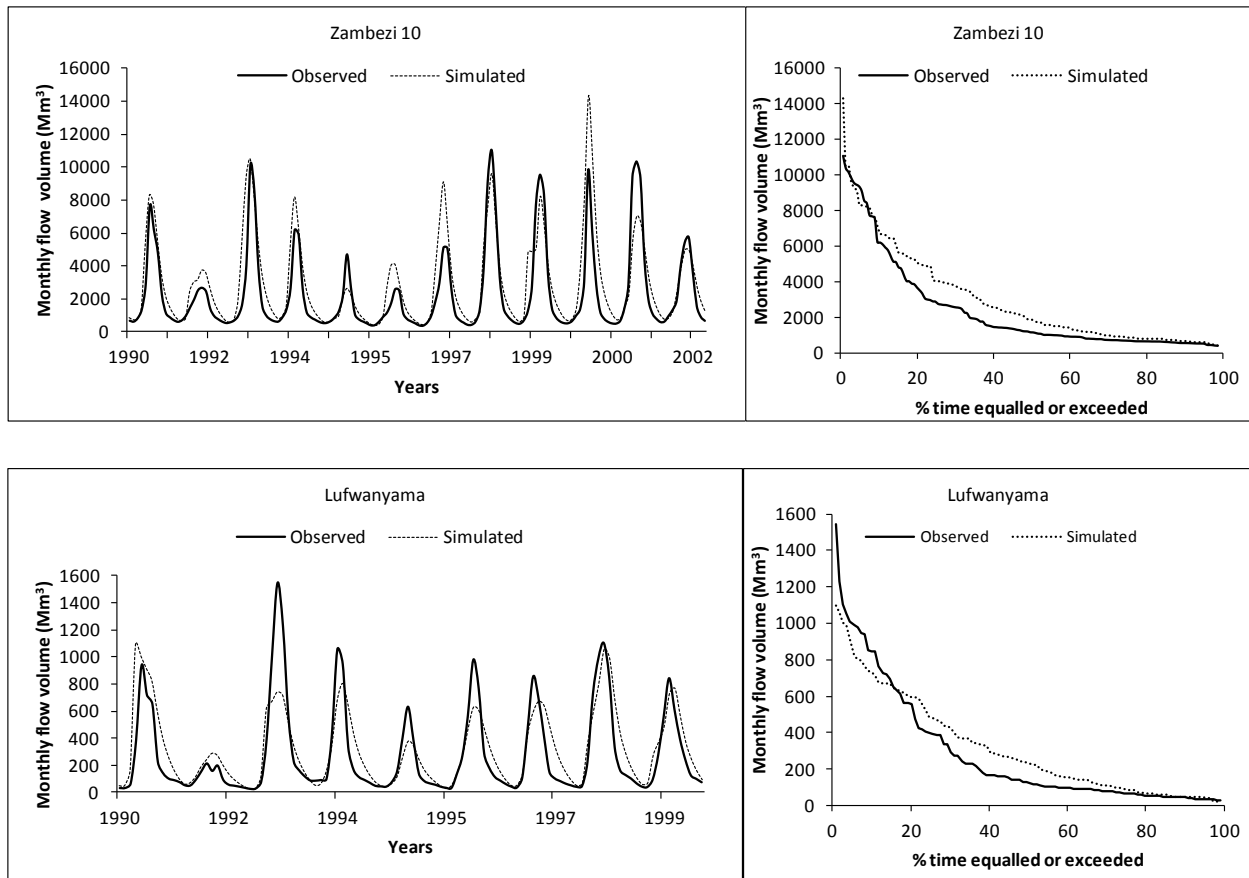


Figure 6.9 Observed and simulated monthly streamflows for validation tests

The model performance for validation was obtained at R^2 and CE values ranging between 0.6 and 0.8 for both the normal and log transformed values. Although the validation results show an increase in the percent bias between the means of the observed and simulated flows compared to the calibration results, the coefficients of determination and efficiency indicate that the model can be used with confidence for other periods that are outside the calibration period.

6.4 Discussion and conclusion

The main objective of this chapter was to establish a hydrological baseline for the Zambezi River basin, with the ultimate goal of using such a baseline for assessing future changes in basin hydrology and exploring the possibility of using simulated soil moisture as an indicator of agricultural droughts. In calibrating the model, uncertainty parameter bounds were generated from a subjective and ‘rule based’ assessment of available basin physical property data and these were used as input to the uncertainty version of the Pitman model in order to generate a

parameter space that could inform the manual calibration process. The behavioural parameters, based on statistical objective function assessments were refined using manual calibration to establish regional parameters for the Zambezi basin.

Based on untransformed and transformed data, the coefficients of determination (R^2) and efficiency (CE) that were used to assess the model performance were both above 0.7 for most of the sub-basins, except for the drier areas of the basin where the performance objectives ranged between 0.44 and 0.67. These results suggest, in general, that the modified Pitman model is capable of reproducing the hydrological response characteristics of the various sub-basins of the Zambezi. However, any modelling process is linked to uncertainties from various sources. Since this study relied on an initial interpretation of the physical property data, it is possible in cases where there was bias in the calibration results that the data were poor or inadequate for interpreting the physical process relationships or, due to subjectivity, the physical data could have been misinterpreted. Data paucity is identified as one of the sources of uncertainty in the calibration process for the Zambezi basin. The problem of capturing the peak flows may be attributed to limitations in the rainfall data in individual months or in wet seasons and also to the inability of the sparse raingauge networks to capture the storms that mainly characterise the rainfall patterns in the dry areas particularly in Zimbabwe (Mazvimavi, 2003) and the extremely high rainfall in wetter parts of the Zambezi basin. It is the same rainfall stations that are used to extrapolate the CRU rainfall data that were used in this study, which implies that this problem may have been translated to the CRU rainfall data. It was observed in Chapter 5 that the Zambezi basin has low runoff coefficients implying that any small errors in the rainfall time series can result in under or over-estimation of the flows and this effect is observed to some extent from the flow duration curves obtained from the calibration process. Uncertainty also arises from a lack of time series of evaporation data (this study used fixed seasonal distributions of potential evaporation) and it is possible that the spatial variation of the potential evaporation data may not have been adequately represented in the model. Apart from input data, uncertainties arise from the subjective parameter estimation approach and it is also possible that in some cases the model is unable to adequately represent the streamflow responses to rainfall in certain years of the calibration period.

The uncertainty version of the Pitman model assisted in generating the parameter space and identifying the behavioural parameters which were then used to guide the manual calibration. High flows were observed to be particularly sensitive to changes in ST while the POW function which determines the rate of decrease of runoff with moisture storage was found to have an impact on runoff when adjusted. It is appreciated that FT plays the role of maintaining a balance between runoff and evaporation (Pitman, 1973) and any changes made may upset the balance, mostly at the expense of evapotranspiration. In some cases changes in FT necessitated changes in the evaporation moisture storage parameter R. It was realised though, that FT had little effect during the very wet periods. One of the notable experiences during the calibration process was the difficulty encountered in modelling the river flows in the drier parts of the basin such as the Lake Kariba drainage area, where the Gwai and Mupfure sub-basins are found, in addition to some sub-basins in the Lake Malawi drainage area. In these drier areas, it was clear that river flows are extremely sensitive to small shifts in the rainfall regime which may not be adequately represented by either local or CRU data. The use of parameter constraints for guiding model calibration in both gauged and ungauged sub-basins proved to be useful as shown by the final calibration results. This approach can be useful especially in areas where the observed data are limited for model calibration. The need to consider uncertainty in hydrological modelling cannot be overlooked as it will improve the quality of model-based decisions in water resources management. It is hoped that improved access to high quality datasets of the basin physical properties would allow the application of enhanced approaches of parameter estimation (e.g. Kapangaziwiri and Hughes, 2008), thus contributing to increased confidence in model simulations for the basin.

Even though there are slight variations between the model results for the calibration and the validation periods, especially in terms of the percent bias, the validation results are still satisfactory implying that the model can also be used with confidence. The fact that the model was able to simulate the hydrology of the basin under dry and wet conditions indicates that it can be used to assess flow conditions under varying climates. With respect to soil moisture simulations, no validations could be made due to the fact that there were no available observed soil moisture data. It was confirmed, however, that in areas with deeper soils such as the Upper Zambezi and Kafue, the ST value is higher than for the shallower soils that are found in dry areas of the Lake Kariba sub-basin. In the absence of ground-based soil moisture data, it is worth

exploring the use of satellite derived soil moisture data to validate the calibration process, but this will also depend on the availability and ease of access to such data. Finally, while the modified Pitman model has been able to adequately capture the hydrology of the Zambezi River basin, especially under conditions of limited data, hydrological modelling in ungauged catchments still remains a challenge. Issues of data quality and their spatial and temporal representativeness are very important if reliable results are to be obtained but most of the streamflow data that were accessed for this study had a lot of gaps and could not be used to model other sub-basins of the Zambezi. For those areas where there are no observed hydrological data the process of regionalisation can be applied, however, there will always be some uncertainty as long as the data (both climate and physical basin characteristics) are inadequate or of poor quality.

CHAPTER 7 VARIABILITY, REGIONAL DROUGHTS AND FOOD SECURITY IN THE ZAMBEZI BASIN

7.1 Introduction

Extreme events such as floods and droughts are among the costliest natural disasters that affect many people especially those from vulnerable communities, such as the Zambezi basin where most of the livelihoods depend on rainfed agriculture. During drought periods, plant growth is the first to be affected because of the limited moisture storage in the soils (Tallaksen and Van Lanen, 2004). Loss of moisture due to a changing and varying climate will impose adverse effects on the environment and on agricultural production. It was demonstrated in Chapter 5 that the present climate variability may continue into the future and it is therefore important to understand and monitor the variability of these events.

This chapter focuses on the relationships that exist between climate variability, agricultural droughts and food security in the Zambezi basin. Two indices, i) the Standardised Precipitation index (SPI, Mckee et al., 1993) and ii) anomalies of simulated soil moisture are used to assess the impacts of drought on agricultural production in the basin during the period 1961-2000. SPI represents the number of standard deviations by which the observed precipitation (transformed to a normal distribution function) deviates from its long-term mean and it is used to measure the severity, spatial extent, and frequency of occurrence of droughts in the Zambezi basin. The simulated soil moisture anomalies are measured as deviations from the long term mean and standardised against the mean.

Since the basin's agricultural production is largely rainfed, the agricultural season extends from October to March (ONDJFM) to coincide with the region's rainy season. In this study the agricultural season has been split into two three monthly periods which extend from October to December (OND) for the planting season and from January to March (JFM) for the growing season. These periods are appropriate to the life cycle of a crop and they are examined for detectable trends during the planting and growing stages. The method used to generate the SPIs in SPATSIM was outlined in Chapter 4 and rainfall is the only input that is required. Catchment

averaged CRU rainfall data were used for this purpose. The soil moisture data are based on outputs from the Pitman model and the calibration of the model for the Zambezi basin is discussed in Chapter 6. Maize production statistics were downloaded from the Food and Agricultural Organization Statistics Division (FAOSTAT, 2012) and they are used to assess and validate the results. Maize was chosen for use in this study for the simple reason that it is the most common rainfed crop in all the Zambezi basin countries.

There are two main sections in this chapter. The first section involves an exploratory assessment of the relationship between SPI and agricultural yield for the whole basin to see if further analyses can be carried out at a regional scale. The second section explores the relationship between simulated soil moisture and agricultural yield. Anomalies of simulated soil moisture are compared to the SPI and to agricultural yield in order to evaluate the potential of using simulated soil moisture as a drought indicator at a regional scale. The SPI analyses are performed both at sub-basin and catchment level but soil moisture analyses are done at the catchment level.

7.2 SPI, droughts and variability in the Zambezi basin

It is important to understand the temporal and spatial characteristics of droughts especially when considering a region's vulnerability to droughts. CRU data for the century long period of 1901 to 2002 were used to generate SPI values for the critical agricultural seasons in the basin based on a six month timescale from October to March (SPI 6) and on three month time scales of October to December (OND) and January to March (JFM).

7.2.1 Variability of agricultural droughts at six month time scales (SPI 6)

Six monthly SPIs (SPI6) for example sub-basins are given in Figures 7.1a-c. The sub-basins are chosen in such a manner that they represent the major sub-basins of the Zambezi (see Figure 3.7). Temporal variation and the severity of SPI6 droughts that occurred in the basin during 1901-2002 are summarised in Table 7.1. In this study analysis is only based on severe (SPI: -1.5 to -1.99) and extreme (SPI: \leq -2.0) drought categories.

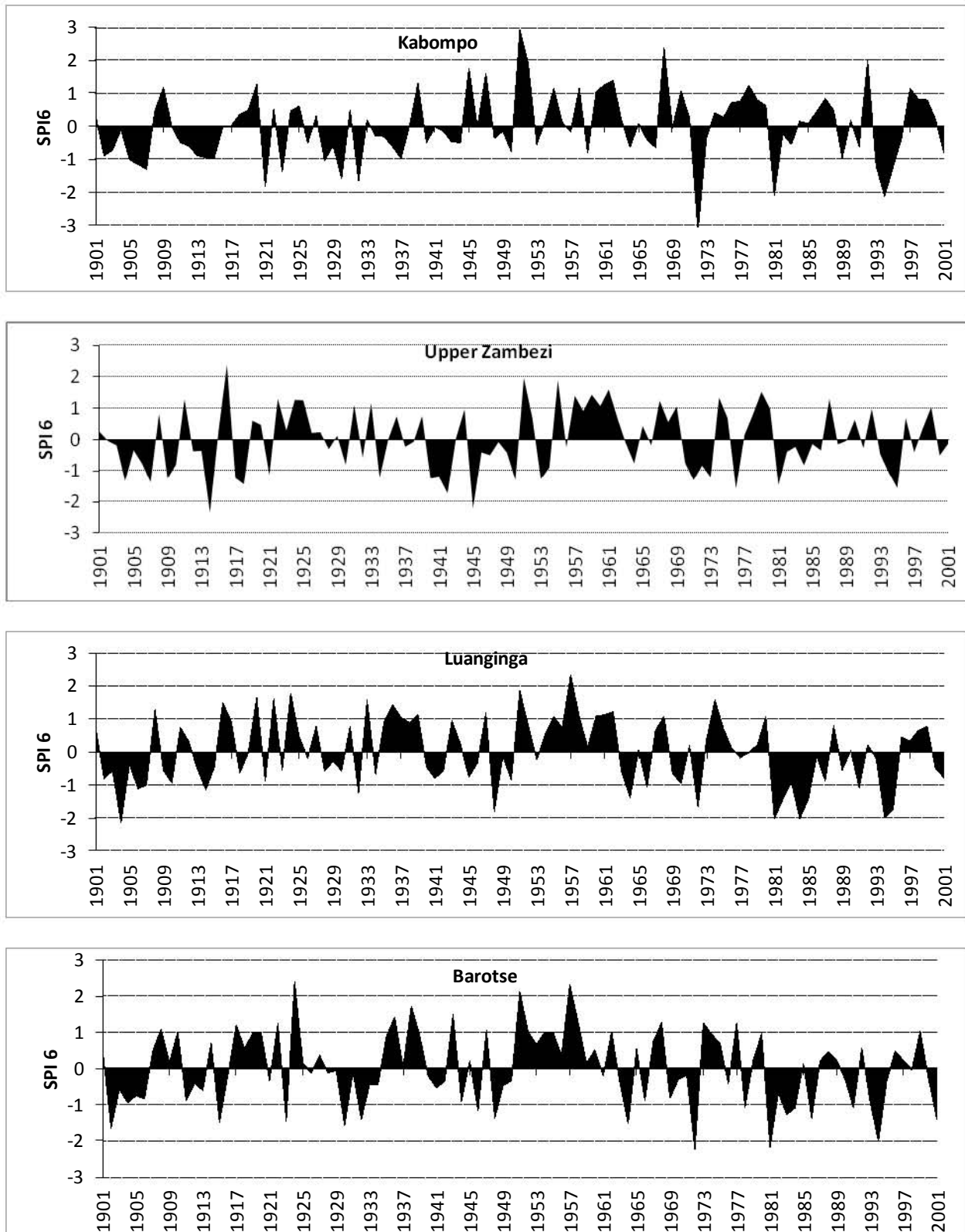


Figure 7.1a 6 month SPIs from the upper sub-basins of the Zambezi

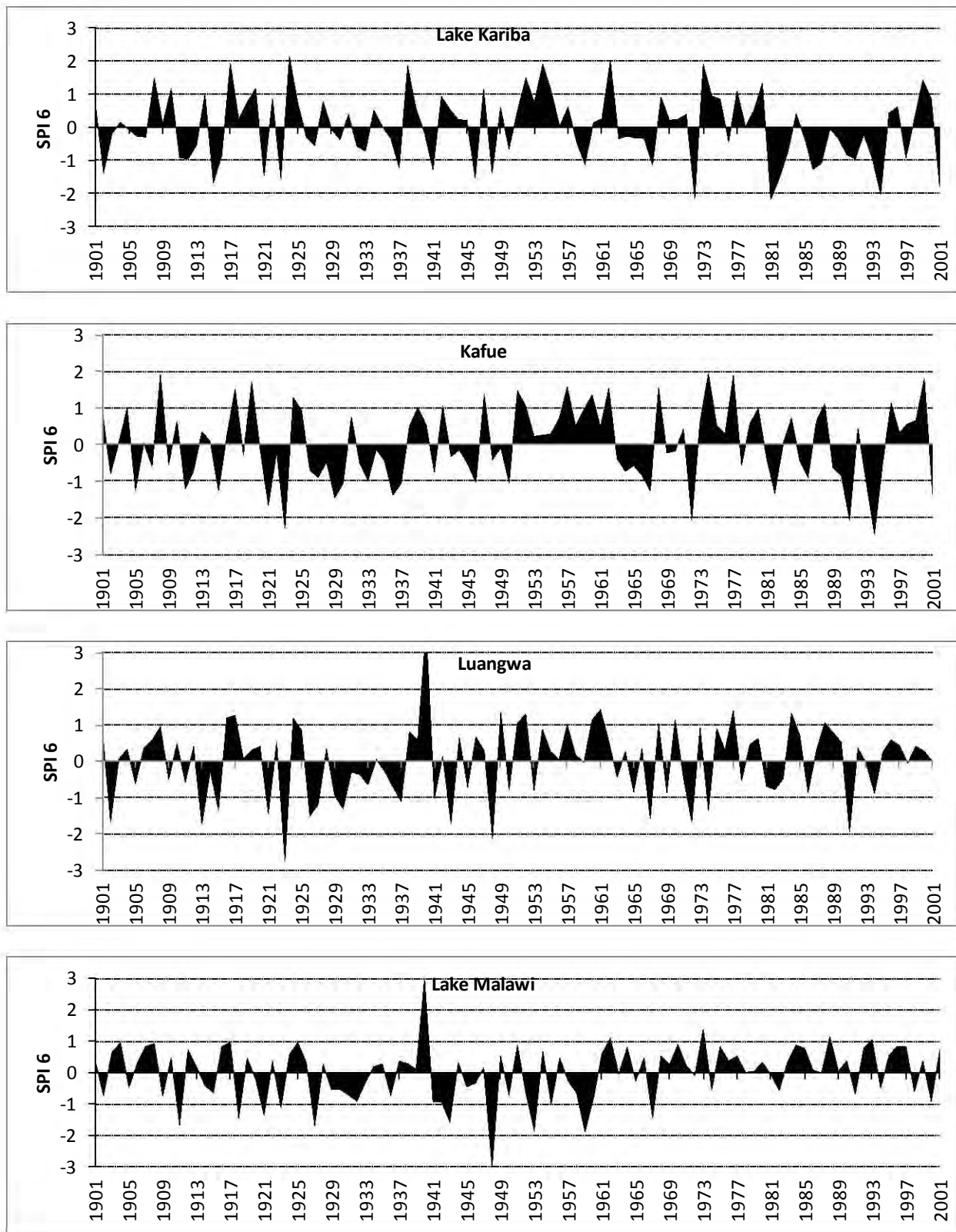


Figure 7.1b 6 month SPIs for Lake Kariba, Kafue Luangwa and Lake Malawi sub-basins

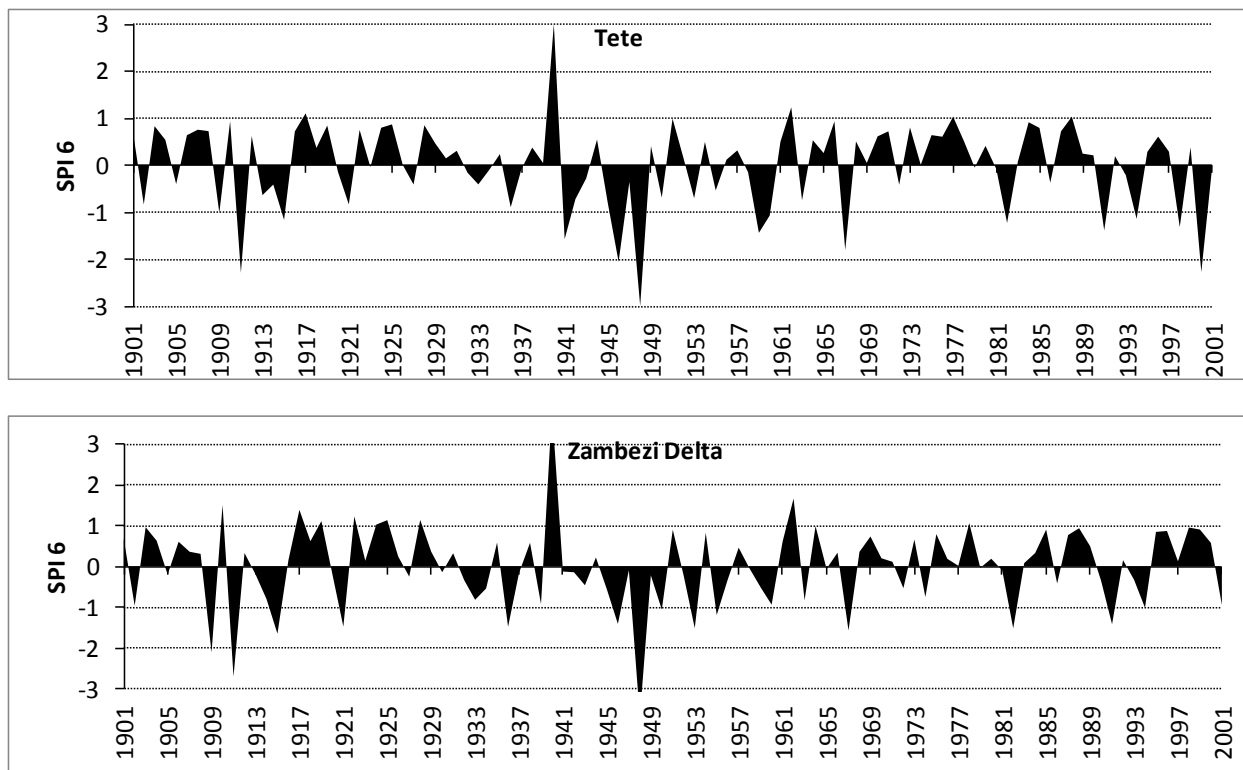


Figure 7.1c 6 month SPIs for Tete and Zambezi Delta

Table 7.1 Severe and extreme SPI 6 droughts between 1901 and 2002

| Sub-basin | Year (starting from October) | | Total |
|---------------|--|------------------------|-------|
| | Severe drought | Extreme drought | |
| Kabompo | 1921, 1930, 1932 | 1972, 1981, 1994 | 6 |
| Upper Zambezi | 1918, 1942, 1976, 1995 | 1914, 1945 | 6 |
| Luanginga | 1948, 1972, 1982, 1985, 1995 | 1904, 1981, 1984, 1994 | 9 |
| Barotse | 1902, 1915, 1923, 1930, 1964 | 1972, 1981, 1994 | 8 |
| Lake Kariba | 1915, 1923, 1945, 1982, 2001 | 1972, 1981, 1994 | 8 |
| Kafue | 1921, 1929 | 1923, 1972, 1991, 1994 | 6 |
| Luangwa | 1902, 1913, 1926, 1943, 1967, 1972, 1991 | 1923, 1948 | 9 |
| Lake Malawi | 1911, 1927, 1943, 1953, 1959 | 1948 | 6 |
| Tete | 1941, 1967 | 1911, 1946, 1948, 2000 | 6 |
| Zambezi Delta | 1915, 1936, 1967, 1982 | 1909, 1911, 1948 | 7 |

Annual, decadal and multidecadal droughts were experienced in various areas of the Zambezi basin during the century long period, this is evidenced by the time spacing between consecutive droughts in each of the example cases. The 1960s-70s were wet years while dry conditions were experienced during the 1980s and 1990s. In terms of severity and spatial extent the year 1972

was the most common extreme drought year during the century long period while both the years 1948 and 1994 were also common under the extreme drought category. Other common droughts were experienced during the years 1913-1915, 1921, 1923, 1967 and 1981. Figure 7.2 illustrates and confirms the spatial extent of droughts during 1921, 1940, 1948 and 1967. During 1940 the eastern part of the basin was extremely wet while most parts experienced normal to near normal conditions. The fact that some sub-basins experienced droughts at different times is a clear indication of spatial variability within the Zambezi basin.

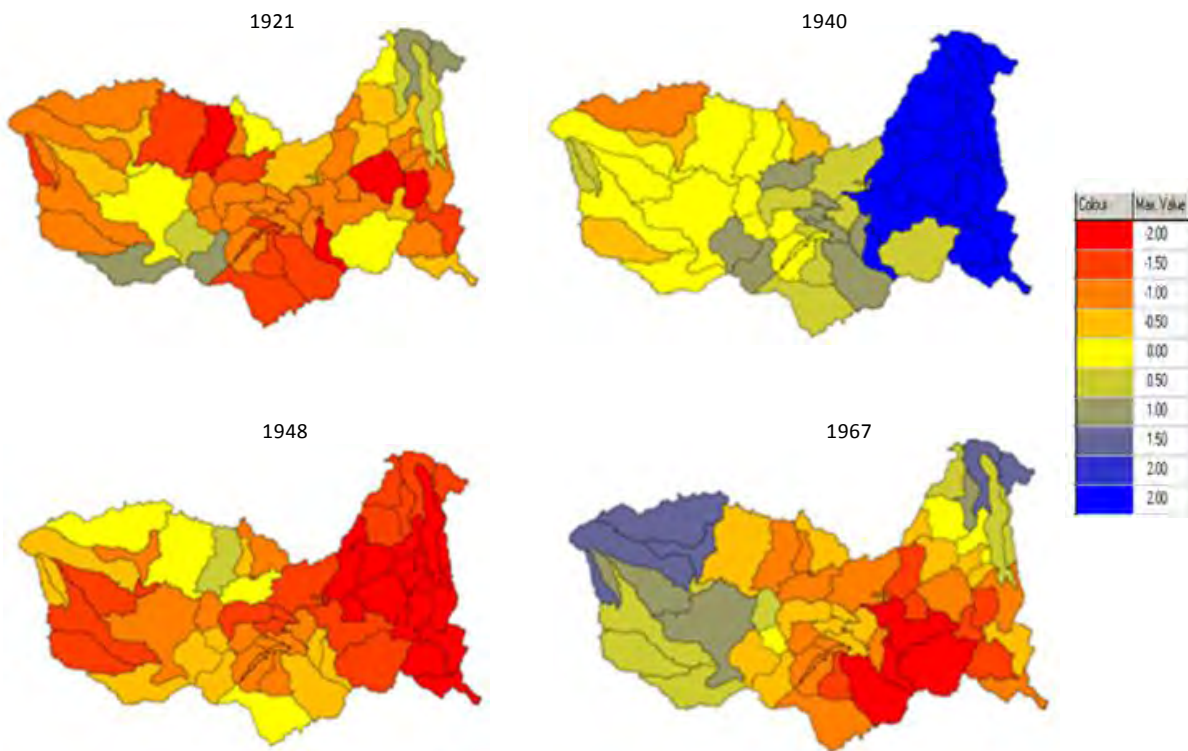


Figure 7.2 6 month SPIs (October to March) for 1921, 1940, 1948 and 1967

7.2.2 Dry and wet spells, 1901-2002

Temporal variation in droughts over the century (1901-2002) is further established by investigating the tendency of successive SPIs to turn into prolonged dry or wet spells. A cumulative sum method is used, this method is justified by the fact that droughts are among some of the cumulative climatic hazards that can affect communities (Manatsa et al. 2010). The Mann Kendall test is also applied to the SPI6 to test for the presence of any significant trends in SPI and in the cumulative sum of the SPIs. Patterns showing the temporal evolution of cumulative SPIs in example sub-basins are depicted in Figure 7.3 and results of the Mann

Kendall's test are presented in Table 7.2. The first half of the century is characterised by relatively short wet and dry spells and the second half of the century shows prolonged periods of alternating wet and dry spells most of which last for an average of 10 years. The periodic tendency of SPI6 is not unusual as it corresponds with the annual, decadal and multidecadal cyclic patterns of rainfall that were observed in the basin (see Chapter 5). Lack of long term persistence in dry conditions can therefore be attributed to the alternate wet and dry conditions. The SPIs do not show any significant trends and again this concurs with observations made in chapter 5 where there were no statistically significant trends in rainfall and streamflows in the Zambezi basin. The cumulative SPIs, however, do show some significant trends over the century.

Table 7.2 Mann Kendall test on SPI6 for the period 1901-2002, $Z_{critical}$ (1.96, $\alpha = 0.05$)

| Sub-basin | Z statistic | Trend | Z statistic | Trend |
|---------------|-------------|-------|----------------|-------|
| | SPI | | Cumulative SPI | |
| Kabompo | 2.11 | yes | 5.34 | yes |
| Upper Zambezi | 0.54 | no | 5.21 | yes |
| Luanginga | 0.87 | no | 6.88 | yes |
| Kafue | 1.02 | no | 1.41 | no |
| Barotse | 0.29 | no | 7.17 | yes |
| Lake Kariba | 0.59 | no | 6.65 | yes |
| Tete | 0.39 | no | -3.48 | yes |
| Zambezi Delta | 0.32 | no | 0.32 | no |
| Luangwa | 0.62 | no | 0.65 | no |
| Lake Malawi | 1.16 | no | -5.23 | yes |

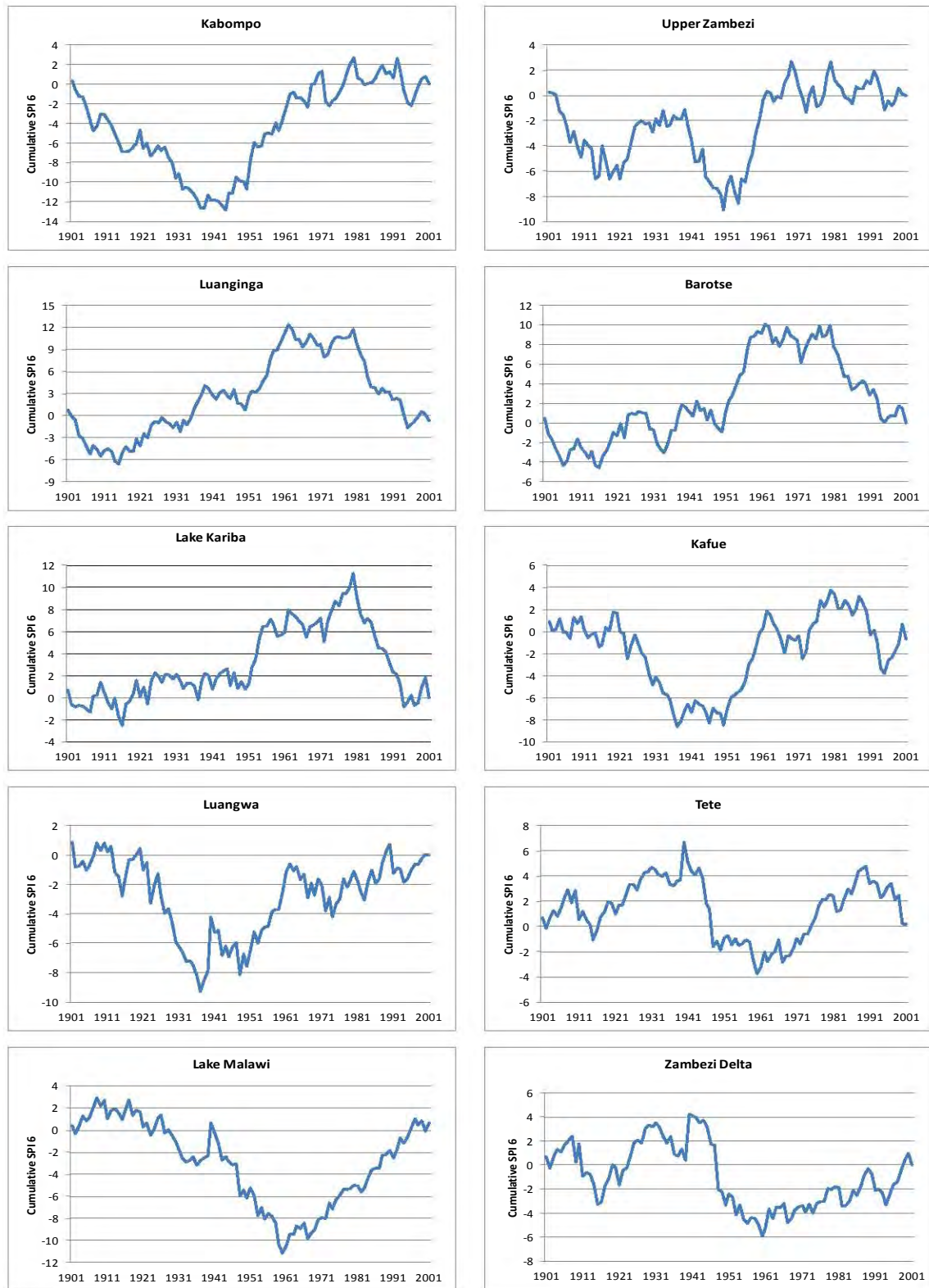


Figure 7.3 Temporal evolution of cumulative SPI 6 during 1901-2002 for the months of October to March

7.2.3 Historical droughts and variability at three month time scales

Historical drought events have been assessed for the period 1961-2000 using the OND and JFM SPIs. This period was chosen based on the FAO crop yield data which starts from 1960 and the CRU rainfall data which goes up to 2002. Figure 7.4 shows the SPIs that were generated in example sub-basins of the Zambezi. The results for both SPIs (OND and JFM) indicate that droughts occurred during the years; 1963-67, 1970-72, 1981-82, 1987,1989,1992,1993, 1994-1996 and 1998. The moderate to extreme drought conditions that occurred in 1972 concur with observations made by other studies (e.g. Mazvimavi, 2010; Hulme, 2001). It is also observed that the frequency of occurrence and timing of the droughts is spatially variable. Figure 7.5 provides a regional overview of the drought events for the 1969-70 and 1981-82 agricultural seasons. Seasonal and decadal variability as well as spatial variability are clearly evident in these results. The difference in the two seasons is seen particularly for the 1969-70 period where the OND season was a very wet season only to be followed by an extremely dry JFM season. Both the OND and JFM SPIs for 1981-82 indicate drought conditions in a considerable part of the basin. The OND season experienced more of the extreme droughts although some areas were under moderate drought conditions. This situation was reversed in the JFM season resulting in more of the moderate droughts and a fewer of the extreme conditions. These results show that it is possible within an agricultural season to have a wet OND (planting) season and a dry JFM (growing) season and vice versa.

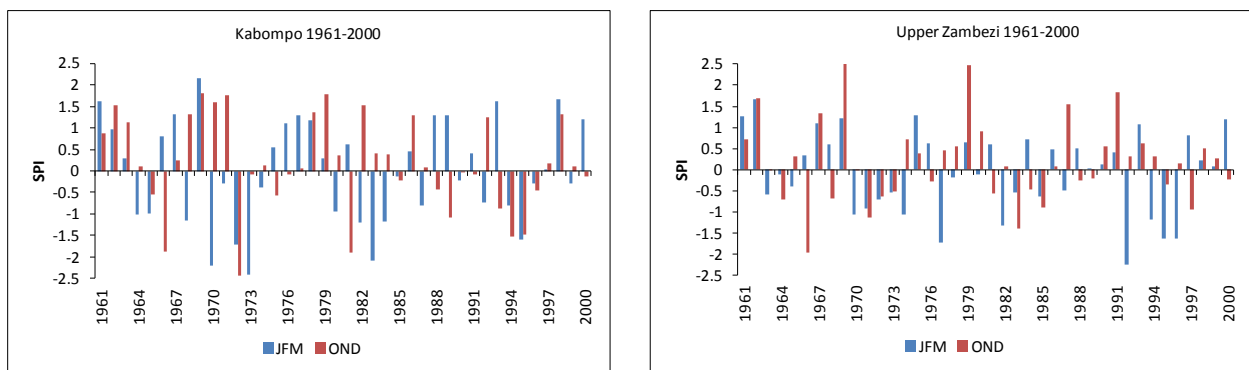


Figure 7.4a Historical JFM and OND SPIs for sub-basins in the Zambezi

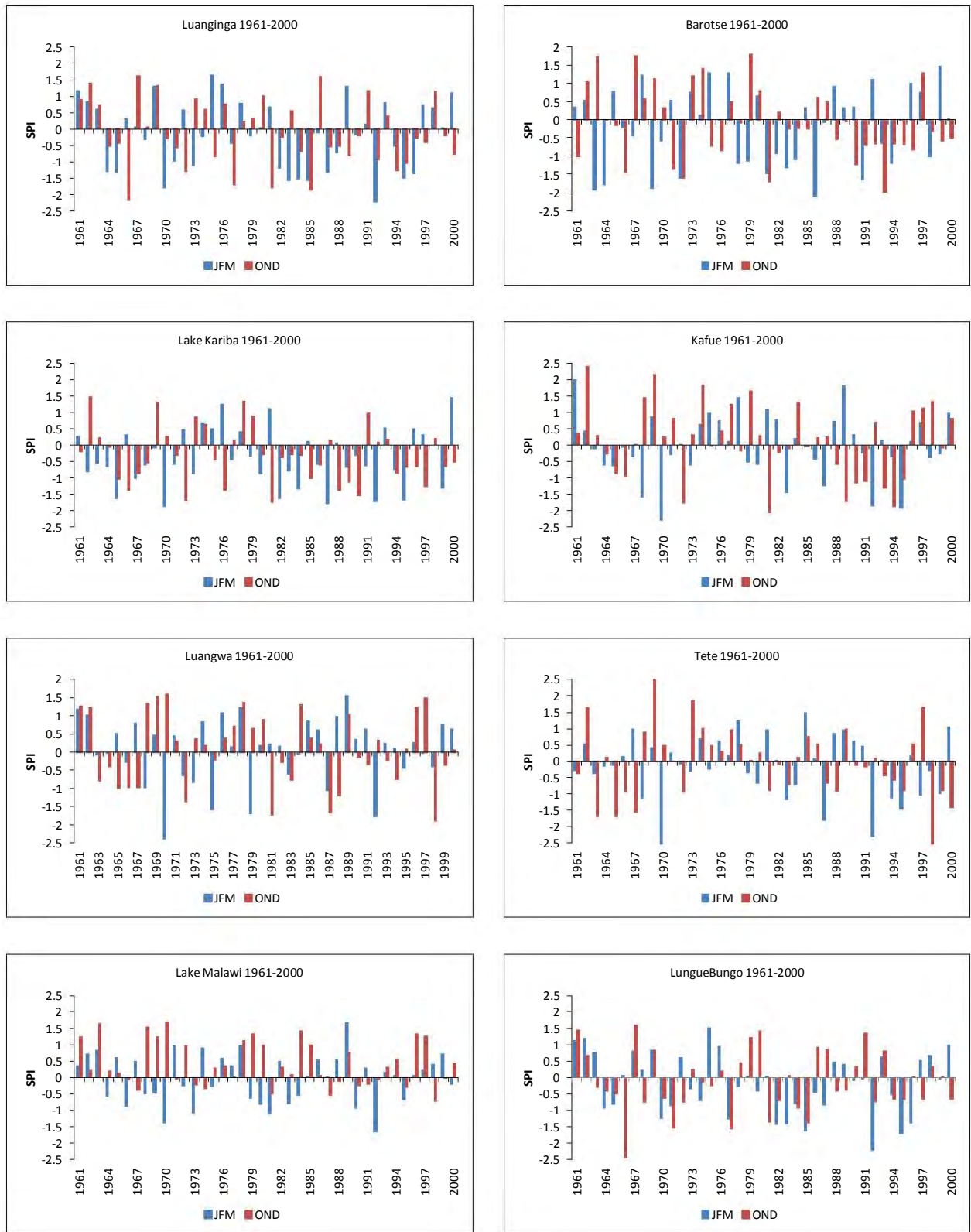


Figure 7.4b Historical JFM and OND SPIs for sub-basins in the Zambezi

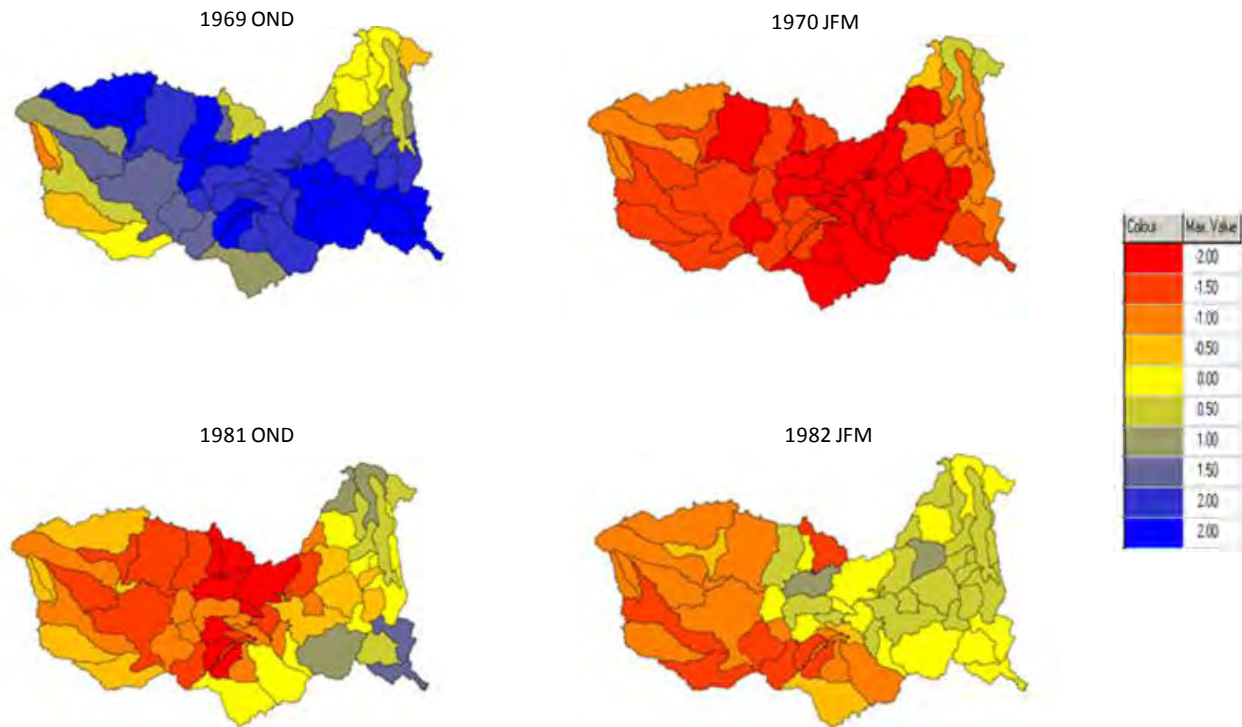


Figure 7.5 3 month SPIs for 1969 OND, 1970 JFM, 1981 OND and 1982 JFM

7.3 Regional droughts and food security relationships in the Zambezi basin

The aim of this section is to quantitatively assess the vulnerability of agriculture to droughts and to establish the role of climate variability in crop production in the Zambezi basin. An exploratory assessment of the relationship between SPI and maize yield is carried out for the Zambezi basin. Further analyses involve the use and evaluation of simulated soil moisture as a drought indicator at the regional scale.

7.3.1 Historical drought and agricultural production in the Zambezi basin

The total annual maize yield obtained from the Zambezi basin countries during the period 1961-2010 is depicted in Figure 7.6. It is observed that the yields are variable across the time series. The amount of crop harvested is largely controlled by the amount of rainfall received and the resulting soil moisture conditions during the agricultural season. In addition non-climate factors such as management, economic, political and policy issues may affect the crop yield. Figure 7.7 presents the individual basin country yields, only four of the basin countries (Zimbabwe,

Zambia, Malawi and Mozambique) are considered as these had a larger contribution to agriculture in the basin during the period of assessment. It is not coincidence that declining yields were experienced during the same years within the individual basin countries. Given the fact that policies vary from country to country it is assumed that climate variability, which happens to be common across the basin could have played a major role in determining the yield deviations from the long term mean.

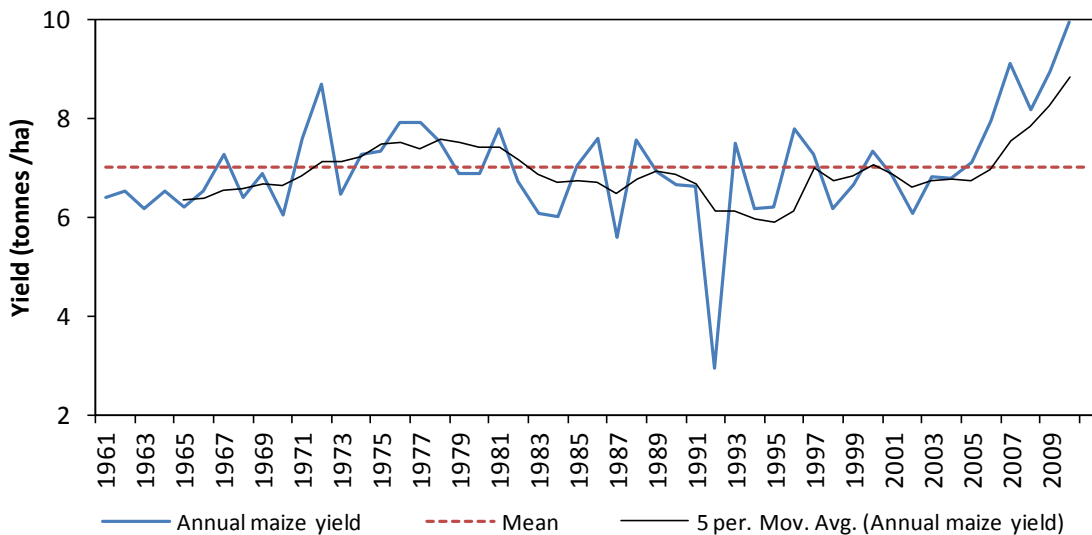


Figure 7.6 Total annual maize yield in the Zambezi basin, calculated from FAOSTAT (2012)

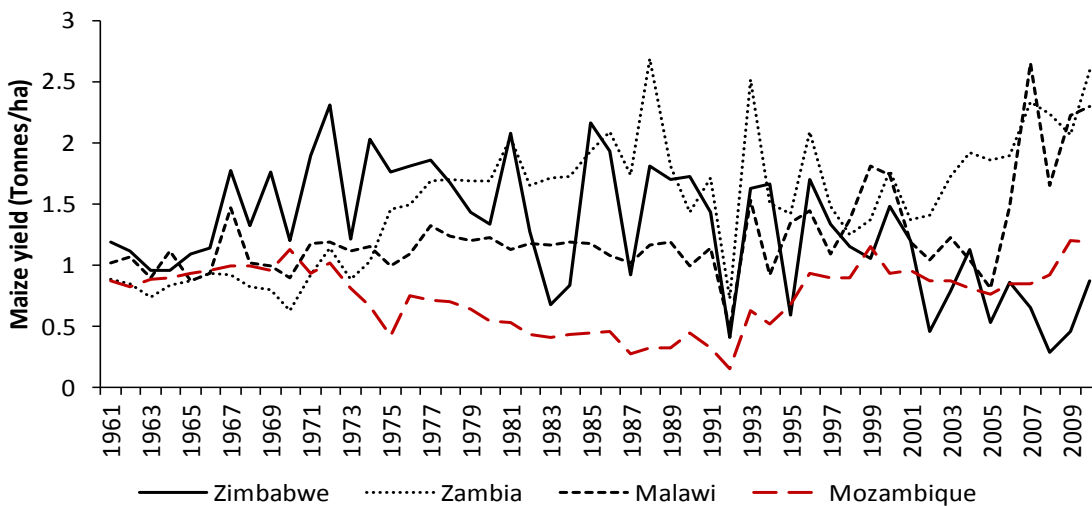


Figure 7.7 Annual maize yields in some of the Zambezi basin countries (1961-2010, source: FAOSTAT, 2012)

To establish if the low yields could have been due to some shortfalls in rainfall the SPIs are generated for the periods in which the low yields were realized. Figure 7.8 provides a regional drought analysis for the Zambezi basin which was carried out by generating SPI indices (OND and JFM) for selected years during the period 1961-2002. It should be noted that when referring to a yield year (e.g. the 1961 yield), it is made up of the previous year's OND season and the same year's JFM season. Therefore the 1961 yield specifically belongs to the 1960-61 agricultural season. The periods selected for presentation are 1969-70, 1982-83 and 1991-92.

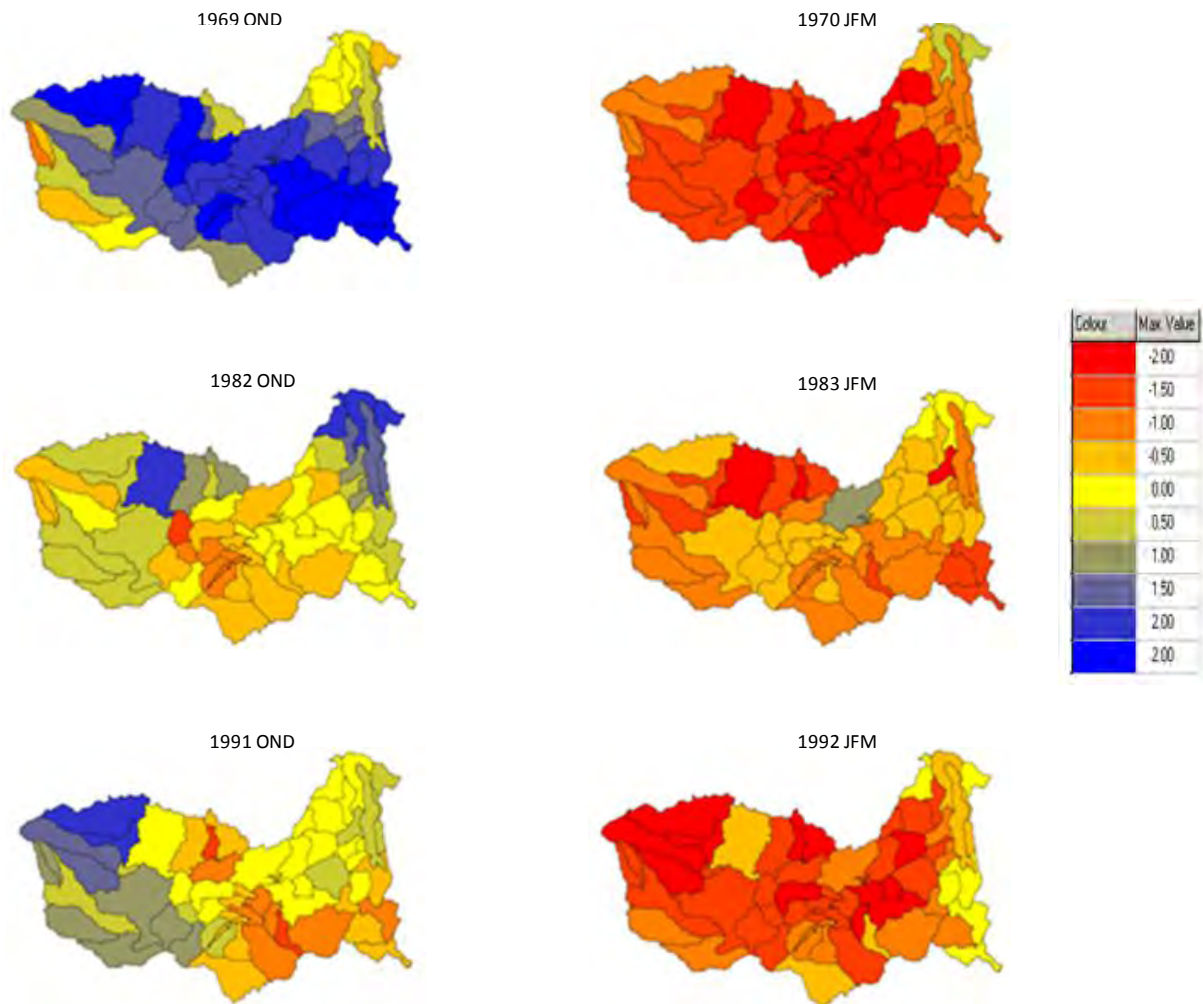


Figure 7.8 SPIs for 1969-70, 1982-83 and 1991-92 (OND and JFM)

It is shown in Figure 7.8 that there were droughts during the years in which low yields were obtained. During 1969-70 the whole basin with the exception of the smaller part of the basin that is occupied by Tanzania experienced severe to extreme droughts. In general, mild to extreme

droughts were experienced during the periods 1982-83 and 1991-93, with extreme drought conditions in at least 50% of the basin. The OND season for 1969-70 was generally wet while the years 1982-83 and 1991-1992 had started experiencing mild droughts in some parts of the basin during the same season. The results obtained suggest that during this period the cropping season was largely impacted by the JFM droughts. The large deviation from the long term mean for the 1991-92 season could be attributed to the fact that the crops did not have sufficient moisture during the planting stage and this was further worsened by the below average moisture conditions that prevailed during the growing season. Since the growth of a crop depends on the availability of soil moisture, the results obtained suggest to some extent that a relationship exists between SPI and soil moisture. Because SPI is a rainfall based index it is only able to explain to some extent the yield obtained and therefore further analysis using a soil moisture based index is necessary in order to establish with confidence the relationship between climate variability and agricultural yield at the regional scale. The assessment of the relationship between soil moisture and yield is addressed in Section 7.5.

7.3.2 SPI and maize yield relationships at sub-basin scales

The previous sections have emphasised the high temporal and spatial variability in the occurrence of agricultural droughts in the Zambezi basin. It is possible that one sub-basin can experience droughts while a neighbouring sub-basin is under normal conditions. This section seeks to establish whether a relationship exists between crop yield and SPI. Apart from natural climate variability, a number of factors influence the crop yield from year to year. Some of these factors include gradual improvements in technology and changes in policy. It is necessary to remove the impacts and long term trends of these factors on crop yield before assessing the impacts that are due to climate variability, this process is called detrending. Detrending ensures a trend free historical record that can be used to predict future yields. In this study raw maize yields were detrended by regressing the average annual yield against the year-of-harvest for each basin country for the period 1961 to 2000. The detrending process involved fitting a regression line whose slope and intercept were used to calculate the expected yield for each year. A relative detrended yield which is the departure of the yield values from the time trend was obtained as a difference of the observed and the expected yield. An absolute detrended yield for each year is

then obtained by adding the expected yield for the last year in the series to the relative detrended yield.

A comparative analysis using Spearman's rank-order correlation (Table 7.3) was also carried to establish the relationship between detrended maize yield and SPI at sub-basin level. In another test, percent deviations from the means of the detrended yield were compared to the SPIs. In this study less emphasis was placed on Angola due to issues of data paucity. Botswana, Namibia and Tanzania were also excluded because of their relatively small contribution to agriculture in the Zambezi basin. Figure 7.9 presents the detrended crop yields for three of the major crop contributing countries in the Zambezi. Mozambique is presented alone in Figure 7.11, this is so that the impacts of (1977-1992) can be seen.

Table 7.3 Rank order correlation coefficients of SPI and detrended maize yield

| Catchment | SPI versus detrended yield | | | | | |
|-------------|----------------------------|---------|----------------|---------|----------------|---------|
| | OND | | JFM | | ONDJFM | |
| | R _s | p-value | R _s | p-value | R _s | p-value |
| Kabompo | 0.46 | 0.001 | 0.35 | 0.027 | 0.42 | 0.001 |
| Luena | 0.35 | 0.028 | 0.28* | 0.096 | 0.46 | 0.003 |
| Luanginga | 0.42 | 0.007 | 0.25* | 0.115 | 0.43 | 0.006 |
| Kafue 4 | 0.43 | 0.003 | 0.08* | 0.643 | 0.32 | 0.045 |
| Zambezi 10 | 0.32 | 0.047 | 0.17* | 0.297 | 0.28 | 0.077 |
| Lake Kariba | 0.10* | 0.192 | 0.13* | 0.417 | 0.21 | 0.045 |
| Gwai | 0.37 | 0.021 | 0.55 | 0.000 | 0.59 | <0.0001 |
| Mupfure | 0.32 | 0.047 | 0.57 | 0.000 | 0.5 | 0.001 |
| Luangwa | 0.43 | 0.006 | 0.29* | 0.072 | 0.25 | 0.118 |
| Mazowe | 0.42 | 0.008 | 0.54 | 0.000 | 0.65 | <0.0001 |
| Lilongwe | 0.02* | 0.320 | 0.11 | 0.167 | 0.17* | 0.290 |
| Namitete | 0.04 | 0.080 | 0.16 | 0.111 | 0.18* | 0.077 |

* not significant at $\alpha=0.05$ level

Detrended maize yields show a temporal variability during the period 1961-2000. The yields indicate that the years 1970-72, 1981-82, 1987 and 1989 and 1991-92 were drought years. With the exception of the Kabompo, the correlations between the detrended maize yields and the SPIs are generally low although most of them are significant at the 95% confidence level. For the JFM season, the correlations for 50% of the sub-basins are statistically insignificant at the 95% confidence level. Apart from the drought years, Zimbabwe had highly variable yields which

exceeded the long term average for 1961-1990 but the yields started to decline after 1995. This illustrates the point that yields may not only be influenced by climatic conditions and in the case of Zimbabwe the high yields obtained during this period could be attributed to good governance and a stable financial base, while at the same time the low yields obtained in the country from around 1995 could be attributed to droughts and changes in land management policies (Richardson, 2007).

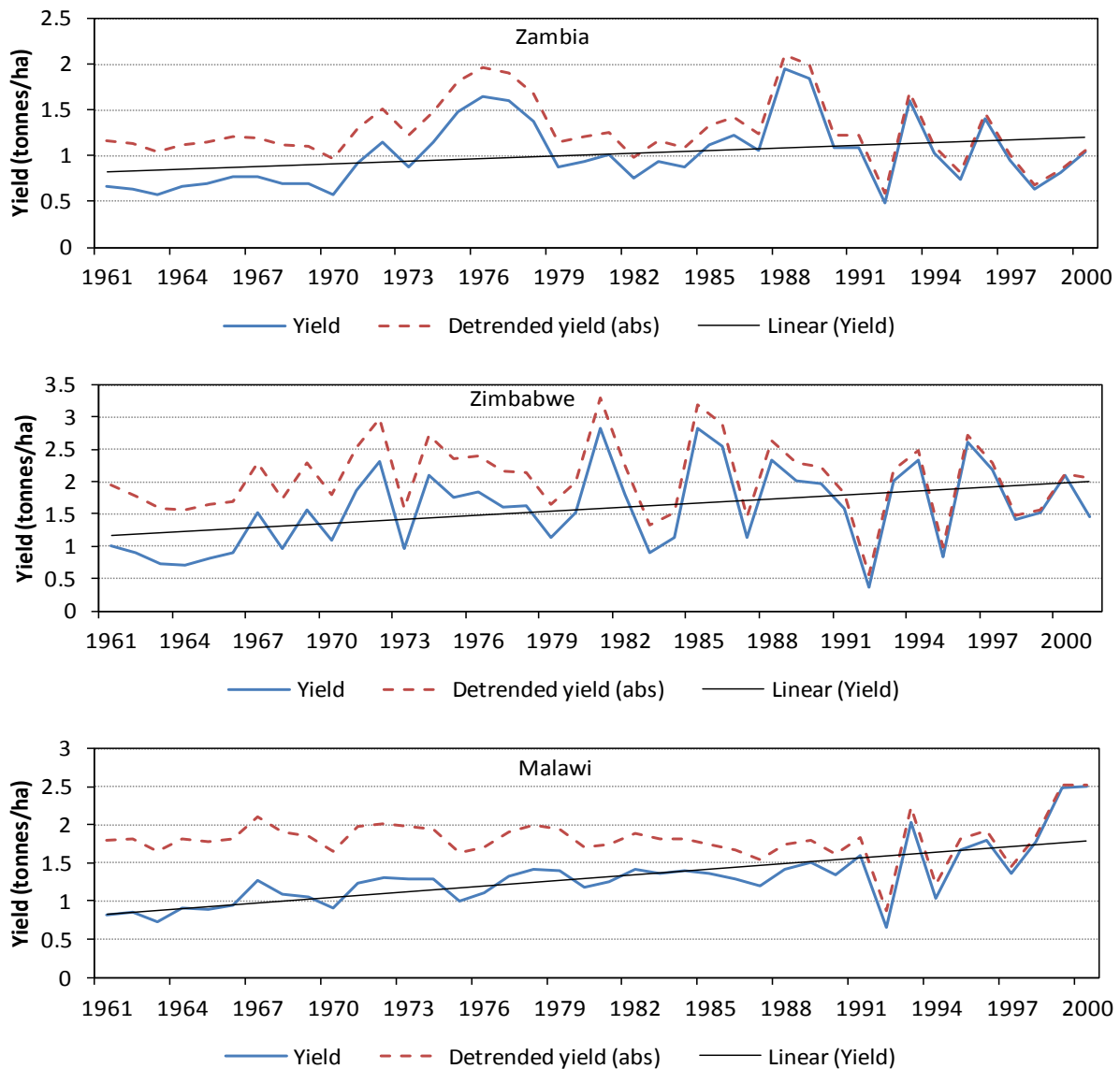


Figure 7.9 Observed and detrended maize yields for Zambia, Zimbabwe and Malawi (source of data: FAO, 2012)

Figure 7.10 illustrates the Zimbabwean case where the total annual rainfall across the country is compared to the normalised detrended yield anomalies for the period 1961-2002. Zimbabwe is an important case example that illustrates a transition from being the bread basket for the Zambezi basin community and the southern African region at large (before the year 2000) to receiving below average yields after the year 2000. Apart from rainfall variability the main cause of this transition is attributable to changing land and governance policies (Richardson, 2007). Between 1971 and 1980 Zimbabwe was experiencing a civil war which resulted in low yields despite the above average rainfall. After gaining independence in 1980 government invested in agriculture through building large storage reservoirs such as dams as well as providing incentives to subsistence-based rural farmers (Glantz et al., 2007) thereby cushioning the country from the impacts of droughts between 1980 and 1995 as seen from the yields. These reforms resulted in Zimbabwe realising high maize yields in the 1980s despite the three agricultural droughts that had been experienced during 1981-82, 1982-84, and 1987-88. Although the 1991-92 season was marked by severe to extreme droughts the maize yield deficit in Zimbabwe has also been attributed to a shift by the commercial farmers from maize production to more commercially and economically viable products such as tobacco (Sachikonye, 1992). Yields also started declining from the year 2000 mainly due to changes in land policy. Also from 1997 there were huge payouts as compensation to the war veterans which could have resulted in less investment in agriculture (Richardson, 2007).

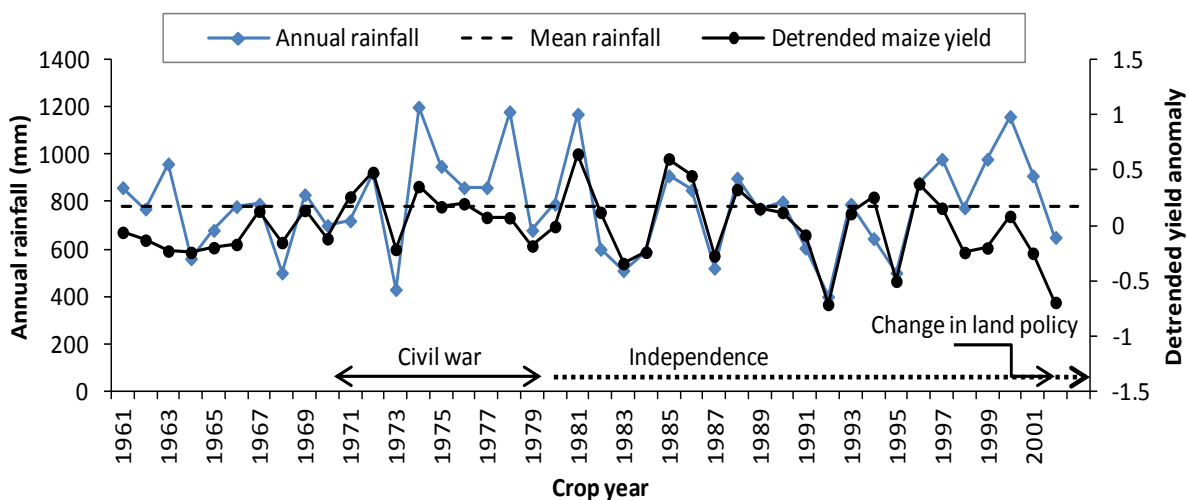


Figure 7.10 Annual rainfall and maize yield in Zimbabwe during 1961-2002

Civil wars seem to have great impact on agriculture in the Zambezi basin. Mozambique on the other hand experienced a downward trend in maize yield between 1961 and 1992 (Figure 7.11) yet during this time only five droughts had been experienced. After 1992 Mozambique started experiencing an upward trend in the yields. Apart from climatic factors, the decline in Mozambican yields largely illustrates the impact of the civil war (1977-1992). Policy factors, such as the Economic Structural Adjustment Programme (ESAP), that were implemented by the World Bank in most of southern Africa also impacted the region's agricultural yield. For example, in 1991 Zambia reduced government expenditure as part of the economic reform which resulted in a 25% decrease in maize production (Glantz et al., 2007) mainly due to lack of agricultural inputs such as fertiliser and a subsequent loss in income. These events also led to reduced planting area in the following season of 1991-92. Therefore in addition to the rainwater deficits of 1991-92 it can be assumed that the agricultural drought impacts were aggravated by policy factors in most parts of the basin.

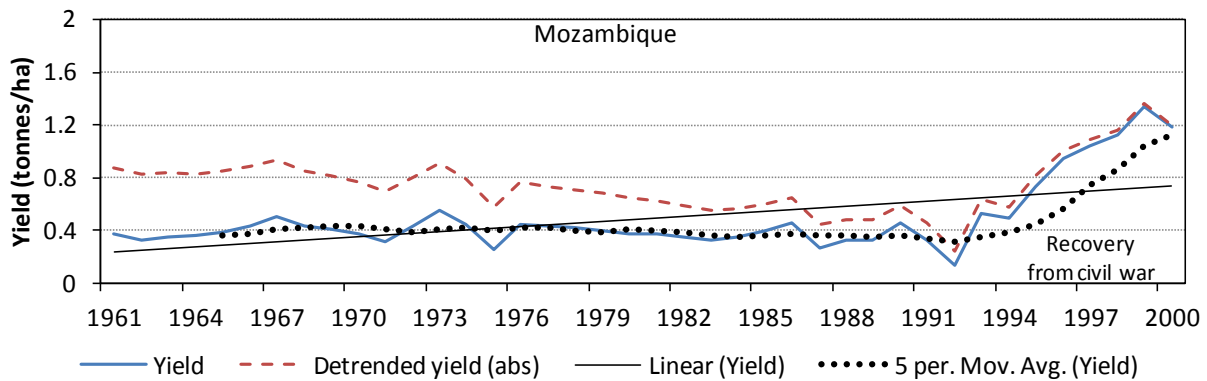


Figure 7.11 Observed and detrended maize yields for Mozambique

Figures 7.12a-c show that the yield deviations are influenced by both OND and JFM seasons and that it is not always the case that a negative SPI in one season will result in a negative yield deviation, neither does a positive SPI imply a positive yield deviation. The worst case scenario though is the one in which the growing season is predominantly dry as was the case during the 1991-92 and 1995-96 seasons for the Kabompo and Kafue sub-basins, the 1987-88 and 1995-96 seasons for Lake Kariba and the 1991-92 season for the Tete catchment. These examples illustrate that water availability during the growing season has more impact on the yield than the planting season moisture. Comparing situations (Figures 7.12a-c) where the severity of SPI

coincides with the yield deviation Table 7.4 shows that there is more coincidence between the growing season and yield deviation than between the planting season and yield deviation. Another example that illustrates this observation is the 1965-66 agricultural year for the Kabompo and Luena catchments in the upstream areas of the Zambezi basin where normal yields ($\pm 10\%$ deviations) were obtained in both sub-basins yet severe (SPI = -1.87 and -1.96 respectively) droughts were experienced during the planting season (OND). The growing season was moderately wet (SPI = 1.32) for the Kabompo and normal (SPI = 0.35) for Luena. It would have been expected that seed germination would fail in both sub-basins given that there was insufficient rainfall during the planting season but it is likely that the moisture deficiency was compensated for by the antecedent conditions of which the previous seasons had normal rainfall in both sub-basins. Further to this, the growing season was wet and this enabled the maize crop to grow to maturity. Jury et al. (1997) confirm that maize crops have a peak sensitivity to rainfall towards the end of January during which time the plants are in the growing phase. It is also possible though, that if the antecedent moisture conditions were poor and given the severely dry conditions the yields may have been adversely affected. Although the growing season moisture has an overriding effect, the results also show that in most cases the deviation in yield depends on the severity of the SPI and the compensatory effects of moisture levels between the planting (OND) and growing (JFM) seasons as well as the antecedent soil moisture conditions.

Table 7.4 Coincidence of SPI and yield deviation

| Catchment | % coincidence of SPI with yield deviation | |
|-----------|---|-----|
| | OND | JFM |
| Kabompo | 67 | 33 |
| Luena | 0 | 100 |
| Kafue | 29 | 71 |
| Mazowe | 40 | 60 |
| Zambezi 8 | 0 | 100 |
| Gwai | 33 | 67 |
| Lilongwe | 29 | 71 |
| Zambezi 4 | 14 | 86 |
| Zambezi 3 | 22 | 78 |

| Kabompo | | | | Luena | | | | Kafue 4 | | | |
|---------|-------|-------|-------|-------|-------|-------|--------|---------|--------|--|--|
| YEAR | OND | Yield | JFM | OND | Yield | JFM | OND | Yield | JFM | | |
| 1960-61 | 0.88 | | 0.97 | 0.71 | | 1.25 | 0.626 | | 1.998 | | |
| 1961-62 | 1.54 | | 0.30 | 1.70 | | 1.66 | 2.213 | | 0.421 | | |
| 1962-63 | 1.12 | | -1.01 | -0.03 | | -0.58 | 0.086 | | -0.123 | | |
| 1963-64 | 0.11 | | -0.99 | -0.69 | | -0.11 | 1.143 | | -0.618 | | |
| 1964-65 | -0.55 | | 0.81 | 0.30 | | -0.39 | -0.906 | | -0.642 | | |
| 1965-66 | -1.87 | | 1.32 | -1.96 | | 0.35 | -0.998 | | -0.062 | | |
| 1966-67 | 0.25 | | -1.16 | 1.34 | | 1.09 | -0.807 | | -0.368 | | |
| 1967-68 | 1.31 | | 2.17 | -0.68 | | 0.60 | 1.439 | | -1.574 | | |
| 1968-69 | 1.80 | | -2.20 | 2.59 | | 1.22 | 1.748 | | 0.868 | | |
| 1970-71 | 1.61 | | -0.30 | -0.02 | | -1.05 | 1.075 | | -2.306 | | |
| 1971-72 | 1.77 | | -1.71 | -1.14 | | -0.92 | 0.939 | | -0.301 | | |
| 1972-73 | -2.44 | | -2.41 | -0.62 | | -0.70 | -1.906 | | 0.001 | | |
| 1973-74 | -0.08 | | -0.38 | -0.53 | | -0.53 | 0.782 | | -0.61 | | |
| 1974-75 | 0.13 | | 0.56 | 0.71 | | -1.05 | 0.841 | | 0.655 | | |
| 1975-76 | -0.57 | | 1.11 | 0.38 | | 1.29 | -0.1 | | 0.985 | | |
| 1976-77 | -0.08 | | 1.30 | -0.27 | | 0.63 | 0.142 | | 0.749 | | |
| 1977-78 | 0.06 | | 1.17 | 0.46 | | -1.72 | 0.851 | | 0.135 | | |
| 1978-79 | 1.37 | | 0.28 | 0.56 | | -0.18 | 0.396 | | 1.457 | | |
| 1979-80 | 1.77 | | -0.94 | 2.47 | | 0.64 | 1.272 | | -0.52 | | |
| 1980-81 | 0.37 | | 0.61 | 0.91 | | -0.10 | 0.66 | | -0.596 | | |
| 1981-82 | -1.91 | | -1.20 | -0.57 | | 0.61 | -1.181 | | 1.09 | | |
| 1982-83 | 1.52 | | -2.08 | 0.08 | | -1.32 | -0.656 | | 0.767 | | |
| 1983-84 | 0.40 | | -1.19 | -1.41 | | -0.55 | -0.788 | | -1.475 | | |
| 1984-85 | 0.39 | | -0.14 | -0.48 | | 0.71 | -0.089 | | 0.187 | | |
| 1985-86 | -0.22 | | 0.46 | -0.89 | | -0.63 | 0.119 | | -0.033 | | |
| 1986-87 | 1.29 | | -0.81 | 0.08 | | 0.49 | 0.39 | | -0.427 | | |
| 1987-88 | 0.08 | | 1.29 | 1.55 | | -0.49 | -0.892 | | -1.251 | | |
| 1988-89 | -0.42 | | 1.29 | -0.27 | | 0.49 | -0.949 | | 0.708 | | |
| 1989-90 | -1.09 | | -0.23 | -0.21 | | 0.03 | -0.853 | | 1.802 | | |
| 1990-91 | -0.04 | | 0.40 | 0.54 | | 0.13 | 0.341 | | 0.316 | | |
| 1991-92 | -0.09 | | -0.74 | 0.31 | | -2.25 | -0.9 | | -1.866 | | |
| 1992-93 | 1.25 | | 1.62 | 1.84 | | 0.42 | 0.467 | | -0.255 | | |
| 1993-94 | -0.88 | | -0.81 | 0.63 | | 1.08 | 0.079 | | 0.144 | | |
| 1994-95 | -1.52 | | -1.58 | 0.32 | | -1.17 | -0.48 | | -0.377 | | |
| 1995-96 | -1.49 | | -0.29 | -0.35 | | -1.64 | -0.584 | | -1.943 | | |
| 1996-97 | -0.46 | | 0.04 | 0.14 | | -1.63 | -0.56 | | 0.134 | | |
| 1997-98 | 0.17 | | 1.66 | -0.94 | | 0.81 | -0.516 | | 0.689 | | |
| 1998-99 | 1.31 | | -0.28 | 0.50 | | 0.21 | 1.035 | | -0.4 | | |
| 1999-00 | 0.12 | | 1.19 | 0.26 | | 0.07 | -0.479 | | -0.273 | | |

| SPI | Key | % yield deviation |
|------------|-----|-------------------|
| ≥ 1.5 | | ≥25 |
| 1 to 1.5 | | 10 to 25 |
| -1 to +1 | | -10 to +10 |
| -1 to -1.5 | | -10 to -25 |
| ≤-1.5 | | ≤-25 |

Figure 7.12a Correlation of SPI (OND and JFM) with detrended maize yield deviations for the period 1961-2000

| YEAR | Mazowe | | | | Lake Kariba | | | | Gwai | | |
|---------|--------|-------|-------|--|-------------|-------|-------|--|-------|-------|-------|
| | OND | Yield | JFM | | OND | Yield | JFM | | OND | Yield | JFM |
| 1960-61 | -0.62 | | 0.45 | | -0.02 | | 0.26 | | -0.66 | | -0.39 |
| 1961-62 | 1.93 | | 0.34 | | 2.67 | | 0.42 | | 1.49 | | -0.47 |
| 1962-63 | -0.22 | | -0.91 | | 0.66 | | 0.23 | | 0.72 | | -0.85 |
| 1963-64 | 0.62 | | -0.60 | | 0.71 | | -0.73 | | 0.70 | | -1.24 |
| 1964-65 | -0.31 | | 0.32 | | -0.99 | | -0.67 | | -1.09 | | 0.18 |
| 1965-66 | -0.78 | | 1.02 | | -0.24 | | 0.16 | | 0.05 | | 0.12 |
| 1966-67 | -0.78 | | -2.32 | | -0.91 | | -0.17 | | -0.83 | | -0.99 |
| 1967-68 | 0.49 | | 0.53 | | 0.34 | | -0.83 | | -0.18 | | 0.51 |
| 1968-69 | 2.60 | | -2.44 | | 2.26 | | 1.00 | | 0.63 | | -2.27 |
| 1970-71 | 1.34 | | -0.43 | | 0.72 | | -1.76 | | -0.16 | | -0.50 |
| 1971-72 | 0.85 | | 0.27 | | -0.11 | | -0.03 | | -0.43 | | 1.27 |
| 1972-73 | -0.51 | | -0.74 | | -2.64 | | 0.62 | | -1.64 | | -1.03 |
| 1973-74 | 1.95 | | -0.12 | | 1.03 | | -1.50 | | 1.89 | | 0.66 |
| 1974-75 | 1.63 | | -0.24 | | 1.69 | | 1.75 | | 0.74 | | 0.98 |
| 1975-76 | 0.33 | | 1.01 | | 0.40 | | 0.04 | | -0.62 | | 0.47 |
| 1976-77 | 0.32 | | 1.24 | | -0.98 | | 0.90 | | -0.57 | | 1.20 |
| 1977-78 | 1.22 | | 1.22 | | 0.91 | | 0.02 | | 2.16 | | 1.14 |
| 1978-79 | 1.07 | | -0.45 | | 1.40 | | 0.88 | | 0.30 | | -0.75 |
| 1979-80 | 0.63 | | -1.23 | | 1.55 | | -0.90 | | 0.88 | | -0.11 |
| 1980-81 | 0.99 | | 0.99 | | 0.66 | | -0.40 | | 1.00 | | 1.23 |
| 1981-82 | 0.74 | | -0.20 | | -2.07 | | 1.32 | | -0.36 | | -0.92 |
| 1982-83 | -0.57 | | -1.37 | | -1.27 | | -1.68 | | -0.77 | | -1.25 |
| 1983-84 | 0.12 | | -0.87 | | -0.69 | | -1.18 | | -0.44 | | -1.17 |
| 1984-85 | 0.54 | | 1.57 | | -0.58 | | -0.47 | | 0.00 | | 0.82 |
| 1985-86 | 1.08 | | -0.09 | | -0.51 | | 0.83 | | 0.90 | | -1.54 |
| 1986-87 | 0.33 | | -1.50 | | 0.54 | | -0.03 | | -0.04 | | -1.65 |
| 1987-88 | 0.49 | | 0.06 | | -1.06 | | -1.89 | | 1.04 | | -0.04 |
| 1988-89 | 0.02 | | 0.04 | | -1.10 | | -0.71 | | -0.79 | | -0.40 |
| 1989-90 | 1.28 | | -0.38 | | -1.25 | | 0.52 | | -0.50 | | -0.02 |
| 1990-91 | 0.15 | | 0.04 | | -1.00 | | 0.23 | | -1.66 | | 0.70 |
| 1991-92 | -1.45 | | -1.40 | | 0.38 | | -1.32 | | -0.86 | | -0.87 |
| 1992-93 | -0.24 | | -0.10 | | 0.38 | | -0.43 | | 0.64 | | -0.50 |
| 1993-94 | -0.72 | | -1.34 | | -0.01 | | -0.37 | | 0.64 | | -0.74 |
| 1994-95 | -1.09 | | -0.71 | | -1.21 | | -1.02 | | -0.07 | | -0.52 |
| 1995-96 | -0.22 | | 0.79 | | -0.07 | | -1.80 | | 0.81 | | 0.65 |
| 1996-97 | 1.21 | | -1.67 | | -0.09 | | 0.65 | | 0.14 | | 0.05 |
| 1997-98 | 0.41 | | -0.64 | | -0.69 | | 0.88 | | -0.71 | | -0.43 |
| 1998-99 | -1.43 | | -1.30 | | 0.97 | | -0.68 | | 0.07 | | -0.18 |
| 1999-00 | -0.28 | | 0.97 | | -0.37 | | -0.21 | | -0.46 | | 1.60 |

| SPI | Key | % yield deviation |
|------------|-----|-------------------|
| ≥ 1.5 | | ≥25 |
| 1 to 1.5 | | 10 to 25 |
| -1 to +1 | | -10 to +10 |
| -1 to -1.5 | | -10 to -25 |
| ≤-1.5 | | ≤-25 |

Figure 7.12b Correlation of SPI (OND and JFM) with detrended maize yield deviations for the period 1961-2000

| YEAR | Lilongwe | | | Zambezi 4 | | | Zambezi 3 | | |
|---------|----------|-------|-------|-----------|-------|--------|-----------|-------|-------|
| | OND | Yield | JFM | OND | Yield | JFM | OND | Yield | JFM |
| 1960-61 | 1.12 | | 0.59 | -0.38 | | 0.535 | -1.52 | | 0.76 |
| 1961-62 | 0.07 | | 0.95 | 1.65 | | -0.366 | -0.25 | | 0.73 |
| 1962-63 | 1.73 | | -0.71 | -1.71 | | -0.164 | 1.89 | | -0.69 |
| 1963-64 | 0.40 | | 0.53 | 0.13 | | -0.125 | -0.27 | | 0.31 |
| 1964-65 | -0.02 | | -0.98 | -1.70 | | 0.156 | 0.73 | | 0.50 |
| 1965-66 | -0.30 | | 0.57 | -0.94 | | 0.988 | -0.27 | | 1.01 |
| 1966-67 | -0.66 | | -0.47 | -1.56 | | -1.164 | 0.33 | | -1.30 |
| 1967-68 | 1.58 | | -0.57 | 0.88 | | 0.417 | -0.97 | | 0.33 |
| 1968-69 | 1.24 | | -1.13 | 2.51 | | -3.071 | 0.63 | | -3.09 |
| 1970-71 | 1.72 | | 0.99 | 0.48 | | 0.266 | 2.26 | | -0.26 |
| 1971-72 | -0.17 | | -0.12 | -0.02 | | -0.087 | 1.64 | | 0.25 |
| 1972-73 | 1.08 | | -0.67 | -0.95 | | -0.296 | 1.26 | | -0.49 |
| 1973-74 | -0.23 | | 0.90 | 1.86 | | 0.682 | 0.00 | | 0.61 |
| 1974-75 | -0.47 | | 0.03 | 1.01 | | -0.255 | 0.87 | | -1.46 |
| 1975-76 | 0.28 | | 0.55 | 0.48 | | 0.617 | 1.48 | | 0.49 |
| 1976-77 | 0.40 | | 0.36 | 0.29 | | 0.196 | 0.68 | | 0.25 |
| 1977-78 | -0.34 | | 0.73 | 0.95 | | 1.238 | 1.00 | | 1.05 |
| 1978-79 | 1.06 | | -0.73 | 0.50 | | -0.343 | 0.55 | | -0.02 |
| 1979-80 | 1.53 | | -1.18 | 0.00 | | -0.673 | 1.15 | | -0.37 |
| 1980-81 | 1.21 | | -1.06 | 0.27 | | 0.957 | 0.47 | | 0.18 |
| 1981-82 | -0.51 | | 0.50 | -0.91 | | 0.03 | 0.65 | | 0.09 |
| 1982-83 | 0.52 | | -0.79 | -0.12 | | -1.185 | -0.22 | | -1.42 |
| 1983-84 | 0.09 | | -0.33 | -0.72 | | -0.721 | -0.21 | | 0.18 |
| 1984-85 | 1.31 | | -0.22 | 0.13 | | 1.467 | -0.05 | | 0.83 |
| 1985-86 | 0.50 | | 0.34 | 0.77 | | 0.092 | 0.72 | | 0.25 |
| 1986-87 | -0.19 | | 0.12 | 0.53 | | -1.819 | 1.44 | | -1.48 |
| 1987-88 | -0.41 | | 0.27 | -0.69 | | 0.836 | 0.93 | | 0.73 |
| 1988-89 | -0.29 | | 1.61 | -0.92 | | 0.943 | 0.40 | | 1.26 |
| 1989-90 | 0.55 | | -0.57 | 0.97 | | 0.613 | -0.10 | | -0.17 |
| 1990-91 | -0.29 | | 0.31 | -0.14 | | 0.454 | 0.79 | | 0.47 |
| 1991-92 | -0.02 | | -1.01 | -0.20 | | -2.33 | -0.31 | | -1.01 |
| 1992-93 | -0.14 | | 0.48 | 0.10 | | 0.001 | -0.78 | | 0.26 |
| 1993-94 | 0.39 | | -0.07 | -0.44 | | -1.132 | 0.05 | | -0.60 |
| 1994-95 | 0.31 | | -0.67 | -0.58 | | -1.469 | 0.45 | | -1.68 |
| 1995-96 | 0.10 | | 0.44 | -0.90 | | 0.169 | 0.08 | | 0.29 |
| 1996-97 | 1.40 | | 0.55 | 0.54 | | -1.044 | 0.19 | | -0.38 |
| 1997-98 | 1.00 | | 0.63 | 1.64 | | -0.283 | 1.75 | | -0.10 |
| 1998-99 | -0.18 | | 0.73 | -2.70 | | -1.002 | 0.78 | | -0.95 |
| 1999-00 | -0.06 | | 0.08 | -0.89 | | 1.045 | -0.76 | | 0.52 |

| SPI | Key | % yield deviation |
|------------|-----|-------------------|
| ≥ 1.5 | | ≥25 |
| 1 to 1.5 | | 10 to 25 |
| -1 to +1 | | -10 to +10 |
| -1 to -1.5 | | -10 to -25 |
| ≤-1.5 | | ≤-25 |

Figure 7.12c Correlation of SPI (OND and JFM) with detrended maize yield deviations for the period 1961-2000

The fact that negative SPIs are sometimes associated with positive yield deviations could also be explained in part by the fact that soils with a good moisture retention capacity are less susceptible to droughts (depending on the amount of moisture retained and the amount of plant

water requirements) especially if wet years precede the dry years or vice versa, this is particularly so in semi arid areas (Tallaksen and van Lanen, 2004). An example is the Kabompo sub-basin where, for the 1968-69 the planting season was very wet and the growing season was extremely dry yet very high maize yields (above the long term average of 1916-2000) with a positive deviation $\geq 25\%$ were obtained.

7.4 Discussion

This part of the study focussed on the spatial and temporal patterns of agricultural droughts in the Zambezi basin. Detrended maize yields for the period 1960-2000 were compared to annual rainfall amounts and the results indicated the potential impacts of any changes in rainfall patterns on agricultural production. An attempt was made to relate the SPI to the detrended agricultural yield in the basin. An analysis of the century long time series (1901-2002) based on the six monthly agricultural SPI (SPI6) revealed high variability of agricultural droughts in the Zambezi basin. The SPIs varied temporally and spatially, with varying degrees of severity between the different sub-basins. Some of the historical droughts as observed from the SPIs (OND, JFM, SPI6) occurred during the years 1948, 1964, 1967, 1972-73, 1981-82, 1984-85, 1991-92, 1994-95 and 2000-2001.

A cumulative sum procedure was applied to the SPI6 for the period 1901-2002. It was observed from the cumulative SPIs that a statistically significant periodic pattern existed between the dry and wet spells experienced during the twentieth century. It is suggested from this observation that if the dry spells are prolonged then the associated impacts will be amplified. In the context of climate change and extreme events, it is already being postulated (Trenberth et al., 2007) that the occurrence of flood and drought events may be a result of a changing climate through global warming. The observation made so far in this study shows a statistically insignificant trend in the dry and wet spells over the whole century suggesting that the patterns of variability are reasonably stationary and that climate change signals are not evident. The recurring pattern of dry and wet spells over a century long period seems to suggest that this is an ongoing trend which may persist into the future. Other studies (e.g Manatsa et al., 2010, Mazvimavi, 2008) undertaken in some parts of the Zambezi basin have also revealed a similar pattern of variability. Since SPI is derived from rainfall as a single input variable it is expected that SPI should follow

to a large extent the same pattern that is portrayed by the rainfall and as such, SPI is able to capture the variability in past drought events in the Zambezi basin.

On a regional scale the maize yield time series for the period 1961-2010 (FAOSTAT, 2012) were assessed and below normal yields were experienced during 1961-65, 1969-71, 1982-84 and 1991-93. When considering plant growth, soil moisture deficiency within a matter of days may have devastating effects especially during the most critical growth stage. It is clear that daily variations and the distribution of rainfall within a month are important for plant growth but SPI is generated at monthly time scales since only monthly rainfall data were available for this study. The daily data that were available were not adequate to cover the entire basin. The three monthly time scales (OND and JFM) used represent agricultural droughts during the planting and growing seasons respectively. The results revealed that for the years 1969-70, 1982-83 and 1991-1992 the below average yields had largely been a result of moisture deficiencies during the growing (JFM) season. The negative impact of the JFM deficiency on crop yield can be explained by the fact that JFM is the growing and grain filling season, and if crops are deprived of moisture they would have no chance to grow and mature.

Statistically significant but weak correlations were observed between the SPI and maize yield deviations. This observation is explained by the fact that SPI is a rainfall-based index which may not be adequate to define the soil moisture droughts and is therefore not able to account for the available soil moisture conditions that largely affect the development of a crop. Soil moisture content is a reflection of the amount of rainfall retained locally after the processes of runoff and evapotranspiration have occurred. SPI is limited in that it does not account for deficits arising from evapotranspiration, infiltration and runoff. Furthermore SPI does not incorporate surface air temperatures and cannot be able to account for the effect of surface warming on the wet and dry spells.

This part of the study has shown that periodic droughts continue to be a recurring phenomenon in the Zambezi basin and that yield deficits are influenced to some extent by the nature and extent of drought. Although it may be agreed that under normal circumstances (excluding war and epidemics) climatic variability is one of the major factors that influences the interannual variability of agricultural production (Gommes,1998), this study demonstrates that it is difficult

to estimate with any degree of accuracy the amount of deviation that may be a direct effect of variability in rainfall. It is possible that even after detrending, some extraneous factors may not have been fully eliminated. The type of technology, administrative procedures and agricultural and government policies are some of the factors that may influence the amount of agricultural yield. Discrepancies may also arise from the way the input data are generated or gathered. Data quality is still a contentious issue, the CRU rainfall data used in this study are derived from sparse raingauges that are found within the Zambezi basin. Bordi *et al.* (2001a;b) state that the quality of the SPI result can only be as good as the data used to generate it. Although the rainfall data were spatially interpolated before generating the SPI, it is possible that the input data at a given point may not always depict an accurate large scale picture (due to sparsness and poor quality) of the prevailing conditions from which the yields were derived (Easterling, 1988).

7.5 Simulated soil moisture and agricultural droughts

This section explores the viability of using a soil moisture based index as an agricultural drought indicator. Soil moisture is an important hydrological variable because it is the medium through which the runoff, infiltration and evapotranspiration processes are integrated. Because soil characteristics are highly variable in time and space, it is difficult to obtain data sets that address the soil properties at finer scales, moreover soil data that cover the entire basin are not available and it is for this reason that simulated soil moisture is used in this study.

7.5.1 Soil moisture SPI relationship

To assess the historical drought situation in relation to food security in the Zambezi basin, the relationship of the anomalies of simulated soil moisture with SPI and with detrended maize yields for the period 1961-2000 are evaluated. Despite the fact that simulated soil moisture and SPI are not independently related, it must be noted that determining the relationship between these two variables is also a way of validating the methodologies used in their derivation. Spearman's rank correlation coefficient and wavelet analysis (a two-dimensional time and frequency analysis tool) are used to assess the relationships (Table 7.5, Figures 7.13 and 7.14). The advantage of wavelet analysis over other methods is that it incorporates the time localisation of frequencies in the time series (Torrence and Compo, 1998; Torrence and Webster, 1999), so that the derived results are not only based on the frequency of occurrence but they are also

synchronised to the time of occurrence. There is a significant relationship between the soil moisture anomalies and the SPIs at the 95% confidence level. Strong correlations ($R_s > 6.5$) between soil moisture and SPI are observed for most of the sub-basins except for Lilongwe and Zambezi 4. For Kabompo and Luena the correlation is weak for the JFM season while for Kafue 4 and Lake Kariba the correlation is weak for the OND season.

Table 7.5 Correlation of soil moisture anomaly with SPI ($\alpha = 0.05$), R_s : Spearman's correlation coefficient

| Catchment | Soil versus SPI | | | | | |
|------------|-----------------|---------|-------|---------|--------|---------|
| | OND | | JFM | | ONDJFM | |
| | R_s | p-value | R_s | p-value | R_s | p-value |
| Kabompo | 0.81 | <0.0001 | 0.45 | 0.029 | 0.84 | <0.0001 |
| Luena | 0.67 | <0.0001 | 0.47 | 0.002 | 0.64 | <0.0001 |
| Luanginga | 0.80 | <0.0001 | 0.70 | <0.0001 | 0.86 | <0.0001 |
| Kafue 4 | 0.58 | 0.000 | 0.71 | <0.0001 | 0.86 | <0.0001 |
| Zambezi 10 | 0.82 | <0.0001 | 0.89 | <0.0001 | 0.92 | <0.0001 |
| Zambezi 8 | 0.57 | 0.000 | 0.65 | <0.0001 | 0.74 | <0.0001 |
| Gwai | 0.95 | <0.0001 | 0.94 | <0.0001 | 0.97 | <0.0001 |
| Mupfure | 0.66 | <0.0001 | 0.80 | <0.0001 | 0.81 | <0.0001 |
| Luangwa | 0.70 | <0.0001 | 0.71 | <0.0001 | 0.94 | <0.0001 |
| Mazowe | 0.98 | <0.0001 | 0.89 | <0.0001 | 0.94 | <0.0001 |
| Lilongwe | 0.37 | 0.042 | 0.48 | 0.046 | 0.58 | 0.032 |
| Zambezi 4 | 0.43 | 0.032 | 0.58 | 0.038 | 0.64 | 0.031 |

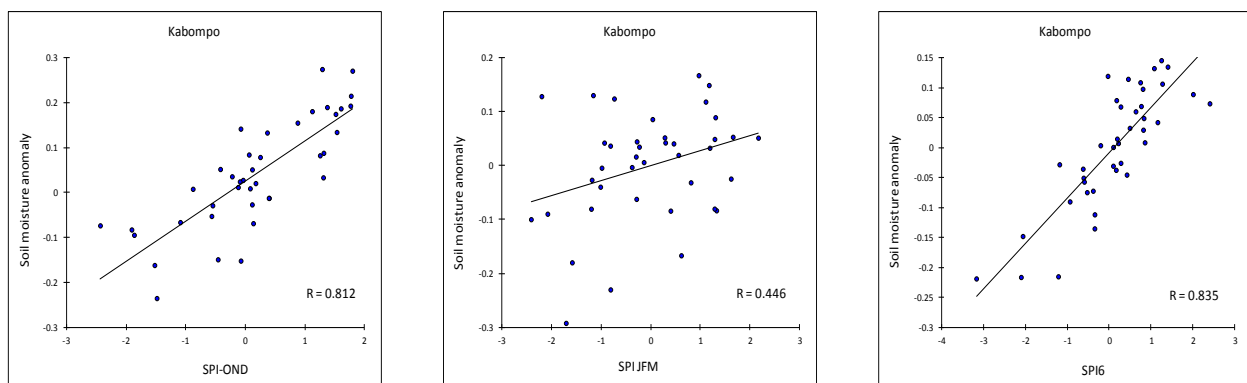


Figure 7.13a Correlations of soil moisture and SPI

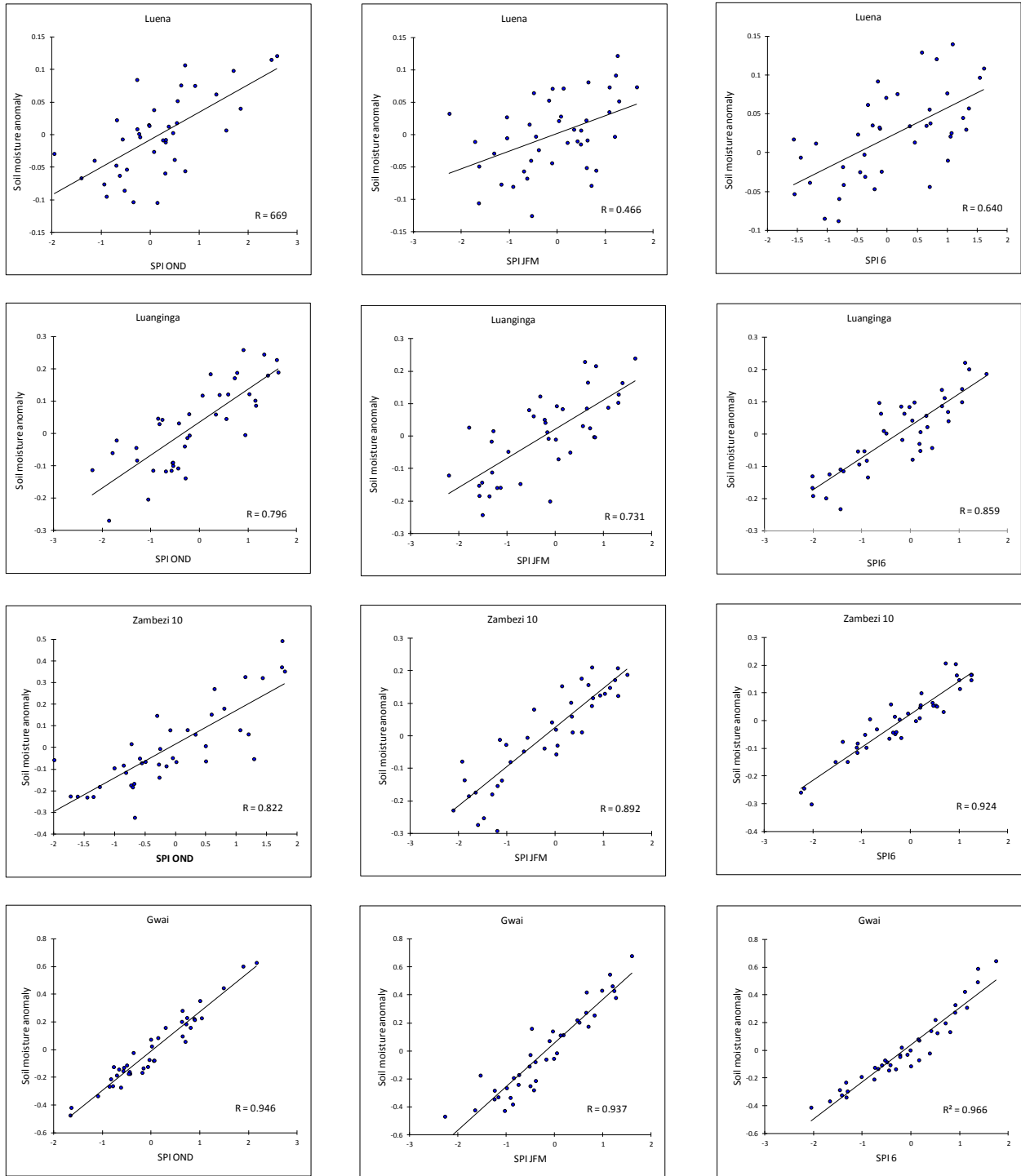


Figure 7.13b Correlations of soil moisture and SPI

The relationship between soil moisture and SPI is further confirmed by the wavelet analysis method. The wavelet power spectra for the Kabompo and Kafue 4 catchments are depicted in Figure 7.13. Temporal fluctuations in both soil moisture and SPI are observed over the 40-year period. In all cases, peaks occur at 1-4, 4-8 and 8-16 year bands and the power is evenly distributed across the entire period. The 1-4 year band is the most dominant, but it should be noted that the 1- year band always represents the natural annual cycle of precipitation. The peaks in the 2-4 and 4-8 year bands are most likely attributed to the ENSO cycles whose range is normally 2-10 years (Glantz et al., 2007).

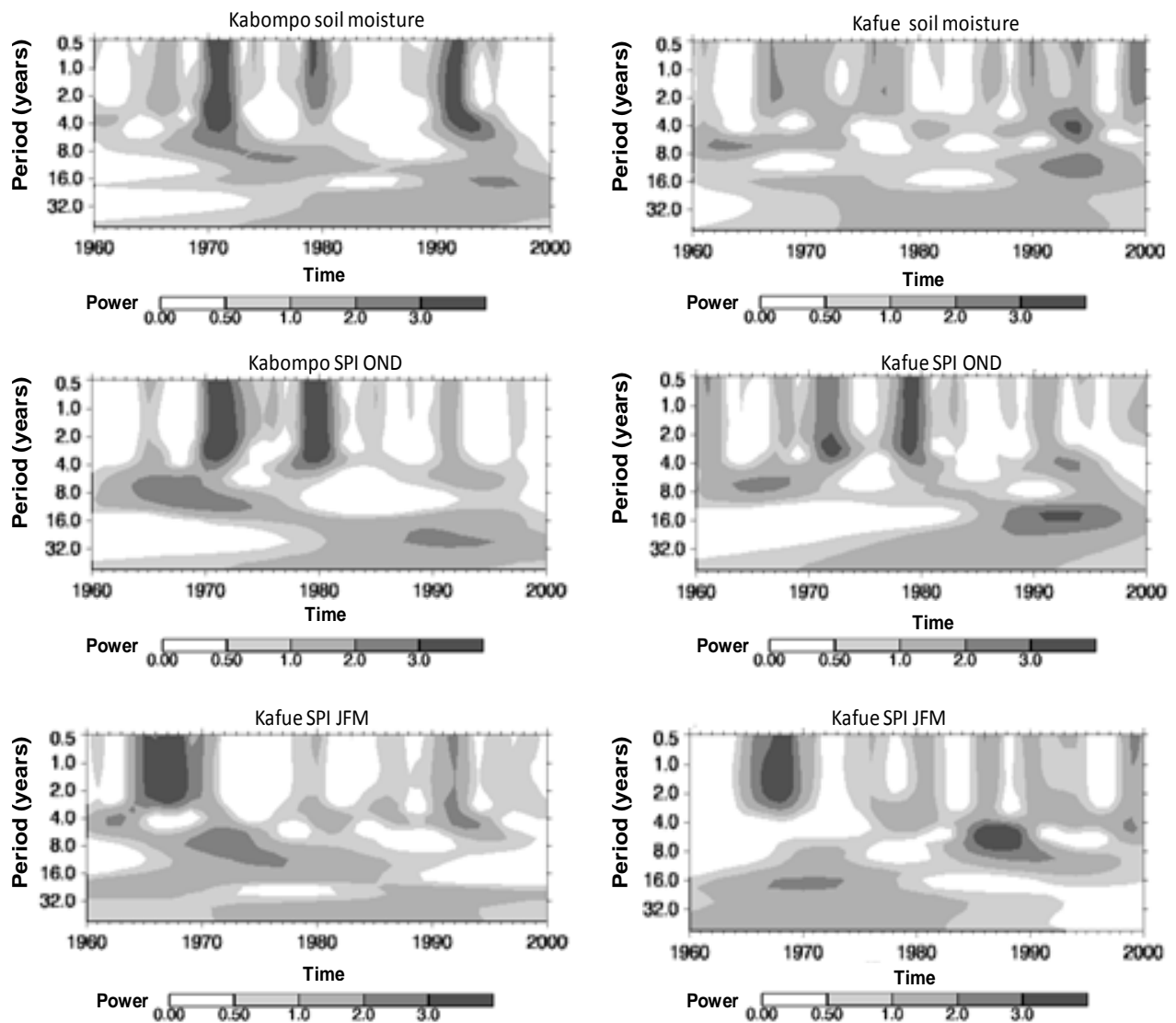


Figure 7.14 Wavelet power spectra of soil moisture and SPI for the Kabompo and Kafue.

The covariance between the two variables during the period 1960-2000 is presented as Fourier squared coherencies (R^2) in Table 7.6. The Fourier squared coherency is applied to identify the frequency bands within which the time series of SPI and soil moisture are covarying. Both the OND and JFM SPIs are equally comparable in coherencies with soil moisture and the R^2 values range between 0.79 and 0.98 at the 95% significance level. These very high coherencies are indicative of a strong covariance between SPI and soil moisture. It should be noted that the coherencies between soil moisture and SPI are higher than the corresponding correlations that were obtained using the Pearson's rank correlation and this may be due to the ability of the wavelet analysis method to explore the relationships in two-dimensional way that considers both the frequency and time domains. Even though the SPI was not designed to be a direct measure of soil moisture content, the strong relationship observed between SPI and soil moisture anomalies is clearly associated with the fact that precipitation is a major driving factor for the two variables. Although the relationship between soil moisture and SPI is not independent it is important to appreciate that evapotranspiration, as well as other hydrological processes (runoff, groundwater recharge, etc.) play a major role in determining the patterns of soil moisture variation. Also it must be noted that determining the relationship between these two variables is also a way of validating the methodologies used in their derivation. The following section explores the possibility of using the simulated soil moisture as an agricultural drought indicator by drawing relationships with detrended maize yields in the Zambezi basin.

Table 7.6 Coherency between SPI and soil moisture

| SPI coherency with soil moisture at 95% significance | | |
|--|---------|---------|
| Catchment | SPI-OND | SPI-JFM |
| Kabompo | 0.915 | 0.813 |
| Luena | 0.912 | 0.924 |
| Luanginga | 0.881 | 0.952 |
| Kafue 4 | 0.883 | 0.941 |
| Zambezi 10 | 0.924 | 0.912 |
| Zambezi 8 | 0.933 | 0.964 |
| Gwai | 0.982 | 0.973 |
| Mupfure | 0.864 | 0.882 |
| Luangwa | 0.861 | 0.900 |
| Mazowe | 0.983 | 0.962 |
| Lilongwe | 0.792 | 0.813 |
| Zambezi 4 | 0.911 | 0.942 |

7.5.2 Soil moisture yield relationship

Scatter plots and time series graphs representing the relationship between simulated soil moisture and detrended maize yields are presented in Figures 7.15a-c and the correlation statistics are shown in Table 7.7. Correlations are performed between the simulated soil moisture conditions for the different time scales of the agricultural season (OND and JFM) and the detrended yield. The results are also assessed against the correlation between the corresponding SPI and the detrended maize yield which is given in brackets in Table 7.7. Strong correlations (>0.8) between soil moisture anomalies and detrended yield are observed in the Kabompo while the Luena, Luanginga, Kafue 4, Luena, Gwai, Mupfure and Mazowe catchments exhibit moderate correlations (>0.5 to 0.65) between the soil moisture anomalies and the detrended yields. Insignificant correlations are obtained for the Lake Malawi (Lilongwe and Namitete) catchments. In general the relationships between soil moisture and detrended maize yield are stronger and more significant than the relationships between SPI and detrended maize yield.

Table 7.7 Rank order correlation coefficients of soil moisture and detrended maize yield

| Catchment | Soil vs. detrended yield | | | | | |
|------------|--------------------------|---------|----------------|---------|----------------|---------|
| | OND | | JFM | | ONDJFM | |
| | R _s | p-value | R _s | p-value | R _s | p-value |
| Kabompo | 0.90 (0.46) | <0.0001 | 0.93 (0.35) | <0.0001 | 1.00 (0.42) | <0.0001 |
| Luena | 0.63 (0.35) | <0.0001 | 0.59 (0.28*) | 0.000 | 0.64 (0.46) | <0.0001 |
| Luanginga | 0.51 (0.42) | 0.001 | 0.51 (0.25*) | 0.004 | 0.57 (0.46) | 0.000 |
| Kafue 4 | 0.66 (0.43) | <0.0001 | 0.37 (0.08*) | 0.02 | 0.51 (0.32) | 0.001 |
| Zambezi 10 | 0.45 (0.32) | 0.004 | 0.16* (0.17*) | 0.297 | 0.29* (0.28) | 0.045 |
| Zambezi 8 | 0.21*(0.10*) | 0.336 | 0.28* (0.13*) | 0.54 | 0.32* (0.21) | 0.187 |
| Gwai | 0.31 (0.37) | 0.046 | 0.59 (0.55) | 0.000 | 0.61 (0.59) | <0.0001 |
| Mupfure | 0.60(0.32) | <0.0001 | 0.60 (0.57) | <0.0001 | 0.53 (0.51) | 0.001 |
| Luangwa | 0.51 (0.43) | 0.001 | 0.22 (0.29*) | 0.325* | 0.32 (0.25) | 0.048 |
| Mazowe | 0.41 (0.42) | 0.011 | 0.64 (0.05) | <0.0001 | 0.63 (0.65) | <0.0001 |
| Lilongwe | 0.23* (0.02*) | 0.154 | 0.22* (0.11) | 0.107 | 0.41 (0.17*) | 0.008 |
| Namitete | 0.10*(0.04) | 0.135 | 0.26*(0.16) | 0.104 | 0.21* (0.18*) | 0.204 |

* not significant at $\alpha = 0.05$ level, ()SPI versus yield

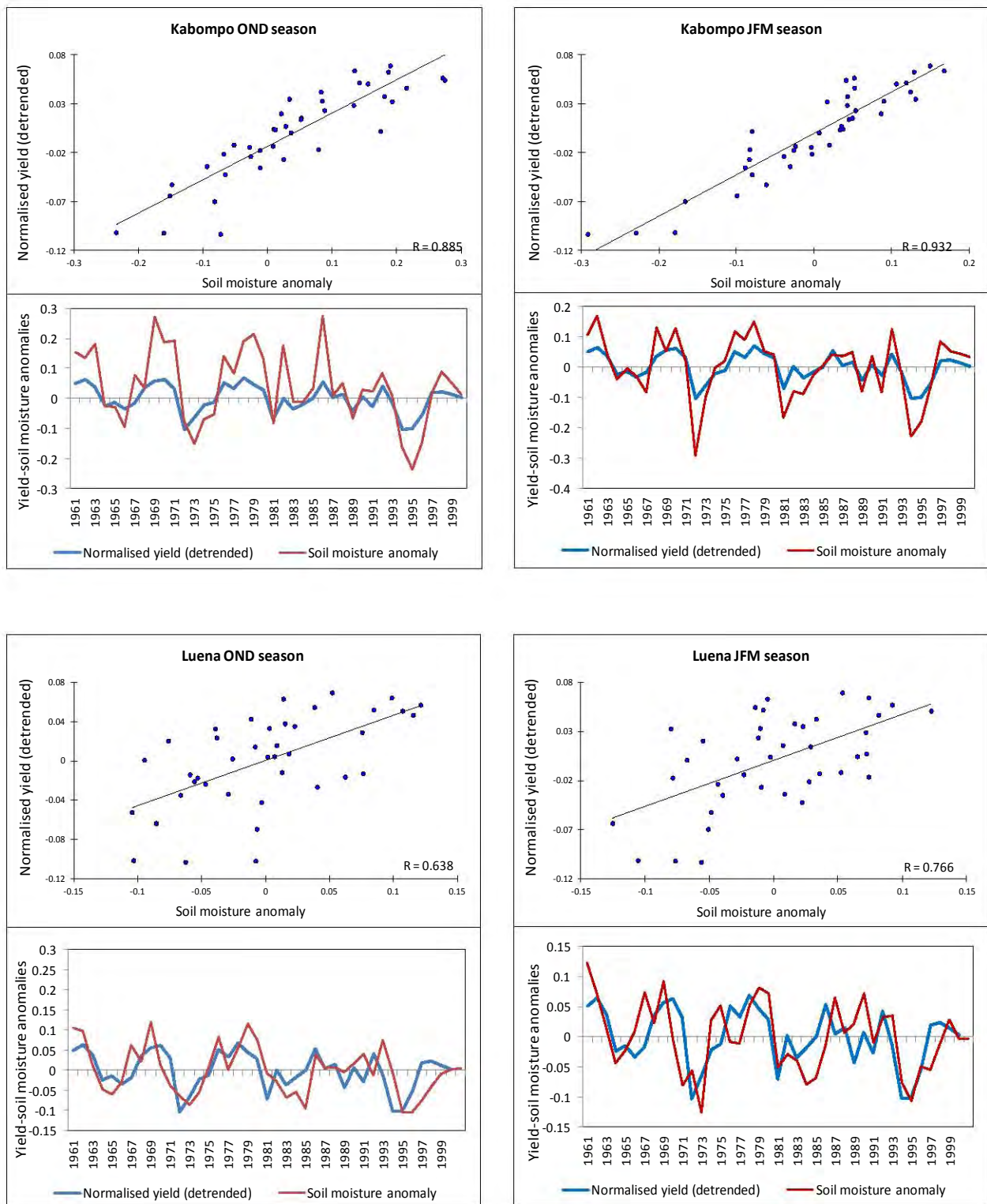


Figure 7.15a Correlations between soil moisture anomalies and detrended maize yields

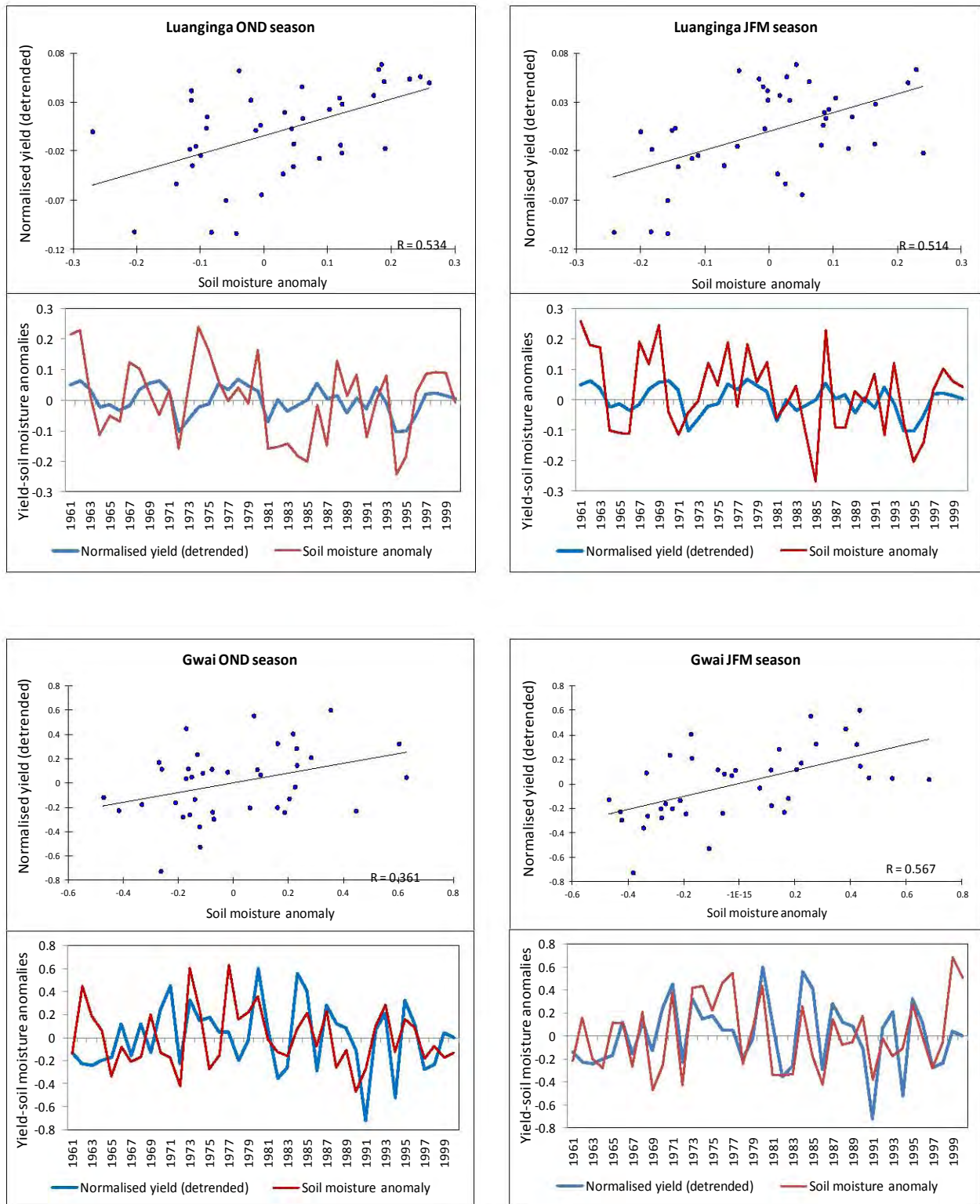


Figure 7.15b Correlations between soil moisture anomalies and detrended maize yields

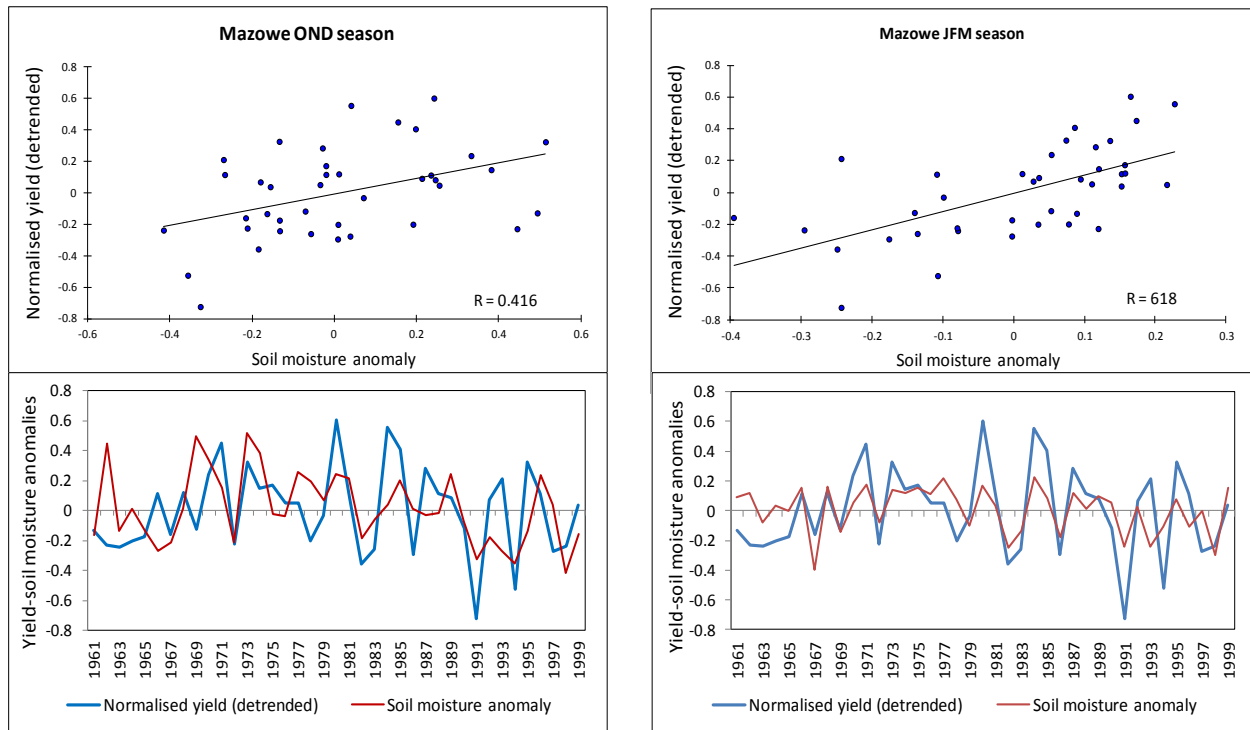


Figure 7.15c Correlations between soil moisture anomalies and detrended maize yields

Wavelet power spectra for the soil moisture anomalies and detrended maize yields are depicted in Figure 7.15 using example cases of the Luena and Mazowe catchments. The spectra for the soil moisture and maize yield show strong peaks in the 1-4 and 4-8 year bands. Moderate to high variability in soil moisture and the yield is observed in all cases except for the 6-10 year maize yield band for the Mazowe sub-basin where variability was low between 1961 and 1980 (mainly due to the impacts of civil war). The coherencies between the soil moisture and maize yield spectra are presented in Table 7.8 and Figure 7.16. High coherency (>0.8 , strong correlation) is exhibited within the 1-4 year band in all the cases while the coherency ranges from 0.4 to 0.8 in the 4-8 year band. Strong relationships are depicted in which 80% of the example cases (both OND and JFM) show coherencies greater than 0.8 and the remaining 20% have coherencies between 0.55 and 0.7 at the 95% confidence level.

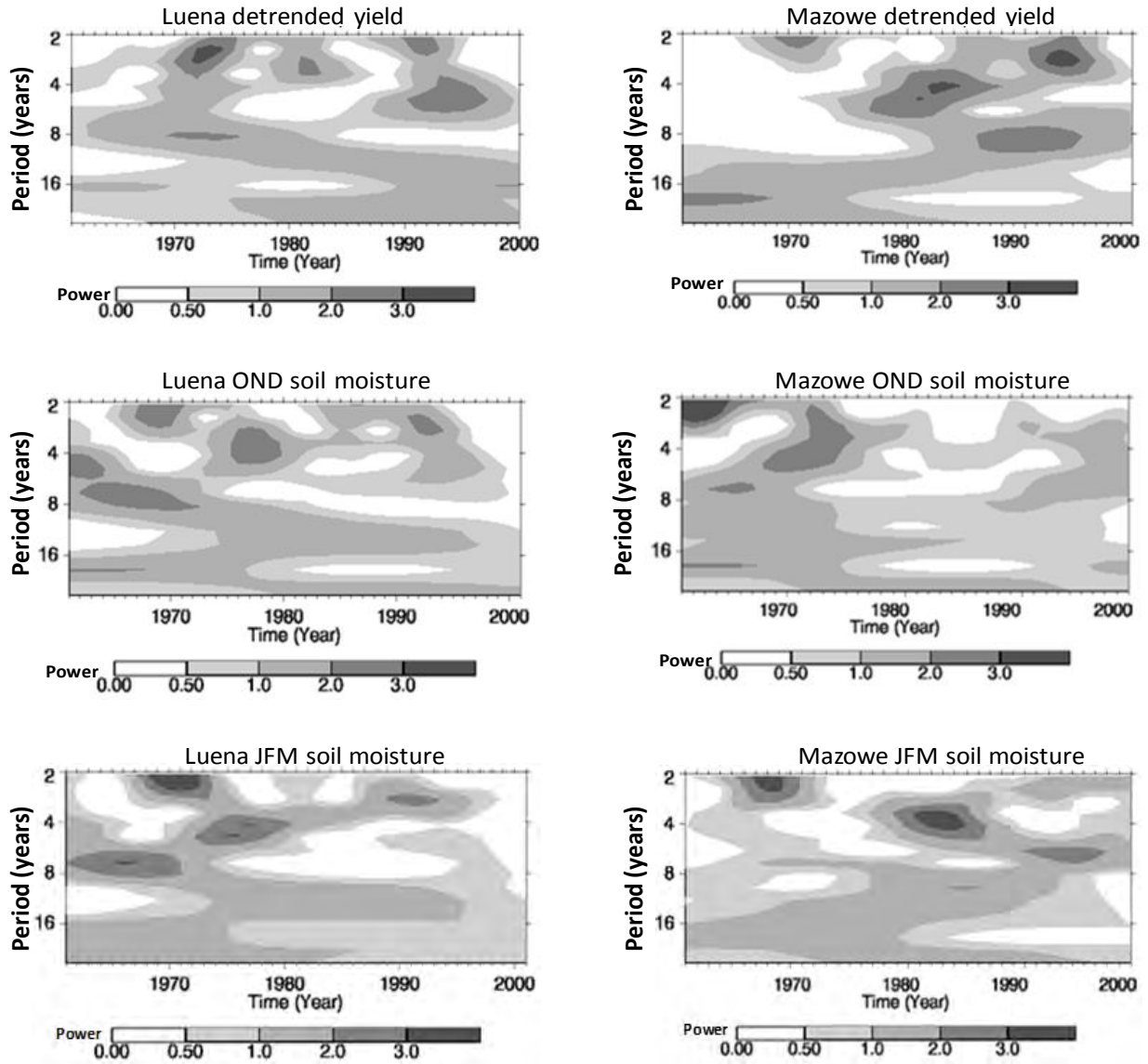


Figure 7.16 Wavelet power spectra of soil moisture and detrended maize yield for Luena and Mazowe

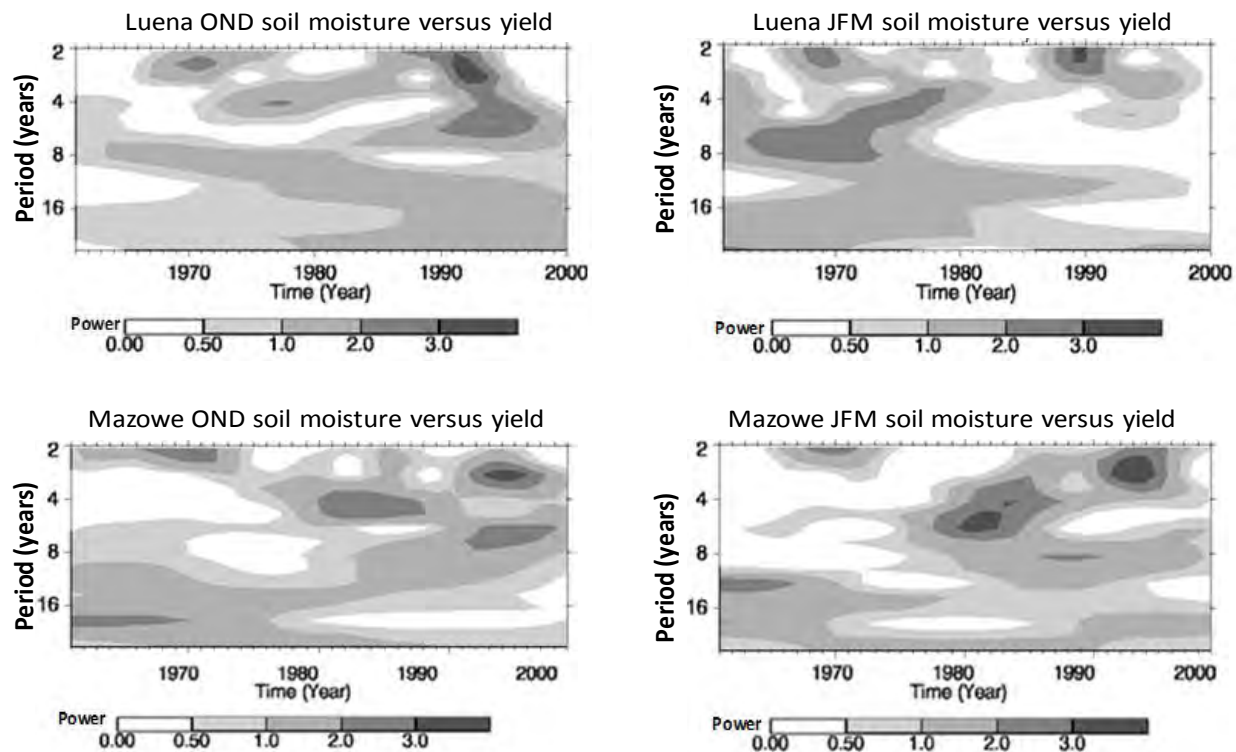


Figure 7.17 Wavelet coherence between soil moisture and detrended maize yield for Luena and Mazowe.

Table 7.8 Coherency between soil moisture and detrended maize yields

| Soil moisture coherency with maize yield at 95% significance | | |
|--|-------|-------|
| Catchment | OND | JFM |
| Kabompo | 0.995 | 0.997 |
| Luena | 0.837 | 0.766 |
| Luanginga | 0.847 | 0.769 |
| Kafue 4 | 0.871 | 0.827 |
| Zambezi 10 | 0.743 | 0.777 |
| Zambezi 8 | 0.691 | 0.626 |
| Gwai | 0.727 | 0.864 |
| Mupfure | 0.760 | 0.827 |
| Luangwa | 0.897 | 0.644 |
| Mazowe | 0.808 | 0.784 |
| Lilongwe | 0.911 | 0.727 |
| Namitete | 0.557 | 0.736 |
| Zambezi 4 | 0.661 | 0.560 |

7.6 Discussion and conclusion

This chapter explored the possibility of using SPI and simulated soil moisture as agricultural drought indicators for the Zambezi basin. The results suggest strong coherencies between soil moisture and SPI and this is attributed to the fact that both variables are mainly driven by regional precipitation. Considering soil moisture and SPI with respect to maize yield, a stronger correlation exists between soil moisture and detrended maize yield than between SPI and the detrended yield. The relationship between SPI and maize yield deviation suggest a compensatory effect between the rainfall conditions of the planting (OND) and growing (JFM) seasons although the JFM season was considered to be more critical to the maize yield than the OND season. Positive yield deviations were obtained even if the OND season was under a water deficit as long as the subsequent JFM season was wet. In some cases positive yield deviations were observed even with negative SPI values indicating that deficit rainfall amounts may not necessarily cause a drop in the yield. Rather the amount of deficit or the severity of the SPI mattered together with the antecedent moisture conditions as these helped the seeds to germinate. As long as the growing season was wet the plants would prosper and therefore a positive deviation could still be realised. A poor relationship was, however, observed between SPI and detrended maize yield and this was attributable to the fact that SPI is a rainfall based index which does not take into consideration other variables such as evapotranspiration, runoff and infiltration. SPI was therefore considered inadequate for monitoring soil moisture droughts. Despite the shortfalls SPI still remains an approximate indicator for the cumulative effect of rainfall deficits and particularly for meteorological droughts and can therefore be used as a preliminary indicator of the drought conditions that can inform the monitoring of other types of droughts.

The development of a crop relies on available soil moisture and the type of soil is important as it determines the moisture retention capacity of a soil. It was clear in this study that antecedent moisture conditions were important such that if the previous season was wet while the subsequent season (for example the planting season) was dry plants could still prosper. It is clear that soil moisture conditions play a major role in all the developmental stages of a crop and this is evidenced by the stronger correlation of soil moisture with the yield for both the OND and JFM seasons. The use of a soil moisture-based agricultural drought index clearly has an

advantage over SPI in that the index incorporates soil moisture dynamics which are very important in the mapping of an agricultural drought and in determining the agricultural yield. Based on the preceding results it can be concluded that a simulated soil moisture based index is a better indicator for agricultural droughts than the rainfall based SPI. Though generating SPI is quick, simple and requires no hydrological expertise, in addition to a single input data (rainfall) requirement, SPI has limitations of not being able to account for water deficits arising from evapotranspiration, infiltration and runoff and it does not consider the intensities and temporal distributions of rainfall within the time scale under consideration e.g. a month. Due to the standardised nature of the index, SPI is not capable of distinguishing the severity of droughts between different locations since the same value of SPI at two different locations does not necessarily mean that the two locations experienced the same water deficits, these deficits are only treated in respect of the conditions within a specific location. On the other hand, using simulated soil moisture index has an advantage of being generated from a hydrological modelling approach that takes into account the effects of evapotranspiration, groundwater storage, interflow, surface runoff and monthly rainfall distributions. Hydrological modelling is, however, resource intensive, time consuming and it requires knowledge about the hydrological responses of the catchment as well as understanding how hydrological models operate. The fact that good correlations were obtained between maize yields and simulated soil moisture suggest that the Pitman model can be confidently applied to the Zambezi basin. Nonetheless, both the SPI and simulated soil moisture may not be perfect due to the type of input rainfall data, and lack of a time series of evapotranspiration data in the case of the Pitman model.

Variability and cyclic patterns in the SPI and the simulated soil moisture were evident from the cumulative SPI plots and from the wavelet spectra, this variability mostly emanates from the highly variable rainfall patterns that have been observed in the Zambezi basin (Chapter 5). The observed cycles especially between the 2-8 year bands can be associated with the global teleconnections of the ENSO cycles which recur within a range of 2 to 10 years (Glantz et al., 2007). Several studies (e.g. Tyson 1986; Rasmusson, 1990; Nicholson, 2000; Dai et al, 2004) have linked the Zambezi basin droughts as well as the southern African droughts to the periodic recurrence of the warm El Niño events. Cane et al. (1994) noted a strong statistical relationship between Zimbabwean maize yields and the equatorial Pacific sea surface temperatures while

Manatsa et al. (2010) reported a significant relationship between the southern oscillation index (SOI) and SPI. In a study looking at the growing season rainfall characteristics for the maize crop in southern Africa, Tadross et al. (2007) noted that crop failure was predominant during El Niño events. According to Nicholson and Kim (1997) drought events in the basin arise when SSTs in the tropical Pacific Ocean increase such that the westerly winds become pronounced in the downstream tropical Atlantic Ocean resulting in dry air and a stronger continental high pressure cell. These processes induce changes in the central tropical Indian Ocean SSTs producing a dipole whereby during the warm El Niño events increased convective rainfall occurring over eastern Madagascar is counteracted by droughts over southern Africa (Mason and Jury, 1997). Since the SSTs and ENSO are naturally occurring events and the El Niño events are cycles that operate within a range of 2-10 years (although uncertain) it is likely that these events will continue into the future such that the wet and dry spells will persist and droughts will continue to impact agricultural yield. Using past variability in rainfall, it is possible to make seasonal predictions of rainfall which can be incorporated into hydrological models to give more reliable predictions of the droughts.

It has been realised in this study that although climate variability is the major contributing factor to agricultural droughts in the Zambezi basin, it is not the only factor that influences agricultural yields. Lal (2011) noted a declining trend in global crop production and attributed the decline to reduced investments in agricultural research and irrigation. There are other non-climate factors that may be policy or economically driven that also impacted the maize yield. This chapter has demonstrated the use of SPI and simulated soil moisture indices as predictors of agricultural droughts and as indicators of food security in the Zambezi basin. Relations between antecedent soil moisture conditions and rainfall variability can go a long way towards improving the predictability of the basin's water and agricultural resources. Such predictions can then be used as input to food security models which will in turn inform the management of adequate mitigation measures. So far in southern Africa the FEWS NET (Famine Early Warning Systems Network) programme is involved in providing information and analyses of data through forecasting crop yields as a way of providing early warning signals to food insecure areas of the region. DEWFORA (Drought Early Warning and Forecasting to Strengthen Preparedness and Adaptation to Droughts in Africa) is another programme whose objective is to provide early

warning and response to mitigate the impact of droughts in Africa. Both programmes aim to forecast and provide timely warning signals in order to minimize vulnerabilities that arise from the effects of severe weather events. However, the challenge is on what can be predicted in view of prevailing climate variability at longer time scales that are essential for drought forecasting. This situation is worsened by the fact most of the region is data sparse. What it means therefore, is that there is need for coordinated interaction between scientists, climatologists and forecasting organizations in order to convert model predictions to useful information that can be used to mitigate and reduce drought induced vulnerabilities.

CHAPTER 8 IMPACTS OF CLIMATE CHANGE ON WATER RESOURCES IN THE ZAMBEZI BASIN (2046-2065)

8.1 Introduction

Quantifying the effects of climatic change on streamflow and other hydrological variables is crucial as water managers need to be well prepared to deal with such effects in the future. Streamflow represents an integrated catchment response and it is therefore the best hydrological indicator of the impacts of climate change on water resources while soil moisture can be used as a hydrological indicator for agricultural droughts. Although it is possible to quantify a basin's hydrological response to changes in climate, the process is made more difficult by the limited availability of data particularly for rainfall and runoff and by the direct impact of human activities on water resources. However, it is still important that climate change predictions be made so that future management plans are informed with the best available estimates. This chapter provides a preliminary attempt towards integrating the predicted climate change scenarios and the hydrological responses of the Zambezi basin. The near future period of 2046-2065 is considered and it is referred to in this study as the 2050s (on average). It should be emphasised that this study is not meant to provide a comprehensive assessment of climate change in the Zambezi basin but to generate a generalised overview of the likely patterns of future hydrological conditions in the basin with respect to climate change and to contribute to the information required for the future management of water resources in the basin.

Although some predictions of the hydrological response of the Zambezi basin to changes in climate have been reported, most of these predictions (e.g. Arnell, 1999; Manabe et al., 2004; Milly et al, 2005) are based on large scale global climate models which tend to overlook the impacts of climate change at local or regional scales. Results of such findings are generalised over the whole basin although the basin is characterised by high spatial and temporal variability in the climate and hydrological variables. When such information is used to inform decision making in various areas of the basin it is likely that inadequate mitigation measures may be implemented based on a largely generalised climate signal. This study therefore aims to assess the climate change impacts at a scale (sub-basin) which takes into consideration the variable hydroclimatic characteristics of the basin.

To simulate the basin's response to future climates three GCM model outputs for the A2 emissions scenario consisting of ECHAM, GFDL and IPSL were used as input to the Pitman rainfall-runoff model which was calibrated for the Zambezi basin. The assessment is based on future changes in rainfall and potential evapotranspiration derived from the climate models and on the hydrological variables of runoff and soil moisture simulated by the hydrological model. The A2 emissions scenario (Nakicenovic et al., 2000) used in this study describes a world of high population growth and less rapid economic development. Unlike other scenarios, this scenario was used because it was available in a format (downscaled) that was required for this study. GCMs generate large global scale data which are difficult to use at smaller regional or local scales and the process of downscaling is required before the GCMs can be used with the local scale or regional hydrological models. The GCMs used in this study were statistically downscaled (Hewitson and Crane, 2006) by the Climate Systems Analysis Group (CSAG) of the University of Cape Town. These GCMs are a subset of the CMIP3 (Coupled Model Inter-comparison Project) multi-model dataset that was used as input to the Fourth Assessment Report of the Intergovernmental Panel on Climate Change (IPCC, Solomon et al., 2007). The data consist of daily rainfall and maximum and minimum temperatures for a baseline period of 1961 to 2000, a near future period of 2046 to 2065 as well as a far future period of 2081-2100. Although CSAG has to date downscaled at least nine GCMs only three of the spatially downscaled GCMs (ECHAM, GFDL and IPSL) were used for this study as these had finer spatial resolutions than the rest of the GCMs that were available. This study is only based on the near future period because it was difficult to access the downscaled GCMs for the far future period and also other sources of data that are available do not have sufficient spatial data for a basin-wide analysis.

The calibrated Pitman model, which is a semi distributed monthly time step rainfall-runoff model, is used to simulate the hydrological response of the Zambezi basin to future climate change scenarios. This model requires as input estimates of monthly rainfall and potential evapotranspiration. The GCM outputs of rainfall are provided at the daily time scale and for purposes of this study these daily data are converted to a monthly time series by using an inverse distance weighting method (Wilk et al., 2006) and making use of the spatial interpolation method under the 'Procedure' application in SPATSIM as illustrated in Figure 8.1. In this study the

hydrological model has been calibrated on historical (CRU) data and therefore the future input data needs to be referenced to the historical input data. Initial investigations indicated that there are large differences in the climate patterns between the downscaled GCMs for the baseline period and equally large differences between the GCM data and the historical data used for the hydrological model calibration. The following section discusses the bias corrections that were considered essential before the future climate data could be used with the hydrological model calibrated on historical data.

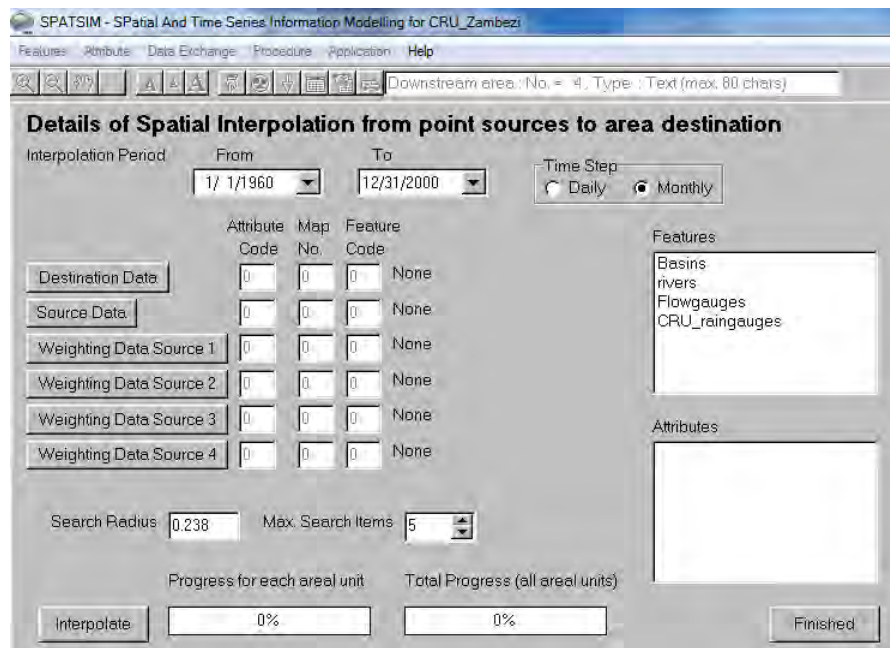


Figure 8.1 Conversion of the GCM daily rainfall to monthly rainfall in SPATSIM

8.2 Bias correction for the rainfall and temperature inputs

GCMs are mathematical representations of the atmospheric, oceanic and continental processes and the interactions that take place between these processes (Christensen et al., 2007). However there is uncertainty linked to the GCMs that emanates from the highly complex nature of the models, limited knowledge of the processes involved and the subsequent parameterisations (Nobrega et al., 2011). In addition uncertainties arise from the scale mismatch between the GCMs and the local or regional representations which necessitate the downscaling of the GCMs. Because of these uncertainties some biases exist in the simulation of both temperature and precipitation for the baseline conditions such that there is wide variation between the baseline

and the historically observed variables of climate. Such biases are illustrated in Figure 8.2 where a seasonally varying bias is observed between the GCM baseline estimates of rainfall and the historical CRU TS2.1 rainfall time series for the period 1961-2000. In order to remove the bias, a bias correction approach is applied to both rainfall and temperature. This step is essential particularly if the climate scenarios are to be used with hydrological models otherwise the results obtained will be meaningless in view of solving practical water resource problems in the future (Green et al., 2006). The bias correction methods used in this study were described in Chapter 4 and are briefly outlined below.

8.2.1 Bias correction for rainfall

The bias correction for rainfall involves the use of standard deviates based on square root transformed monthly rainfall data (Hughes et al., 2012) which are applied to convert the future monthly rainfall into standard deviates of the baseline monthly rainfall distribution. The standard deviates are then rescaled using the distribution statistics of the historical rainfall data to obtain a corrected future rainfall time series. This procedure is carried out in SPATSIM and the process is aimed at ensuring that the future rainfall conditions are related to the historical distribution statistics while at the same time maintaining the differences between the baseline and future scenarios. Other approaches such as the quartile based mapping of cumulative frequency distributions (e.g. Li et al., 2010) and logarithmic transformation are available to transform the data but these result in magnified differences between the baseline and the historical data while seasonality is not preserved in the future rainfall. The bias corrected outputs of the three GCMs (ECHAM, GFDL and IPSL) are presented in Figure 8.2 and are based on two case examples of the Zambezi. It is evident that the seasonal distributions of the baseline rainfall outputs of the GCMs are not fully representative of the historical rainfall. The GCMs over- and under-estimate the historical rainfall, the wet season rainfall months of September to November are overestimated and the months December to March are under-estimated while the dry season months are consistently over-estimated. It is noted that the baseline distribution amounts for ECHAM and IPSL are closer to the historical amounts while there is a big discrepancy for the GFDL model both for the wet and dry season months. The bias corrected outputs produce improved seasonal distribution patterns that are closer to the historically observed rainfall with

little change in the future. For the GFDL model the month of March illustrates a potential problem with this bias correction approach.

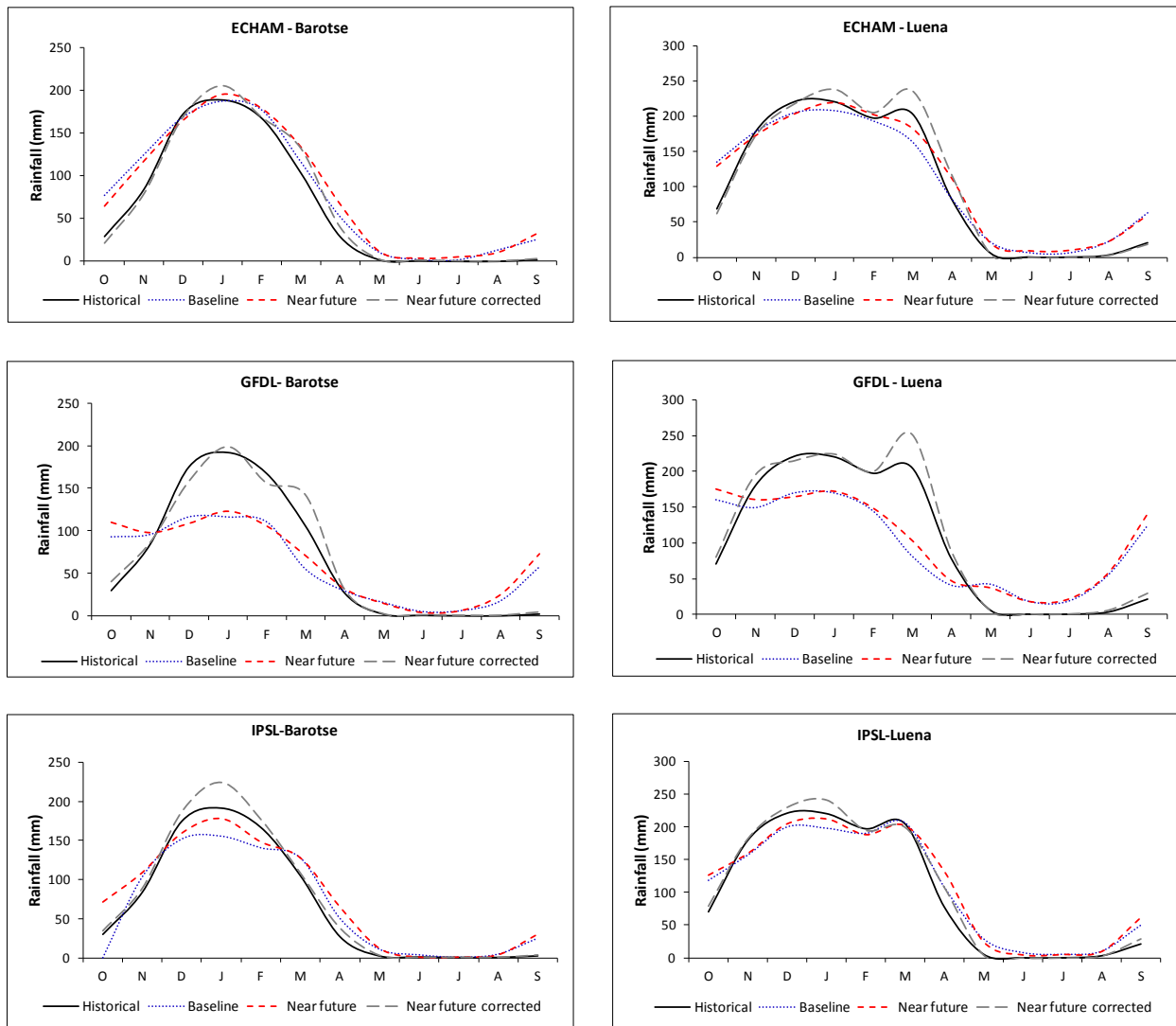


Figure 8.2 Example of rainfall bias correction for the Barotse and Luena using the ECHAM, GFDL and IPSL

8.2.2 Bias correction and change in potential evapotranspiration

In addition to precipitation, estimates of potential evaporation are also required as input to the Pitman model, but, instead of evaporation data, the available CSAG data sets consist of minimum and maximum temperature data for the baseline and future climates. These temperature data are first converted to potential evapotranspiration using the Hargreaves approach (Allen et al., 1998), as described in Chapter 4, so that they can be used with the Pitman

model. Percentage increases in potential evaporation from the baseline to the near future are estimated and the same increases are applied to the historical seasonal distributions used in the model calibration. Apart from temperature, this approach does not take into consideration all the other climate variables (e.g. relative humidity, wind speed) that impact on the evaporative demand, it is simply assumed that such factors remain constant. This is because the available GCM outputs do not provide any information from which such variables can be evaluated. The changes in potential evapotranspiration are highlighted in Table 8.1, these results are for some example sub-basins which are chosen to represent each of the major drainage areas in the Zambezi basin. In general the three GCMs predict increases ranging from 8 to 20% across the entire basin, suggesting that the Zambezi basin will become warmer by the 2050s. When classified according to the scheme given in Figure 8.3 the changes predicted by the three GCMs all fall under the same category (which is why only one map is presented for all the GCMs). It should be noted that in arid areas the evaporation component plays a major role in the water balance such that a slight over-estimation may result in huge evaporative losses thus generating smaller runoff. Likewise an under-estimation of the evaporation component may result in over-simulated flows and again such results may be meaningless with regard to solving real water problems.

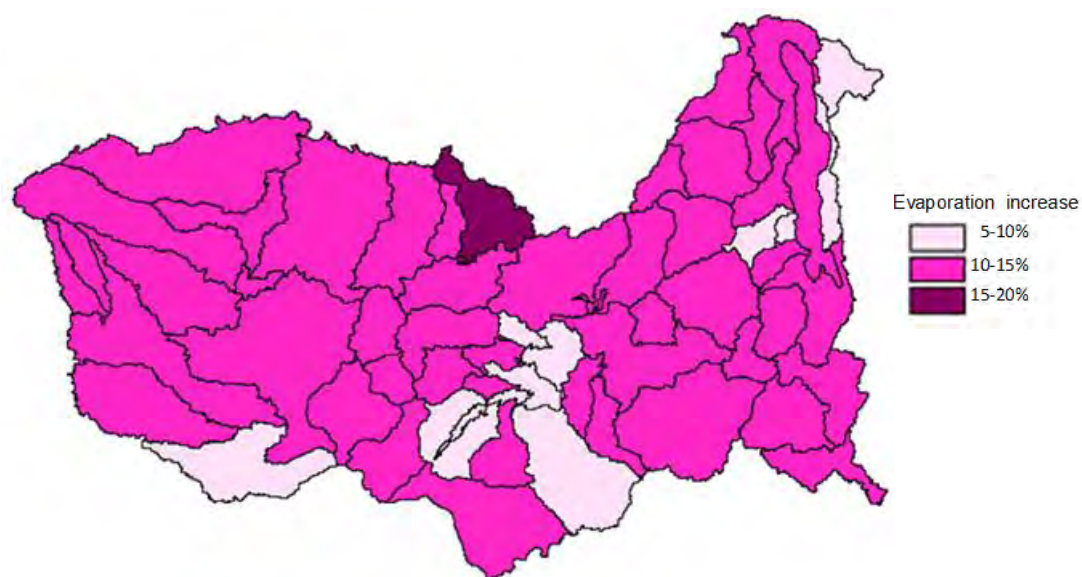


Figure 8.3 Annual evapotranspiration increases predicted by ECHAM, GFDL, and IPSL models

Table 8.1 Mean monthly potential evapotranspiration changes for example catchments

| Catchment | Mean monthly evapotranspiration increases (%), ECHAM | | | | | | | | | | | |
|----------------|---|-------------|-------------|-------------|-------------|-------------|-------------|-------------|-------------|-------------|-------------|-------------|
| | Oct | Nov | Dec | Jan | Feb | Mar | Apr | May | Jun | Jul | Aug | Sep |
| Luena | 13.6 | 13.3 | 11.2 | 11.4 | 11.0 | 11.3 | 12.3 | 11.6 | 17.1 | 17.3 | 9.9 | 11.3 |
| Cuando 1 | 13.4 | 11.2 | 11.4 | 12.3 | 11.7 | 11.3 | 13.5 | 14.6 | 20.3 | 19.1 | 11.7 | 12.8 |
| Zambezi 10 | 13.2 | 11.8 | 11.0 | 11.9 | 11.6 | 11.5 | 13.0 | 14.3 | 20.0 | 18.3 | 10.3 | 11.3 |
| Zambezi 8 | 11.9 | 11.6 | 11.5 | 13.0 | 14.3 | 20.0 | 18.3 | 10.3 | 11.3 | 13.2 | 11.8 | 11.0 |
| Kafue 4 | 13.6 | 13.3 | 11.2 | 11.4 | 11.0 | 11.3 | 12.3 | 11.6 | 17.1 | 17.3 | 9.9 | 11.3 |
| Zambezi 5 | 13.0 | 12.3 | 10.7 | 11.3 | 11.1 | 11.3 | 12.3 | 11.9 | 17.8 | 17.1 | 9.4 | 11.3 |
| Luangwa 1 | 13.9 | 13.4 | 12.3 | 11.8 | 11.0 | 11.6 | 11.2 | 10.6 | 15.2 | 17.4 | 12.3 | 13.6 |
| Zambezi 4 | 9.0 | 9.1 | 7.6 | 7.6 | 7.2 | 8.0 | 7.0 | 7.4 | 10.7 | 10.7 | 6.9 | 8.0 |
| Shire | 12.5 | 12.6 | 10.6 | 10.4 | 10.2 | 9.7 | 9.0 | 8.6 | 13.7 | 14.7 | 8.9 | 10.9 |
| Mazowe | 11.5 | 11.7 | 9.9 | 10.3 | 10.4 | 10.5 | 10.3 | 11.0 | 15.3 | 15.3 | 8.5 | 10.7 |
| Average | 12.6 | 12.0 | 10.7 | 11.1 | 10.9 | 11.6 | 11.9 | 11.2 | 15.8 | 16.0 | 10.0 | 11.2 |
| Catchment | Mean monthly evapotranspiration increases (%), GFDL | | | | | | | | | | | |
| | Oct | Nov | Dec | Jan | Feb | Mar | Apr | May | Jun | Jul | Aug | Sep |
| Luena | 12.8 | 13.1 | 10.8 | 10.8 | 9.4 | 15.9 | 12.2 | 9.9 | 11.5 | 9.8 | 11.6 | 11.6 |
| Cuando 1 | 12.0 | 11.3 | 10.6 | 11.1 | 9.7 | 15.0 | 10.0 | 12.8 | 10.8 | 12.2 | 12.6 | 13.4 |
| Zambezi 10 | 12.4 | 12.3 | 9.9 | 10.7 | 9.5 | 15.3 | 9.8 | 10.7 | 10 | 10.7 | 13.3 | 12.8 |
| Zambezi 8 | 10.7 | 9.5 | 15.3 | 9.8 | 10.7 | 10.0 | 10.7 | 13.3 | 12.8 | 12.4 | 12.3 | 9.9 |
| Kafue 4 | 12.8 | 13.1 | 10.8 | 10.8 | 9.4 | 15.9 | 12.2 | 9.9 | 11.5 | 9.8 | 11.6 | 11.6 |
| Zambezi 5 | 12.7 | 13.1 | 10.6 | 11.6 | 9.5 | 16.7 | 11.8 | 10.9 | 11.4 | 9.9 | 12 | 12.3 |
| Luangwa 1 | 11.8 | 11.6 | 10.9 | 11.3 | 10.4 | 12.4 | 14.2 | 14.9 | 13.2 | 13.4 | 12.7 | 12.3 |
| Zambezi 4 | 10.4 | 11.6 | 9.1 | 9.7 | 8.4 | 12.5 | 10.8 | 9.0 | 9.0 | 7.6 | 9.3 | 9.0 |
| Shire | 12.6 | 13.4 | 10.7 | 10.9 | 9.9 | 14.2 | 15.1 | 12.5 | 13.0 | 11.1 | 12.1 | 11.3 |
| Mazowe | 12.4 | 13.5 | 10.4 | 11.1 | 9.8 | 15.9 | 12.7 | 11.1 | 10.5 | 9.0 | 11.3 | 11.5 |
| Average | 12.1 | 12.3 | 10.9 | 10.8 | 9.7 | 14.4 | 11.9 | 11.5 | 11.4 | 10.6 | 11.9 | 11.6 |
| Catchment | Mean monthly evapotranspiration increases (%), IPSL | | | | | | | | | | | |
| | Oct | Nov | Dec | Jan | Feb | Mar | Apr | May | Jun | Jul | Aug | Sep |
| Luena | 10.6 | 11.2 | 11.2 | 10.2 | 9.7 | 10.4 | 12 | 11.5 | 13 | 14.3 | 11.5 | 11.1 |
| Cuando 1 | 10.7 | 11.4 | 11.5 | 9.4 | 9.0 | 9.8 | 10 | 10.5 | 11.1 | 14.3 | 9.5 | 10.8 |
| Zambezi 10 | 10.5 | 12.3 | 11.1 | 8.9 | 9.2 | 9.6 | 10.9 | 10.9 | 13.5 | 16.2 | 10.8 | 11.6 |
| Zambezi 8 | 8.9 | 9.2 | 9.6 | 10.9 | 10.9 | 13.5 | 16.2 | 10.8 | 11.6 | 10.5 | 12.3 | 11.1 |
| Kafue 4 | 10.6 | 11.2 | 11.2 | 10.2 | 9.7 | 10.4 | 12.0 | 11.5 | 13.0 | 14.3 | 11.5 | 11.1 |
| Zambezi 5 | 10.4 | 10.8 | 10.8 | 9.9 | 9.4 | 10.2 | 11.5 | 10.9 | 13.0 | 14.5 | 11.3 | 11.4 |
| Luangwa 1 | 4.1 | 5.1 | 5.8 | 4.4 | 3.3 | 3.9 | 7.4 | 7.8 | 7.5 | 7.5 | 7.0 | 5.9 |
| Zambezi 4 | 7.5 | 8.3 | 8.6 | 7.8 | 7.3 | 7.7 | 8.2 | 7.9 | 8.8 | 10.0 | 8.2 | 7.7 |
| Shire | 10.1 | 11.3 | 11.3 | 10.0 | 9.3 | 9.6 | 11.0 | 10.4 | 13 | 14.7 | 12.7 | 11.7 |
| Mazowe | 9.1 | 10.7 | 9.9 | 9.3 | 8.8 | 8.8 | 9.9 | 9.5 | 12.6 | 13.8 | 11.7 | 11.0 |
| Average | 9.2 | 10.1 | 10.1 | 9.1 | 8.7 | 9.4 | 10.9 | 10.2 | 11.7 | 13 | 10.6 | 10.3 |

8.3 Future scenarios of change in rainfall

This section assesses the changes in rainfall in the Zambezi basin by the 2050s. The changes are examined based on the percentage differences between the downscaled and bias corrected future rainfall and the historical rainfall (1961-2000).

Bias corrected and historical mean monthly rainfall distributions representing example sub-basins are presented in Figure 8.4. The results show that seasonality is largely preserved and there are no indications of a shift to an earlier or later wet season. The GFDL model, however, seems to suggest a change from a unimodal type of rainfall in which there is one peak rain period (around January) to a bimodal rainfall pattern whereby two peak rainfall periods (January and March) will be experienced within the wet season for the upstream catchments such as Kabompo, Luena, and areas around Lake Malawi. This could be related to the topographic set up of an area where it is possible that there might be fluctuations in the prevailing winds especially in high relief areas. It is possible that this deviation may also be a result of the bias correction approach and limitations of the square root transformation method. Comparing the three GCMs, the IPSL model predicts large changes in the peak (December to February) rainfall distribution amounts. Basin-wide the seasonal changes in precipitation are more pronounced for the wet season months of December to April and there is almost no notable change throughout the dry season (May to September).

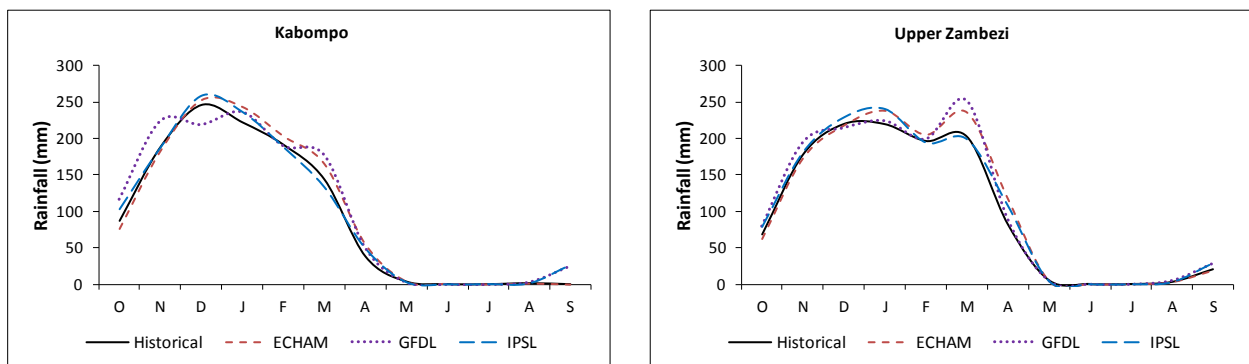


Figure 8.4a Seasonal distributions of monthly rainfall for the historical (1961-2000) and bias corrected near future (2046-2065) rainfall in example sub-basins

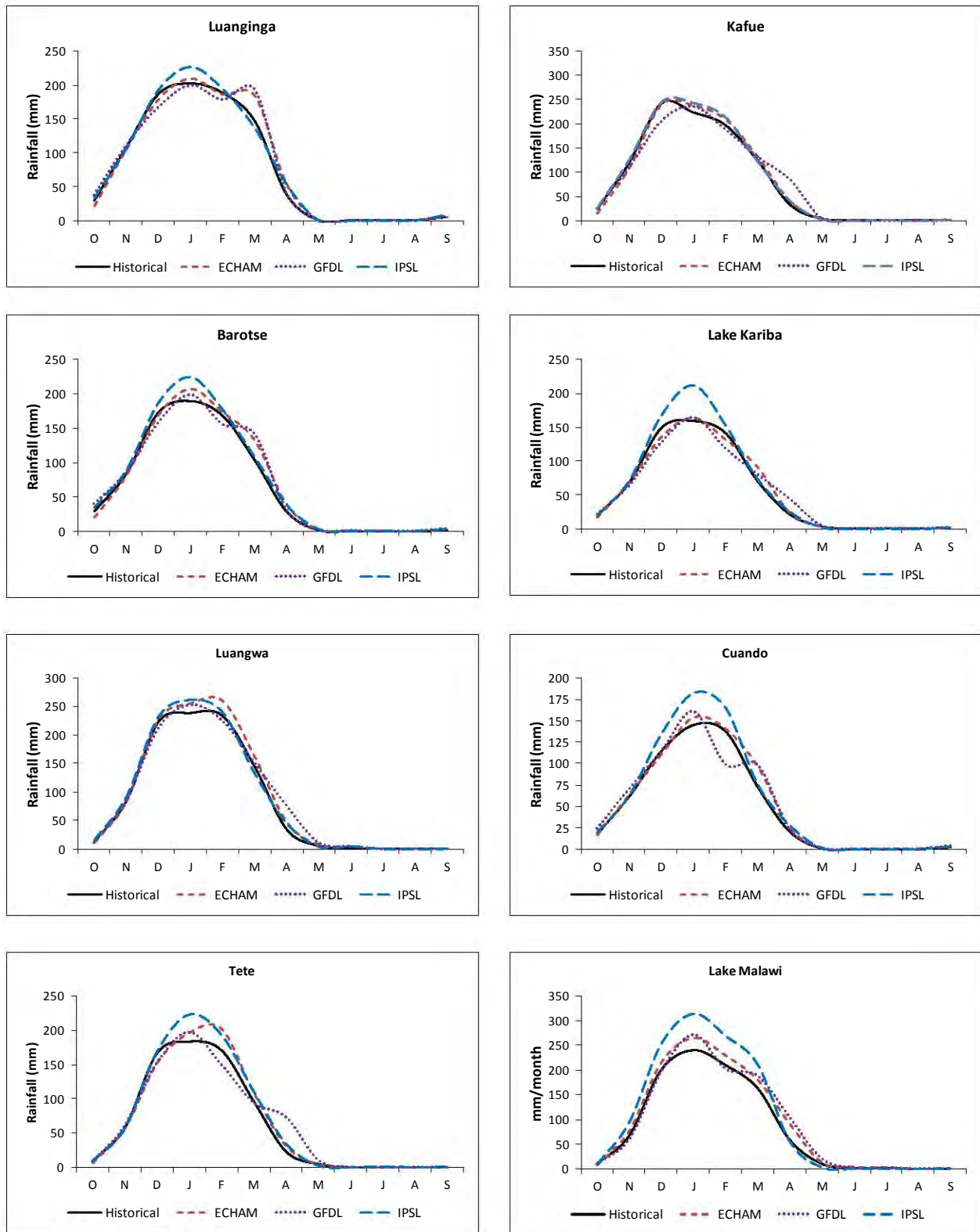


Figure 8.4b Seasonal distributions of monthly rainfall for the historical (1961-2000) and bias corrected near future (2046-2065) rainfall in example sub-basins

The changes in magnitude and frequency of occurrence of rainfall in response to climate change and with respect to the historical rainfall are reported in Figures 8.5 and 8.6. All three GCM predictions indicate no substantial changes in the near future rainfall although there is a distinct variation in the very high rainfall events particularly for the ECHAM model (Figure 8.6). The predicted changes deviate from the historical rainfall by amounts in the range of -2 to 10%, only the GFDL model predicts a change slightly above 10% for Luena (the most upstream sub-basin).

Generally there is no consensus between the three GCMs as to the direction of change of the future rainfall with respect to the historical baseline conditions of the various sub-basins in the Zambezi. Using the example sub-basins, predictions by ECHAM range from -0.3 to 5% and the IPSL model predicts changes in the range of 2 to 6.5%. The GFDL model records the largest increase with changes in the range of -0.5 to 12%. Even though the dry season rainfall is projected to increase, the increases are still very close to the zero line (no rainfall) which characterises the historical pattern of the dry season in the Zambezi basin. In real terms, these increases are negligible and do not contribute to the overall changes in rainfall across the basin. Overall there is a high variation in the future rainfall changes between sub-basins and between seasons and this may be an indication of climatic variability within the Zambezi basin. A regional overview of the predicted changes in annual rainfall in the Zambezi basin is presented in Figure 8.7. A general classification is assigned to the different categories of change in rainfall by the 2050s. According to INGC (2009), climate change is categorised as marginal if the change is within $\pm 10\%$, a moderate change is expected for both increasing and decreasing rainfall if the respective changes are between ± 10 and $\pm 25\%$. The changes are considerable if the decrease is $\leq -25\%$ or the increase is $\geq 25\%$. The same classification has been adopted in this study. One classification map is presented as the predicted changes for all the GCMs fall within the same ranges but the specific magnitudes of change are different for each sub-basin and for each GCM. Minor changes in annual rainfall ranging between -10% and 10% are predicted for the larger part of the basin while moderate changes are projected for some areas.

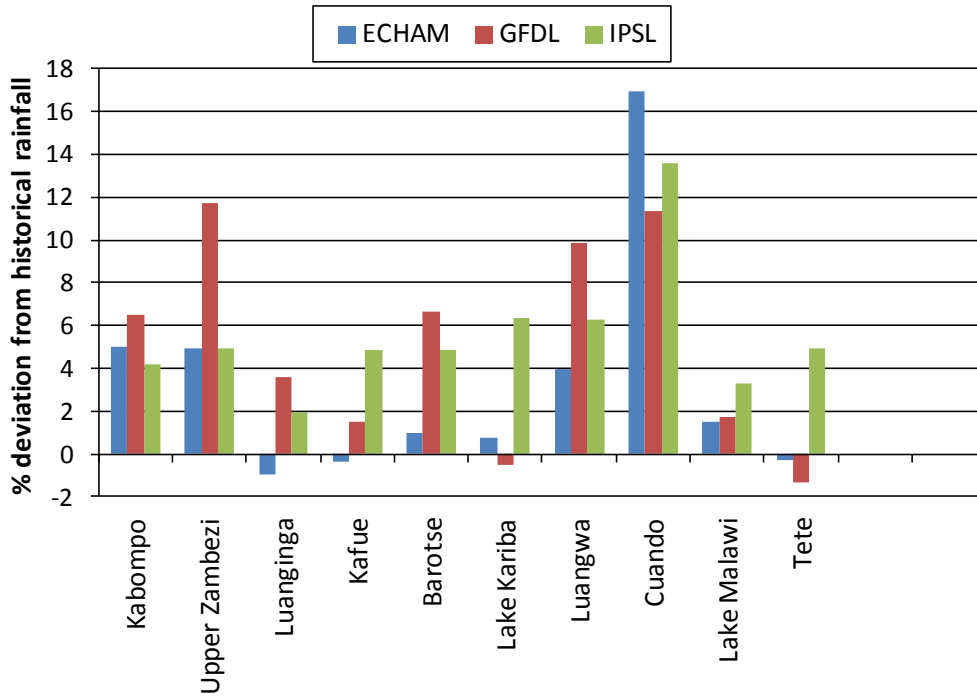


Figure 8.5 Near future changes in mean monthly rainfall relative to the historical rainfall

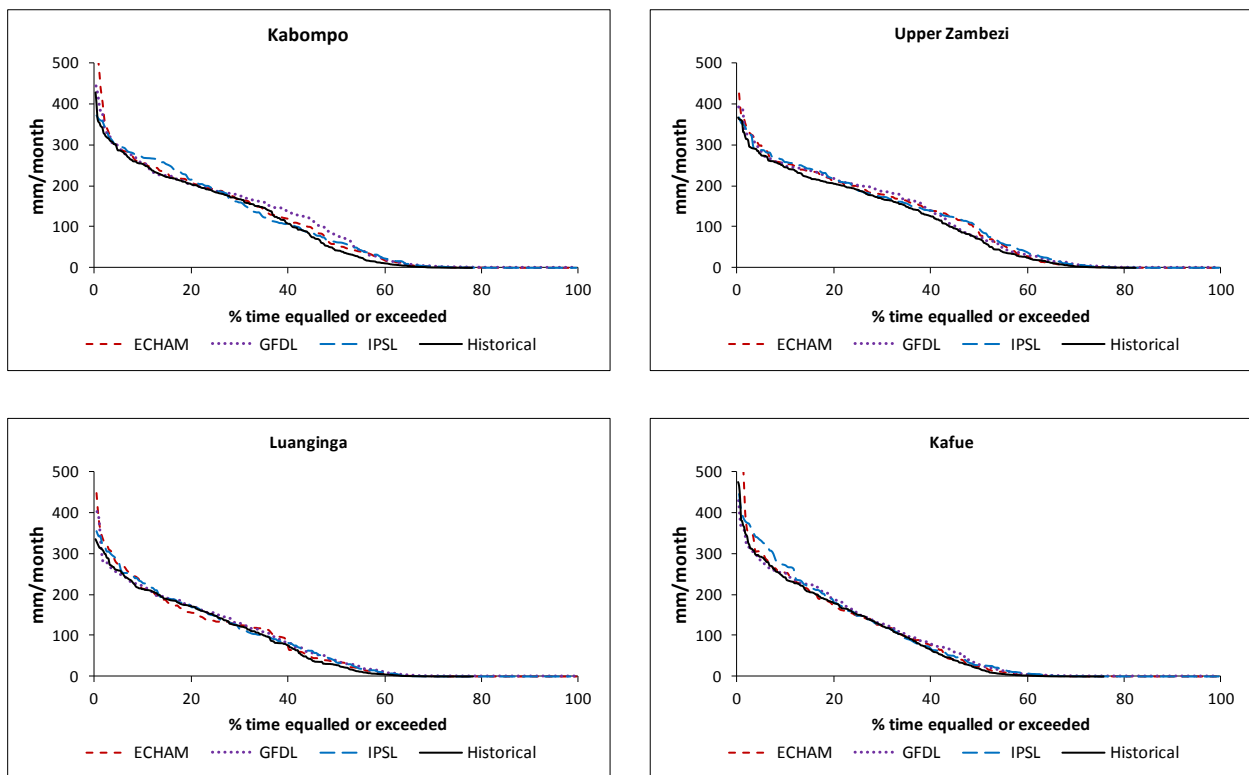


Figure 8.6a Predicted changes in long term mean monthly rainfall in the Zambezi River basin

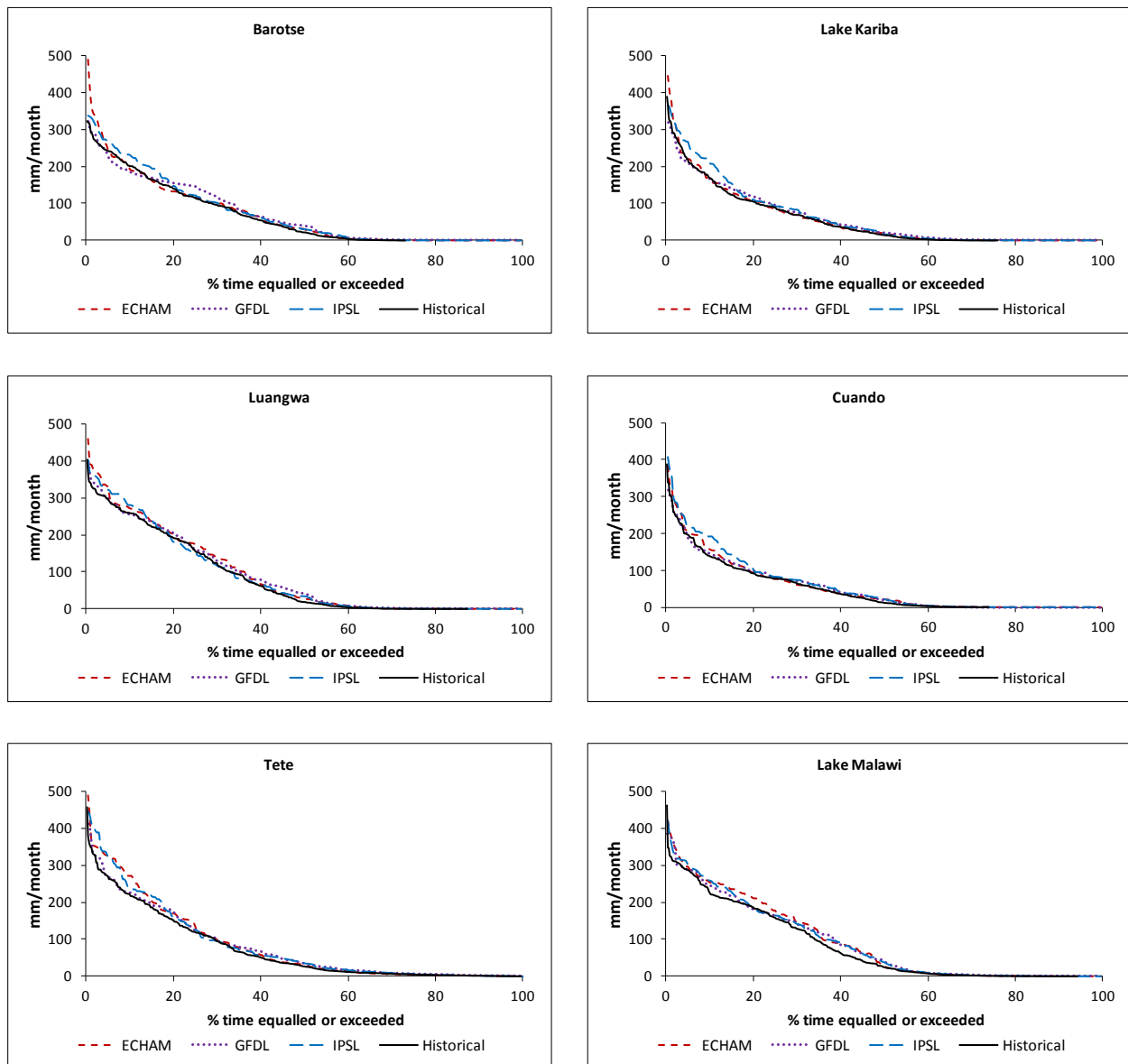


Figure 8.6b Predicted changes in long term mean monthly rainfall in the Zambezi River basin

8.4 Hydrological impacts of climate change (2046-2065)

Changes in rainfall, soil moisture and evaporation as a result of changing climates can have significant impacts on the catchment runoff (Schulze, 2005). As a basis for managing water resources in the future it is important to account for the changes in runoff as these have a direct bearing on the basin's water supply. This section quantifies the hydrological responses of the Zambezi basin to the near future scenarios of climate change. The impacts of human activities

(e.g. landuse changes) have not been considered as part of this study and therefore the assessment is only based on the effects of the GCM scenarios. Streamflow and soil moisture are simulated by forcing the calibrated Pitman model (see Chapter 6) with the spatially downscaled and bias corrected rainfall and potential evapotranspiration outputs of the ECHAM, GFDL and IPSL models. The climate change impacts are assessed based on the simulated streamflow mainly at gauged catchments along the mainstream (see Figure 6.3) and on simulated soil moisture storage. Two versions of the Pitman model are employed in this part of the study. First the ordinary version of the model (Hughes et al., 2006) which uses a single set of calibrated basin parameters is used to simulate and quantify the near future hydrological conditions of the Zambezi basin. Based on the simulated streamflow and soil moisture, the future changes are assessed relative to the historical conditions. It is acknowledged that there are various uncertainties associated with the hydrological model of which the key uncertainties arise from input data, model structure and model parameterisation (Hughes et al., 2011b). These uncertainties are inherently transferred to the climate change signal when a hydrological model is used to assess the basin's response to climate change. Added to the hydrological model uncertainties are uncertainties arising from the GCM such as the nature of the greenhouse gas emissions, methods used to downscale the GCM, the bias correction for the baseline and the choice of the GCM. An attempt is made in this study to examine the uncertainties arising from both the hydrological model and the GCMs. The calibrated hydrological model together with the optimum uncertainty parameter ranges assigned in the initial calibration process (Chapter 6) are forced with the bias corrected GCM outputs of rainfall and potential evapotranspiration and the uncertainty version of the Pitman model is applied to generate an ensemble of future climates. The uncertainties arising from hydrological modelling and from the GCMs are assessed based on the envelopes of uncertainty generated from the uncertainty version of the Pitman model.

8.4.1 Changes in streamflow

The predicted changes in streamflows by the 2050s based on magnitude, duration and frequency of occurrence and using example catchments are illustrated in Figure 8.7. Overall there are some notable changes in the high flow events while the low flow events are expected to be less impacted by the changes in climate. In most cases the low flows are very similar in magnitude to the historical flow conditions; the only exception is the Kabompo where the historical low flow

conditions are expected to be reduced in the near future. Changes in the monthly streamflow distribution amounts relative to the historical streamflows are shown in Figure 8.8. These changes are calculated as percent deviations of the long term mean monthly streamflow values of the future climate from the historical means.

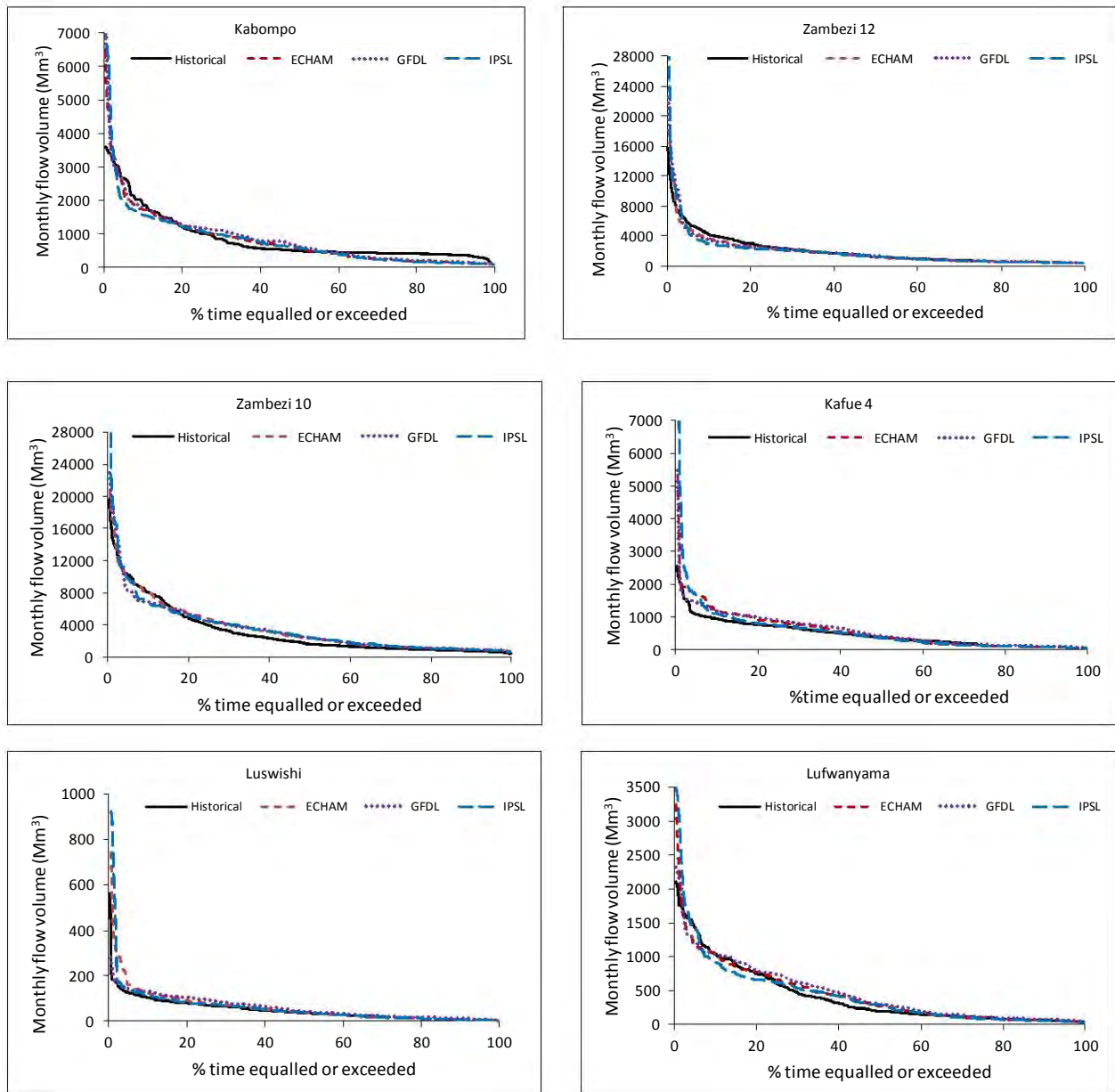


Figure 8.7a Flow duration curves for the historical and near future streamflows.

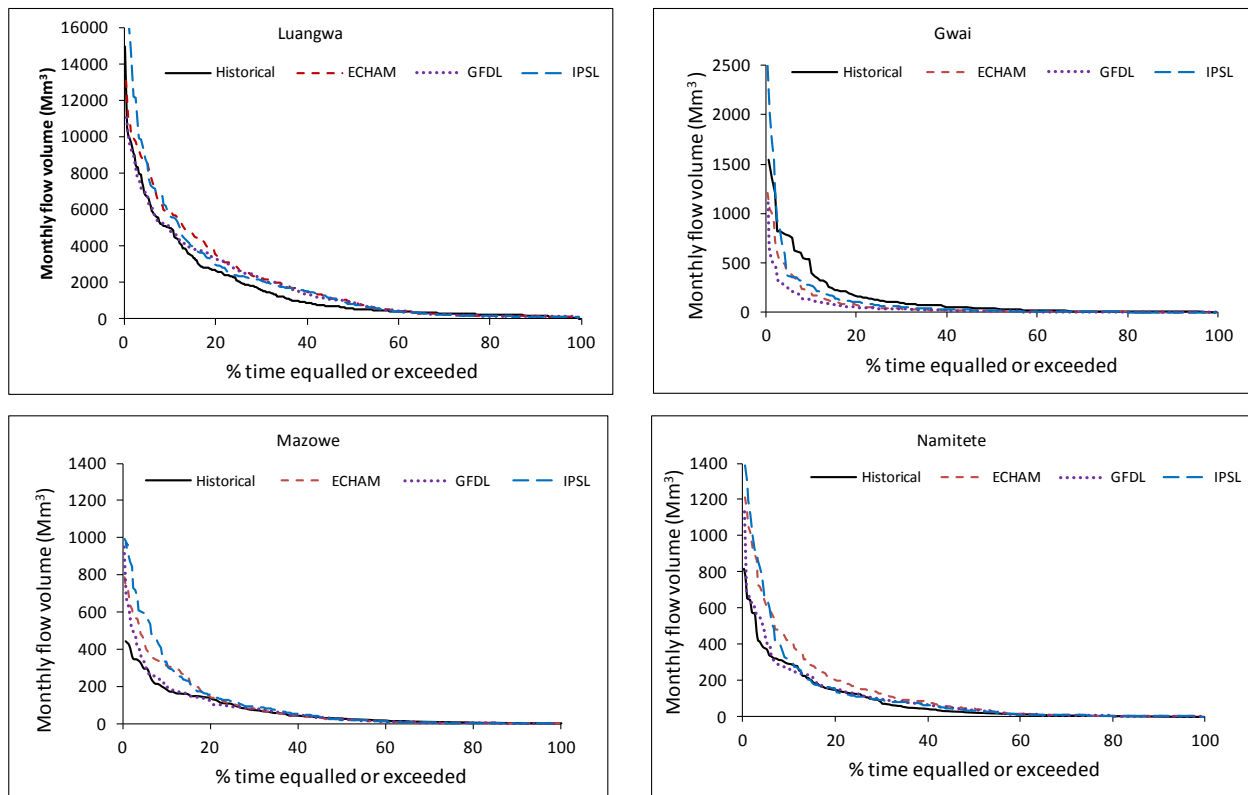


Figure 8.7b Flow duration curves for the historical and near future streamflows. (Case examples based on gauged catchments)

Mixed changes in streamflow are observed for the three GCM scenarios. For most of the upstream catchments (e.g. Kabompo and Zambezi 12) streamflow is expected to remain constant or to decrease from February to September, with slight increases between October and December for Zambezi 12 and between December and January for Kabompo. For the Kafue (Kafue 4, Lufwanyama and Luswishi) and the Luangwa some notable increases are expected between May and June while changes in the remaining months are minimal. No changes are expected in streamflow for the months January to March in the Barotse while for the Gwai catchment some marked increases are predicted between April and July. The Gwai catchment is one of the most arid areas in the basin and therefore any changes relative to the historical low flows tend to produce some high percentage increases while the actual contribution to annual flows is negligible. The dry conditions that characterise the basin also render the streamflows highly sensitive to changes in rainfall. Reduced streamflows are expected from July to December in the Mazowe and Namitete catchments and no substantial changes are expected for the remaining months except for January where changes greater than 50% are expected. Overall prolonged dry

conditions are expected in most parts of the basin. Future changes in the mean annual streamflow for some of the catchments are presented in Table 8.2. For all the catchments, except Gwai and for all GCMs, when averaged across the year, no considerable (<25%) changes are anticipated by the 2050s.

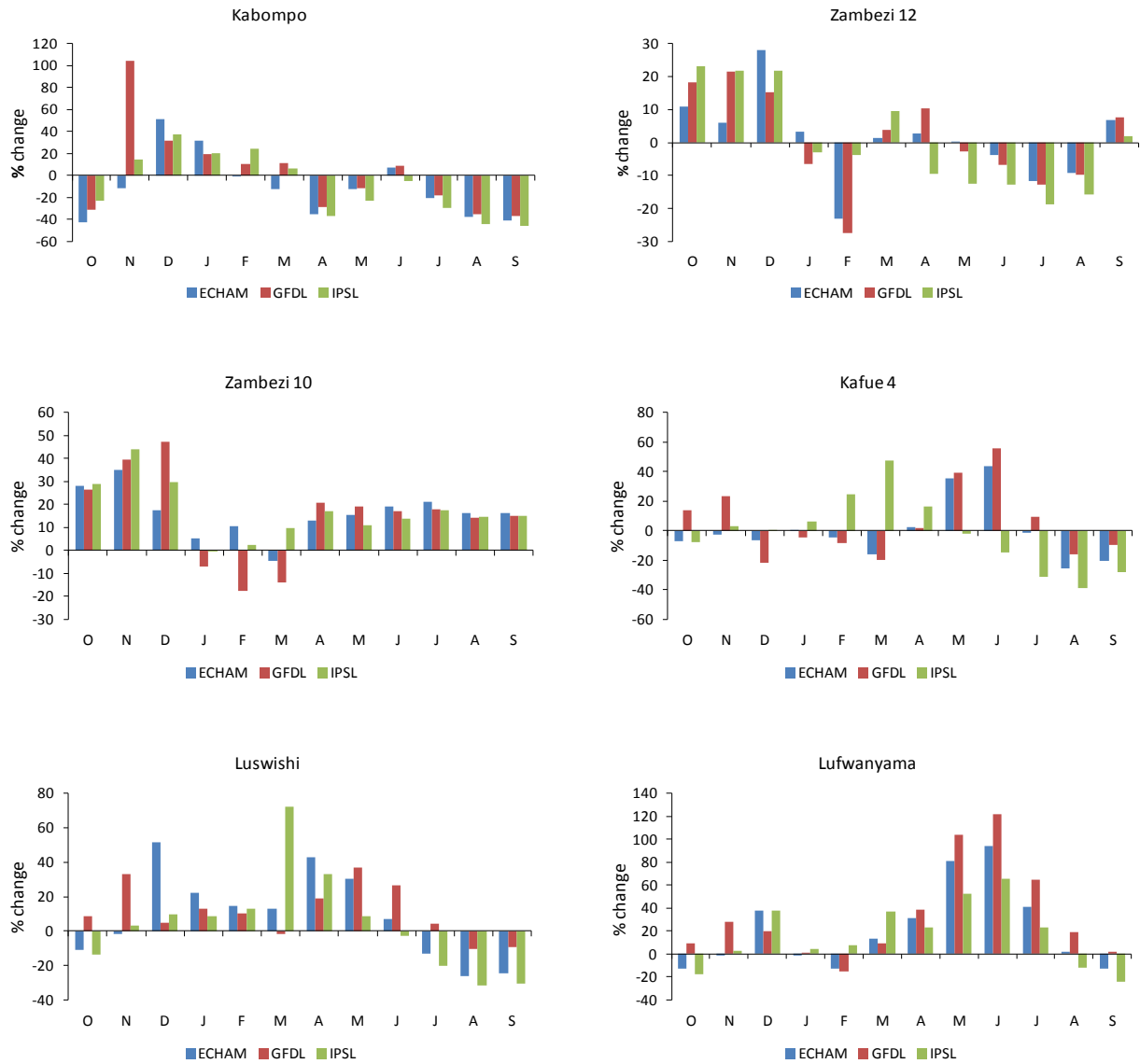


Figure 8.8a Future changes in streamflow relative to the historical flow

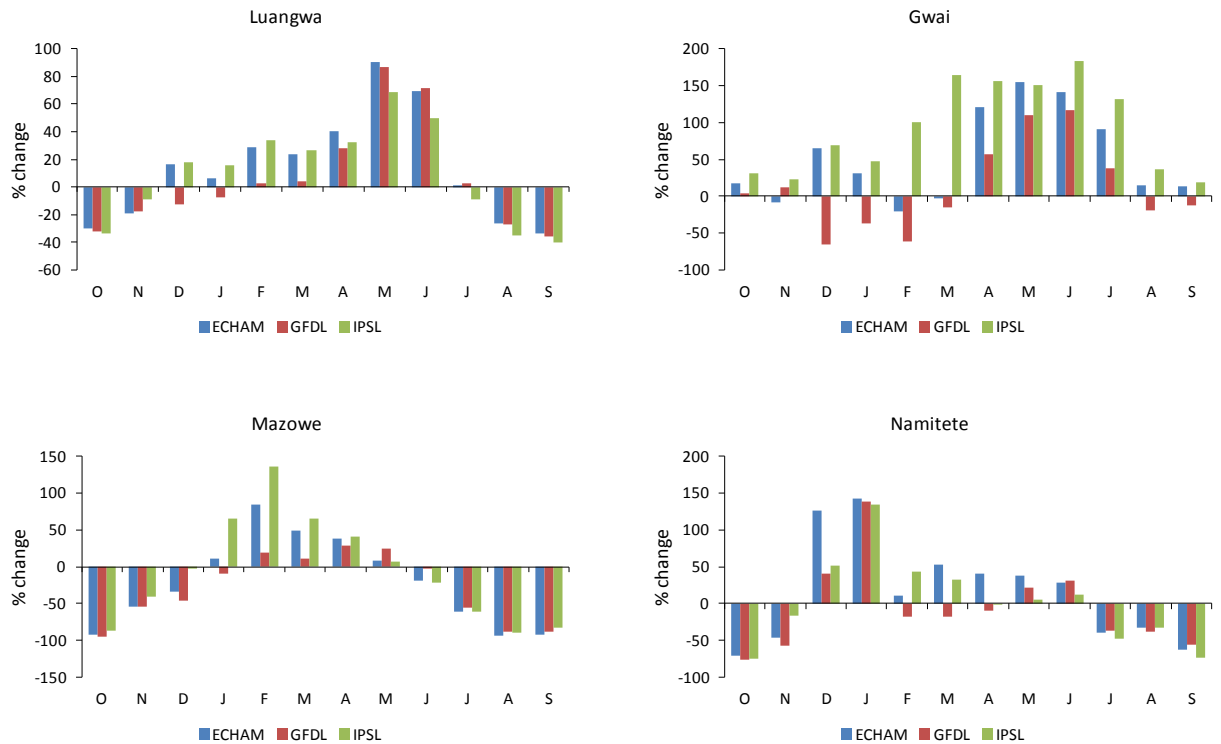


Figure 8.8b Future changes in streamflow relative to the historical flow

Table 8.2 Changes (%) in mean annual, 90th and 10th percentile streamflows with respect to the historical streamflows

| Catchment | ECHAM | | | GFDL | | | IPSL | | |
|------------|-------|------|-------|-------|-------|-------|------|------|-------|
| | MAR | 90% | 10% | MAR | 90% | 10% | MAR | 90% | 10% |
| Kabompo | -10.4 | 47.2 | 16.4 | 1.9 | 51.7 | 36.0 | -8.8 | 46.4 | 0.4 |
| Zambezi 12 | 0.9 | -1.0 | 10.4 | 0.9 | -48.8 | 27.3 | 0.1 | 6.0 | 3.6 |
| Zambezi 10 | 16.1 | 18.5 | 39.5 | 14.9 | 13.1 | 41.0 | 16.9 | 27.0 | 35.5 |
| Kafue 4 | -0.2 | 28.0 | 12.9 | 5.1 | 23.9 | 42.6 | -2.1 | 17.7 | 5.5 |
| Luswishi | 8.8 | 57.3 | 10.2 | 11.2 | 5.9 | 38.7 | 4.1 | 56.4 | 4.1 |
| Lufwanyama | 15.5 | 26.9 | -37.2 | 18.5 | 22.2 | -20.9 | 11.5 | 43.2 | -44.6 |
| Luangwa | 13.9 | 14.2 | 11.5 | 5.2 | -2.7 | 8.4 | 9.8 | 34.1 | -0.3 |
| Mazowe | -21.5 | 64.4 | -96.0 | -23.0 | 32.2 | -57.1 | -5.9 | 81.3 | -87.5 |
| Namitete | 15.4 | 82.1 | -23.1 | -6.7 | 23.3 | -29.2 | 2.4 | 86.1 | -33.8 |

8.4.2 Uncertainty in future climate change projections

A comparison of the uncertainties arising from hydrological model parameterisation and from the GCMs is presented in Figure 8.9. The assessment is illustrated by two example catchments,

Lufwanyama and Kafue 4, the results show the lower and upper uncertainty limits of the predicted streamflow and the envelopes bracket the possible streamflow outcomes.

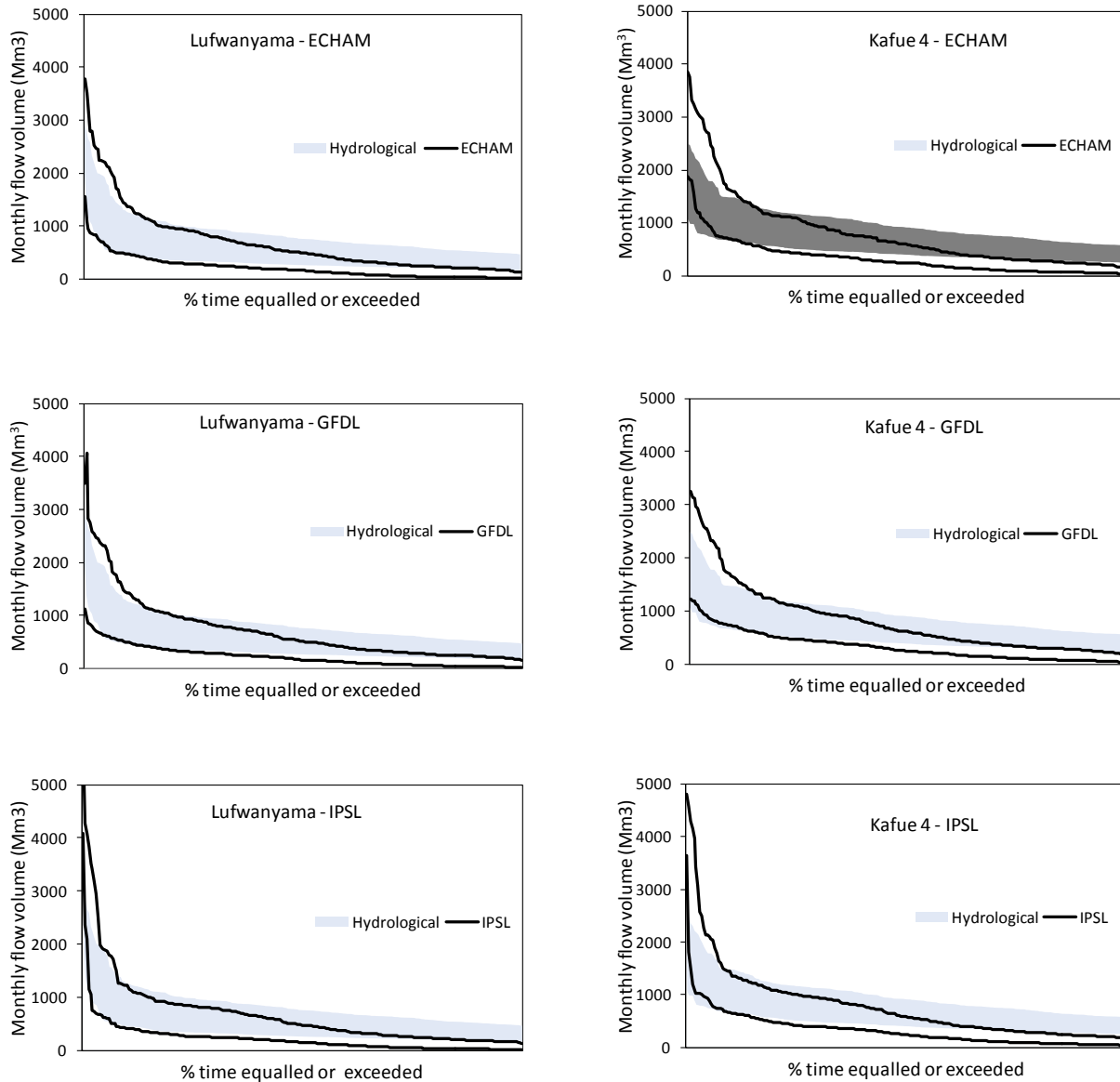


Figure 8.9 Comparison of the hydrological model parameter uncertainty and GCM uncertainty

There seems to be smaller uncertainty associated with estimating the low flow components of the flow duration curve and this uncertainty increases gradually towards the high flows for both the hydrological model and the GCM uncertainty bands. At the same time hydrological model uncertainty is shown to be higher than the GCM uncertainty at low to medium flows while the

GCM uncertainty envelope is much bigger for the high flow components of the duration curve. Comparing the uncertainties between the different GCMs there is not much difference in the magnitude of uncertainty for the low to the moderately high flows but there is a marked variation at extremely high flows where the GFDL model presents larger uncertainties compared to ECHAM and IPSL. This observation can be attributed to the larger bias observed in the GFDL rainfall change especially during March.

8.5 Changes in soil moisture storage

Soil moisture conditions for both the historical and the near future conditions are simulated using the calibrated Pitman model. The impacts of climate change are assessed through the percent deviation of the mean monthly future conditions of soil moisture from the historical mean conditions. The wet season soil moisture conditions are expected to increase while a decline is anticipated during the dry season in the near future period. These observations are reported in Figure 8.10. For all the GCM predictions, irrespective of the magnitude of change, the wet season extending from October to May is predicted to have increased soil moisture storage. The dry winter season, made up of the months of June, July, August and September is likely to experience declining soil moisture conditions. The future changes are, however, expected to vary temporally and spatially, reflecting the variable nature of the basin's water resources. Generally the high rainfall and upstream areas of the basin (e.g. Kabompo and Luanginga) are predicted to have smaller increases (up to 5% on average) in the wet season soil moisture and decreases of up to 5% in the dry season compared to the areas that are further downstream. This may be attributed to the fact that soils in the upstream areas have high absorption capacities in addition to the prevailing high rainfall conditions. On average it is expected from all the GCMs that the Zambezi basin may experience increases of 5% to 15% in wet season soil moisture and decreases of 5% to 40% during the dry season.

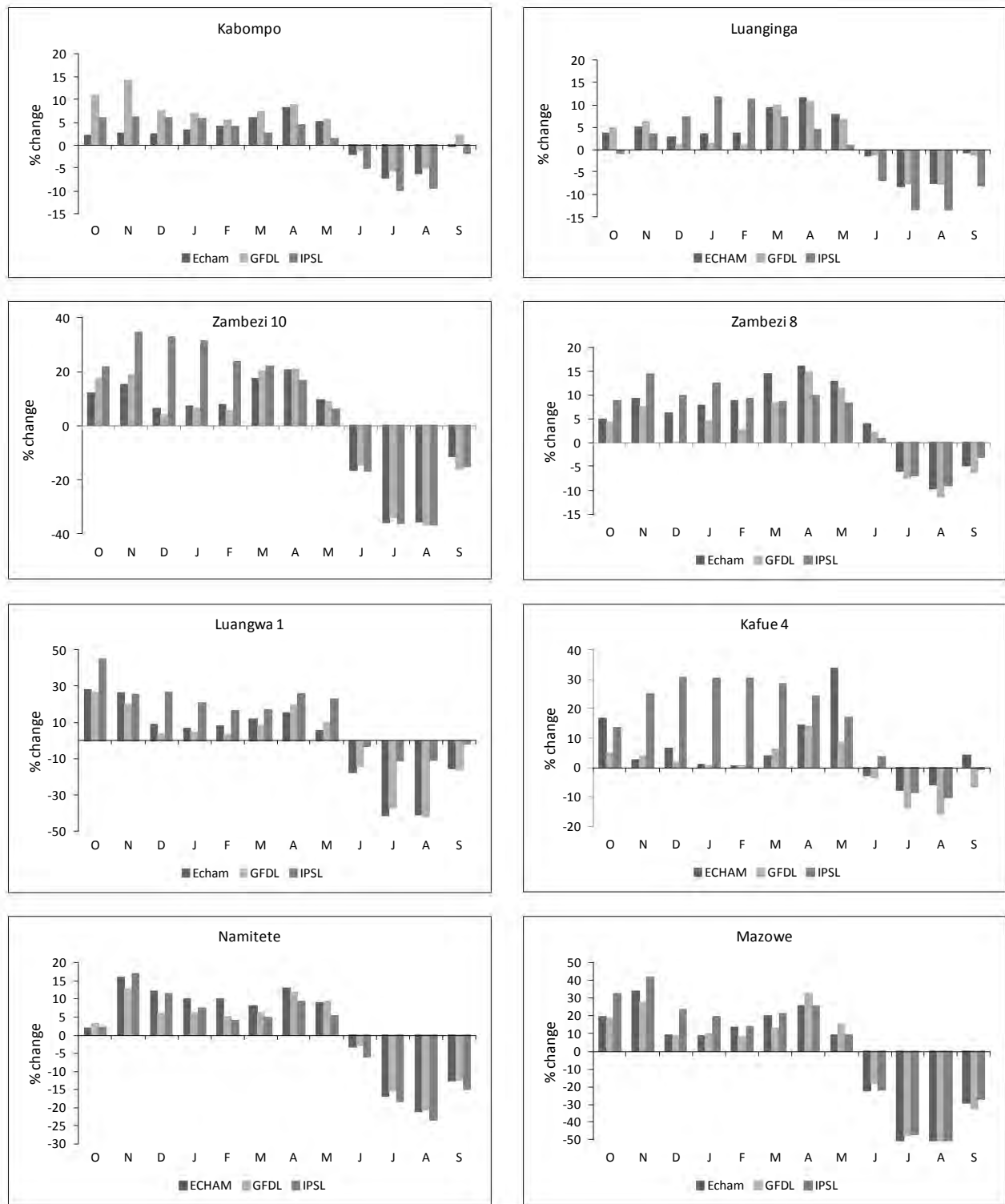


Figure 8.10 Changes in soil moisture relative to historical conditions

8.6 Extreme drought events

The Standardised Precipitation Index (SPI) is used to assess the historical and future drought conditions in the Zambezi River basin. The historical droughts are derived from the CRU rainfall for the period 1961-2000 and future droughts are generated from the bias corrected precipitation of the three GCMs for the period 2046-2065. Catchment averaged rainfall is applied in all cases. In the African context, droughts are normally measured by the state of agricultural produce for a particular year and this study therefore focuses mainly on agricultural droughts whose SPI is generated at three-month time scales. In the Zambezi basin the agricultural season extends from October (when sufficient soil moisture has accumulated after the onset of the rains) to March. Two three-monthly time scales of October, November, December (OND) for the planting season and January, February, March (JFM) for the growing season are used. Both the time scales coincide with the rain season in the Zambezi basin. For assessment, dry conditions are indicated by negative SPI (≤ -0.99) and wet conditions occur when the SPI ≥ 0.99 . The SPIs generated from the near future rainfall conditions are illustrated in Figures 8.11 a-c.

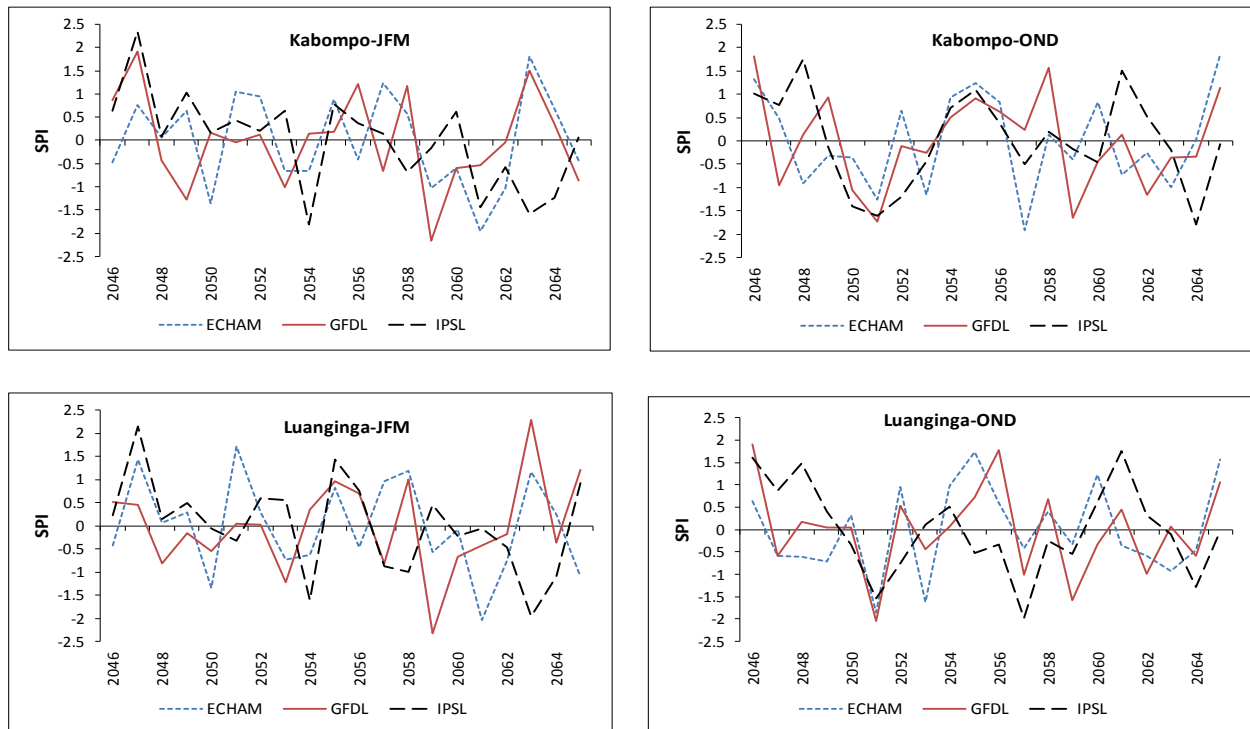


Figure 8.11a Predicted JFM and OND SPIs for 2046-2065

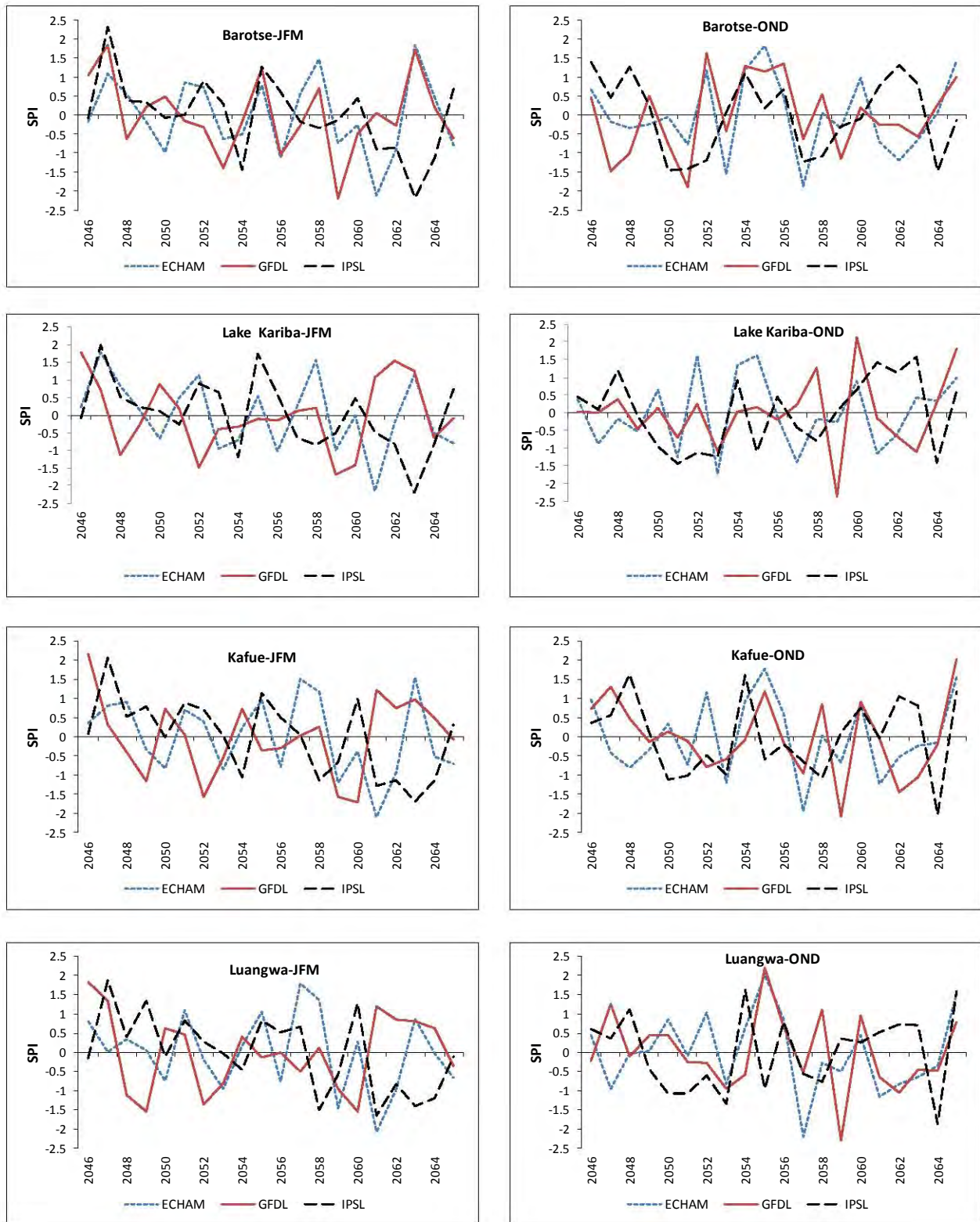


Figure 8.11b Predicted JFM and OND SPIs for 2046-2065

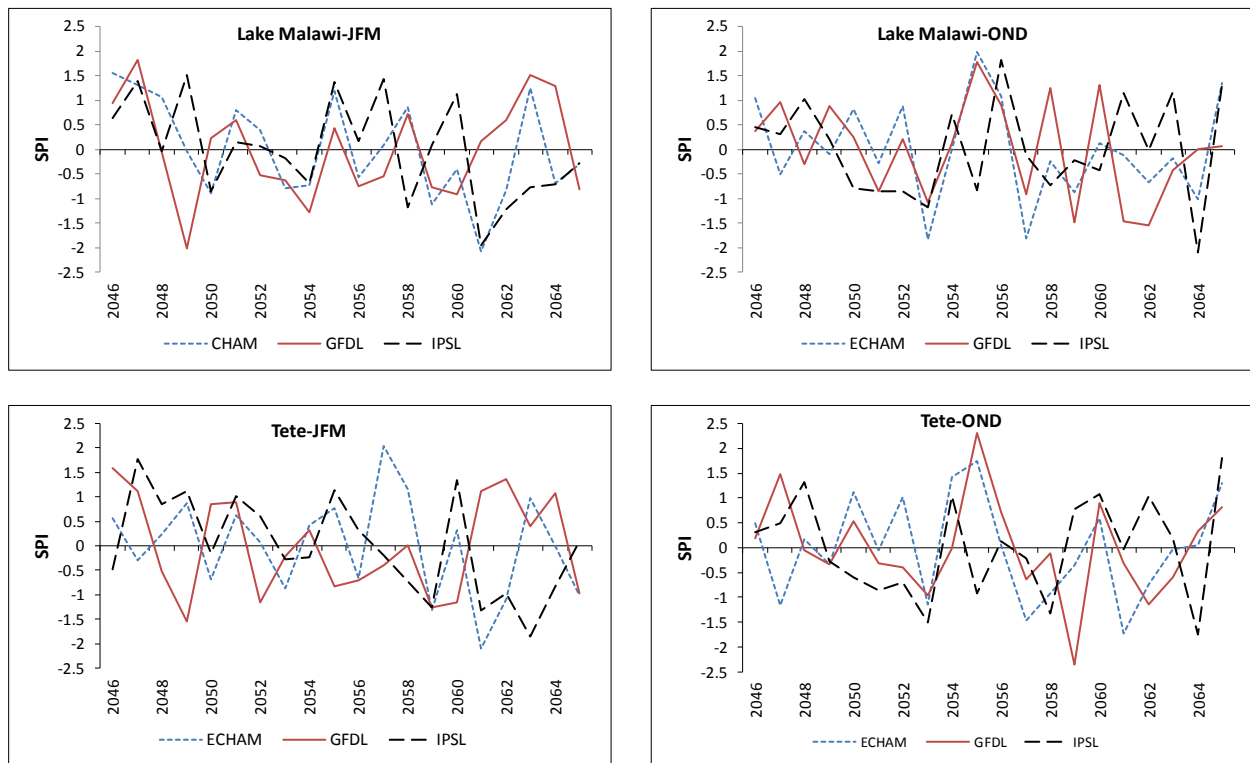


Figure 78.11c Predicted JFM and OND SPIs for 2046-2065

To determine the frequency of occurrence and severity of droughts in the future the number of drought events in each of the time scales (OND and JFM) is compared to the historical droughts. The frequency and severity of occurrence of future drought events is assessed and presented in Figures 8.12a-b. The severities are classified as, N: normal, MD: moderately dry, MW: moderately wet, SD: severely dry, VW, very wet, ED: extremely dry, EW: extremely wet. Using the example cases, the prevalence of normal conditions is expected to rise on average by a range of $\pm 20\%$ and to occur at least 70% of the times in the near future. Moderate and severely dry conditions are generally simulated to increase but only by small margins that may not exceed 10%. For the Kabompo sub-basin, the ECHAM and IPSL models predict moderate to severely dry conditions to increase slightly while a decrease is simulated by the GFDL model. For Luanginga, the only notable change is a slight increase in the moderately dry conditions. For the Barotse and Victoria Falls, slight increases are expected only in the extreme droughts. In the Kafue basin, severe and moderate drought conditions are expected to increase by up to 10%. An observable change for the Luangwa is an expected increase of 5-10% in moderately dry conditions.

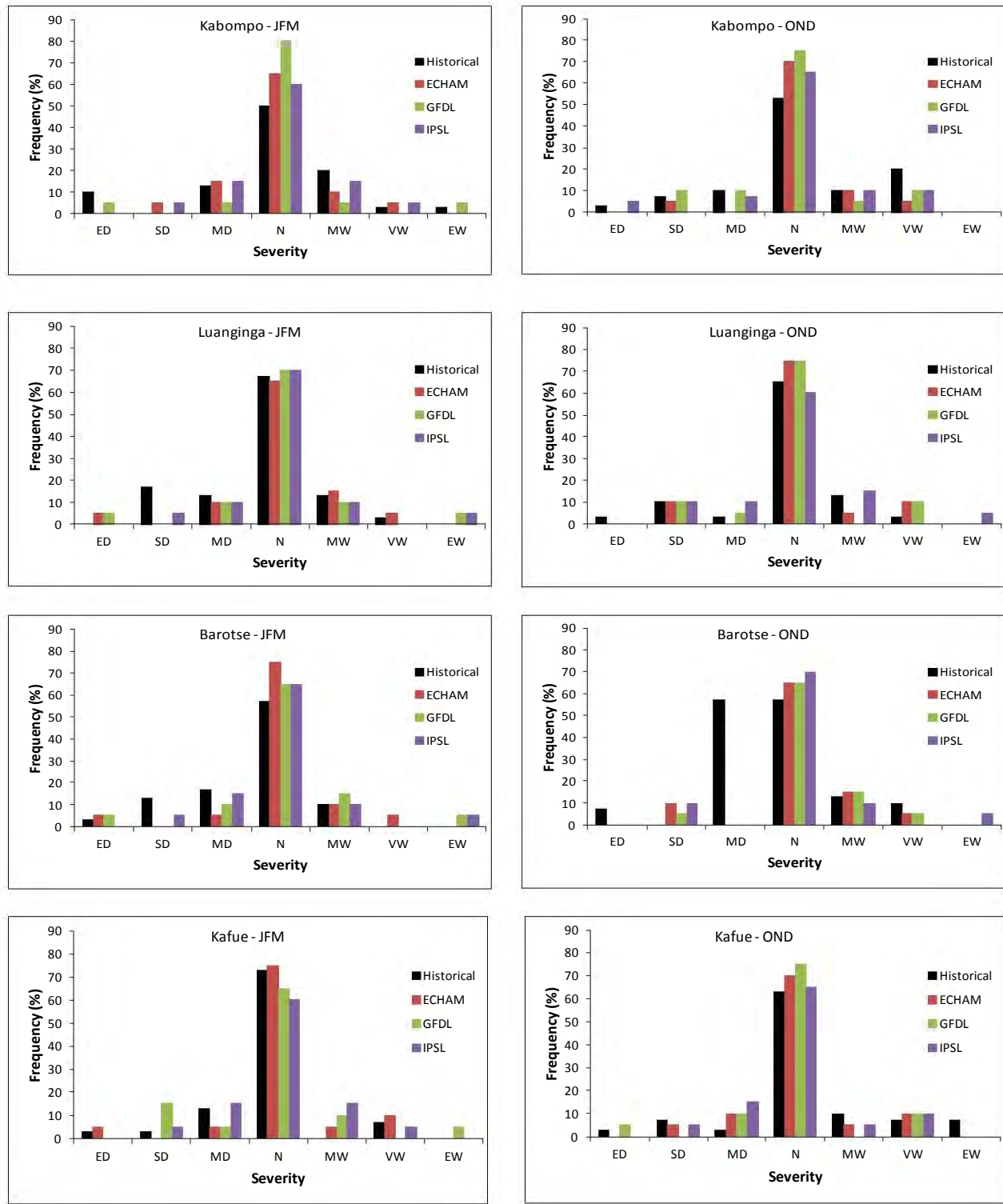


Figure 8.12a Frequency and severity of droughts for the near future seasons, JFM and OND

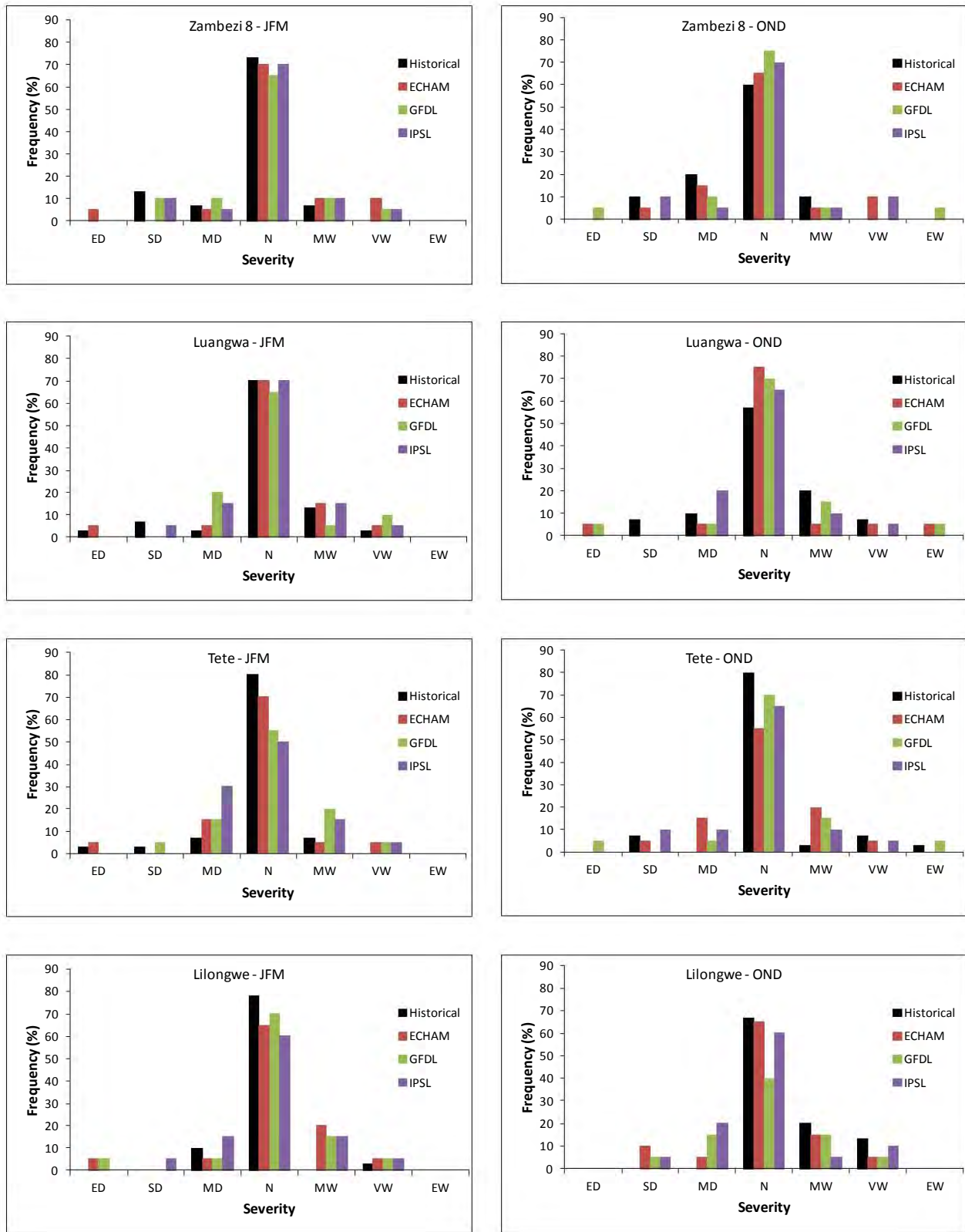


Figure 8.12b Frequency and severity of droughts for the near future seasons, JFM and OND

Conditions in Tete and in the Lilongwe sub-basin are expected to shift from normal, through a decrease of 10-20%, and this decrease is transferred to a 5-10% increase in the moderate to extremely dry conditions. It has been observed that normal conditions are likely to prevail 70% of the times in the near future, likewise, the soil moisture content is expected to remain in the normal ranges 70% of the time since a strong correlation was established between SPI and soil moisture. The implication of such soil moisture conditions is that they may be able to sustain the basin's crop yields thereby preventing the occurrence of agricultural droughts. However, extra precaution would need to be taken to introduce other agricultural methods that may boost the yields particularly in view of the fact that the basin's needs change from time to time (e.g. due to increasing population).

8.7 Climate change and climate variability

It is important to establish whether future changes in climate will be influenced by interannual variability or by the impact of anthropogenic climate change. Adopting the method of Jung et al. (2012), the signal to noise ratio (S/N) for streamflow is evaluated in order to perform the assessment. S/N is calculated (Jung and Kunstmann, 2007) as:

$$S/N = \frac{|\bar{X}_{future} - \bar{X}_{historical}|}{\sigma}$$

where, \bar{X}_{future} and $\bar{X}_{historical}$ are the mean monthly or annual values of the predicted future streamflows and the historically observed streamflows respectively and σ is the mean of standard deviations of the historical and future mean monthly or annual streamflows. The predicted changes are expected to be a result of anthropogenic impacts or increased variability if, $S/N > 1$, and if $S/N < 1$ the changes are assumed to lie within the historical range of variability. This assessment only considers the signal to noise ratio for the long term mean monthly streamflows and the results are presented in Table 8.3.

Table 8.3 Climate variability and climate change: signal to noise ratio for streamflow

| ECHAM | | | | | | | | | | | | |
|--------------|-------------|-------------|-------------|-------------|-------------|-------------|-------------|-------------|-------------|-------------|-------------|-------------|
| Sub-basin | Oct | Nov | Dec | Jan | Feb | Mar | Apr | May | Jun | Jul | Aug | Sep |
| Kabompo | 0.17 | 0.13 | 0.25 | 0.51 | 0.54 | 0.53 | 0.66 | 0.68 | 0.30 | 0.36 | 0.72 | 0.39 |
| Zambezi 12 | 0.46 | 0.18 | 0.33 | 0.06 | 0.50 | 0.02 | 0.05 | 0.01 | 0.14 | 0.50 | 0.43 | 0.33 |
| Luanginga | 0.86 | 0.73 | 2.44 | 1.58 | 0.74 | 0.53 | 0.70 | 0.88 | 0.82 | 0.92 | 1.67 | 1.99 |
| Barotse | 2.31 | 2.68 | 1.52 | 0.40 | 0.56 | 0.38 | 0.68 | 0.83 | 1.16 | 1.45 | 1.49 | 1.67 |
| Zambezi 8 | 1.50 | 1.96 | 2.34 | 1.13 | 0.63 | 0.55 | 0.56 | 0.66 | 0.79 | 0.98 | 1.23 | 1.40 |
| Gwai | 0.29 | 0.06 | 0.22 | 0.18 | 0.15 | 0.02 | 0.31 | 0.39 | 0.73 | 0.62 | 0.15 | 0.18 |
| Lufwanyama | 0.00 | 0.25 | 0.13 | 0.22 | 0.35 | 0.15 | 0.50 | 0.71 | 0.26 | 0.55 | 1.04 | 0.74 |
| Kafue 4 | 0.20 | 0.09 | 0.07 | 0.01 | 0.13 | 0.33 | 0.05 | 0.68 | 0.67 | 0.03 | 0.70 | 0.63 |
| Luswishi | 0.28 | 0.04 | 0.32 | 0.30 | 0.27 | 0.13 | 0.40 | 0.45 | 0.16 | 0.33 | 0.72 | 0.68 |
| Luangwa | 2.44 | 0.91 | 0.17 | 0.09 | 0.56 | 0.47 | 0.93 | 2.05 | 1.60 | 0.04 | 1.20 | 2.15 |
| Mazowe | 0.45 | 0.17 | 0.04 | 0.54 | 1.05 | 1.12 | 1.09 | 1.24 | 0.29 | 0.96 | 2.50 | 1.76 |
| Namitete | 1.16 | 0.10 | 0.63 | 0.75 | 0.25 | 0.63 | 0.51 | 0.11 | 0.94 | 2.06 | 1.11 | 1.03 |
| GFDL | | | | | | | | | | | | |
| Sub-basin | Oct | Nov | Dec | Jan | Feb | Mar | Apr | May | Jun | Jul | Aug | Sep |
| Kabompo | 0.20 | 0.69 | 0.15 | 0.41 | 0.71 | 0.62 | 0.75 | 0.85 | 0.40 | 0.30 | 0.65 | 0.19 |
| Zambezi 12 | 0.75 | 0.26 | 0.26 | 0.16 | 0.65 | 0.04 | 0.20 | 0.09 | 0.27 | 0.59 | 0.50 | 0.39 |
| Luanginga | 0.79 | 0.58 | 2.48 | 1.62 | 0.51 | 0.41 | 0.56 | 0.74 | 0.69 | 0.88 | 1.76 | 2.32 |
| Barotse | 2.49 | 2.04 | 1.44 | 0.32 | 0.08 | 0.18 | 0.76 | 0.91 | 1.20 | 1.48 | 1.57 | 1.78 |
| Zambezi 8 | 1.58 | 2.13 | 2.57 | 0.34 | 0.50 | 0.17 | 0.39 | 0.68 | 0.86 | 1.04 | 1.28 | 1.46 |
| Gwai | 0.07 | 0.07 | 0.45 | 0.31 | 0.51 | 0.11 | 0.40 | 0.77 | 0.84 | 0.40 | 0.31 | 0.21 |
| Lufwanyama | 0.81 | 1.07 | 0.01 | 0.29 | 0.31 | 0.10 | 0.65 | 1.10 | 0.71 | 0.08 | 0.58 | 0.26 |
| Kafue 4 | 0.43 | 0.66 | 0.31 | 0.10 | 0.28 | 0.45 | 0.04 | 0.89 | 1.00 | 0.22 | 0.49 | 0.31 |
| Luswishi | 0.22 | 0.63 | 0.05 | 0.24 | 0.26 | 0.03 | 0.35 | 0.80 | 0.61 | 0.11 | 0.29 | 0.27 |
| Luangwa | 2.74 | 0.67 | 0.17 | 0.14 | 0.06 | 0.09 | 0.75 | 2.28 | 1.75 | 0.10 | 1.31 | 2.43 |
| Mazowe | 0.91 | 0.14 | 0.11 | 0.37 | 0.35 | 0.55 | 0.86 | 1.34 | 0.67 | 0.69 | 2.34 | 1.21 |
| Namitete | 1.90 | 0.00 | 0.31 | 0.74 | 0.10 | 0.06 | 0.10 | 0.42 | 0.86 | 1.85 | 1.34 | 0.73 |
| IPSL | | | | | | | | | | | | |
| Sub-basin | Oct | Nov | Dec | Jan | Feb | Mar | Apr | May | Jun | Jul | Aug | Sep |
| Kabompo | 0.26 | 0.25 | 0.24 | 0.49 | 0.70 | 0.52 | 0.45 | 0.29 | 0.07 | 0.67 | 1.00 | 0.61 |
| Zambezi 12 | 0.60 | 0.51 | 0.40 | 0.08 | 0.06 | 0.10 | 0.19 | 0.43 | 0.47 | 0.79 | 0.73 | 0.08 |
| Luanginga | 2.03 | 2.47 | 1.99 | 1.23 | 0.99 | 0.51 | 0.54 | 0.69 | 0.66 | 0.79 | 1.48 | 2.72 |
| Barotse | 2.16 | 2.20 | 1.56 | 0.50 | 0.60 | 0.61 | 0.52 | 0.60 | 0.95 | 1.24 | 1.31 | 1.48 |
| Zambezi 8 | 1.41 | 1.85 | 2.15 | 1.46 | 0.79 | 0.66 | 0.62 | 0.57 | 0.59 | 0.75 | 0.93 | 1.22 |
| Gwai | 0.36 | 0.13 | 0.29 | 0.30 | 0.24 | 0.22 | 0.22 | 0.48 | 0.80 | 0.71 | 0.29 | 0.22 |
| Lufwanyama | 0.18 | 0.36 | 0.20 | 0.38 | 0.63 | 0.32 | 0.30 | 0.24 | 0.20 | 0.98 | 1.45 | 1.15 |
| Kafue 4 | 0.23 | 0.10 | 0.01 | 0.13 | 0.43 | 0.37 | 0.24 | 0.06 | 0.43 | 1.03 | 1.30 | 0.87 |
| Luswishi | 0.36 | 0.08 | 0.13 | 0.18 | 0.30 | 0.38 | 0.33 | 0.19 | 0.07 | 0.53 | 0.90 | 0.88 |
| Luangwa | 2.68 | 0.26 | 0.24 | 0.22 | 0.47 | 0.37 | 0.60 | 1.59 | 1.18 | 0.31 | 1.60 | 2.56 |
| Mazowe | 0.04 | 0.39 | 0.38 | 0.93 | 1.21 | 0.98 | 0.98 | 1.30 | 0.24 | 0.97 | 2.70 | 0.81 |
| Namitete | 1.73 | 0.29 | 0.53 | 0.63 | 0.39 | 0.37 | 0.03 | 0.81 | 1.34 | 2.45 | 1.07 | 1.48 |

For all the three models, the predicted changes across the Zambezi basin are expected to lie within the historical range of variability ($S/N < 1$) at least 80% of the time in the near future. Exceptions include Luanginga, Barotse and Zambezi 8 sub-basins where, generally the months of July to January exhibit values of $S/N > 1$. These sub-basins are directly connected with Luanginga upstream of the Barotse and the Barotse upstream of Zambezi 8 in the western part of the Zambezi basin. The observation may be an indication of the differences in the geophysical properties and of the attenuation of streamflow that characterises this part of the basin (see Chapter 6). The Luangwa is also made up of a marked gradation in topography from the upstream to the downstream areas and this may also be a cause of the high signal to noise ratio in this drainage area. Based on the fact that a larger part of the basin is expected to experience changes influenced by natural variability it is highly probable that the few observations of high S/N ratio may be due to increased variability rather than anthropogenic climate change. The Mazowe sub-basin also exhibits some high S/N values but mainly for the dry season months, this signal may not be significant since the sub-basin is virtually dry during the dry season.

8.8 Discussion and conclusion

This study gives insight into the hydrological responses of the Zambezi basin to future changes in climate. The predicted changes in the hydroclimatic variables of the Zambezi basin by the 2050s are discussed. Some biases were observed in the GCM rainfall baselines with respect to the historical CRU rainfall (1961-2000). Bias correction using the square root transformation approach was applied in order to obtain a rainfall pattern which would produce a realistic hydrological change signal when the GCM outputs are transferred to the hydrological model. Most of the bias was removed for the three GCMs except that the month of March proved to be problematic for the GFDL model. The results indicate that the bias correction approach has an influence on the results as evidenced by the larger bias for the GFDL prediction. An example is the Luena sub-basin where, the predicted changes in rainfall are 11.7% for GFDL, 4.90% for ECHAM and 4.92% for IPSL. There is no consensus among the GCMs on the direction of change in precipitation in the Zambezi basin. The timing of the seasons is expected to remain the same in the near future and overall no substantial changes in rainfall are expected across the basin. These findings suggest no evidence of any marked impacts of climate change on rainfall or that the changes are too small compared to the basin's natural variability.

The three GCMs predict that conditions in the Zambezi basin will become warmer resulting in a postulated accelerated potential evapotranspiration rate. Unlike the mixed direction of change in rainfall, unidirectional increases in potential evapotranspiration are predicted in the entire basin and these changes are of a similar range of magnitude for all the GCMs. Nonetheless, there is some degree of uncertainty in the projected changes as the potential evapotranspiration estimates are only derived from temperature without giving due consideration to the other key driving variables which include vapour pressure, net radiation and wind speed (Rosenberg et al, 1989). Contrary to the GCM projections that evaporative demand increases due to increased temperatures, some studies carried out in the northern hemisphere and in southern Africa (e.g. Roderick and Farquhar, 2005; Hoffman et al., 2011) reveal a decrease in the pan evaporation rates with increasing temperature. This is attributed to decreased wind speed and reduced solar radiation at the earth's surface as well as increased cloud cover and aerosol concentrations in the atmosphere (Eamus and Palmer, 2004). These findings imply that there may be many uncertainties if the predictions are only based on changes in temperature.

All the GCMs predicted a general but marginal increase in the high flow components of the flow duration curves, while the dry season flows are simulated to decrease slightly or to remain relatively constant. Predictions of the seasonal streamflows are mixed in direction suggesting that they may be uncertain. Although rainfall is predicted to increase, the small margin of change in streamflow is a result of increases in potential evapotranspiration which happen to be higher than the changes in rainfall. Assessing climate variability versus climate change, the results suggest that the predicted changes are minimal and will most likely fall within the historical range of variability.

It was observed in this study that there are significant uncertainties in the hydrological predictions of the basin's response to climate change. These uncertainties are attributed to both hydrological modelling and the GCM model uncertainty. In terms of the hydrological model uncertainty, input data were identified as one of the major sources of uncertainty. Over and above the input data uncertainty is the model structural uncertainty which arises mainly from the applied process descriptions and from the distribution of inputs in the model. In addition, the Pitman model uses a monthly time step which may be too coarse in view of solving agricultural issues where, lack of rainfall within a period of a day or a week may have drastic impacts on the

development of a crop. Lack of knowledge of how the future will be like in terms of greenhouse gas emissions and poor understanding of the climate system in response to these emissions are some of the sources of GCM uncertainties. These uncertainties have resulted in some GCMs simulating a region's climate better than others (Xu et al., 2011) and differences were apparent in the projections derived from the three GCMs used in this study. Some limitations may also arise from the manner in which the GCM data are processed starting from downscaling to the bias removal approach used in this study. Like most of the climate change impact studies, an 'offline' simulation which relies on transferring the climate change signal from the GCM to the hydrological model was used. Such an approach can introduce some uncertainties in the prediction of hydrological change in the future. Furthermore, GCMs are not as good at predicting precipitation as they are at predicting temperature (Solomon et al., 2007).

Soil moisture content is generally predicted to increase during the wet season and to decrease in the dry season. The expected decreases can be attributed to the projected increases in temperature and evapotranspiration. In the upstream areas such as the Kabompo and Luena, high rainfall amounts and the high absorption capacity of the soils make it possible to quickly attain the soil moisture storage capacity which allows a larger interflow. The differences in magnitude of change between the various sub-basins can also be linked to the different soil types that predominate in each area. High temporal fluctuations were observed in the SPI time series for the period extending from 2046 to 2065 and these fluctuations which are an indication of climatic variability in the basin, seem to override the expected increase in the frequency of occurrence of the drought events within the same period. It is concluded that variability in rainfall will still assume a major role in the future. The signal to noise ratio between the historical and near future streamflows also confirms that future changes will fall within the historical range of variability. Given the high dependence of the basin population on rainfed agriculture, there is need to minimise the threats of climate variability and change to agriculture and food security. If variability persists, it will continue to complicate the prediction process which is very crucial in determining whether there will be dry or wet conditions in the seasons that follow, thereby making it difficult for plans to be made when considering the agricultural season. Effort should be increased in assessing the variabilities through improved data sources and such assessments

should be an ongoing process that is aimed at informing the prediction process towards reducing the basin vulnerabilities.

This study has generated some preliminary estimates of the effects of future changes in climate on water resources in the Zambezi basin. Overall the research findings indicate a warmer basin climate and a generally increasing trend in precipitation but only with slight changes in the basin streamflows by the 2050s. The results also indicate increased normal conditions and the possibility of a lower frequency of occurrence of severe to extreme drought events. The study also reveals that there is a high degree of uncertainty around the magnitude and direction of change of the basin's hydrological responses to future GCM scenarios and this makes it difficult to evaluate the effectiveness of the simulated results. One unique feature of this study is that an attempt has been made to assess the changes at the sub-basin scale unlike the large scale global projections that were made by some of the previous studies (e.g. Arnell, 1999). Simulating the changes at sub-basin scales ensures that most of the detail pertaining to hydrological change is captured and this is very important especially in large basins that are characterised by high variability in climate and in physical basin properties. Obtaining information at local scales is very important since most of the water resource problems are encountered at local scales and it is therefore important to provide sub-basin specific information which can assist in bringing forward interventions that are unique to the sub-basin. There is, however, a large range of uncertainty in the quantitative prediction of the basin's hydrological responses and the results obtained in this study should therefore be taken as indicators of trends of change in the future and not as precise amounts of the real changes. It is concluded in general that the predicted impacts of climate change will be minimal in the near future and that the hydrological conditions are likely to remain within the historical range of variability.

CHAPTER 9 CONCLUSION AND RECOMMENDATIONS

9.1 Introduction

In contrast to other studies which focus on hydropower dams along the main river of the Zambezi, the focus of this study was to assess the basin's hydrological responses to climate variability and change at the sub-basin scale.

The availability of water resources and how they are managed has significant impacts on society and the economy. Water resources are already under pressure from increasing demand due to development, population growth and competing interests among the basin countries. Climate variability which tends to occur at different spatial and temporal scales in large basins such as the Zambezi is recognized as one of the drivers to the availability of water. It is also a major constraint to water resources management. Conclusions of this study postulate that this variability will persist into the future resulting in continued pressure on water resources and will continue to impact negatively on the livelihoods of the basin population. Protecting the basin population from the adverse impacts of climate variability and change on water resources requires good understanding of climatic fluctuations and their drivers as well as hydrological processes in relation to water resources management. It is also important to understand variability and climate change at different temporal and spatial scales within the basin as this will allow effective and local specific adaptation solutions. Appropriate predictions and early warning signals are also required that will allow adequate and timely adaptation strategies and prevent the risk of making wrong decisions that are based on insufficient information. This can only be possible provided there are enough data (in terms of quality and quantity) and analysis tools to assess the historical hydroclimatic events upon which the future predictions can be made. There is also need for decision support systems which enable the estimation of future water resources and allow sharing of knowledge and effective communication among stakeholders.

9.2 Data issues and decision support tools

Managing water resources revolves around quantifying and allocating water for various uses in addition to building water resources infrastructure. For this to be possible large amounts of accurate and relevant data that are of a scale appropriate to the area being addressed, together

with information describing the data must be readily available and easily accessible. The question remains whether there are enough data and analysis tools that are appropriate to the problem of defining climate variability and change with respect to water resources. The Zambezi basin is limited in climate and hydrological data, the major challenge being the sparseness of observed data, missing values and short hydrological records. This problem is worsened by deteriorating gauging networks, reduced budgets and most likely the lack of adequate monitoring capacity within the national hydrological agencies. The Zambezi Water Information System (ZAMWIS), a web-based and information systems portal for the Zambezi basin is purportedly in place but was difficult to access at the time this study was conducted. The Southern African Development Community Hydrological Cycle Observing System (SADC HYCOS) is another potential source of data for the Zambezi basin but regrettably there are many formalities that have to be addressed (largely unsuccessful) before one can access the data. Due to these limitations and in order to meet the set objectives, this study resorted to the use of global data sets, which ironically are easier to access compared to the local data (from local water authorities). Global data sets have an advantage of having more detailed spatial and temporal coverage and the CRU TS2.1 rainfall grids were therefore used for the greater part of this study. In addition to hydroclimatic data, it is important to have knowledge of the water uses and developments particularly in the upstream areas of the basin as these assist in adequately quantifying the basin runoff and assessing the downstream impacts. However, there seems to be inadequate knowledge of the specific water demands and their location in the basin.

It is also crucial to have in place data analysis and management tools that are appropriate to the effective management of water resources. To assess the patterns of variability, a range of statistical methods starting from the simplest regression to more complex approaches such as the Mann Kendall and Fourier spectral analysis were employed in this study. In order to create a holistic and integrated approach to the management of water resources, water resources management tools are required which enable estimation and allocation of the predicted water resources. According to Loucks et al. (2005), *“Decision-makers don’t know what they want until they know what they can get. And how do modellers know what decision-makers will need before even they do? Also how will modellers know what is the right amount of information, especially if they are to have that information available, and in the proper form, before or at the time, not*

after, it is needed?” Clearly modellers can only have answers provided a decision making framework is available to accommodate interactive modelling and provide some display technologies and data analysis facilities that can be easily understood and interpreted. A variety of software packages are available for decision support in water resources management.

Most of the assessments carried out to meet the objectives of this study were facilitated through the data storage, data processing and analysis and the modelling facilities provided in SPATSIM. This software package is intended to provide a user friendly platform for managing and processing data in addition to running different hydrological models (Hughes and Forsyth, 2006). Its robustness is demonstrated through the various applications performed in this study which included data storage, generating areal averaged rainfall through inverse distance weighting, generating regional drought maps through the rendering facility, converting the massive daily GCM rainfall data sets to monthly data for use with the Pitman model, performing the bias correction for rainfall and potential evaporation, running the hydrological model (both the ordinary and uncertainty versions) and finally providing a TSOF platform to graphically view (e.g. time series, scatter plots, flow duration curves and seasonal distributions) and statistically analyse the modelling results.

9.3 Variability and its implications for droughts and food security

It is widely acknowledged that the measurement of climate and hydrological variables is important for monitoring changes in climate as they are related to water resources and for input into predictive models. Understanding variability will help interpret and give meaning to the observed measurements which can then be used to inform future water resource plans. While there is some evidence in the literature to indicate high interannual and interdecadal variability in rainfall and streamflow in the basin, this evidence is based on very coarse assessments of the basin and only a few studies have focused on the spatial and temporal variability at a more detailed sub-basin scale. Adopting a sub-basin response to the management of water resources in the context of climate variability implies that potential adaptation options should also be made at the sub-basin scale. This study derives its strength from the assessment of changes in various sub-basins rather than focusing on a globalised overview of the basin. The results showed marked annual and interdecadal climate variability to be an intrinsic feature of the basin while at

the same time having significant consequences for the management of the basin's water resources. This variability is postulated to persist into the future. Due to data limitations, the available data are not capable of representing the full extent of natural variability making it difficult to predict the return period of extreme hydrological events, however, it is still important to recognize this variability as it enables risk assessment for such extremes. Understanding and quantifying this variability can inform the design and management of water resources in the future while reliable predictions can be used to formulate adaptive strategies that can reduce the risk of climatic impacts on water resources.

The series of recurrent droughts that have occurred in the basin over the last century have largely been a consequence of high levels of variability in rainfall and streamflow events. These droughts have caused a lot of suffering amongst the basin population whose majority depend entirely on rainfed agriculture as their main source of livelihood. The drought of 1991/1992, for example, is reported to be the most severe drought in the Zambezi basin during the 20th century, resulting in a 45% decrease in cereal production (FAO, 2004). It has been shown in this study that rainfall is the major constraint to agricultural yield in the basin. The postulated persistence of variability in the near future is likely to pose negative impacts on the basin's food security. While practicing optimal water use may be beneficial, timely monitoring and prediction of the occurrence of droughts will result in improved water and food security. Many indices are available to monitor droughts and the SPI has advantages over other indices in that it is simple with low data requirements and can represent different time scales depending on the user's choice. It can be used effectively to monitor droughts by indicating their onset, magnitude and severity but its weakness is that it relies on rainfall as the only input variable and it does not adequately represent the agricultural droughts. Although the generation of a soil moisture based agricultural drought index is more cumbersome, this study shows that the index is a better indicator for agricultural drought. Observations made during the study indicate that climate and hydrology are not the only drivers to the basin's food security but there are other drivers which may be influenced by policy and the prevailing political environment.

9.4 Modelling the hydrological impacts of climate change

The importance of water in the socio-economic development of the Zambezi basin justifies the need to understand how changes in the global climate will impact the availability and reliability of water resources. Predictions show that future changes in streamflows are likely to remain within the historically observed ranges of variability but there is no clear indication as to how or by how much these changes will occur. This implies that future water resources management should be planned in light of the continued variability and under greater uncertainty conditions. In a basin where there is already an imperfect fit between water demand and the available water resources (Manabe et al., 2004) and where no marked increases are expected in the amount of water available, it is inevitable that socioeconomic development and a growing basin population will result in increased water demand and increased pressure on the water resource.

Clearly, any model prediction in hydrology is uncertain but it should also be emphasised that there are many uncertainties in GCM predictions. Uncertainty arises from limited knowledge of the global climatic processes and their feedbacks, the choice of the GCM, the downscaling techniques used in reducing the GCM scale to match the regional scale, the bias-correction approaches used in trying to match the GCM rainfall baseline with the historically observed rainfall and the manner in which the transformed data are transferred to the hydrological model. These uncertainties make it difficult to obtain reliable estimates of the future climates. It is important for water resource plans to acknowledge these uncertainties in the context of historical variability. Because of the uncertainty associated with the future predictions, it is emphasised that the results given in this study do not provide the exact estimates of change in water supply in the future, but only an approximate indication of what the future trend is likely to be and may therefore be used as a guide to the future management of water resources in the Zambezi basin.

9.5 Recommendations

This section gives some suggestions and recommendations to improve water resources research and to better inform water resources management in the Zambezi basin.

To produce more certain results there is need to improve monitoring and data collection and to ensure that the monitoring networks are consistently maintained and that well trained people are

in place to monitor the results. Since ZAMWIS and SADC HYCOS (and others not mentioned here) are already operational, with the responsibility of being repositories of climate and hydrological data for the Zambezi basin and the southern African region at large, it is suggested that such organisations should continuously update the climate and hydrological records and that they should make the data readily available, especially for uses that are intended to improve the management of water resources. To address some of the data limitations, it is worth exploring the use of satellite data in conjunction with the gauged data. In order to obtain a comprehensive basin-wide assessment of the basin's hydrological responses, effort should also be made to produce detailed information on water related developments in the basin such as land use and land changes as well as various water demands.

Responses to climate variability in the past have been reactive and in view of the predicted variabilities, this approach is at risk of being inadequate. It becomes necessary to consider the implementation of well-timed and appropriate adaption strategies. Necessary adaptation measures do not only rely on structural designs but also on accurate predictions and early warning systems that will safeguard against the adverse impacts of climate variability. To avoid regretful decisions means of improving the predictions and reducing the uncertainties should also be explored while a better understanding of how climate variability and change will affect the water resources is still needed.

In this study the patterns of variability were assessed based on rainfall, it is recommended that in addition to rainfall trends, variability be assessed against other biophysical drivers such as the ENSO events that are also well known to influence the climate of the basin. Given that there is no strong evidence to suggest any marked changes in rainfall and streamflow and in view of the fact that the predicted changes will mostly lie within the historical range of variability, it would be reasonable to base the future plans on the historically observed variability provided that appropriate data and analysis tools are available to assess the variability. Most of the analyses are premised on long term changes and impacts but it was observed in this study that although there are long term cycles of variability in rainfall and streamflow, there are strong fluctuations within the cycles such that dry periods persist within a wet cycle and vice versa. These short term fluctuations suggest the need for improved variability predictions based on short to medium term forecasts, particularly where rainfed agriculture is the major activity and where the adaptation

strategies are needed to address the real issues on the ground (especially for the local subsistence farmers). It is therefore emphasised that it is not only the skill of the forecasting tools that matters but also the implications of the decisions made from the forecasts.

Over the past century the Zambezi basin has been subjected to a series of droughts with significant impacts on the rural-based population. This is a clear indication of the vulnerability of the basin's water resources and food security to climatic anomalies. Preventing such negative impacts from recurring in the future calls for a well informed predictive system which takes into consideration the hydrological and agricultural dynamics of the basin. It is recommended that agricultural authorities should also promote drought resistant crops to avert the impacts of droughts on the basin's food security. This study only focused on drought as one of the climatic hazards that can impact a region's food security. Since floods and cyclones are among some of the aggravating factors it is recommended for further studies to also consider the impacts of these hazardous events. Cooperation between water institutions, governments and other stakeholder communities is, however, required to ensure that vulnerabilities are minimised. So far in southern Africa programmes such as FEWS, FEWSnet and DEWFORA have been implemented to ensure timely early warning forecasts, but these can only be successful provided there is co-ordinated cooperation among the stakeholders. It is also recommended that agricultural authorities should also promote drought resistant crops to avert the impacts of droughts on the basin's food security. This study only focused on drought as one of the climatic hazards that can impact a region's food security. Since floods and cyclones are among some of the aggravating factors it is recommended for further studies to also consider the impacts of these hazardous events.

It is clear that uncertainty will continue to pose a threat to the basin's water management plans since it is quite difficult to tell when, where and by how much the water resources will respond to a variable and changing climate. If this uncertainty is not addressed, it is likely to constrain the adaptation strategies resulting in adverse impacts on socioeconomic livelihoods and the environment. It is crucial therefore that uncertainty be acknowledged and incorporated into the water resources management and methods of making decisions based on the uncertainties should be identified. This will ensure a 'no regrets' (Todd et al., 2010) situation whereby a range of likely outcomes are generated upon which the water resource plans and adaptation strategies can

be made. This range of possibilities will avert a situation whereby incorrect decisions are made based on a single outcome whose prediction may be in variation with the manner in which the future climate may unfold. For holistic and sustainable water resource management strategies it is recommended that future research efforts be focussed on the impacts of climate change on water quality, the various socio-economic attributes and the environment in general.

9.6 Conclusion

A preliminary attempt has been made to contribute to the prediction of climate variability and climate change on the hydrology of the Zambezi River basin. It is concluded from this study that what is important is to incorporate variability and to manage uncertainty in planning for the basin's future water resources. This implies sustained efforts to reduce the risks of climate variability and change while maintaining flexible management options that are able to deal with the extremes of both low and high hydrological events. Finally, it is recognized that the potential impacts of climate variability and change are wide-ranging and this clearly calls for multi-disciplinary approaches towards appropriate adaptation strategies, especially for a basin where there are users with different interests.

REFERENCES

- Allen, R., Pereira L.S., Raes, D. and Smith, M., 1998. Crop evapotranspiration: guidelines for computing crop water requirements. FAO Irrigation and Drainage, Paper No. 56, Rome, Italy, 300 pp.
- Allen, R., Myles, R. and Ingram, W. J., 2002. Constraints on future changes in climate and the hydrologic cycle. *Nature*, 419 (6903), 224–232.
- Andersson, L., Wilk, J., Todd, M.C., Hughes, D.A., Earle, A., Kniveton, D., Layberry, R. and Savenije, H.H.G., 2006. Impact of climate change and development scenarios on flow patterns in the Okavango River. *J. Hydrol.*, 331, 43–57.
- Andreu, J., Capilla, J. and Sanchis, E., 1991. AQUATOOL. A computer assisted support system for water resources research management including conjunctive use. In: D.P. Loucks and J.R. da Costa (eds.), *Decision support systems*. Berlin, Springer-Verlag, 333–355.
- Ao, T., Ishidaira, H., Takeuchi, K., Kiem, A.S., Yoshitani, J., Fukami, K. and Magome, J., 2006. Relating BTOPMC model parameters to physical features of MOPEX basins. *J. Hydrol.*, 320(1-2), 84–102.
- Arnell, N.W., 1999. Climate change and global water resources. *Global Environ. Change*, 9, S31-S49.
- Arnell, N.W., 2011. Uncertainty in the relationship between climate forcing and hydrological response in UK catchments. *Hydrol. Earth Syst. Sci.*, 15, 897–912.
- Arnell, N. W., 2003. Effects of IPCC SRES emissions on river runoff: a global perspective. *J. Hydrol. Earth Syst. Sci.*, 7(5), 619-641.
- Arnold, J.G., Srinivasan, R., Muttiah, R.S. and Williams, J.R., 1998. Large area hydrologic modeling and assessment, Part I: model development. *J. Am. Water Resour. Assoc.*, 34(1), 73–89.
- Ashton, P.J., 2000. Southern African water conflicts: are they inevitable or preventable? In: Solomon, H. and Turton, A.R. (eds.), *Water Wars: Enduring Myth or Impending Reality*, Africa Dialogue Monograph Series No. 2. The African Centre for the Constructive Resolution of Disputes (ACCORD), Durban, South Africa, 62–105.
- Ashton, P.J., Love, D., Mahachi, H. and Dirks, P.H.G.M., 2001. An Overview of the Impact of Mining and Mineral Processing Operations on Water Resources and Water Quality in the Zambezi, Limpopo and Olifants Catchments in Southern Africa. Contract Report to the Mining, Minerals and Sustainable Development (SOUTHERN AFRICA) Project, by CSIR Environmentek, Pretoria, South Africa and Geology Department, University of Zimbabwe, Harare, Zimbabwe. Report No. ENV-P-C 2001-042, 64–177.
- Bailey, A.K. and Pitman, W.V., 2005. The Water Resources 2005 Project (WR2005). Wetlands (with 2005 enhancements), Pitman 2005. WRC Report No.: K5/1491. Water Research Commission, South Africa.
- Bardossy, A., 2007. Calibration of hydrological model parameters for ungauged catchments. *J. Hydrol. Earth Syst. Sci.*, 11, 703–710.
- Bastiaansen, C., 1990. Wetland types of Western Province and their suitability for rice cultivation. Land and Water Management Project, Department of Agriculture.
- Bates, B.C.Z., Kundzewicz, S., Wu, S. and Palutikok, J.P., 2008. *Climate Change and Water*, Technical Paper on the Intergovernmental Panel on Climate Change IPCC Secretariat, Geneva 210pp.

- Beilfuss, R. and dos Santos, D., 2001. Patterns of hydrological change in the Zambezi Delta, Mozambique. Working paper 2: Programme for the sustainable management of Cahora Bassa Dam and the Lower Zambezi Valley, 158pp.
- Beilfuss, R. and Brown, C. (eds.), 2006. Assessing environmental flow requirements of the Zambezi Delta: Application of the DRIFT model (Downstream response to imposed flow transformations). University of Eduardo Mondlane, Maputo, Mozambique.
- Benke, K.K., Pettit, C.J. and Lowell, K.E., 2011. Visualisation of spatial uncertainty in hydrological modelling. *Spatial Science*, 56(1), 73–88.
- Beven, K.J., 1989. Changing ideas: The case of physically based models. *J. Hydrol.*, 105(1-2), 157–172.
- Beven, K.J., 2005. *Rainfall-runoff modelling: The Primer*. John Wiley and Sons, 360pp.
- Beven, K.J., 2006. A manifesto for the equifinality thesis. *Hydrol. Process*, 320, 18-36.
- Beven, K.J. and Binley, A.M., 1992. The future of distributed models-model calibration and uncertainty prediction, *Hydrol. Process.*, 6 (3), 279–298.
- Beven, K.J. and Freer, J., 2001. Equifinality, data assimilation, and data uncertainty estimation in mechanistic modelling of complex environmental systems using the GLUE methodology. *J. Hydrol.*, 249, 11–29.
- Beven, K.J., Smith, P.J. and Freer, J.E., 2008. So just why would a modeller choose to be incoherent? *J. Hydrol.*, 354, 15–32.
- Beyene, T., Lettenmaier, D.P. and Kabat, P., 2010. Hydrological impacts of climate change on the Nile River basin: implications of the 2007 IPCC scenarios. *Clim. Change*, 100, 433–461.
- Booth, A., Chenje, M. and Johnson, P., 1994. *State of the Environment in Southern Africa*. Harare, Zimbabwe: SARDC: IUCN, Regional Office for Southern Africa; Maseru, Lesotho : SADC, Environment and Land Management Sector Coordination Unit. 332p.
- Bordi, I., Frigio, S., Parenti, P., Speranza, A. and Sutera, A., 2001a. The analysis of the Standardised Precipitation Index in the Mediterranean area: regional patterns. *Annali di Geofisica (Ann. Geofis)*, 44(5–6), 979–993.
- Bordi, I., Frigio, S., Parenti, P., Speranza, A. and Sutera, A., 2001b. The analysis of the Standardised Precipitation Index in the Mediterranean area: large scale patterns. *Annali di Geofisica (Ann. Geofis)*, 44(5-6), 965–978.
- Boughton, W. and Chiew, F., 2007. Estimating runoff in ungauged catchments from rainfall, PET and the AWBM model. *Environmental Modelling & Software* 22, 476–487.
- Box, G.E.P. and Jenkins G.M., 1976. *Time Series Analysis: Forecasting and Control*, 2nd Edition. Holden-Day, San Francisco.
- Bourgeois, S., Thomas Kocher, T. and Peter Schelander, P., 2003. *ETH Seminar: Science and Politics of International Freshwater Management 2003/04: Case study-Zambezi River*. ETH, EAWAG, Swiss Federal Institute of Technology, Zurich.
- Brandon, J., 2011. Planetary-scale tropospheric systems. www.recreationalflying.net/tutorials. Accessed January, 2012.
- Brauner, S., 2011. *Environmental Sampling and Monitoring Primer. Nonparametric Estimation Slope: Sen's Method in Environmental Pollution*. <http://www.cee.vt.edu/ewr/environmental/teach/smprimer/sen/sen.html>. Accessed January 2012.
- Brown, C., Greene A., Block, P. and Giannini, A., 2008. Review of downscaling methodologies for Africa climate applications. Technical Report 08-05: IRI Downscaling Report. International Research Institute for Climate and Society IRI Columbia University. 31pp.

- Burns, D.A., Klaus, J. and McHale, M.R., 2007. Recent climate trends and implications for water resources in the Catskill Mountain region, New York, USA. *J. Hydrol.*, 336(1-2), 155–170.
- Burroughs, W.J., 2007. *Climate Change: A Multidisciplinary Approach*. 2nd Edition, Cambridge University Press, 378pp.
- Byun, H.R. and Wilhite, D. A., 1999. Objective quantification of drought severity and duration. *J. Climate*, 12, 2747–2756.
- Calder, I.R., Hall, R.L., Bastable, H.G., Gunston, O.S., Chirwa, A. And Kafundu, R., 1995. The impact of land use change on water resources in sub-Saharan Africa: a modelling study of Lake Malawi. *J. Hydrol.*, 170, 123-135.
- Cane, M.A., Eshel, G. and Buckland, R.W., 1994. Forecasting Zimbabwe Maize Yield using Eastern Equatorial Pacific Sea-Surface Temperature. *Nature*, 370(6486), 204–205.
- Cap-Net, 2009. *IWRM as a Tool for Adaptation to Climate Change; a Training Manual and Facilitator’s Guide*. Cap-Net, Pretoria, South Africa.
- Carter, T. R., Parry, M. L., Harasawa, H. and Nishioka S., 1994. IPCC technical guidelines for assessing climate change impacts and adaptations, IPCC Special Report to Working Group II of IPCC, London, 72pp.
- Chagutah, T., 2007. Recent floods in the Zambezi basin-a result of climate Change? In: *The Zambezi*, SARDC, 6(3), 1–7.
- Chenje, M. and Johnson, P. (eds.), 1996. *Water in Southern Africa*. Harare, SADC Environment and Land Sector Coordination Unit.
- Chenje, M. (ed.), 2000. *State of the Environment in the Zambezi Basin 2000*. Report by Southern African Development Community (SADC-ELMS and WSCU), World Conservation Union (IUCN), Zambezi River Authority (ZRA) and Southern African Research and Documentation Centre - Musokotwane Environment Resource Centre for Southern Africa (SARDC-IMERCSA). Maseru, Lusaka, Harare. 334 pp.
- Chibuye, H., 2008. *Zambezi River Basin-Key features and Challenges from Climate Change*. Transboundary Water Cooperation-Climate Change Workshop. 1-2 December 2008. Copenhagen.
- Chiew, F.H.S., 2007. Estimation of rainfall elasticity of streamflow in Australia. *Hydrol Sci. Journ.*, 51(4), 613–625.
- Chiew, F.H.S., Whetton, P.H., McMahon, T.A. and Pittock, A.B., 1995. Simulation of the impacts of climate change on runoff on soil moisture in Australian catchments. *J. Hydrol.*, 167, 121–147.
- Chiew, F.H.S., Teng, J., Vaze, J., Post, D.A., Perraud, J.M., Kirono, D.G.C. and Viney, N.R., 2009. Estimating climate change impact on runoff across southeast Australia: Method, results and implications of the modeling method. *Water Resour. Res.*, 45, W10414. doi:10.1029/2008WR007338. 17pp.
- Chiew, F.H.S. and McMahon, T.A., 1993. Detection of trend or change in annual flow of Australian rivers. *Int. J. Climatol.*, 13, 643–653.
- Chiew, F.H.S. and McMahon, T.A., 2002. Global ENSO-streamflow teleconnections, streamflow forecasting and interannual variability. *Hydrol. Sci. Journ.*, 47, 505–522.
- Chung, C.F., Lopez, A. and New, M., 2011. *Modelling Impact of Change on Water Resources*. John Wiley and Sons, 200pp.
- Christensen, H.B., Hewitson, B., Busuoiu A., Chen, A., Gao, X., Held, I., Jones, R., et al., 2007. *Regional Climate Projections*. *Climate Change 2007: The Physical Science Basis*.

- Contribution of Working Group I to the Fourth Assessment Report of the Intergovernmental Panel on Climate Change. Cambridge, UK, New York, US, Cambridge University Press, 847–940.
- Christensen, N.S., Wood, A.W., Voisin, N., Lettemaier, D.P. and Palmer, R.N., 2004. The effects of climate change on the hydrology and water resources of the Colorado River basin. *Clim. Change*, 62, 337–363.
- Conway, D., 2002. Extreme rainfall events and lake level changes in East Africa: recent events and historical precedents. In: *The East African great lakes: limnology, palaeolimnology and biodiversity. Advances in Global Change Research*, 12, 63–92, Dordrecht: Kluwer.
- Conway, D. and Hulme, M., 1996. The impacts of climate variability and future climate change in the Nile basin on water resources in Egypt. *Int. J. of Water Res. Development*, 12, 261–280.
- Cubasch, U., Waskewitz, J., Hegerl, G. and Perlwitz, J., 1995. Regional climate changes as simulated in time-slice experiments. *Clim. Change*, 31, 273–304.
- Dai, A., Trenberth, E. and Qian, Taotao, 2004. A global dataset of Palmer Drought Severity Index for 1870-2002: Relationship with soil moisture and effects of surface warming. *J. Hydrometeorol.*, 1117–1130.
- Danish Hydraulic Institute, (DHI), 1997. MIKEBASIN: operating manual and description. Denmark, Hørsholm.
- DELFT Hydraulics, 2004. RIBASIM River basin simulation program operating manual and description. Netherlands, Delft.
- Delworth, T.L., Broccoli, A.J., Rosati, A., Stouffer, R.J., Balaji, V., Beesley, J.A., et al., 2006. GFDL's CM2 global coupled climate models. Part I: formulation and simulation characteristics. *J. Climate*, 19, 643–674.
- De Bruine, B.A., Grobler, A.J. and Crerar, S.E., 1993. Evaluation of a specialized rainfall-runoff model for catchments in Namibia. *Proc. 6th South African National Hydrology Symposium, Pietermaritzburg, Sept. 1993*, 225–233.
- Donohue, R.J., McVicar, T.R. and Roderick, M.L., 2010. Assessing the ability of potential evaporation formulations to capture the dynamics in evaporative demand within a changing climate. *J. Hydrol.*, 386, 186-197.
- Eamus, D. and Palmer, A.R., 2004. Research Letter: Is Climate Change a Possible Explanation for Woody Thickening in Arid and Semi-Arid Regions? *Research Letters in Ecology*, 2007, 37364, doi:10.1155/2007/37364, 5 pp.
- Easterling, W.E., 1988. Improving the detection of agricultural drought: a case study of Illinois corn production. *Agricultural and Forest Meteorology*, 43, 37–47.
- Elasha, B.O., Medany, M., Niang-Diop, I., Nyong, T., Tabo, R. and Vogel, C., 2006. Background paper on impacts, vulnerability and adaptation to climate change in Africa. African Workshop on Adaptation Implementation of Decision 1/CP.10 of the UNFCCC, Accra, Ghana.
- Engelbrecht, F., 2005. Simulations of Climate and Climate Change over Southern Tropical Africa with the Conformal-Cubic Atmospheric Model. In: Schulze R.E. (ed.) *Climate Change and Water Resources in Southern Africa: Studies on Scenarios, Impacts, Vulnerabilities and Adaptation*. Water Research Commission, Pretoria, RAS, WRC Report 1430/1/05. Chapter 14, 57–74.

- Euroconsult Mott MacDonald, 2007. Rapid Assessment: Final Report Integrated Water Resources Management Strategy for the Zambezi River Basin. SADC-WD/ ZRA, SIDA, Lusaka, Zambia. 188pp.
- Euroconsult Mott MacDonald, 2008. Integrated Water Resources Management Strategy and Implementation Plan for the Zambezi River Basin, Summary. SADC-WD/ ZRA, SIDA, Lusaka, Zambia. 35pp.
- FAO, 2003. The digital soil map of the world and Food and Agricultural Organisation of the United Nations. Land and Water Development Division, FAO, Rome, Italy. <http://www.fao.org/ag/agl/agll/key2soil.stm>.
- FAO, 2004. Drought impact mitigation and prevention in the Limpopo River basin: A situation analysis. Land and Water Discussion Paper 4. Rome, Food and Agricultural Organisation of the United Nations.
- FAOSTAT, 2012. <http://faostat.fao.org/site/567/DesktopDefault.aspx?PageID=567#anchor>.
- Farquharson, F. and Sutcliffe, J.V., 1998. Regional variations of African river flows. In: Water Resources Variability in Africa During the 20th Century. Servat, E., Hughes, D.A., Fritsch, J.M. and Hulme, M. (eds). IAHS Special Publication, 252, 161–170. IAHS, Wallingford, UK.
- Flint, L., 2006. Climate change, vulnerability and the potential for adaptation. Case study: the Upper Zambezi Valley region of Western Zambia. University of Copenhagen, Denmark.
- Folland, C.K., Palmer, T.N. and Parker, D.E., 1986. Sahel rainfall and worldwide sea temperatures, 1901-1985. *Nature*, 320, 602–607.
- Fowler, H.J., Blenkinsop, S. and Tebaldi, C., 2007. Linking climate change modelling to impact studies: recent advances in downscaling techniques for hydrological modeling. *Int. J. Clim.*, 27(12), 1547–1578.
- Gandolfi, C., Guariso, G. And Togni, D., 1997. Optimal flow allocation in the Zambezi River System. *Water Resour Manage.*, 11, 377–393.
- Fuller, W.A., 1976. Introduction to statistical time series. John Wiley & Sons, Inc., New York.
- Giorgi, F., 2005. Climate Change Prediction. *Clim. Change*, 73(3), 239–265.
- Giorgi, F. and Francisco, R., 2000. Evaluating uncertainties in the prediction of regional climate change. *Geophys. Res. Lett.* 27, 1295–1298.
- Giorgi, F., Hewitson, B. C., Christensen, J. H., Hulme, M., vonStorch, H., Whetton, P. H., Jones, R. G., Mearns, L. O. and Fu, C., 2001. Regional Climate Information: Evaluation and Projections. In Houghton, J. T., Ding, et al. (Eds.). *Climate Change 2001: The Scientific Basis*, Chapter 10, Contribution of Working Group I to the Third Assessment Report of the Intergovernmental Panel on Climate Change (IPCC), Cambridge University Press, Cambridge, UK, 583–638.
- Giorgi, F. and Mearns, L.O., 1991. Approaches to regional climate change simulation: A review. *Reviews of Geophysics*, 29(2), 191–216.
- Glantz, M.H., Betsill, M. And Crandall, K., 2007. Food Security in Southern Africa: Assessing the Use and Value of ENSO Information. University Corporation for Atmospheric Research, National Oceanic and Atmospheric (NOAA) Administration Proposal No. GC95–014.
- Glantz, M., Katz, R., and Nicholls N. (eds.), 1991, *Teleconnections Linking Worldwide Climate Anomalies*, Cambridge University Press, Cambridge, U.K.
- GLC, 2000. Global land cover map for Africa in the year 2000. <http://www-gem>.
- Gleick, P.H. (Lead Author), 2000. *Water: The Potential Consequences of Climate Variability and Change for the Water Resources of the United States*. The Report of the Water Sector

- Assessment Team of the National Assessment of the Potential Consequences of Climate Variability and Change for the U.S. Global Change Research Program. 160pp.
- Gleick, P.H., 1986. Methods for evaluating the regional hydrologic impacts of global climatic changes. *J. Hydrol.*, 88, 97–116.
- Gleick, P.H., 1989. Climate Change, Hydrology and Water Resources. *Reviews of Geophysics*, 27(3), 329–344.
- Gommes, R., 1999. Climate-related risk in agriculture. A note prepared for the IPCC Expert Meeting on Risk Management Methods Toronto, AES, Environment Canada, 29 April–1 May 1998.
- Gommes, R. and Hoefsloot, P., 1998. Gaps in maps, estimation of missing data in agricultural statistics maps. Proc. Of the COST (EU Committee on Science and Technology) meeting in Volterra on the Spatial Interpolation of Climatic and Meteorological data. Italy, 1997.
- Goulden, M., Conway, D. and Persechino, A., 2008. Adaptation to climate change in international river basins in Africa: a review. Working Paper 127. Tyndall Centre for Climate Change Research, 37pp.
- Graham, L.P., Andreasson, J. and Carlsson B., 2007. Assessing climate change impacts on hydrology from an ensemble of regional climate models, model scales and linking methods: a case study on the Lule River basin. *Climatic Change*, 81(1), 293–307.
- GRDC (The Global Runoff Data Center), 2003. 56068, Koblenz, Germany.
- GRDC, 2007. Major River Basins of the World / Global Runoff Data Centre. Koblenz, Germany, Federal Institute of Hydrology (BfG).
- Greene, A., Goddard, L. and Lall, U., 2006. Performance-based multimodel climate change scenarios 1: low-frequency temperature variations. *J. Climatology*, 19, 4326–4343.
- Gudmundsson, L., Tallaksen, L.M., Stahl, K., Clark, D.B., Dumont, E., Hagemann, S., Bertrand, N., Gerten, D., Heinke, J., Hanasaki, N., Voss, F. And Koirala, S., 2012 Comparing large-scale hydrological model simulations to observed runoff percentiles in Europe. *J. Hydrometeo*. 13 (2), 604-620.
- Gupta, H.V. and Sorooshian, S., 1985. The relationship between data and the precision of parameter estimates of hydrologic models. *J. Hydrol.*, 81, 57–77.
- Gupta, V.K., Sorooshian, S. and Yapo, P.O., 1998. Toward improved calibration of hydrologic models: Multiple and non-commensurable measures of information. *Water Resour. Res.*, 34(4), 751–764.
- Guttman, N.B., 1998. Comparing the Palmer Drought Index and the Standardized Precipitation Index. *American Water Resources Association*, 34 (1), 113–121.
- Haddeland, I., Clark, D.B., Franssen, W., Ludwig, F., Voß, F., Arnell, N.W., Bertrand, N., Best, M., Folwell, S., Gerten, D. Gomes, S., Gosling, S.N., Hagemann, S., Naota Hanasaki, N., Harding, R., Heinke, J. Kabat, P., Koirala, S., Oki, T., Jan Polcher, J., Stacke, T., Viterbo, P., Weedon, G.P. and Yeh, P., 2011. Multimodel Estimate of the Global Terrestrial Water Balance: Setup and First Results. *J. Hydrometeor*, 12, 869–884.
- Hamed, K.H., 2008. Trend detection in hydrologic data: The Mann-Kendall trend test under the scaling hypothesis. *J. Hydrol.*, 349, 350–363.
- Hargreaves, G. H. and Allen, R.G., 2003. History and evaluation of Hargreaves evapotranspiration equation. *J. Irrig. Drain. Eng.*, 129, 53–63.
- Hay, L.E. and Clark M.P., 2003. Use of statistically and dynamically downscaled atmospheric model output for hydrologic simulations in three mountainous basins in the western United States. *J. Hydrol.*, 282(1–4), 56–75.

- Hastenrath, S., 1996. *Climate Dynamics of the Tropics*. Updated edition from *Climate and Circulation of the Tropics*. Atmospheric Sciences Library. Kluwer Academic Publishers, Dordrecht, Netherlands, 488pp.
- Hayes, M.J., Svoboda, M.D., Wilhite, D.A. and Vanyarkho, O.V., 1999. Monitoring the 1996 Drought Using the Standardized Precipitation Index. *Bull. Amer. Meteor. Soc.*, 80(3), 429–438.
- Heim, R.R., 2002. A review of twentieth-century drought indices used in the United States. *Bull. Amer. Meteor. Soc.*, (83), 1149–1165.
- Held, I.M., Lyons, S.W. and S. Nigam, 1989. Transients and the Extratropical Response to El-Nino. *Atmos. Science.*, 46, 163–174.
- Helsel, D.R. and Hirsch, R.M., 1992. *Statistical methods in water resources*. Studies in Environmental Science, 49. Elsevier, Amsterdam, The Netherlands.
- Herold, C., 2003. WQ 2000: Development of an Interactive Surface Water Quality Information and Evaluation System for South Africa. Water Research Commission, Report No. 950/01/03, Pretoria, South Africa.
- Hesse, C., Krysanova, V., Pazolt, J. And Hattermann, F.F., 2008. Eco-hydrological modelling in a highly regulated lowland catchment to find measures for improving water quality. *Ecological Modelling*, 218(1-2), 135-148.
- Hewitson, B. C. and Crane, R.G., 1996. Climate downscaling: Techniques and applications. *Clim. Res.* (7), 85–95.
- Hewitson, B.C. and Crane, R.G., 2006. Consensus between GCM climate change and projections with empirical downscaling: Precipitation downscaling over South Africa. *Int. J. Climatol.*, 26, 1315–1377.
- Hoerling, M., Hurrell, J., Eischeid, J. and Philips, A., 2006. Detection and Attribution of Twentieth-Century Northern and Southern African Rainfall Change. *J. Climate*, 19, 3989–4008.
- Hoffman, M.T., Cramer, M.D., Gillson, L. and Wallace M., 2011. Pan evaporation and wind run decline in the Cape Floristic Region of South Africa (1974-2005): Implications for vegetation responses to climate change. *Climate Change*, 109, 437–452.
- Hughes, D.A., 1995. Monthly rainfall–runoff models applied to arid and semiarid catchments for water resource estimation purposes. *Hydrol. Sci. Journ.*, 40 (6), 751–769.
- Hughes, D.A., 1997. Southern African FRIEND: The Application of Rainfall-Runoff Models in the SADC Region. Water Research Commission, Report, No. 235/1/97, Pretoria.
- Hughes, D.A., 2004a. Three decades of hydrological modelling research in South Africa, *South African J. Sci.*, 100, 638–642.
- Hughes, D.A., 2004b. Incorporating ground water recharge and discharge functions into an existing monthly rainfall-runoff model. *Hydrol. Sci. Journ.*, 49(2), 297–311.
- Hughes, D.A., 2006. Water resources estimation in less developed regions-issues of uncertainty associated with a lack of data. In *Predictions in Ungauged Basins: Promises and Progress*, IAHS Publ., 303, 72–79.
- Hughes, D.A., Andersson, L., Wilk J. and Savenije, H.H.G., 2006. Regional calibration of the Pitman model for the Okavango River. *J. Hydrol.*, 331, 30–42.
- Hughes, D.A. and Forsyth, D., 2006. A generic database and spatial interface for the application of hydrological and water resource models, *Comp. Geosci.*, 32, 1389–1402.

- Hughes, D.A., Forsyth, D. and Watkins, D.A., 2000. An integrated software package for the analysis and display of hydrological or water resources time series data. Water Research Commission Report No. 876/2/00, Pretoria, South Africa.
- Hughes, D.A., Kapangaziwiri, E., Mallory, S.J.L., Wagener, T. and Smithers, J., 2011b. Incorporating uncertainty in water resources simulation and assessment tools in South Africa. WRC Report No. 1838/1/11, ISBN 978-1-4312-0128-0, 149pp.
- Hughes, D.A., Kapangaziwiri, E. and Sawunyama, T., 2010. Hydrological model uncertainty assessment in southern Africa. *J. Hydrol.*, 387, 221–232.
- Hughes, D.A., Kingston, D. G. and Todd, M. C., 2011a. Uncertainty in water resources availability in the Okavango River Basin as a result of climate change. *Hydrol. Earth Syst.*, 15, 931–941.
- Hughes D. A., Mantel S., Mohobane T., 2012. An assessment of the skill of downscaled GCM outputs in simulating historical patterns of rainfall variability. Submitted Paper.
- Hughes, D.A., Murdoch, K.A. and Sami, K., 1994. A hydrological model application system: a tool for integrated river basin management. In: Kirby, C., White, W.R. (eds.), *Integrated River Basin Development*. Wiley, Chichester, UK, 397–406.
- Hughes, D.A., and Sami, K., 1994. A semi-distributed, variable time interval model of catchment hydrology: structure and parameter estimation procedures. *J. Hydrol.*, 155, 265–291.
- Hughes, D.A., Sawunyama, T. and Kapangaziwiri, E., 2008. Incorporating estimation uncertainty into water resource development planning in ungauged basins in southern Africa. BHS 10th Hydrology Symposium, Exeter, 2008, 7–12.
- Hulme, M. and Brown, O., 1998. Portraying climate scenario uncertainties in relation to tolerable regional climate change. *Clim. Res.*, 10, 1–14.
- Hulme, M. and Carter, T.C., 1999. In *Representing Uncertainty in Climate Change Scenarios and Impact Studies: ECLAT-2 Red Workshop Report*. T. Carter, M. Hulme and D. Viner (eds.). Climatic Research Unit, Norwich.
- Hulme, M., Doherty, R., Ngara, T., New, M. and Lister, D., 2001. African Climate Change 1900–2100. *Climate Res.*, 17, 145–168.
- Hundecha, Y. and Bardossy, A., 2004. Modeling of the effects of land use changes on the runoff generation of a river basin through parameter regionalization of a watershed model. *J. Hydrol.*, 292, 281–295.
- HYDRO 1K-Africa, 2001. USGS-NASA Distributed Active Archive Center. <http://edcdaac.usgs.gov/gtopo30/hydro/africa.asp>
- INGC., 2009. Main report: INGC Climate Change Report: Study on the Impact of Climate Change on Disaster Risk in Mozambique. Asante, K., Brundrit, G., Epstein, P., Fernandes, A., Marques, M.R., Mavume, A, Metzger, M., Patt, A., Queface, A., Sanchez del Valle, R., Tadross, M., Brito, R. (eds.). INGC, Mozambique, 338pp.
- IPCC, 2001a. *Climate Change 2001: Impacts, Adaptation, and Vulnerability*. Contribution of Working Group II to the Third Assessment Report of the Intergovernmental Panel on Climate Change. McCarthy, M.C., O.F. Canziani, N.A. Leary, D.J. Dokken and K.S. White (eds.). Cambridge University Press, Cambridge, 1031 pp.
- IPCC, 2001b. *Climate Change 2001: The Scientific Basis*. Contribution of Working Group I to the Third Assessment Report of the Intergovernmental Panel on Climate Change Houghton, J. T., Y. Ding, D. J. Griggs, M. Noguer, P. J. van der Linden, X. Dai, K. Maskell, and C. A. Johnson (eds.). Cambridge University Press, Cambridge, United Kingdom and New York, NY, USA, 881pp.

- IPCC, 2001c. Climate Change 2001: Synthesis Report. Contribution of Working Groups I, II, and III to the Third Assessment Report of the Intergovernmental Panel on Climate Change Watson, R.T. and the Core Writing Team (eds.). Cambridge University Press, Cambridge, 398 pp.
- IPCC, 2008: Climate Change and Water. IPCC Technical Paper VI. <http://www.ipcc.ch/ipccreports/tp-climate-change-water.htm>
- IPCC, 2007. Climate Change: The Physical Science Basis. Cambridge University Press, Cambridge. 996pp.
- IPCC, 1996. Climate Change 1995: Economic and social dimensions of climate change. Contribution of working group III of the Second Assessment Report of the Intergovernmental Panel on Climate Change. Bruce, J.P., H. Lee and E.F. Haites (eds.). Cambridge University Press, Cambridge 179–224 .
- IPCC, 1997. The Regional Impacts of Climate Change: An Assessment of Vulnerability. Summary for Policy Makers. Geneva, Switzerland.
- IPCC, 2007. Climate Change 2007: Impacts, Adaptation and Vulnerability. Contribution of Working Group II to the Fourth Assessment Report of the Intergovernmental Panel on Climate Change. Cambridge University Press, Cambridge UK. 976pp.
- IPSL, 2005. The new IPSL climate system model: IPSL–CM4'. Institut Pierre Simon Laplace des Sciences de l'Environnement Global, Paris, France, 73 pp.
- IWMI (International Water Management Institute), World Water and Climate Atlas. www.iwmi.ggiar.org/WAtlas?default.aspx. Accessed 2009.
- Jacob, D. and van den Hurk, B., 2009. Climate Change Scenarios at the Global and Local scales in Climate change adaptation in the water sector. Ludwig F., Kabat P., van Schaik H. and van der Valk (eds.) 23–33. Earthscan UK and USA.
- Jakeman, A.J. and Letcher, R.A., 2003. Integrated assessment and modelling: features, principles and examples for catchment management. Environ. Model. Soft., 18, 491–501.
- Jewitt, G.P.W. and Gorgens, A.H.M., 2000. Scale and Interfaces in the context of integrated water resources management for the rivers of the Kruger National Park. WRC Report 627/1/00.
- Johnson, T. and Weaver C., 2009. A Framework for Assessing Climate Change Impacts on Water and Watershed Systems. Environmental Management, 43(1), 118–134.
- Jones, P.D., Murphy, J.M. and Noguer, M., 1995. Simulation of climate change over Europe using a nested regional-climate model: assessment of control climate, including sensitivity to location of lateral boundaries. Quart. J. Roy Met. Soc., 121, 1413–1449.
- Jung, J. and Kunstmann, H., 2007. High resolution regional climate modelling for the Volta Basin of West Africa. Geophysical Res. Atmos., 123, d23108.
- Jung, J., Wagner, S. and Kunstmann, H., 2012. Joint climate-hydrology modelling: an impact study for the data-sparse environment of the Volta Basin in West Africa. J. Hydrol. Res., 43(3), 231–248.
- Jury, M.R. and Gwanzantini, M.E., 2002. Climate Variability in Lake Malawi, Part 2: Sensitivity and Prediction of Lake Levels. Int. J. Climatol., 22, 1303–1312.
- Jury, M.R., Mulenga, H.M. and Mason, S.J., 1999. Exploratory Long Range Models to Estimate Summer Climate Variability over Southern Africa. J. Climate, 12, 1892–1899.
- Jury, M.R., Weeks, S. and Gondwe, P.M., 1997. Satellite vegetation as an indicator of climate variability over southern Africa. S. African J. Sci., 93, 34–38.

- Kabat, P. and van Schaik, H., 2003 (co-ordinating lead authors). Climate changes the water rules: How water managers can cope with today's climate variability and tomorrow's climate change. Dialogue on Water and Climate. ISBN 90-327-0321-8. 120pp.
- Kampata, J.J., Parida, B.P. and Moalafhi, D.B., 2008. Trend analysis of rainfall in the headstreams of the Zambezi River Basin. *Phys. Chem. Earth*, 33, 621–625.
- Kapangaziwiri, E., 2010. Regional application of the Pitman monthly rainfall-runoff model in southern Africa incorporating uncertainty. PhD thesis, Rhodes University.
- Kapangaziwiri, E., 2008. Revised parameter estimation methods for the Pitman monthly model, MSc Thesis, Rhodes University, Grahamstown, South Africa. <http://eprints.ru.ac.za/1310/>.
- Kapangaziwiri, E. and Hughes, D.A., 2008. Towards a physically-based parameter estimation method for the Pitman monthly rainfall-runoff model. *Water SA.*, 32(2),183–191.
- Kapangaziwiri, E., Hughes D.A. and Wagener, T., 2009. Towards the development of a consistent uncertainty framework for hydrological predictions in South Africa. New approaches to hydrological prediction in data sparse regions. Proc. Symposium HS2 at the Joint IAHS & IAH Convention, Hyderabad, India, September 2009. IAHS Publ.,333, 84–93.
- Karl, T.R. and Trenberth, K.E., 2003. Modern Global Climate Change. *Science*, 302(5651), 1719–1723.
- Karpauzos, D.K., Kavalieratou, S. and Babajimopoulos, C., 2010. Trend analysis of precipitation data in Pieria Region (Greece). *European Water*, 30, 31–40.
- Kavetski, D., Kuczera, G. and Franks, S.W., 2006. Bayesian analysis of input uncertainty in hydrological modelling: 2. Application. *Water Resour. Res.* (42), W03408, doi: 10.1029/2005WR004376, 10pp.
- Kay, A.L., Davies, N.H., Bell, V. A. and Jones, R.G., 2009. Comparison of uncertainty sources for climate change impacts: Flood frequency I England. *Clim. Change* 92(1–2), 41–63.
- Kendall, M.G., 1975. Rank Correlation Methods. 4th Edition, Charles Griffin, London. 202pp.
- Kestin, T.A., Karoly, J., Yano, I. and Rayner, N.A., 1998. Time-frequency variability of ENSO and stochastic simulations. *J. Climate*, 7, 81–105.
- Keyantash, J. and Dracup, J.A., 2002. The quantification of drought: An evaluation of drought indices. *Bull. Amer. Meteor. Soc.*, 83, 1167–1180.
- Kiehl, J. T. and Trenberth K. E., 1997: Earth's annual global mean energy budget. *Bull. Amer. Meteor. Soc.*, 78, 197–208.
- Killingtveit, A. and Saelthun, N.R., 1995. Hydrology: Hydropower Development. Norwegian Institute of Technology, Division of Hydraulic Engineering, Trondheim.
- Kim, U. and Kaluarachchi, J.J., 2008. Application of parameter estimation and regionalization methodologies to ungauged basins of the Upper Blue Nile River Basin, Ethiopia. *J. Hydrol.* (362), 39–56.
- Kingston, D. G. and Taylor, R. G, 2010. Sources of uncertainty in climate change impacts on river discharge and groundwater in a headwater catchment of the Upper Nile Basin, Uganda, *Hydrol. Earth Syst. Sci.*, 14, 1297–1308.
- Kingston, D. G., Thompson, J. R. and Kite, G., 2010. Uncertainty in climate change projections of discharge for the Mekong River Basin. *Hydrol. Earth Syst. Sci. Discuss*, 7, 5991–6024.
- Kirchoff, C.J. and Buckley, J. W, 2008. Sustainable Water Management of the Zambezi River Basin. *The Journal of the International Institute Spring* 2008, 10.

- Kirono, D.G.C, Hennessy, K., Mpelasoka, F. and Kent, D., 2011. Approaches for generating climate change scenarios for use in drought projections: a review. CAWCR Technical Report No. 034. ISSN: 1836-019X .
- Knutti, R., 2011. Should we believe model predictions of future climate change? *Phil. Trans. R. Soc.*, 366, 4647–4664.
- Kogan, F.N., 1995. Droughts of the late 1980s in the United States as derived from NOAA polar-orbiting satellite data. *Bull. Amer. Meteor. Soc.*, 76(5), 655–668.
- Kokkonen, T., Jakeman, A., Young, P. and Koivusalo, H., 2003. Predicting daily flows in ungauged catchments: model regionalization from catchment descriptors at the Coweeta Hydrologic Laboratory, North Carolina. *Hydrol. Process.*, 11, 2219–2238.
- Koutsoyiannis, D., 2011. Scale of water resources development and sustainability: small is beautiful, large is great. *Hydrol. Sciences* 56(4), Special Issue, 553–575.
- Krasovskaia, I. and Gottschalk, L., 1995. Analysis of regional drought characteristics with empirical orthogonal functions. In *New Uncertainty Concepts in hydrology and Water Resources: International J. Hydrol. Series. Kundzewicz Z.W. (ed.)*. Cambridge University Press, 163–167.
- Krishnamurti, V. and Shukla, J., 2007. Intraseasonal and Seasonally Persisting Patterns of Indian Monsoon Rainfall. *Climate*, 20, 3–20.
- Kuczera, G., Kavetski, D., Franks, S. and Thyer, M., 2006. Towards a Bayesian total error analysis of conceptual rainfall-runoff models: Characterising model error using storm-dependent parameters. *J. Hydrol.*, 331(1–2), 161–177.
- Kuczera, G. and Mroczkowski, L., 1998. Assessment of hydrologic parameter uncertainty and the worth of data. *Water Resour. Res.* 34(6), 1481–1489.
- Kumambala, P.G., 2010. Sustainability of water resources development for Malawi with particular emphasis on North and Central Malawi. PhD thesis. University of Glasgow. <http://theses.gla.ac.uk/1801/>, 412pp.
- Kundzewicz, Z.W., Mata, L.J., Arnell, N.W., Doll, P., Kabat, P. et al, 2007. Freshwater resources and their management. In *Climate Change 2007: Impacts, Adaptation and Vulnerability. Contribution of Working Group II to the Fourth Assessment Report of the Intergovernmental Panel on Climate change*. M.L. Parry, O.F. Canziani, Palutikof J.P., van der Linden P.J., Hanson (eds). Cambridge University Press, Cambridge, UK, 173–210.
- Kundzewicz, Z. W., 1997. Water resources for sustainable development. *Hvdrol. Sci.Journ.*, 42(4), 467–480.
- Kundzewicz, Z.W. and Robson, A.J., 2004. Change detection in hydrological records - review of the methodology. *Hydrol. Sci. Journ.*, 49(1), 7–19.
- Kundzewicz, Z.W. and Robson, A.J., 2000 (eds.). *Detecting trend and other changes in hydrological data*. World Climate Programme: World Climate Programme Data and Monitoring. WCDMP-54, WMO/TD, 1013. WMO, Geneva, Switzerland. Lam, D.C. and Swayne, D.A., 1993. An expert system approach of integrating hydrological database, models and GIS: Application of the RAISON System. In: *Application of Geographic Information Systems in Hydrology and Water Resources Management*. Proc. HydroGIS–93 Conference, Vienna. IAHS Publ., 211.
- Lamb, P.J., 1978. Large-scale tropical Atlantic surface circulation patterns associated with Sub-Saharan weather anomalies. *Tellus* 30, 240–251.

- Lal, M., 2011. Implications of climate change in sustained agricultural productivity in South Asia. *Reg. Environ Change*, 11: S790S94. DOI 10.1007/s10113-010-0166-9.
- Lempert, R.J., Groves, D.G. Popper S.W. and Bankes, S.C., 2006. A General, Analytic Method for Generating Robust Strategies and Narrative Scenarios. *Management Science*, 52(4), 514–528.
- Lempert, R.J. and Collins, M.T., 2007. Managing the risk of uncertain threshold response: Comparison of robust, optimum and precautionary approaches. *Risk Analysis*, 27(4), 1009–1026.
- Le Treut, H., Somerville R., Cubasch U., Ding Y., Mauritzen C., Mokssit A., Peterson, T. and Prather M., 2007. Historical Overview of Climate Change. In: *Climate Change 2007: The Physical Science Basis. Contribution of Working Group I to the Fourth Assessment Report of the Intergovernmental Panel on Climate Change*. Cambridge University Press, Cambridge, United Kingdom and New York, NY, USA. 94–127.
- Legates, D.R., McCabe Jr. G.J., 1999. Evaluating the use of ‘Goodness of Fit’ Measures in Hydrologic and Hydroclimatic Model Validation. *Water Resour. Res.*, 35(1), 233–241.
- Liu, Y. and Gupta, H.V., 2007. Uncertainty in hydrological modelling: Towards an integrated data assimilation framework. *Water Resour. Res.*, 43. W07401, doi: 10.1029/2006 WR 005756.
- Lockwood, M. and Frohlich, C., 2007. Recent oppositely-directed trends in solar climate forcings and the global mean surface air temperature. *Proc. R. Soc. A*, 463, 2447–2460.
- Loucks, D.P., van Beek, E., Stedinger, J.R., Dijkman, J.P.M. and Villars, M.T, 2005. *Water Resources Systems Planning and Management: An Introduction to Methods, Models and Applications: Studies and Reports in Hydrology* Paris, UNESCO PUBLISHING ISBN 92-3-103998-9, 677pp.
- Love, D., Uhlenbrook, S., Twomlow, S. and van der Zaag, P., 2010. Changing hydroclimatic and discharge patterns in the northern Limpopo basin, Zimbabwe. *Water SA*, 36(3), 335–350.
- Ludwig R., May, I., Turcotte, R., Vescovi, L., Braun, M., Cyr, J.F., Fortin, L.G., Chaumont, D., Biner, S., Chartier, I., Caya, D. and Mauser, W., 2009. The role of hydrological model complexity and uncertainty in climate change impact assessment. *Adv. Geosci.*, 21, 63–71.
- Lyons, R. P., Kroll, C. N. and Scholz, C.A., 2011. An energy-balance hydrologic model for the Lake Malawi Rift Basin, East Africa. *Global and Planetary Change*, 75, 83–97.
- Madsen, H., 2003. Parameter estimation in distributed hydrological catchment modelling using automatic calibration with multiple objectives. *Advances in Water Resources*, 26(2), 2005–16.
- Manabe, S., Milly, P.C.D. and Wetherald, G., 2004. Simulated long-term changes in river discharge and soil moisture due to global warming. *Hydrol. Sci. Journ*, 49(4), 625–642.
- Manatsa, D., Mukwada, G., Siziba, E. and Chinyanganya, T., 2010. Analysis of multidimensional aspects of agricultural droughts in Zimbabwe using the Standardized Precipitation Index. *Theo Appl. Climatology* DOI 10.1007/s00704-010-0262-2.
- Mann, H.B., 1945. Non parametric tests against trend. *Econometrica* 13, 245–259.
- Mason, S. J., 2001. El Niño, climate change, and Southern African climate. *Environmetrics*, 12, 327–345.
- Mason, S. J., 1995. Sea surface temperature-South Africa rainfall associations, 1910–1989. *Int. J. Climatol.* 15, 119–135.

- Mason, S. J. and Jury, R.M., 1997. Climate fluctuations in southern Africa. A reflection on underlying processes, precursors and predictability. *Progress in Physical Geography*, 21, 23–50.
- Mazvimavi, D. and Wolski P., 2006. Long-term variations of annual flows of the Okavango and Zambezi Rivers. *Phys. Chem. Earth*, 31, 944–951.
- Mazvimavi, D., 2003. Estimation of Flow Characteristics of Ungauged Catchments Case Study in Zimbabwe. Published PhD. Thesis, ISBN 90-5808-950-9, 188pp.
- Mazvimavi, D., 2008. Investigating possible changes of extreme rainfall in Zimbabwe. *Hydrol. Earth Syst. Sci. Discuss.*, 5, 1765–1785.
- Mazvimavi, D., 2010. Investigating changes over time of annual rainfall in Zimbabwe. *Hydrol. Earth Syst. Sci.*, 14, 2671–2679.
- McKee, T.B., Doesken, N.J. and Kleist, J., 1993. The relationship of drought frequency and duration to time scales. *Proceedings of the 8th Conference on Applied Climatology*. AMS, Boston, MA, pp. 179–184.
- McMahon, T.A., Finlayson, B.L., Haines, A. and Srikanthan R., 1987. Runoff variability: a global perspective. In *The Influence of Climate Change and Climatic Variability on the Hydrologic Regime and Water Resources (Proceedings of the Vancouver Symposium, August 1987)*. IAHS Publ., 168, 3–11.
- McMahon, T.A, Peel, M.C, Vogel, R.M, and Pegram, G.G.S, 2007a. Global streamflows-Part 3: Country and climate zone characteristics. *J. Hydrol.*, 347, 272–291.
- McMahon, T.A, Vogel, R.M, Pegram, G.G.S., Peel, M.C. and Etkin D., 2007b. Global streamflows-Part 2: Reservoir storage-yield performance. *J. Hydrol.*, 347, 260–271.
- McMahon, T.A, Vogel, R.M, Peel, M.C. and Pegram G.G.S., 2007c. Global streamflows-Part 1: Characteristics of annual streamflows. *J. Hydrol.*, 347, 243–259.
- McWilliams, J. C., 2007 Irreducible imprecision in atmospheric and oceanic simulations. *Proc. Natl Acad. Sci. USA*, 104, 8709–8713.
- Mearns, E., Laugier, M., Daw, J., Kaatz, L., Waage, M. and Water, D., 2010. Decision Support Planning Methods: Incorporating Climate Change Uncertainties into Water Planning. Water Utility Climate Alliance (WUCA) White paper. 113pp.
- Meehl, G.A., 1993. A coupled air-sea biennial mechanism in the tropical Indian Ocean and Pacific regions: Role of the oceans. *J. Climate*, 6, 31–41.
- Mendelsohn, F. (ed.), 1961. *The Geology of the Northern Rhodesian Copperbelt*. Macdonald, London. 523 pp.
- Meigh, J.R., McKenzie, A.A. and Sene, K.J., 1999. A grid-based approach to water scarcity estimates for eastern and southern Africa. *Water Resour. Manage.*, 13, 85–115.
- Milly, P.C.D., Betancourt, J., Falkenmark, M., Hirsch, R.M., Kundzewicz, Z.W., Lettenmaier, D. and Stoufer, R.J., 2008. Stationarity Is Dead: Whither Water Management? *Science*, 319, 573–574.
- Milly, P.C.D. and Dunne, 2002. Macroscale water fluxes 2. Water and energy supply control of their interannual variability. *Water Resour. Res.*, 38, 1206. DOI: 10.1029/ 2001 WR 00 0 760.
- Milly, P.C.D., Dunne, K.A. and Vecchia, A.V., 2005. Global pattern of trends in streamflow and water availability in a changing climate. *Nature*, 438(7066), 347–350.
- Milly, P.C.D., Wetherald, R.T., Dune and K.A., Delworth, T.L., 2002. Increasing the risk of threats in a changing climate. *Nature*, 415, 514–517.
- Mitchell, T.D. and Hulme, M., 1999. Predicting regional climate change: living with uncertainty. *Prog. Phys. Goegr*, 23(1), 57–78.

- Mitchell, T.D. and Jones, P.D. 2005. An improved method of constructing a database of monthly climate observations and associated high-resolution grids. *Int. J. Climatol.*, 25, 693-712.
- Muchinda, M., Dandaula, H., Hyera, T.M. and Mutambirwa C., 2000. Physical Features and Climate. In *State of the Environment Zambezi Basin 2000*. Chenje, M. (ed.) Maseru/Harare/Lusaka: SADC/IUCN/ZRA/SARDC.
- Mukheibir, P., 2008. Water Resources Management Strategies for Adaptation of Climate-Induced Impacts in South Africa. *Water Resour. Manage.*, 22, 1259–1276.
- Murphy, J., 2000. Predictions of climate change over Europe using statistical and dynamical downscaling techniques. *J. Climatol.* 20(5), 489–501.
- Mwelwa, E.M., 2004. The application of a monthly time step Pitman rainfall-runoff model to the Kafue river basin of Zambia. MSc. Thesis, Rhodes University.
- Nobrega, M. T., Collischonn, W., Tucci, C. E. M. and Paz, A. R., 2011. Uncertainty in climate change impacts on water resources in the Rio Grande Basin, Brazil, *Hydrol. Earth Syst. Sci.*, 15, 585–595.
- Nakayama, M. (ed), 2003. *International Waters in Southern Africa*. United Nations University Press, 306pp.
- Nakicenovic, N., Alcamo, J., Davis, G., de Vries, B., Fenhann, J., Gaffin, S. et al., 2000. *Emissions Scenarios: A special report of Working Group III of the Intergovernmental Panel on Climate Change*. Cambridge University Press, Cambridge, UK and New York, USA, 599 pp.
- Nash, L. and Gleick, P., 1993a. The Colorado River basin and climate change. Report EPA 230-R-93-009. Washington DC: US Environmental Agency.
- Nash, L. and Gleick P., 1993b. The sensitivity of streamflow in the Colorado Basin to climatic changes. *J. Hydrol.*, 125, 221–241.
- Nash, J. E. and Sutcliffe, J. V., 1970. River flow forecasting through conceptual models. Part 1: A discussion of principles. *J. Hydrol.*, 10(3), 282–290.
- Ndiritu, J., 2005. Long-term trends of heavy rainfall in South Africa. *Regional Hydrological Impacts of Climate change: Hydroclimatic Variability*. In *Proceedings of Symposium S6, the 7th IAHS Scientific Assembly at Foz do Iguacu, Brazil, April, 2005*. IAHS Publ., 296, 178–183.
- Ndiritu, J., 2009. A comparison of automatic and manual calibration using the Pitman model. *Phys. Chem. Earth*, 34, 729–740.
- Nemec, J. and Schaake, J., 1982. Sensitivity of Water Resource Systems to Climate Variation. *Hydrol. Sci. Journ*, 1(27), 327–343.
- Neuman, S.P., 2003. Maximum likelihood Bayesian averaging of uncertain model predictions. *Stochastic Environ. Res. and Risk Assess.*, 17, 291–305.
- New, M., 1999. In *Representing Uncertainty in Climate Change Scenarios and Impact Studies: ECLAT-2 Red Workshop Report*. T.Carter, M. Hulme and D. Viner (eds.) Climatic Research Unit, Norwich.
- New, M., Lister, D., Hulme, M. and Makin, I. 2000. A high-resolution data set of surface climate over global land areas. *Climate Res.*, 21, 1–25.
- Nicholson, S.E, 2000. The nature of rainfall variability over Africa on time scales of decades to millennia. *Global and Planetary Change*, 26, 137–158.

- Nicholson, S.E., 1996. A review of climate dynamics and climate variability in eastern Africa. In: Johnson, T.C., Odada, E. ŽEds. , The Limnology, Climatology and Paleoclimatology of the East African Lakes. Gordon & Breach, 25–56.
- Nicholson, S.E. and Kim J., 1997. The relationship of the El Niño Southern Oscillation to African rainfall. *Int. J. Climatol.*, 17, 117–135.
- Nijssen, B., O'Donnell, G.M., Hamlet, A.F and Lettenmaier, D.P., 2001. Global Sensitivity of Global Rivers to Climate Change. *Climatic Change*, 50, 143–175.
- Pabon, J.D. and Dorado Delgado, J., 2008. Intraseasonal variability of rainfall over Northern South America and Caribbean Region. *Ingenieria de Recursos Naturales y del Ambients*, 7, 26–38.
- Palmer, M.A., Lettenmaier, D.P., Poff, N.L., Postel, S.L., Richter, B., Warner, R., 2009. Climate Change and River Ecosystems: Protection and Adaptation Options. *Environmental Management* 44, 1053–1068
- Palmer, W. C., 1965. Meteorological drought. U.S. Department of Commerce Weather Bureau Research Paper, 45, 1–58.
- Palmer, W.C., 1968. Keeping track of crop moisture conditions, nationwide: the Crop Moisture Index. *Weatherwise* 21, 156–161.
- Pandey, S., Bhandari, H. and Hardy, B. (eds.), 2007. Economic costs of drought and rice farmers' coping mechanisms: a cross-country comparative analysis. International Rice Los Baños (Philippines): International Rice Research Institute (IRRI), 203 pp.
- Panu, U.S. and Sharma, T.C., 2002. Challenges in drought research: some perspectives and future directions. *Hvdrol. Sci. Journ.*, 47(S), Special Issue: Towards Integrated Water Resources Management for Sustainable Development S19–S30.
- Pappenberger, F. and Beven, K., 2006. Ignorance is bliss: or seven reasons not to use uncertainty analysis. *Water Resour. Res.*, 42, W05302, doi: 10.1029/2005WR004820.
- Parajka, J., Merz, R. and Bloßschl, G., 2005. A comparison of regionalization methods for catchment model parameters. *Hydrol. Earth Syst. Sci.*, 9, 157–171.
- Parry, M.L. and Carter, T., 1998. Climate Impact and Adaptation Assessment: a guide to the IPCC approach. Earthscan, London 166pp.
- Peel M.C., McMahon T.A and Finlayson, B.L., 2004. Continental differences in the variability of annual runoff: update and reassessment. *J. Hydrol.*, 295, 185–197.
- Peel, M.C., McMahon, T.A. and Finlayson, B.L., 2002. Variability of annual precipitation and its relationship to El Niño-Southern Oscillation. *J. Climate*, 15(6), 545–551.
- Peel, M.C., McMahon, T.A., Finlayson, B.L. and Watson, F.G.R., 2001. Identification and explanation of continental differences in the variability of annual runoff. *J. Hydrol.*, 250, 224–240.
- Pettitt, A. N., 1979. A non-parametric approach to the change point problem. *Appl. Statist.*, 28, 126–135.
- Phillipon, N., Camberlin, P. and Fauchereau, N., 2002. Empirical predictability study of October-December east African rainfall, *Q.J.R. Meteorological Society*, 128, 2239–2256.
- Pilgrim, D.H., Chapman, T.G. and Doran, D.G., 1988. Problems of rainfall-runoff modelling in arid and semi-arid regions. *Hydrol. Sci. J.*, 33(4), 379–400.
- Pitman, W.V., 1973. A mathematical model for generating river flows from meteorological data in South Africa. Report No. 2/73, Hydrological Research Unit, University of the Witwatersrand, Johannesburg, South Africa.

- Population Reference Bureau, 2009. World population data sheet. 17pp. www.prb.org/pdff09/09wpds_eng.pdf.
- Quiring, S.M. and Papakryiakou, T.N., 2003. An evaluation of agricultural drought indices for the Canadian prairies. *Agricultural and Forest Meteorology*, 118, 49–62.
- Randrianasolo, A., Ramos, M.H. and Andreassian, V., 2011. Hydrological ensemble forecasting at ungauged basins: using neighbor catchments for model setup and updating. *Adv. Geosci*, 29, 1–11.
- Rasmusson, E.M., 1990. Intraseasonal and interannual climate variability. *Climatic Change*, 16, 153–171.
- Rauscher, C., 2001. *Fundamentals of Spectrum Analysis*. Rohde & Schwarz GmbH & Co. KG, Germany, 221pp.
- Reason, C.J.C. and Mulenga, H., 1999. Relationships between South African rainfall and SST anomalies in the southwest Indian Ocean, *Int. J. Climatol.*, 19, 1651–1673.
- Reason, C.J.C. and Rouault, M., 2005. Links between the Antarctic Oscillation and winter rainfall over western South Africa. *Geophysical Res. Letters*, 32, L077705, doi: 10.1029/2005GL022419.
- Refsgaard, J.C., van der Sluijs, J.P., Hojberg, A.L. and Vanrolleghem, P.A., 2007. Uncertainty in the environmental modelling process: A framework and guidance. *Environmental Modelling & Software*, 22, 1543–1556.
- Rial, J. A., Pielke, R. A. Sr., Beniston, M., Claussen, M., Canadell, J., Cox, P., Held, H., DeNoblet-Ducoudre, N., Prinn, R., Reynolds, J. F. and Salas, J. D.: 2004, ‘Nonlinearities, feedbacks, and critical thresholds within the Earth’s climate system. *Clim. Change*, 65, 11–38.
- Richard, Y., Fauchereau, N., Pocard, I., Rouaoult, M. and Trzaska, S., 2001. 20th century droughts in southern Africa: Spatial and temporal variability, teleconnections with oceanic and atmospheric conditions. *Int. Journal of Climatology*, 18, 329–345.
- Richardson, C.J., 2007. How much did droughts matter? Linking rainfall and GDP growth in Zimbabwe. *African Affairs*, 106(424), 463–478.
- Roderick, M.L. and Farquhar G.D., 2004. Changes in Australian pan evaporation from 1970 to 2002. *J. Climatol.*, 24, 1077–1090.
- Roderick, M.L. and Farquhar G.D., 2005. Changes in New Zealand pan evaporation since the 1970s. *J. Climatol.*, 25, 2031–2039.
- Roeckner, E., Arpe, K., Bengtsson, L., Claussen, M., Dumenil, L., Giorgetta, M., Schlese, U. and Schulzweida, U., 1996. The atmospheric general circulation model ECHAM-4: model description and simulation of present-day climate. Max-Planck Institute for Meteorology, Report No. 218, Hamburg, Germany, 90pp.
- Rosenberg, N.J., McKenney, M.S. and Martin, P., 1989. Evapotranspiration in a greenhouse-warmed world: a review and a simulation. *Agricultural and Forest Meteorology*, 47, 303–320.
- Rouault, M. and Richard, Y., 2003. Intensity and spatial extension of drought in South Africa at different time scales. *Water SA* 29(4), 489–500.
- Sachikonye, L.M., 1992. Zimbabwe: Drought, Food, and Adjustment-Review of African Political Economy, 53, 88–94.
- SADC, 1996. Food, Agriculture and Natural Resources. Report to SADC Annual Consultative Conference, SADC, Gaborone, 1996.
- SADC, 2011. Water Sector ICP Collaboration Portal. <http://www.icp-confluence-sadc.org/rbo/66>

- Salathe, E.P., 2003. Comparison of various precipitation downscaling methods for the simulation of streamflow in a rainshadow river basin. *Int. J. Climatol.* 23(8), 887–901.
- Salecwickz, A., 1996. Impact of climate change on operation of Lake Kariba hydropower scheme. *Water resources management in the face of climatic/hydrologic uncertainties*. Kluwer Academic Publishers, 300–321.
- SARDC, 2008, Southern African Environment Outlook. SADC, SARDC, IUCN, UNEP, Gaborone/Harare, Nairobi, 56pp.
- SARDC-IMMERCISA, 2007. Action on climate change to advance sustainable development in the Zambezi Basin. *The Zambezi*, 7(3), 8pp.
- Sawunyama, T., 2008. Evaluating uncertainty in water resources estimation in southern Africa: A case study of South Africa. Unpublished PhD. Thesis, Rhodes University, Grahamstown, South Africa.
- Schulze, R.E., 1994. Hydrology and Agrohydrology: A text to accompany the ACURU 3.00 Agrohydrological Modelling System. Water Research Commission, Report TT69/95, Pretoria.
- Schulze, R.E., 2005a. Setting the scene: the current hydroclimatic landscape in Southern Africa. In Schulze R.E. (ed.). *Climate change and water resources in Southern Africa: studies on scenarios, impacts, vulnerabilities and adaptation*. Water Research Commission (WRC) Report 1430/1/05: 6, 84–94.
- Schulze, R.E., 2000. Modelling hydrological responses to land use and climate change: A southern African perspective. *Ambio*, 29(1), 12–22.
- Schulze, R.E., 1986. The ACURU model for agrohydrological decision-making: structure, options and application. Proc. Second South African National Hydrology Symp. University of Natal, Pietermaritzburg, Dept. Agric. Engineering, ACURU report 21, pp. 345–362.
- Scott, P.A., Stone, D.A. and Allen, M.R., 2004. Human contribution to the European heatwave of 2003. *Nature*, 432, 610–613.
- Sen, P.K., 1968. Estimates of the regression coefficient based on Kendall's tau. *Journal of the American Statistical Association*, 63, 1379–1389.
- Sharma, A., Dadhwal, V.K., Jeganathan, C. and Tolpekin, V., 2009. Drought monitoring using the Standardised Precipitation Index: A case study for the state of Karnataka, India. *Geospatial Application Papers: Environment-Forest*, 6pp. www.gisdevelopment.net/application/natural_hazards/drought.
- Sharma, T.C. and Nyumbu, I. L., 1985. In W.L. Handlos and G.W. Howard, (eds). *Some hydrologic characteristics of the Upper Zambezi Basin. Development Prospects for the Zambezi Valley in Zambia*. Lusaka: Kafue Basin Research Committee of the University of Zambia, 29–43.
- Shamir, E., Imam, B., Morin, E., Gupta, H.V. and Sorooshian, S., 2005. Application of temporal streamflow descriptors in hydrologic model parameter estimation. *Water Resour. Res.*, 41. W06021, doi:10.1029/2004WR003409.
- Shela, O.N., 2000. Management of shared river basins: the case of the Zambezi River. *Water Policy*, 2, 65–81.
- Shepard, D., 1968. A two-dimensional interpolation function for irregularly-spaced data. *Proceedings of the 23rd ACM National Conference*, New York, NY, USA, 517–524.
- Shongwe, M. E., van Oldenborgh G. J., van den Hurk, B. J. J. M. de Boer B., Coelho C. A. S. and van Aalst, M. K., 2009: Projected changes in mean and extreme precipitation in Africa under global warming. Part I: Southern Africa. *J. Climate*, 22, 3819–3837.

- Shrestha, D.L., Kayastha, N., Solomatine, D. P., 2009. A novel approach to parameter uncertainty analysis of hydrological models using neural networks. *Hydrol. Earth Syst. Sci.*, 13, 1235–1248.
- Shumway, R.H., 1988. *Applied Statistical Time Series Analysis*. Englewood Cliffs, New Jersey, Prentice Hall.
- Siegel, S. and Castellan, N.J., 1988. *Non-parametric Statistics for the Behavioural Sciences*. McGraw Hill, New York, USA.
- Singh, C. R., Thompson, J. R., French, J. R., Kingston, D. G. and Mackay, A. W., 2010. Modelling the impact of prescribed global warming on runoff from headwater catchments of the Irrawaddy River and their implications for the water level regime of Loktak Lake, northeast India. *Hydrol. Earth Syst. Sci.*, 14, 1745–1765.
- Sivapalan, M., Takeuchi, K., Franks, S., Schertzer, D., O'Connell, P.E., Gupta, V.K., McDonnell, J.J., Pomeroy, J.W., Uhlenbrook, S., Zehe, E. and Lakshmi, V., 2003. IAHS Science Decade on Prediction in Ungauged Basins (PUB), 2003–2012: Shaping an exciting future for hydrological sciences. *Hydrol. Sci. Journ.*, 48(6), 857–880.
- Smakhtin, V.U. and Hughes, D.A., 2004. Review, Automated estimation and analyses of drought indices in South Asia. Working Paper 83, Drought Series paper 1, Colombo, Sri Lanka. International Water Management Institute, 24pp.
- Smith, L. A., 2002. What might we learn from climate forecasts? *Proc. Natl Acad. Sci. USA* 99, 2487–2492.
- Smith, P.J., Beven, K.J. and Tawn, J.A., 2008. Detection of structural inadequacy in process-based hydrological models: A particle-filtering approach. *Water Resour. Res.* 44, W01410, doi:10.1029/2006WR005205, 11pp.
- Solomon, S., Qin D., Manning, M., Chen, Z., Marquis, M., Averyt, K.B., Tignor, M. and Miller, H.L. (eds.), 2007. *Regional Climate Projections*. In *Climate Change 2007: The Physical Science Basis*. Contribution of the Working Group I to the Fourth Assessment Report of the Intergovernmental Panel on Climate Change. Cambridge University Press, Cambridge, United Kingdom and New York, NY, USA, 996 pp.
- Sorooshian, S. and Gupta, H.V., 1985. The analysis of structural identifiability: Theory and application to conceptual rainfall-runoff models. *Water Resour. Res.* 21(4), 487–495.
- Stainforth, D.A., Allen, M.R., Tredger, E.R. and Smith L.A., 2007. Confidence, uncertainty and decision support relevance in climate predictions. *Phil. Trans R Soc A*, 365, 2145–2161.
- StatSoft, Inc., 2009. STATISTICA (data analysis software system), version 9.0. www.statsoft.com.
- Swain, A., Swain, R.B., Themne, r A. and Krampe, F., 2011. *Climate Change and Risk of Violent Conflicts in Southern Africa*. Global Crisis Solutions, South Africa. ISBN 978-0-620-50465-2, 118pp.
- Sutcliffe, J.V and Knott., D.G., 1987. Historical variations in African water resources, in S.I. Solomon, M. Beran and W. Hogg (eds.). *The influence of climate change and climatic variability on the hydrologic regime and water resources*. IAHS Publication No. 168, 463–476. Oxfordshire.
- Tadross, M., Suarez, P., Lotsch, A., Hachigonta, S., Mdoka, M., Unganai, L., Lucio, F., Kamdonyo, D. and Muchinda, M., 2007. IPCC Regional Expert Meeting on Regional Impacts, Adaptation, Vulnerability and Mitigation. Nadi, Fiji, June 20-22, 193–204.

- Tallaksen, L.M. and Van Lanen, H.A.J. (eds.), 2006. *Developments in Water Science: Hydrological Drought-processes and Estimation Methods for Streamflow and Groundwater*. Elsevier, 579pp.
- Tang, C. and Piechota, T.C., 2009. Spatial and temporal soil moisture and drought variability in the Upper Colorado River Basin. *J. Hydrol.*, 379, 122–135.
- Tate E., Sutcliffe J., Conway D., Farquharson F., 2004. Water balance of Lake Victoria: update to 2000 and climate change modelling to 2100. *Hydrol. Sci.*, 49(4), 563-574.
- Taylor, W.A., 2000. Change-Point Analysis: A powerful new tool for detecting changes. <http://www.variation.co/cpa/tech/changepoint.html>.
- Thiaw, W. M., Barnston, A. G., and Kumar, V., 1999. Predictions of African Rainfall on the Seasonal Timescale. *Geophys. Res.*, 104(31), 589–597.
- Thiemann, T., Trosset, M. and Gupta H.V., 2001. Bayesian recursive parameter estimation for hydrologic models. *Water Resour. Res.*, 37(10), 2521–2535.
- Thomas, H.E., 1965. Reality of drought is always with us. *Natural History*, 74, 50–62.
- Thorne, R., 2010. Uncertainty in the impacts of projected climate change on the hydrology of a subarctic environment: Liard River Basin, *Hydrol. Earth Syst. Sci. Discuss.*, 7, 3129–3157.
- Tilmant, A., Kinzelbach, W., Beevers, L. and Juizo, D., 2010. Optimal Water Allocation in the Zambezi Basin. *International Environmental Modelling and Software Society (IEMS), 2010 International Congress on International Environmental Modelling and Software. Modelling for Environment's Sake. Fifth Biennial Meeting, Ottawa, Canada, 10pp.*
- Timberlake, J. (ed.), 1998. *Biodiversity of the Zambezi Basin Wetlands. Phase I: Review and Preliminary Assessment of Available Information. Volume I: Main Report. The Zambezi Society and Biodiversity Foundation for Africa, Harare, Zimbabwe, 124 pp.*
- Tirivarombo, S. and Hughes, D.A., 2011. Regional droughts and food security relationships in the Zambezi River Basin. *Phys. Chem. Earth*, 36, 977–983.
- Todd, M.C., Taylor, R. G., Osborn, T. J., Kingston, D. G., Arnell, N. W. and Gosling, S. N., 2011. Uncertainty in climate change impacts on basin-scale freshwater resources, preface to the special issue: the QUEST-GSI methodology and synthesis of results. *Hydrol. Earth Syst. Sci.*, 15, 1035–1046.
- Todd, M. C., Taylor, R. G., Osborn, T., Kingston, D., Arnell, N.W., and Gosling, S. N., 2010. Quantifying the impact of climate change on water resources at the basin scale on five continents a unified approach, *Hydrol. Earth Syst. Sci. Discuss.*, 7, 7485–7519.
- Todd, M. and Washington, R., 1999. Tropical temperate links in southern African and southwest Indian Ocean satellite-derived daily rainfall. *Int. J. Climatol.*, 19, 1601–1616.
- Torrence, C. and Compo, G.P., 1998. A Practical Guide to Wavelet Analysis. *Bull. Amer. Meteor. Soc.*, 79, 61–78.
- Torrence, C. and Webster, P.J., 1999. Interdecadal changes in the ENSO-monsoon system. *J. Climate*, 12(8), 2679–2690.
- Trenberth, K. E., Branstator, G. W., Karoly, D., Kumar, A, Lau., N. C. and Ropelewski, C., 1998. Progress during TOGA in understanding and modeling global teleconnections associated with tropical sea surface temperatures. *J. Geophys. Res. -Oceans*, 103, 14291–14324.
- Trenberth, K. E., Dai, A., Rasmussen, R. M. and Parsons D. B., 2003. The changing character of precipitation. *Bull. Amer. Meteor. Soc.*, 84, 1205–1217.

- Trenberth, K.E, Jones, P.D, et al., 2007. Observations: surface and atmospheric climate change. In: Solomon S., Qin D., Manning M., Marquis M., Averyt K., Tignor M.M.B., Miller H.L. Jr., Chen Z. (eds.) *Climate Change 2007: The Physical Science Basis. Contribution of Working Group I to the Fourth Assessment Report of the Intergovernmental Panel on Climate Change*. Cambridge University Cambridge, United Kingdom and New York, 235–336.
- Tshimanga, R., 2012. Hydrological uncertainty analysis and scenario-based streamflow modelling for the Congo River Basin. PhD thesis, Rhodes University, South Africa. <http://eprints.ru.ac.za/2397/>.
- Tumbare, J., 2004. The Zambezi River: Its threats and opportunities: 7th River Symposium, 1–3 September 2004, Brisbane.
- Tyson, P.D, 1986. *Climate change and variability over southern Africa*. Oxford University Press, Cape Town, 220pp.
- UN, 1992. United Nations Framework Convention on Climate Change. FCCC/INFORMAL/84, GE.05-62220 (E) 200705, 25pp. <http://unfccc.int/resource/docs/convkp/conveng.pdf>
- UN, 2006a. United Nations Population Reference Bureau. [http://www.prb.org/pdf06/06 World Data Sheet.pdf](http://www.prb.org/pdf06/06_World_Data_Sheet.pdf)
- UN, 2006b. UN-Water: Coping with water scarcity. A strategic issue and priority for system-wide action. UN-Water Thematic Initiatives. August 2006, 12pp.
- UNEP, 2006. *Climate Change and Variability in Southern Africa: Impacts and Adaptability in the Agricultural Sector*, UNEP and ICRAF.
- UNESCO, 1997. Southern Africa FRIEND. Technical Documents in Hydrology 15. UNESCO, Paris.
- Van den Hurk B, Jacob D., 2010. The Art of Predicting Climate Variability and Change in Climate change adaptation in the water sector. Ludwig F., Kabat P., van Schaik H., van der Valk (eds.). Earthscan UK and USA, 9–21.
- Van Jaarsveld, A.S., Biggs, R., Scholes, R.J., Bohensky, E., Reyers, B., Lynam, T., Musvoto, C. and Fabricius, C., 2005. Measuring conditions and trends in ecosystem services at multiple scales: the Southern African Millennium Ecosystem Assessment (SAfMA) experience. *Phil. T. Roy. Soc. B.*, 360, 425–441.
- Van Vuuren, D.P. and O’Neill, B.C., 2006. The Consistency of IPCC’s SRES scenarios to recent literature and recent projections. *Climatic Change* (2006), 75, 9–46.
- Valimba, P., 2004. Rainfall variability in southern Africa, its influences on streamflow variations and its relationships with climatic variations. PhD thesis, Rhodes University, 219pp.
- Vicente-Serrano, S.M., 2006. Differences in spatial patterns of drought on different time scales: An analysis of the Iberian Peninsula. *Water Resources Management*, 20, 37–60.
- Vicente-Serrano, S.M. and Lopez-Moreno J.I., 2005. Hydrological response to different time scales of climatological drought: an evaluation of the Standardized Precipitation Index in a mountainous Mediterranean basin. *Hydrol. Earth Syst. Sci.*, 9, 523–533.
- Viner, D., 2003. A qualitative assessment of the sources of uncertainty in climate change impact assessment studies. In *Climatic Change: Implications for the hydrological cycle and for water management*. *Advances in Global Change Research*, 10, 139–149.
- Vrugt, J. A., Gupta, H. V., Bouten, W. and Sorooshian, S., 2003a. A Shuffled Complex Evolution Metropolis algorithm for optimization and uncertainty assessment of hydrologic model parameters, *Water Resour. Res.*, 39(8), 1201.

- Vrugt, J. A., Gupta, H. V., Bastidas, L. A., Bouten, W. and Sorooshian, S. 2003b. Effective and efficient algorithm for multi-objective optimization of hydrologic models, *Water Resour. Res.*, 39(8), 1214.
- Vrugt, J.A., Diks, C.G.H., Gupta, H.V., Bouten, W., Jacobus, M. and Verstraten, J.M, 2005. Improved treatment of uncertainty in hydrologic modeling: Combining the strengths of global optimization and data assimilation. *Water Resour. Res.*, 41. W01017, doi: 10.1029/2004WR003059.
- Wagener, T. and Collat, J., 2007. Numerical and visual evaluation of hydrological and environmental models using the Monte Carlo analysis toolbox. *Environ. Model. Soft.*, 22(7), 1021–1033.
- Wagener, T., McIntyre, N., Lees, M.J., Wheater, H.S. and Gupta, H.V., 2003. Towards reduced uncertainty in conceptual rainfall-runoff modeling: Dynamic identifiability analysis. *Hydrol. Process.*, 17, 455–476.
- Wagener, T. and Wheater, H.S., 2006. Parameter estimation and regionalization for continuous rainfall-runoff models including uncertainty. *J. Hydrol.*, 320(1–2), 132–154.
- Wamukonya, N. and Rukato, H., 2001. Climate change implications for Southern Africa: a gendered perspective, Southern African Gender Network (SAGEN), Minerals and Energy Policy Center (MEPC), 36pp.
- Washington, R. and Todd, M., 1999. Tropical-temperate links in southern African and southwest Indian Ocean satellite-derived daily rainfall. *Int. J. Climatol.*, 19, 1601–1616.
- Webster, P.J., Holland, G.J., Curry, J.A. and Chang, H.R., 2005: Changes in tropical cyclone number, duration and intensity in a warming environment. *Science*, 309, 1844–1846.
- Wheater, H. S, 2008. Modelling Hydrological Processes in arid and semi-arid areas: An introduction to the workshop. In : *Hydrological modelling in Arid and Semi-Arid Areas*. Wheater, H., Sorooshian, S. and Sharma, K.D. (eds.). Cambridge University Press, Cambridge.
- Wheater, H. S, Jakeman, A.J. and Beven, K.J., 1993. Progress and directions in rainfall-runoff modeling. In *Modeling Change in Environmental Systems*, Jakeman A.J., Beck M.B., McAleer M.J., (eds.). John Wiley & Sons, UK, 101–132.
- Wilby, R.L., 2005. Uncertainty in water resource model parameters used for climate change impact assessment. *Hydrol. Process.*, 19(16), 3201–3219.
- Wilby, R.L., 2007. Decadal forecasting techniques for adaptation and development planning. A briefing document on available methods, constraints, risks and opportunities. DFID Report. October 2007, 54pp.
- Wilby, R.L., Dawson, C.W., Barrow, E.M., 2002. SDSM: a decision support tool for the assessment of regional climate change impacts. *Environ. Model. Soft.*, 17, 147 – 159.
- Wilby, R.L. and Harris, I., 2006. A framework for assessing uncertainties in climate change impacts: Low-flow scenarios for the River Thames, UK. *Water Resour. Res* 42(2), W02419. (doi:10.1029/2005WR004065).
- Wilby, R.L. and Wigley, T.M.L., 1997. Downscaling general circulation model output: a review of methods and limitations. *Progress in Physical Geography*, 21(4), 530–548.
- Wilhite, D.A., and Glantz, M.H., 1985. Understanding the drought phenomenon: The role of definitions. *Water Int.*, 10(3), 111–120.
- Wilk, J., Kniveton, D., Andersson, L., Layberry, R., Todd, M.C., Hughes, D., Ringrose, S. and Vanderpost, C., 2006. Estimating rainfall and water balance over the Okavango River basin for hydrological applications. *J. Hydrol.*, 331, 18–29.

- Winsemius, H.C., 2009. Satellite data as complementary information for hydrological modeling. Published PhD thesis, 1st Edition ISBN: 978-90-6562-207-5. 186pp.
- Winsemius, H.C., Savenije, H.H.G. and Bastiaanssen, W.G.M., 2008. Constraining model parameters on remotely sensed evaporation: justification for distribution in ungauged basins? *Hydrol. Earth Syst.Sci.*, 12, 1403–1418.
- Winsemius, H.C., Savenije, H.H.G., Gerrits, A.M.J., Zapreeva, E.A. and Klees, R., 2006. Comparison of two model approaches in the Zambezi river basin with regard to model reliability and identifiability. *Hydrol. Earth. Syst. Sci.*, 10, 339–352.
- Wolski, P., Todd, M.C., Murray-Hudson., M.A., Tadross., M., 2011. Multidecadal variability in hydroclimate of Okavango river system, southwest Africa, in the past and under changing climate. Paper submitted to *J. Hydrol.*
- WMO (World Meteorological Organisation), 1987. Water resources and climate change: Sensitivity of water resources systems to climate change and variability. Report WCAp-4, WMO/TD (247), 50pp.
- WMO, 2000. Detecting trends and other changes in hydrological data. WCDMP 45, WMO TD 1013, 157 pp.
- Wood, A. W., Leung, L. R., Sridhar, V. and Lettenmaier, D. P., 2004. Hydrologic Implications of Dynamical and Statistical Approaches to Downscaling Climate Model Outputs. *Climatic Change*, 62, 189–216.
- Wood, A.W., Maurer, E.P., Kumar, A. and Lettenmaier, D.P., 2002. Long range experimental hydrologic forecasting for the eastern U.S. *Geophys. Res.*, 107, (D20), 4429.
- World Bank, 2005. World development indicators. www.worldbank.org/data.
- World Bank, 2010. The Zambezi River Basin: A Multi-Sector Investment Opportunities Analysis. Volume 4, Modelling, Analysis and Input data. The International Bank for Reconstruction and Development/The World Bank, 158pp.
- World Climate Programme, 2007. Expert meeting on water manager needs for climate information in water resources planning. Geneva, Switzerland, 18–20 December 2006. Final Report. WCASP-74. WMO/TD-No. 1401.
- Xu, C.Y., 1999. Climate Change and hydrologic models. A review of existing gaps and recent research developments. *Water Resour. Manage.*, 13(5), 369–382.
- Xu, C.Y., 2000. Modelling the effects of climate change on water resources in Central Sweden. *Water Resour. Manage.*, 14(3), 177–189.
- Xu C.Y. and Singh, V.P., 1998. A Review on Monthly Water Balance Models for Water Resources Investigations. *Water Resour. Manage.*, 12, 31–50.
- Xu C.Y. and Singh, V.P., 2004. Review on Regional Water Resources Assessment Models under Stationary and Changing Climate. *Water Resour. Manage.*, 18, 591–612.
- Xu, H., Taylor, R. G. and Xu, Y., 2011. Quantifying uncertainty in the impacts of climate change on river discharge in sub-catchments of the Yangtze and Yellow River Basins, China, *Hydrol. Earth Syst. Sci.*, 15, 333–344.
- Yadav, M., Wagener, T. and Gupta, H., 2007. Regionalization of constraints on expected watershed response behavior for improved predictions in ungauged basins. *Adv. Water Resour.*, 30, 1756–1774.
- Yates, D.N. and Strzepek, K.M., 1998. Modeling the Nile basin under climatic change. *Hydrol. Eng.* 3(2), 98–108.
- ZACPRO 6.1.2 (Zambezi Action Plan Project 6.1.2), 1998. INTRODUCTORY VOLUME Water Resources and Hydrological Modelling.

- Zagona, E.A., Fulp, T., Shane, R., Magee, T. and Goranflo, H.M., 2001. RIVERWARE: A generalized tool for complex reservoir system modelling. *American Water Res. Assoc.*, 37(4), 913–929.
- Zelenhasic, E. and Salvai, A., 1987. A method of streamflow drought analysis. *Water Resour. Res.*, 23 (10), 156–168.
- Zhang, Y., Wallace, J. M. and Battisti, D. S., 1997. ENSO-like interdecadal variability: 1900–93. *J. Climate*, 10, 1004–1020.
- Zhang, C., 1993. Large-scale variability of atmospheric deep convection in relation to sea surface temperature in the tropics. *J. Climate*, 10, 1898–1913.
- Zhang, X., Srinivasan, K., Zhao, K. and Van Liwew, M., 2009. Evaluation of global optimization algorithms for parameter calibration of a computationally intensive hydrologic model. *Hydrol. Process.*, 23(3), 430–441.
- Zhang, X., Srinivasan, R. and Hao, F., 2007. Predicting Hydrologic response to Climate Change in the Luohe River Basin Using the SWAT model. *American Society of Agricultural and Biological Engineers. Transactions of the ASABE*, 50(3), 901–910.
- Ziervogel, G., Johnston, P., Matthew, M. and Mukheibir, P., 2010. Using climate information for supporting climate change adaptation in water resource management in South Africa. *Climate Change*, 103, 537–554.
- Zinyama L., Whitlow R, 2004. Changing patterns of population distribution in Zimbabwe. *Geology Journ.*, 13, 365–384.
- ZRA (Zambezi River Authority), 2009.